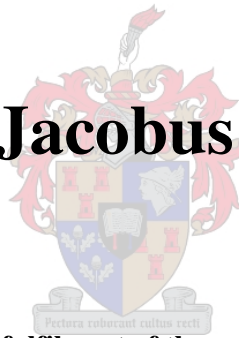


*Process development and commissioning of  
a bioreactor for mass culturing of USAB  
granules by process induction and  
microbial stimulation*

**BY**

**Pierrie Jacobus van Zyl**



Thesis submitted in partial fulfilment of the requirements for the degree of

**Master of Science in Engineering  
(Chemical Engineering)  
In the Department of Process Engineering  
At the University of Stellenbosch**

**Supervisors: L Lorenzen, E R Els**

**STELLENBOSCH  
DECEMBER 2004**

# Declaration

---

I, the undersigned, hereby declare that the work contained in this thesis is my own original work, except where specifically acknowledged in the text. This thesis has not, partially or entirely been submitted at any university for any degree in the past.

.....

Pierrie Jakobus van Zyl

December 2004



# *Synopsis*

---

The Up-flow Anaerobic Sludge Blanket Reactor (UASB) provides a state-of-the-art solution to effluent treatment by anaerobic digestion: sludge production is dramatically lower than in other digestion processes, and energy is gained from the system if the produced biogas is converted to electricity and/or heat. The UASB is a modified fluidised bed reactor, with the solid state 'catalyst' being granulated anaerobic sludge, and the liquid phase the effluent that needs to be treated. A gas cap is installed to serve as a carbon dioxide and methane collector. This biogas (carbon dioxide and methane) is produced by the stepwise decomposition of complex carbohydrates and proteins via a consortium of micro-organisms living in a symbiotic environment known as a granule. A typical UASB reactor has an organic removal rate of 89-93% Chemical Oxygen Demand (COD) and operates optimally at loadings of 9.8-11 kg COD/ m<sup>3</sup> reactor volume/day. Unfortunately, one major problem hampers the efficiency of this reactor to such an extent that the unit is only economically viable in exceptional cases; if the reactor is inoculated with un-granulated anaerobic sludge, start-up times of up to 12 months can be expected.

The lengthy start-up times motivated the search for an artificial way to cultivate USAB granules. Early research (done on lab-scale, 400ml vessel volumes) proved that, under a specified set of environmental conditions, granule growth can occur in an artificial environment. Yet these laboratory-scale vessels did not facilitate scale-up or the study thereof. This led to the main problem statement of this research project: namely to design, commission, and optimise bench-scale bioreactors that will generate granulated anaerobic sludge in an incubation period of 20 days. These units should also facilitate the determining of parameters that will assist in the design of a scale-up to a UASB granule producing reactor of economically viable size. Two bench-scale reactors were initially designed specifically to "mimic" the motion found in the laboratory-scale vessels. The results from these initial reactors proved that granulation cannot only be enhanced, but granules can actually be cultivated from dispersed anaerobic sludge in a larger artificial environment over an incubation period of only 20 days.

The results were still far from satisfactory, as the granules produced were irregular in shape and the yield of usable granules (2.2 kg/m<sup>3</sup> reactor volume) insufficient. A third test reactor was designed to "mimic" roller table movement and baffles were included. These results were much better and the yield was 4.4 kg/m<sup>3</sup> reactor volume at a baffle tipspeed of 0.0055 m/s. The optimisation was extended further to include the inoculation sludge and the feed medium. A C:N:P ratio of 10:1:4 proved to yield the best results. Monovalent anions, hydrogen concentration and a pH-level outside the 6.5 to 7.2 range evidently had an inhibitory effect on the granulation rate. After the optimisation study the third test unit produced a usable granule yield of 15.2 kg/m<sup>3</sup> reactor volume over the 20-day incubation period.

The incubation period can be separated into 3 distinct phases, namely the acidification, stabilisation and growth phases. From the mass balance it was found that most of the COD and nutrients were used for ECP production in the acidification phase. During the stabilisation phase, the COD and nutrients were mostly used for nucleus formation, and finally in the growth phase the COD was used for granule growth. To study the effect the internal surface area of the reactor has on the granulation process, 3 scale-down versions of the third test unit were constructed. Within the studied range, a yield of usable granules of 40 kg/m<sup>2</sup> reactor internal surface area was obtained.

# Opsomming

---

Die Opwaartse-vloei Anaërobe Slyk Bed Reaktor (UASB) bied 'n uitstekende alternatiewe oplossing vir die behandeling van afloopwater deur anaërobe vertering: slykproduksie is aansienlik laer as in alternatiewe verteringsprosesse en energie kan genereer word (indien die gevormde biogas na elektrisiteit of hitte omgeskakel word. Die UASB is 'n aangepaste gefuidiseerde bedreaktor met gegranuleerde anaërobiese slyk as (vastestof-fase) katalisator en die vloeibare fase as die afloopwater wat behandel moet word. 'n Driefase skeier dien as verwisslingsruimte om die biogas (koolstofdiksied en metaan) van die granules en afloopwater te skei. Hierdie biogas word gevorm deur die stapsgewyse ontbinding van komplekse koolhidrate en proteïene deur 'n konsortium van mikro-organismes in 'n simbiotiese omgewing bekend as 'n granule. 'n Tipiese UASB reaktor het 'n organiese verwyderingsvermoë van 89 – 93 % chemiese suurstof aanvraag (COD) en funksioneer optimaal by beladings van 9.8 – 11 kg COD/m<sup>3</sup> reaktorvolume/dag. Ongelukkig kan die inleidende fase (indien die reaktor met nie-gegranuleerde anaërobiese slyk gevoer word) tot so lank as 12 maande neem, wat die eenheid slegs in uitsonderlike gevalle ekonomies lewensvatbaar maak.

On laasgenoemde rede is die ondersoek na 'n kunsmatige wyse om granules te kweek, begin. Vroeëre laboratoriumstudies (400 ml reaktorvolumes) het bewys dat, onder voorafbepaalde omstandighede, granules wel kan groei in 'n kunsmatige omgewing. Dog, hierdie reaktors het nie ruimte vir verskaling en die studie daarvan gelaat nie. Die huidige studie poog gevolglik om werkbank-skaal reaktors te ontwerp, (vermagtig) en te optimiseer om sodoende, binne 'n inkubasie-periode van 20 dae, gegranuleerde anaërobiese slyk te produseer. Die eenhede moet verder die studie van die parameters wat die verskaling van 'n UASB-granule-produiserende reaktor van ekonomies-lewensvatbare omvang beïnvloed, fasiliteer. Twee werkbank-grote reaktors is ontwerp, spesifiek om die beweging van die laboratoriumreaktors na te boots. Die resultate gelewer deur hierdie reaktors het bewys dat, nie net kan granulasie bevorder word nie, dit kan inderdaad vanuit (fyn) anaërobiese slyk in 'n groter kunsmatige omgewing binne 'n inkubasie periode van slegs 20 dae gekultiveer word.

Die resultate was egter steeds onbevredigend, aangesien die vorm van die granules onreëlmatig en die massa bruikbare granules (2.2 kg/m<sup>3</sup> reaktorvolume) heeltemal te laag is. 'n Derde toetsreaktor is ontwerp om die beweging van die roltafels na te boots. Hierdie keer was die resultate aansienlik beter: 4.4 kg/m<sup>3</sup> reaktovolume teen 'n keerplaatkantelspoed van 0.0055 m/s. Ook die geïnkuleerde slyk en voermedium is onder oënskou geneem, 'n C:N:P verhouding van 10:1:4 toon die beste resultate. Die studie wys verder dat monovalente anione, die konsentrasie waterstof en 'n pH-vlak buite die 6.5 tot 7.2 speelruimte, granulasie inhibeer. Na afloop van die studie het die derde eenheid 15.2 kg/m<sup>3</sup> reaktorvolume bruikbare granules gelewer, binne die 20 dag inkubasie periode.

Die inkubasie-periode kan in drie definitiewe fases verdeel word, naamlik die suurvormingsfase, die stabiliseringsfase en die groeifase. Die massabalans toon dat die meerderheid van die COD en voedigstowwe tydens die suurvormingsfase vir die produksie van ekstra-sellulere polimere (ESP) aangewend is. Tydens die stabiliseringsfase is dit meestal gebruik vir nukleus-vorming. COD word in die groeifase vir granulegroeï vanaf die gevormde nukleie gebruik. Om die effek van die intrinsieke reaktoroppervlak op die granulasieproses te bestudeer, is drie afgeskaalde weergawes van die derde eenheid ontwerp. Binne die bestudeerde speelruimte, is die opbrengs van bruikbare granules van 40 kg/m<sup>2</sup> binneoppervlakruimte opgemerk.

# Acknowledgements

---

- 1 **Amy Barty:** Your love, support and friendship is truly a life changing experience, and it came at a time when it was most needed. Thank you for being a part of my life and work.
- 1 **Leon Lorenzen:** Your extensive experience in being a study leader made this project a remarkable experience. Thank you for all the support and lightning fast workshop. You are a blessing to any master's study.
- 1 **Pierre van Zyl (Senior):** Thank you for all the love and support and dedication to your child's education through the years. Above all thank you for the love of nature and the environment you so diligently cultivated in your family. If it was not for this, this thesis would never have been.
- 1 **Rina van Zyl:** Thank you for believing in your son, and never being more than a phone call away. You are the best mother any student can ask for.
- 1 **Andre and Jacques van Zyl:** Thank you for all the friendship and support, you are both brothers and role models anyone can be proud of.
- 1 **E R Els:** The design and construction of the first two bench-scale reactors and gas measuring units are much appreciated.
- 1 **TJ Britz:** Thank you for giving me the opportunity to work in the magnificent field of microbial digestion; I will carry the experience with me for the rest of my life.
- 1 **G Scott, P Moolman, R Rabe, B Rousseau, G Sigge, C Lampregt:** Your support, friendship and humour made every day at work a true pleasure.
- 1 **WRC:** For funding the project
- 1 **NRF:** For financial aid.
- 1 **The staff at the Department of Process Engineering at the University of Stellenbosch:** Working with you was a true pleasure, thank you.
- 1 And finally in humble acknowledgement of the Almighty God, for granting all of us this beautiful gift of life and without Who's strength this work could never have been done.

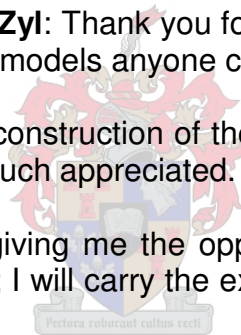


# Table of Contents

---

---

<b><u>Chapter</u></b>	<b><u>Page</u></b>
<i>Declaration</i> .....	ii
<i>Synopsis</i> .....	iii
<i>Opsomming</i> .....	iv
<i>Acknowledgements</i> .....	v
<i>Table of Contents</i> .....	vi
<i>List of Figures</i> .....	ix
<i>List of Tables</i> .....	xi
<i>List of Abbreviations</i> .....	xii
<b>1. Introduction</b> .....	<b>1</b>
<b>2. Literature Review</b> .....	<b>8</b>
<b>2.1 Introduction</b> .....	<b>8</b>
2.1.1 The Definition of Anaerobic Digestion .....	8
2.1.2 The History of Anaerobic Digestion.....	10
2.1.3 Anaerobic Waste Treatment Methods .....	11
<b>2.2 The Up-flow Anaerobic Sludge Blanket Reactor (UASB)</b> .....	<b>13</b>
2.2.1 General Discussion and Characteristics.....	13
2.2.2 Applications .....	15
2.2.3 Performance .....	16
2.2.4 Shortcomings .....	17
<b>2.3 Granule Composition</b> .....	<b>17</b>
2.3.1 Definition of UASB Granules.....	18
2.3.2 Inorganic Species .....	18
2.3.3 Organic Species (Extra Cellular Polymers) .....	19
<b>2.4 Granule Structure and Population</b> .....	<b>20</b>
2.4.1 Macroscopic Granule Structure .....	20
2.4.2 Microscopic Granule Structure .....	21
<b>2.5 Granule Formation</b> .....	<b>23</b>
2.5.1 Anaerobic Bio-granulation.....	23
2.5.2 Granulations Accelerators and Inhibitors .....	25
<b>2.6 Bioreactors and Scale-up</b> .....	<b>27</b>
2.7.1 General Scale-up Considerations.....	27
2.7.2 General Design Parameters.....	28
<b>2.8 Matlab® Image Processing</b> .....	<b>28</b>
<b>2.9 Summary</b> .....	<b>29</b>

3. <i>Initial Research and Bench-Scale Commissioning</i> .....	32
3.1 Introduction.....	32
3.2 Reactor Design.....	35
3.2.1 The 4.15 Litre Unit (R <sub>4.15</sub> ) .....	35
3.2.2 The 7.2 Litre Unit (R <sub>7.2</sub> ).....	36
3.2.3 Gas Measuring Unit .....	37
3.3 pH-Manipulation.....	38
3.4 Results and Discussion .....	40
3.4.1 Experimental Run 1 .....	40
3.4.2 Experimental Run 2 .....	41
3.4.3 Experimental Run 3 .....	43
3.4.4 Experimental Run 4 .....	44
3.5 Summary .....	47
4. <i>Phase 3, Reactor Optimisation</i> .....	50
4.1 Phase 3 Problem Statement.....	50
4.2 Background .....	52
4.3 Identification of Sludge Prone to Granulation. ....	53
4.3.1 Settability .....	54
4.3.2 PH .....	55
4.3.3 Specific Gravities.....	56
4.3.4 Granule Size Distribution .....	56
4.3.5 Summarized results .....	57
4.4 Reactor Feed Optimisation .....	58
4.4.1 Base Case and Growth Curve .....	59
4.4.2 Variation of the CaCO <sub>3</sub> Concentration .....	60
4.4.2 Feed Processing Through Filtration and Sterilisation.....	60
4.4.4 Variation of the KH <sub>2</sub> PO <sub>4</sub> Concentration .....	61
4.4.5 pH Manipulación vía Ca(OH) <sub>2</sub> .....	62
4.4.6 Trace Elements.....	62
4.4.7 COD Variation .....	63
4.5 Bioreactor Optimisation with Regards to Mixing Speed.....	64
4.5.1 Experimental Runs 1 to 5.....	64
4.5.2 Experimental Run 6 .....	65
4.5.3 Experimental Run 7 .....	66
4.5.1 Experimental Run 8 .....	67
4.5.1 Experimental Run 9 .....	67
4.3.1 Experimental Run 10 .....	69
4.6 Graphical comparison of results obtained.....	69
4.5.1 Mixing speed vs. Increase in Granular Mass .....	69
4.5.2 Mixing Speed vs. Methane Produced .....	71
4.5.3 Mineral Consumption vs. Mixing speed.....	72
4.5.5 COD Consumed vs. Mixing Speed.....	73
4.7 Optimised Process Output.....	73
4.7.1 Experimental Run 11 .....	73
4.7.2 Experimental Run 12 .....	74
4.8 Summary .....	75
5. <i>Growth Analysis Revision</i> .....	78
5.1 Introduction.....	78
5.2 Programming and Implementation .....	81

<b><u>Chapter</u></b>	<b><u>Page</u></b>
5.3 Materials and Methods.....	82
5.3.1 Sampling Procedure .....	82
5.3.2 Calculations.....	83
5.4 Results and Discussion .....	84
5.4.1 Test Sample, Set 1 (200 ml).....	85
5.4.2 Test Sample, Set 2 (2x100 ml).....	85
5.4.3 Test Sample, Set 3 (5x50 ml).....	85
5.4.4 Visual representation of DIPMUG vs. the actual MUG .....	86
5.5 Summary.....	90
6. <i>ISA Variation</i> .....	92
6.1 Introduction.....	92
6.2 Materials and Methods.....	93
6.2.1 Baffle Tipspeeds .....	94
6.2.2 Reactor Design.....	95
6.2.3 Operating Procedure .....	97
6.3 Results and Discussion .....	97
6.3.1 Daily pH Log .....	98
6.3.2 Growth Curves .....	99
6.3.3 MUG vs. Tipspeed.....	100
6.3.4 MUG vs. Internal Surface Area (ISA) .....	101
6.4 Summary.....	102
7. <i>Mass Balance and Modelling</i> .....	104
7.1 Introduction.....	104
7.2 Theoretical Discussion.....	104
7.3 Results and Discussion .....	107
7.4 Mass Balance and Modelling.....	111
7.4.1 Mass Balance Predictions Compared to TSS values .....	111
7.4.2 Summary of the Final Experimental Run .....	113
7.5 Summary.....	113
8. <i>Final Conclusions and Recommendations</i> .....	116
9. <i>References</i> .....	124
<i>Appendix</i> .....	129
A1. Operational Procedures .....	129
A1.1 Reactor Operation .....	129
A1.2 Feed Composition and Sludge Preparation.....	129
A1.3 Sludge Screening Tests .....	130
A1.3.1 Density ( $\rho$ ).....	130
A1.3.2 Settling time ( $t_s$ ) .....	131
A2 Analytical Procedures .....	137
A2.1 COD Analysis .....	137
A2.2 Sample Preparation for TSS.....	138
A2.3 Total Suspended Solids (TSS) [g/200ml] .....	138
A2.4 Biogas and Methane Production .....	139
A2.5 MUG and DIPMUG Analysis.....	139



<u>Chapter</u>	<u>Page</u>
A4. Chapter 4, Experimental Results.....	146
A5. Chapter 5, Experimental Results.....	170
A5.3 Experimental Results .....	174
A7. Chapter 6, Experimental Results.....	177
A7. Chapter 7, Experimental Results.....	178
A8. WRC Project .....	182

# *List of Figures*

---

<u>Figure</u>	<u>Page</u>
Figure 1.1: Schematic Representation of the UASB Reactor	3
Figure 1.2: Mindmap of WRC Project Layout	5
Figure 2.1: Aerobic digestion and Anaerobic digestion	8
Figure 2.2: A Schematic of the UASB Reactor	14
Figure 2.3: Anaerobic Sludge Granules	21
Figure 2.4: Microbial layout and digestion process inside a UASB granule	22
Figure 3.1: VFA Profiles of the Major Acidic Digestion Products of Sludge	34
Figure 3.2a: R <sub>4,15</sub> , Agitator Included	35
Figure 3.2b: R <sub>4,15</sub> , Outside View	36
Figure 3.3a: R <sub>7,2</sub> , Agitator included	36
Figure 3.3b: R <sub>7,2</sub> , Outside View	37
Figure 3.4: The Gas Measuring Unit	38
Figure 3.5: The Actual pH vs. Time Distribution	39
Figure 3.6: Desired pH vs. Time Distribution	39
Figure 3.7: Experiment 1, pH vs. Time	40
Figure 3.8: Experiment 1, Gas Production vs. Time	40
Figure 3.9: Experiment 2, pH vs. Time	41
Figure 3.10: Experiment 2, Gas Production vs. Time	42
Figure 3.11: Experiment 2, % Methane in Biogas vs. Time	42
Figure 3.12: Experiment 3, pH vs. Time	42
Figure 3.13: Experiment 3, Gas Production vs. Time	43
Figure 3.14: Experiment 3, % Methane in Biogas vs. Time	44
Figure 3.15: Experiment 4, pH vs. Time	45
Figure 3.16: Experiment 4, Gas Production vs. Time	45
Figure 3.17: Experiment 4, TSS Yield per Mass fraction	46
Figure 3.18: Flow patterns in R <sub>7,2</sub>	49
Figure 3.19: Flow patterns in R <sub>4,15</sub>	49
Figure 4.1: R <sub>5,5</sub> , Baffles Included	49
Figure 4.2: Outside view of the third reactor (R <sub>5,5</sub> )	53
Figure 4.3: Settling Velocities of Raw Sludge	54
Figure 4.4: pH's of Raw Anaerobic Sludge	55
Figure 4.5: Specific Gravities of Raw Sludge	56
Figure 4.6: Granule Size Distribution of Raw Anaerobic Sludge	57
Figure 4.7: Raw Anaerobic Digester Sludge	58

<b><u>Figure</u></b>	<b><u>Page</u></b>
Figure 4.8: Granule Growth over 20 Days	60
Figure 4.9: Variation in CaCO <sub>3</sub> Concentration	60
Figure 4.10: Feed Variation	61
Figure 4.11: KH <sub>2</sub> PO <sub>4</sub> Variation	62
Figure 4.12: Feed pH Manipulation with Ca(OH) <sub>2</sub>	63
Figure 4.13: Trace Elements	63
Figure 4.14: COD Variation in Feed	64
Figure 4.15a: Yield <sub>(MUG)</sub> vs. Impellor Tipspeed	70
Figure 4.15b: Yield <sub>(MUG)</sub> vs. Impellor Tipspeed	70
Figure 4.16: Methane Produced vs. Mixing Speed	71
Figure 4.17: KHCO <sub>3</sub> and CaCO <sub>3</sub> Consumed to Maintain pH vs. Mixing Speed	72
Figure 4.18: COD Consumption vs. Mixing Speed	73
Figure 4.19: MUG Timeline	75
Figure 4.20: Flow Patterns in R <sub>5.5</sub> (Red shows the sludge movement)	76
Figure 5.1: Granulated Anaerobic Sludge	78
Figure 5.2: Standard camera set-up for the DIP programme	83
Figure 5.3: Actual MUG vs. DIP MUG for Run 3, 1 litre growth Curve (200 ml)	86
Figure 5.4: Actual MUG vs. DIP MUG for Run 3, 2 litre growth Curve (200 ml)	86
Figure 5.5: Actual MUG vs. DIP MUG for Run 3, 4 litre growth Curve (200 ml)	87
Figure 5.6: Actual MUG vs. DIP MUG for Run 3, 1 litre test samples (2x100 ml)	88
Figure 5.7: Actual MUG vs. DIP MUG for Run 3, Diverse Test Samples (2x100ml)	88
Figure 5.8: Actual MUG vs. DIP MUG for 1, 2 and 4 Litre Reactors	89
Figure 5.9: 4 x 50 ml Actual MUG vs. DIPMUG	89
Figure 6.1: Classic Scale-up Procedure followed in Reactor Design	92
Figure 6.2: Visual representation of the r <sub>b</sub> value	95
Figure 6.3: Front and Side View of Reactors	96
Figure 6.4: Run 2 pH vs. Time 0.00275 m/s.	98
Figure 6.5: Run 3 pH vs. Time 0.0055 m/s.	98
Figure 6.6: Run 4 pH vs. Time 0.01375 m/s.	99
Figure 6.7: Run 2 MUG vs. Time at 0.00275 m/s.	99
Figure 6.8: Run 3 MUG vs. Time at 0.0055 m/s.	100
Figure 6.9: Run 4 MUG vs. Time at 0.01375 m/s.	100
Figure 6.10: MUG <sub>D20</sub> vs. Tipspeed for 1, 3, 4 and 5.5 litre units.	101
Figure 6.11: MUG <sub>D20</sub> vs. Tipspeed for 1, 3, 4 and 5.5 litre units.	101
Figure 7.1: Mass Balance over 5.5 litre reactor	105
Figure 7.2: pH vs. time for Mass Balance on R <sub>5.5</sub>	108
Figure 7.3: Methane in Biogas Production vs. Time	108
Figure 7.4: COD Consumed vs. Time	109
Figure 7.5: Calcium consumption vs. time	109
Figure 7.6: Phosphate Consumption vs. Time	110
Figure 7.7: Nitrogen Consumption vs. Time	110
Figure 7.8: Mass Increase in Each Size Range vs. Time (i)	111
Figure 7.9: Mass Increase in Each Size Range vs. Time (ii)	112
Figure 7.10: Total Biomass Increase in vs. Time	112
Figure 8.1: Mechanical Seal at Reactor Base	122
Figure 8.3: Basic Thickener Design	122
Figure 8.4: PFD of Reactor and Fluidised Bed	123
Figure A1.1: Calibration image used for calibration of the DIP program (particles: 1x10mm; 6x5mm; 5x2mm; 7x1mm and 6x0.4mm)	131
Figure A1.2: Calibration image used for calibration of the DIP program	132
Figure A1.3: DIP Calibrator Output (CLevel = 0.4, Cut = 0.2 mm)	132

<b><u>Figure</u></b>	<b><u>Page</u></b>
Figure A1.4: DIP Calibrator Output (CLevel = 0.4, Cut = 0.5 mm)	133
Figure A1.5: DIP Calibrator Output (CLevel = 0.4, Cut = 1 mm)	133
Figure A1.6: Typical subsample image ready for DIP processing	134
Figure A1.7: Correct DIP program output	135
Figure A1.8: Too high grey scale (CLevel = 0.55)	136
Figure A1.9: Too low grey scale (CLevel = 0.2)	136
Figure A2.1: Chemical Oxygen Demand (COD) Analysis	137
Figure A2.2: Total Suspended Solids (TSS) Procedure	139
Figure A2.3: Standard sampling method used for granulated sludge to obtain the MUG and DIPMUG values	141
Figure A5.1: Main Program Layout of the DIP Program	170
Figure A5.2: Block Flow Diagram of Image Processing Section of the DIP Program	170

## *List of Tables*

<b><u>Table</u></b>	<b><u>Page</u></b>
Table 2.1: Summarised Discussion of Early Digestion Processes	12
Table 2.2: COD Removal Rates of Some Anaerobic Digestion Processes	16
Table 2.3: Mineral compositions of UASB granules (Uemura and Hadara, 1994)	19
Table 2.4: Some of the more common species found in granulated anaerobic sludge	23
Table 2.5: Average composition of PCE (Trnovec and Britz , 1997)	26
Table 4.1: Summarised Results of the Sludge Screening Tests	58
Table 4.2: Experiment 6 Results	66
Table 4.3: Experiment 7 Results	67
Table 4.4: Experiment 8 Results	68
Table 4.5: Experiment 9 Results	69
Table 4.6: Experiment 10 Results	69
Table 4.7: Experiment 11 Results	74
Table 4.8: Experiment 12 Results	74
Table 5.1: Dimensional Analysis [g/200ml] to [kg/m <sup>3</sup> ]	80
Table 6.1: Calculated Reactor Dimensions, for a 1, 2 and 4 litre scale-down of R <sub>5,5</sub>	96
Table 6.2: Comparison of Tipspeeds at a Given Roller Speed	96
Table 7.1: Experiment 13 Results	113
Table A2.1: Dimensional Analysis [g/200ml] to [kg/m <sup>3</sup> ]	140
Table A3.1: Experimental Run 1, R <sub>4,15</sub>	142
Table A3.2: Experimental Run 1, R <sub>7,2</sub>	142
Table A3.3: Experimental Run 2, R <sub>4,15</sub>	143
Table A3.4: Experimental Run 2, R <sub>7,2</sub>	143
Table A3.5: Experimental Run 3, R <sub>4,15</sub>	144
Table A3.6: Experimental Run 3, R <sub>7,2</sub>	144
Table A3.7: Experimental Run 4, R <sub>4,15</sub>	145

<b><u>Table</u></b>	<b><u>Page</u></b>
Table A3.8: Experimental Run 4, R <sub>7.2</sub>	145
Table A4.1: Experimental Run 6, R <sub>4.15</sub>	146
Table A4.2: Experimental Run 7, R <sub>4.15</sub>	148
Table A4.3: Experimental Run 9, R <sub>4.15</sub>	150
Table A4.4: Experimental Run 6, R <sub>7.2</sub>	152
Table A4.5: Experimental Run 7, R <sub>7.2</sub>	154
Table A4.6: Experimental Run 8, R <sub>7.2</sub>	156
Table A4.7: Experimental Run 9, R <sub>7.2</sub>	158
Table A4.8: Experimental Run 6, R <sub>5.5</sub>	160
Table A4.9: Experimental Run 7, R <sub>5.5</sub>	162
Table A4.10: Experimental Run 9, R <sub>5.5</sub>	164
Table A4.11: Experimental Run 10, R <sub>5.5</sub>	166
Table A4.12: Experimental Run 11, R <sub>5.5</sub>	168
Table A5.1: 200 ml Sample MUG and DIPMUG	174
Table A5.2: 2 x 100 ml Sample MUG and DIPMUG	175
Table A5.3: 4 x 50 ml Sample MUG and DIPMUG	176
Table A6.1: Chapter 6, Experimental Results	177
Table A7.1: Experimental Run 13 Results	178

# *List of Abbreviations*

<b>[Abbreviation]</b>	<b>[Explanation]</b>	<b>[Dimension]</b>
Al	Aluminium	
AVG	Average	
BOD	Biological Oxygen Demand	[mg/l]
C	Carbon	
Ca	Calcium	
CaCO <sub>3</sub>	Calcium Carbonate	
Ca(OH) <sub>2</sub>	Calcium Dihydroxide	
Ca-P	Calcium Bound Phosphorous	
CH <sub>4</sub>	Methane	
CLevel	Greyscale Cut-off Value	
COD	Chemical Oxygen Demand	[mg/l]
CO <sub>2</sub>	Carbon Dioxide	
Cu	Copper	
D/d	Day	

[Abbreviation]	[Explanation]	[Dimension]
D <sub>50</sub>	Average Diameter	[mm]
DIPMUG	Image Processor MUG Prediction	[kg/Vr]
DNA	Deoxyribonucleic Acid	
ECP	Extra-Cellular Polymers	
EGSB	Expanded Granular Sludge Bed Reactor	
Fe	Iron	
HRT	Hydraulic Retention Time	[hours]
H <sub>2</sub> O	Dihydrogen Oxide	
ID	Internal Diameter	[m]
ISA	Internal Surface Area	[m <sup>2</sup> ]
K	Potassium	
KHCO <sub>3</sub>	Potassium Hydrogen Carbonate	
KH <sub>2</sub> PO <sub>4</sub>	Potassium Dihydrogen Phosphate	
L <sub>s</sub>	Sludge Level	[m]
Mg	Magnesium	
MI	Mass Increase	[g]
MUG	Mass of granules larger than 0.5 mm per m <sup>3</sup> Reactor Volume	[kg/Vr]
N	Nitrogen	
Na	Sodium	
NaOH	Sodium Hydroxide	
Nu	Number of Identified Granules	
O <sub>2</sub>	Oxygen	
P	Phosphorous	
PCE	Peach Cannery Effluent	
PFD	Process Flow Diagram	
pH	Potential of Hydrogen	[pH-units]
R	Experimental Run	
R <sup>2</sup>	Coefficient of Determination	
R <sub>1</sub>	1 Litre Reactor	
R <sub>2</sub>	2 Litre Reactor	
R <sub>4</sub>	4 Litre Reactor	
R <sub>4.15</sub>	4.15 Litre Reactor	
R <sub>5.5</sub>	5.5 Litre Reactor	

[Abbreviation]	[Explanation]	[Dimension]
R <sub>7.2</sub>	7.2 Litre reactor	
RNA	Ribonucleic Acid	
RPM	Revolutions per Minute	
Si	Silicon	
SO <sub>4</sub>	Sulphate	
SRT	Solids Retention Time	[days]
t <sub>s</sub>	Settling Time	[s]
TSS	Total Suspended Solids	[g]
UASB	Up-flow Anaerobic Sludge Blanket (Reactor)	
V <sub>Biogas</sub>	Biogas Volume	[ml]
VFA	Volatile Fatty Acid	
V <sub>in</sub>	Feed Volume in	[litre]
V <sub>out</sub>	Feed Volume out	[litre]
V <sub>r</sub>	Cubic Meter of Reactor Volume	[m <sup>3</sup> ]
V <sub>Tip</sub>	Baffle Tipspeed	[m/s]
w/w	Weight/Weight	
α	TSS to MUG Conversion Factor	



**THIS THESIS IS DEDICATED TO MY MOTHER: RINA  
VAN ZYL**



# 1. Introduction

---

The turn of the previous century saw many firsts for mankind. One of the most beneficial 'firsts' was the environmental awareness that appeared on a global scale. Issues like global warming due to CO<sub>2</sub> emissions, deforestation and the depletion of the ozone layer were, and still are, prime topics of discussion on news networks around the world. This environmental pressure from the media and masses forced governments around the world to create and comply with new standards for industrial emissions, like the ISO 9001, ISO 14001, HSAS 18001 and the new ISO 17000. Non-conformation to these standards normally leads to severe governmental penalties and lengthy court cases that can be ill afforded in today's competitive economical climate. The food industry is no exception. It is one of the prime water consumers in South Africa. Growing concern over the quality and quantity of fresh water has forced this industry to reduce pollution loading on treatment facilities and environmental pollution.

Considerable interest has been shown in the application of anaerobic digestion to wastewaters from the food industry. The nature of these effluents is such that it often provides ideal conditions for anaerobic digestion. These effluents usually have a high organic content, have little or no toxic minerals present and are often produced only over a short period of time (Britz et al., 1999), like for instance during the midsummer in the canning industry. Anaerobic processes are amenable to such conditions and in particular where seasonal shutdown may take place. Unlike most effluent treatment processes, where large quantities of land, effluent pre-treatment and a large operating costs hamper the applicability of the system, the Up-flow Anaerobic Sludge Blanket Reactor (UASB) provides a state-of-the-art solution to effluent treatment by anaerobic digestion (Lettinga et al., 1997).

The UASB reactor is a modification on the fluidised bed reactor (Fogler, 1999), with the solid phase catalyst replaced with granulated anaerobic sludge, and the liquid phase the waste water or factory effluent. At the top of the UASB a gas cap is installed to serve as a biogas collector (see Figure 1.1). This biogas (mostly carbon dioxide and methane) is produced by the stepwise decomposition of complex carbohydrates and proteins via a consortium of micro-organisms living in a symbiotic environment inside the granules. A



typical UASB reactor has an organic removal rate of 89-93% Chemical Oxygen Demand (COD) and operates optimally at loadings of 9.8-11 kg COD/ m<sup>3</sup> reactor volume / day. COD's of up to 40 000 mg/litre can be processed and it has a hydraulic retention time (HRT) of approximately 10 hours. The solids retention time (SRT) can be up to 18 months (Lettinga et al., 1980; Trmovec and Britz, 1998; Metcalf and Eddy, 2003). Other advantages of this process include low operating costs, high organic loading rate, a net energy benefit from the produced methane and a 40% lower production of sludge, if compared to other waste water digestion processes. The UASB process only functions properly with granulated anaerobic sludge with a particle diameter of between 0.1 and 5 mm which allows for settling velocities up to 60 m/hour. The high settling velocity enables the sludge bed to be fluidised and the high loading rates needed for optimal operation can thus, be attained (Metcalf and Eddy, 2003).

However, one major problem hinders the efficiency of the unit to such an extent that it renders the unit only economically viable in exceptional cases only. If the unit is seeded with readily available un-granulated anaerobic sludge, it can take up to 12 months to form a fully operational granular sludge bed that can handle the loading rates required for optimal operation. In other words, if a UASB is seeded with normal anaerobic digester sludge, a reactor start-up of up to 1 year can be experienced, depending on the ambient temperature and effluent conditions (Agrawal et al., 1997). Many theories exist on how anaerobic bio-granulation occurs and the most relevant of these (from an engineering point of view) will be discussed in the Literature Survey (Chapter 2).

From the lengthy start-up and the long SRT it is clear that there is a large demand for granulated anaerobic sludge, to dramatically shorten the start-up period of the UASB (by inoculating the reactor with artificially cultivated sludge granules). Thus making the unit a more economically viable effluent treatment system. Another reason for the large demand for granulated sludge, is to replace whole sludge beds in the case of accidental poisoning of the reactor volume, which is known to happen, either through acidification of the reactor volume, or foreign chemicals in the effluent. It was with this in mind that the first research work on the artificial enhancement of bio-granulation was done at the Department of Food Sciences in the University of Stellenbosch. This research was done on the batch cultivation of anaerobic bio-granules in lab-scale reactors (Britz et al., 1999; Britz and Van Schalkwyk 2002).

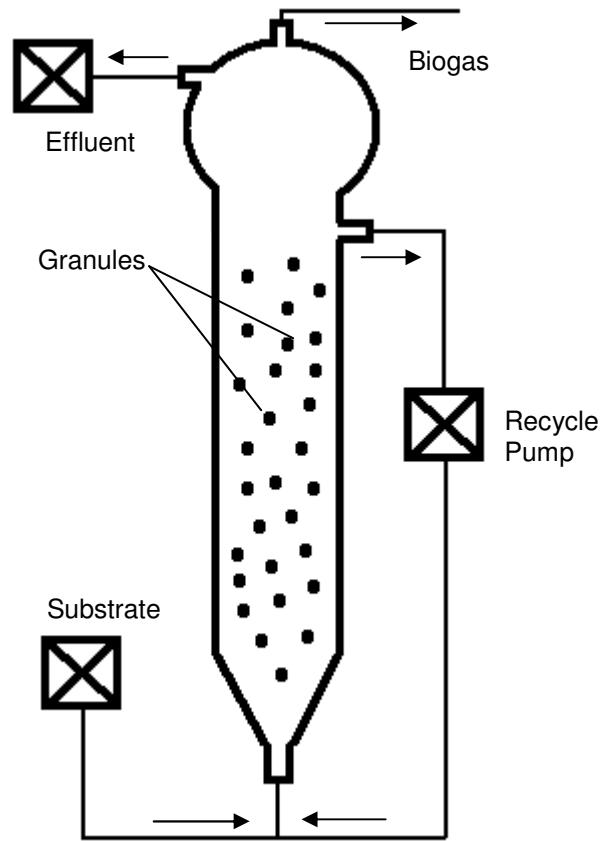


**Figure 1.1: Schematic Representation of the UASB Reactor**

In the abovementioned study, batch cultures with the different carbon sources were inoculated with either anaerobic sludge or granules and grown inside 450 ml vessel volumes in shaker water baths and roller tables over a period of 14 to 20 days. The temperature of the water baths were maintained at 35 °C and the shake-speed was set at 150 rpm or 20 rpm on the roller tables, to induce mixing of the sludge and feed. Bottles containing  $7/9^{\text{th}}$ s (per vessel volume) of sterile growth medium were each inoculated with either  $2/9^{\text{th}}$ s of sludge from an anaerobic tank from the Kraaifontein Sewerage Works, or with granular sludge from SA Breweries. Each day the shaker baths were stopped to allow the sludge to settle,  $2/9^{\text{th}}$ s of the batch unit's volume of used feed was removed and replaced with sterile substrate to simulate bio-granulation. The amount of granules was determined by physically counting the amount of granules formed over a specific period of time by using a round glass container with a graded grid underneath. The aim of this initial study was to determine whether granulated anaerobic sludge could be produced in an artificial environment, simulating the conditions as is experienced by the anaerobic micro-organisms in the up-flow hydraulic

environment that occurs inside the UASB reactor (Britz et al., 1999). From the results obtained from this research, even if it was only done in a qualitative visual manner, it was concluded that anaerobic bio-granules can be cultured in laboratory scale batch reactors if the proper environmental parameters are in place. However, the reactors and methods used in this research did not facilitate scale-up.

Nonetheless, the success of this initial lab-scale work was the motivation for a larger project sponsored by the Water Research Commission (WRC), revolving around the batch cultivation of UASB granules. The final aim of the WRC project was to design a reactor of sufficient volume and to produce enough bio-granules to replace an entire volume of an industrial size UASB sludge bed, within twenty days.

The larger WRC project can be broken down into 5 phases (Appendix A8), Phase 1 being the initial work done in the Department of Food Sciences as was discussed above (WRC Project 667/1/99 hereon forth called 'Britz et al., 1999'). The second phase, Phase 2 (hereon forth called 'Els and Van Zyl, 2002'), of the project was the commissioning of two bench-scale bioreactors with volumes one order of magnitude larger than the vessel volumes used in Phase 1. These reactors were designed to simulate the motion that was induced by the shaker baths on the 450 ml vessel volumes. These bioreactors had the added advantage of facilitating scale-up and the study thereof. The Phase 2 results showed that not only could granulation be enhanced (as was the case in Phase 1), but granules could also be cultivated from dispersed anaerobic digester sludge. However, it was obvious from these experiments that the system was far from optimised and a far higher yield could be obtained. Methods of analysing the granule growth over the 20 day incubation period used at this stage were also found to be far from adequate for a bench-scale study (Els and Van Zyl, 2002).

Phase 3, the research presented in this thesis, is preoccupied with the optimisation of bench-scale reactors specifically designed for the artificial cultivation of UASB granules and with factors that will influence scale-up to Phases 4 and 5 (further up-scaling phases) of the WRC project. The following section is a discussion of the layout of Phase 3, a mind map of this layout is given by Figure 1.2.

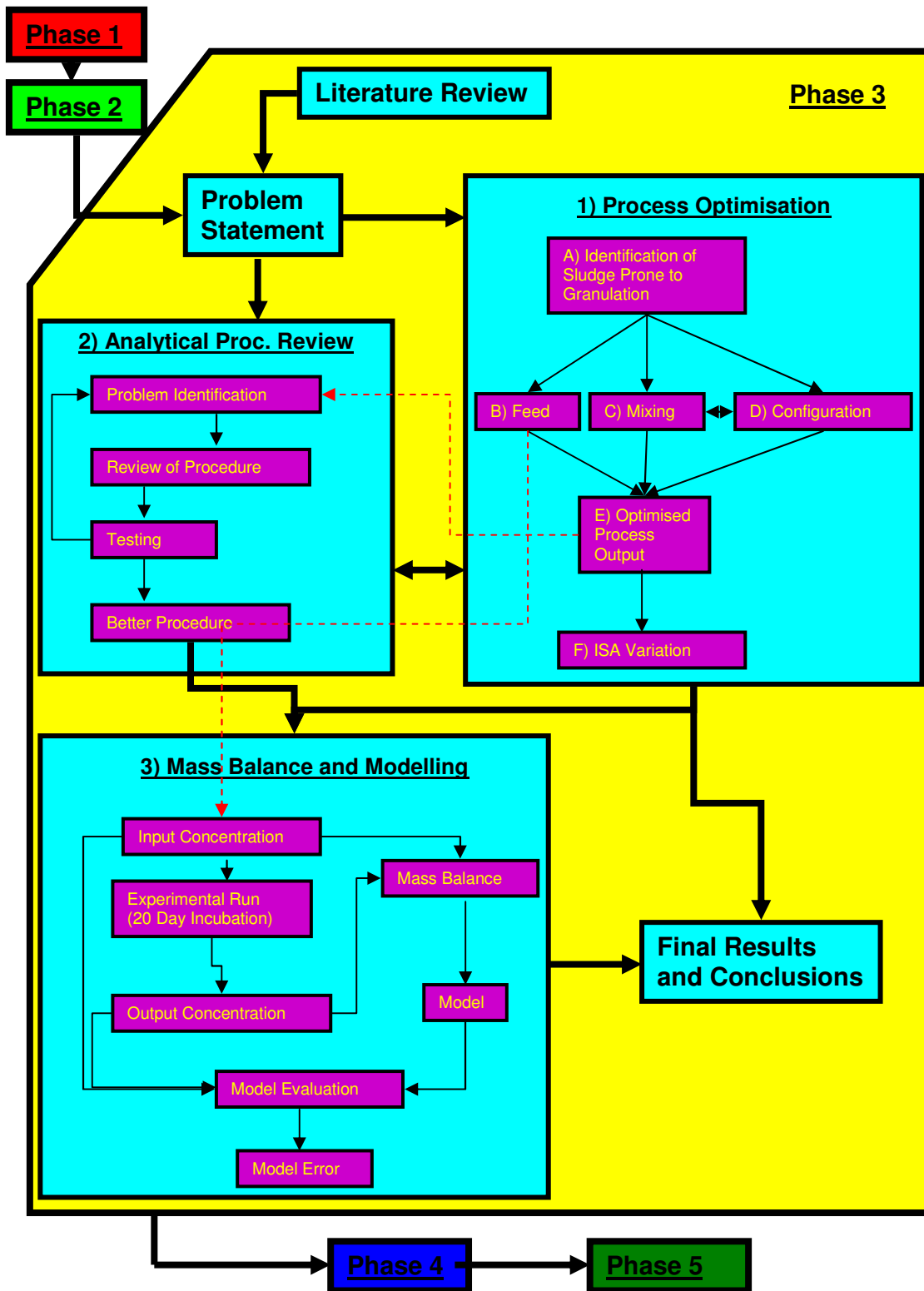


Figure 1.2: Mind Map of WRC Project Layout

From a literature review (Chapter 2) and previous work performed in Phase 1 and 2 of the project (Chapter 3), a problem statement will be defined for the third phase. From the problem statement, it will be clear that Phase 3 entails the use of a bench-scale reactor system for optimisation-, evaluation- and information gathering exercise, which will allow for the conservative scale-up to reactor volumes one order of magnitude larger

(Phase 4) than the bioreactors used in this research. Phase 3 can be broken down into three stages, namely (1) the process optimisation, (2) analytical procedure revision and the (3) mass balance and modelling stage. The aim of the process optimisation section (numbered '1' on Figure 1.2) was to obtain the largest possible yield of granules larger than 0.5 mm in diameter (MUG, Appendix A2.5) over the 20-day incubation period.

The process optimisation started with the identification of anaerobic sludge prone to granulation (beginning of Chapter 4), since it was proven from results obtained in Phases 1 and 2 of the bigger WRC project, that this procedure was of paramount importance to the overall success of any study done on the granulation of anaerobic sludge (Britz and Van Schalkwyk, 2002; Els and Van Zyl, 2002). The next three steps in the process optimisation phase were performed in parallel; feed -, mixing speed – and reactor optimisation (remainder of Chapter 4). Many data points were necessary for the bioreactor feed optimisation therefore; this part of the project was done in bottles on a shaker table, since 15 vessels could be incubated at a time. Another reason for referring back to the Phase 1 incubation method was to save resources and time.

The reactor configuration and mixing speed optimisation (C and D under '1' in Figure 1.2) were done simultaneously. The two previously used bench-scale units and a third reactor, simulating the motion experienced on the roller tables, were seeded with the same sludge and feed and set to the same mixing speed: After the 20 day incubation the procedure was repeated at a different mixing speed. From this, both the reactor configuration giving the best results and the mixing speed giving the highest yield of sludge granules were obtained. The results from these three studies (done in parallel) were then combined in the next step (E), to obtain the optimised process output (late Chapter 4). The procedure was to use an optimised feed in the reactor that gave the best overall yield in the mixing speed optimisation section. The results obtained were also verified to ensure reproducibility. During this section, another parameter that might have an effect on the granulation yield was identified, namely the internal surface area (ISA) of the reactor.

The second section of the Phase 3 study (numbered '2' on Figure 1.2) was the analytical procedure review (Chapter 5). This section was done in parallel with the optimisation study. The analytical procedure review entailed the evaluation of methods used in Phase 1 and 2 to analyse the yields of granules obtained in and during the 20 day incubation, period and if considered necessary, to alter or replace these methods to

produce a more accurate (and/or less time consuming) means of analysis. The results obtained from this section were incorporated in the ISA section of the optimisation study. Three scale-down versions of the reactor that proved best in the optimised process output section, was constructed with varying ISA at a constant shear rate inside the reactors (Chapter 6).

The third section of Phase 3 (numbered '3' on Figure 1.2) was the mass balance and modelling section (Chapter 7). This entailed the observation of rate limiting parameters (mostly identified in the feed optimisation section) and the manner in which they are absorbed (or produced) by the system. The input and output concentrations of the COD, inorganic species in the feed and also the biogas produced were measured at regular intervals in the incubation period. From basic mass balance theory (Fogler, 1999) a model was constructed to predict the accumulation of biomass in the reactor over the 20 day incubation period. This was then compared to the actual yield that was observed and the model was evaluated.

The results obtained from sections 1, 2 and 3 of Phase 3, were then combined to form the final conclusions and recommendations of the project (Chapter 8). Chapter 9 of this thesis is the references followed by the appendices. Phase 4 and 5 on Figure 1.2 and Section 8 in the Appendix, Section A8, are the expected flow of the bigger WRC project on the batch cultivation of UASB granules to shorten the USAB start-up.

# 2. Literature Review

---

## 2.1 Introduction

This literature review starts by defining the concept that is anaerobic digestion by aid of a definition and comparison to the aerobic digestion process. This will be followed by the evolution of the anaerobic digestion, how it gradually became more amenable to various types of effluent and the reactor systems used in the process, from the beginning (early 1800's) to current state-of –the-art high rate anaerobic reactors like the USAB and EGSB systems. After a short discussion of the UASB, the review will move to the theory behind the granulation process. This process occurs spontaneously if dispersed anaerobic sludge is placed in a constant up-flow hydraulic regime (like in a UASB reactor). The next section will discuss general issues around bioreactor scale-up (since this is the main aim of this project) and also give a short discussion on digital image processing, since this will be used later in an attempt to develop a more accurate means of quantifying granule growth. The chapter ends with a summary. This literature review attempts to highlight the engineering aspects of bio-granulation, and bioreactors and only to limited degree biochemistry.

### 2.1.1 The Definition of Anaerobic Digestion

Anaerobic wastewater treatment is the biological treatment of wastewater in the absence of air or elemental oxygen. The organic pollutants are converted by anaerobic micro-organisms to a gas containing methane and carbon dioxide, known as "biogas". Biogas, produced as an end product, consists of 50 – 70% methane, 25 - 45% carbon dioxide and trace amounts of hydrogen, nitrogen and sulphur (Britz et al., 1999). This conversion process form complex carbohydrates to biogas in the absence of oxygen is known as anaerobic digestion (Bushwell and Hatfield, 1936).

If the same microbial consortium (or sludge) is placed in an environment where oxygen is present, aerobic and facultative aerobic species become more prominent and the digestion process is known as aerobic digestion. In order to point out the advantages of

anaerobic- over aerobic digestion, Figure 2.1 displays the principle differences between the two processes. In aerobic treatment, a large fraction of the organic material in wastewater is converted to sludge, which in turn leads to costly solid waste disposal problems. Other problems include high operating costs due to the continuous need for aeration with oxygen of the system and unpleasant odours, mostly due to Volatile Fatty Acids that has not been completely broken down (Metcalf and Eddy, 2003).

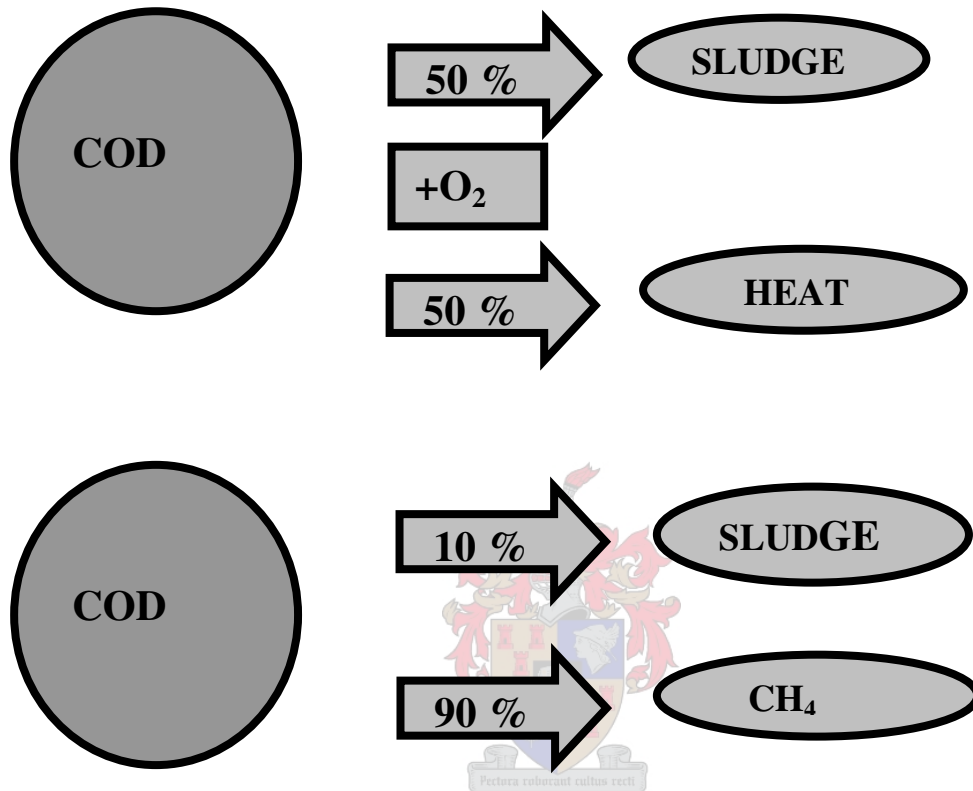


**Figure 2.1: Aerobic Digestion and Anaerobic Digestion**

In anaerobic treatment, the organic material in wastewater is mostly converted into methane, which is a valuable fuel source. Due to the very primitive metabolic processes the conversion of organic polymers to carbon dioxide and/or methane in the absence of oxygen is relatively slow. In the methanogenic species, the resultant effect is that growth rates of these species are very slow and the polymers cannot be completely converted to O<sub>2</sub> and H<sub>2</sub>O (Metcalf and Eddy, 2003). This leads to a much slower accumulation of sludge in the digester than was the case with aerobic digestion. Unlike in aerobic digestion processes, no major process inputs such as O<sub>2</sub> (resulting in high operating costs) is required for the system to run.



## 2.1.2 The History of Anaerobic Digestion

The taming of the anaerobic digestion process began in the late 19<sup>th</sup> and early 20<sup>th</sup> century due to the sanitation concerns of individuals and municipalities. By the 1900's, anaerobic digestion was used in many parts of the world, mostly in the form of anaerobic ponds for the treatment of sewerage. The development of microbiology as a science led to research to identify anaerobic bacteria and the conditions that promoted methane production (Buswell and Hatfield 1936). The benefits of heating, due to the volatility of biogas and mixing waste in closed tanks to enhance and control anaerobic digestion, were introduced in the 1920's. At this stage waste stabilisation as the primary goal. This led to a basic municipal sludge digester design that spread throughout the world, a concept that has not changed much to this day. Only occasional use was made of methane beyond digester heating, because coal- and petroleum-based energy was readily available. China was the first to use wasted biogas for heat, light and cooking (RAP Bulletin 1995).

The early years (in terms of waste treatment) ended with the industrial expansion of the 1960's, when discharge of organic wastes and water pollution became environmentally unacceptable. In the industrialised parts of the world, government programmes and goals pushed the rapid development of aerobic wastewater treatment plants, with cheap electricity driving the development of aerobic processes. Anaerobic digestion was only included in wastewater treatment plants for sludge digestion. In the majority of cases, high-strength wastes were mostly applied or landfills (IEA Bioengineering 1996).

The energy crisis of 1979 triggered an appreciation for successful systems and recognition of the net positive energy benefits associated with anaerobic digestion. The designs and equipment that did not prove economically viable previously, was now being recognized, and new and improved anaerobic digestion technologies were being developed (Koberle, 1995). Currently, energy production and recovery are regarded as equally important, but the focus still remains on anaerobic digestion as an inexpensive technology to stabilise organic waste, reduce COD and suspended solids, with minimal sludge production, and odour reduction. Current goals of some anaerobic digestion systems include odour reduction and nutrient recovery (Wilkie et al., 1995). The types of waste treated with anaerobic digestion have expanded widely; some anaerobic digestion systems have become more complex as industrial applications become more prevalent.

The use of the anaerobic digestion process for treating industrial wastewaters has grown tremendously during the past decade. Industrialists realized that pollution reduction from high-strength organics in industrial wastewater was very costly if done aerobically. Operational costs 10 to 20 times higher than experienced with anaerobic digestion are not uncommon (Metcalf and Eddy, 2003).

### 2.1.3 Anaerobic Waste Treatment Methods

Throughout the years, the maintenance of a high solids retention time (SRT) has probably been one of the major problems in the practical application of the anaerobic digestion process, especially for effluents with a chemical oxygen demand (a measure of the amount of organic material in the water, see Section A2.1 in the Appendix) below 3000 mg/litre. Since the need for processing large volumes of these relatively low chemical oxygen demand (COD) wastes exists, the anaerobic digestion process had to be evaluated again. The only way of economically processing medium COD wastes is, to force large volumes of effluent can be forced through a treatment system in a short period of time. Historically, the SRT of the anaerobic digester was heavily dependant (or even equal to) the hydraulic retention time (HRT) of the wastewater to be treated inside the reactor. For anaerobic digestion to be amenable to the abundance of medium strength (COD =  $\pm 3\ 000$  mg/litre) industrial wastes, a large demand for a process where the biomass retention time is independent of waste water flow rate occurred.

With the mentioned process constraints in mind, the following evolution of high rate anaerobic treatment processes occurred:

- the first attempt was the anaerobic contact process, which in essence is nothing more than a modified anaerobic digester. Washout from the reactor was controlled by a sludge separation and recycle system. This aspect is also the downfall of the system since the separator hampers the practicality of the process due to the land space needed (Lettinga et al., 1980),
- a somewhat modified version of the above-mentioned process is the 'Clarigester' which is based on the upward movement of liquid through a dense blanket of anaerobic sludge. The primary limitation of the Clarigester was the loss of sludge in the 'clarified' effluent. Therefore the loss of sludge was considered the primary limitation of the process (Lettinga et al., 1980),

- The basic anaerobic digester design was modified further by adding an inert support material to a vertical filter bed. In time, the anaerobic micro-organisms would immobilise and attach itself to this support material and enlarge the SRT of the system dramatically. Despite the good results obtained with the anaerobic filter process, further development of this process has nearly been completely abandoned in favour of the Up-flow Anaerobic Sludge Blanket Reactor (UASB) (Lettinga et al., 1980).

Table 2.1 gives a summarised comparison of early digestion processes.

**Table 2.1: Summarised Discussion of Early Digestion Processes**

Reactor Type	Description	Advantages	Disadvantages
<b>Anaerobic Pond</b>	Earthen basin filled with anaerobic sludge	First process capable of partial stabilisation of domestic waste. Low capital and operating costs.	Poor performance due to dead zones and short circuiting. Control problems due to acidification. High energy methane was wasted. Very sensitive to hydraulic shocks. HRT = SRT
<b>Anaerobic Digester</b>	Closed concrete vessel filled with anaerobic sludge (with mechanical mixing)	Far higher % COD stabilisation than with Anaerobic Ponds. Methane could be harvested for digester heating, resulting in increased effectively.	Only for COD levels higher than 3000 mg/litre. Sensitive to hydraulic shock. Large footprint. HRT = SRT
<b>Anaerobic Contact Process</b>	Anaerobic Digester with sludge separation and recycle.	HRT < SRT. HRT far lower than in normal digester	Very large footprint.
<b>Clarigester</b>	Upward movement of liquid through dispersed sludge blanket	HRT < SRT. No mechanical mixing	Very sensitive to hydraulic shocks. Large biomass losses through 'clarified' effluent. Only applicable to a small range of effluents
<b>Anaerobic Filter</b>	Inert support matrix for immobilised bio film.	HRT << SRT. No mechanical mixing	Large footprint. High recycle rates. Influent dispersion problems. Very Long Start-up.

## **2.2 The Up-flow Anaerobic Sludge Blanket Reactor (UASB)**

The processes discussed in Section 2.2 had many problems (Table 2.1), to overcome these the entire anaerobic digestion process had to be redesigned to meet the requirements set by industry. The result was a unit with a relatively small footprint, large throughput rate and short HRT that were capable of producing superior effluent quality. These systems were based on (debatably) one of the most advantageous attribute of anaerobic sludge: the spontaneous granulation under a certain set of parameters (including an up-flow hydraulic regime). The most commonly used reactors that takes advantage of this, is the UASB. Various aspects like the design, performance, applications and shortcomings of the UASB reactor will be discussed in this section.

### **2.2.1 General Discussion and Characteristics**

The UASB process was developed in 1972 by G. Lettinga in the Netherlands, in a strive towards a more efficient and stable anaerobic waste treatment system. From 1974 to 1977, three pilot plants were constructed. In 1978, the first full scale UASB with working volume of 800 m<sup>3</sup> was constructed. Because of its high biomass concentration and rich microbial diversity, the UASB reactor is considered desirable in medium to high-strength organic waste water treatment. High biomass concentration implies that contaminant transformation is rapid and large volumes of organic waste can be treated in compact reactors. (Liu et al., 2003; Batstone et al., 2003). The UASB exhibits positive features such as high organic loadings, low energy demand, short hydraulic retention time, ease of construction and a small footprint (Show et al., 2004).

As can be seen from Figure 2.2, the UASB reactor is nothing more than a fluidised bed reactor- therefore an relatively simple and inexpensive design (Fogler, 1999),. Influent is distributed into the bed at appropriately spaced inlets. The influent passes upwards through an anaerobic sludge bed where the micro-organisms in the granules come into contact with substrates. The “solid state catalyst” is composed of micro-organisms that naturally form granules (pellets) of 0.5 to 2 mm diameter. Granules have a high sedimentation velocity and thus resist wash-out from the system even at high hydraulic loads. Upward flow velocities of up to 60 m/s is not uncommon (Metcalf and Eddy, 2003).

The resulting anaerobic degradation process is responsible for the production of biogas containing  $\text{CH}_4$  and  $\text{CO}_2$ . The upward motion of released gas bubbles causes hydraulic turbulence that leads to reactor mixing without any mechanical parts (Singh and Viraraghavan, 2002). At the top of the reactor, the water phase is separated from sludge solids and the gas in a gas-liquid-solids separator. The three-phase-separator is a gas cap with a settler situated above it. Below the opening of the gas cap, baffles are used to deflect gas to the gas-cap opening (Lettinga et al., 1980).

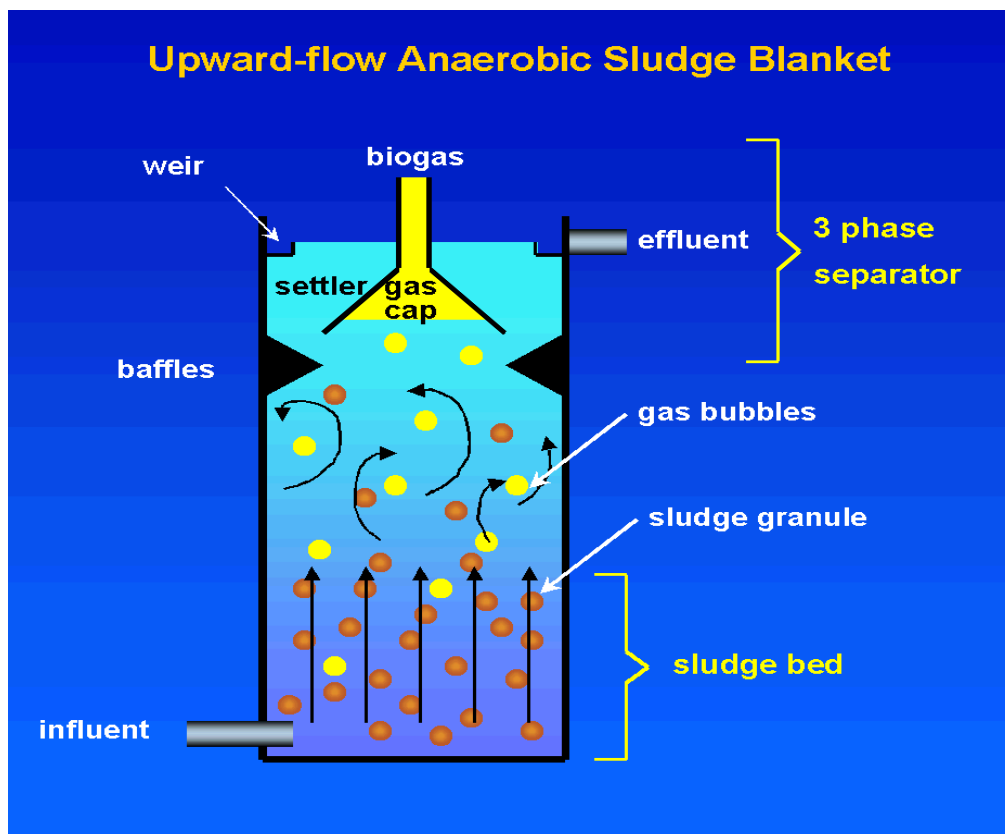


**Figure 2.2: A Schematic of the UASB Reactor**

The adaptation of anaerobic sludge from dispersed digester to granulated UASB sludge can be defined in roughly three stages (Zeew, 1980):

- 1 The initial stage involves the adaptation to the new environment and substrate. In order to prevent inhibition of the breakdown of VFA's the loading rate should not exceed the maximum potential of the seed sludge. This stage is the first few days after start-up.
- 1 During the second phase of adaptation, activity of the sludge increases due to microbial growth and a higher sludge retention time. If operated correctly,

doubling times of 8 to 9 days can be observed in the specific activity (or methane production) in the first few weeks.

- 1 The third stage is the pelletization of the sludge. The first pin size 'granules' can be observed 6 to 8 weeks after start-up. The onset of polarization appears to be mainly dependant on the proper supply of nutrients, as well as the sludge loading rate.

The spontaneous adaptation and pelletization of dispersed anaerobic sludge in the UASB (or EGSB) forms one of the cornerstones of the research done in this project and will be discussed in more detail in Sections 2.3 to 2.7.

## 2.2.2 Applications

Due to growing concern for the preservation of the environment, industries are increasingly required to reduce their impact on the environment. Because of this, adequate treatment of food processing effluents is assuming growing importance, as industries addressed the issue of responsible environmental management (Trnovec and Britz., 1997). In a recent survey (Frankin, 2001), 1215 full-scale high rate anaerobic reactors have been carefully documented. Since the 1970's these have been built throughout the world for the treatment of various types of effluents. An overwhelming majority of the existing full-scale plants (72% of all plants) are based on the UASB or EGSB (slightly modified UASB) design concept developed by Lettinga in The Netherlands. This statistic emphasizes the fact that anaerobic granular sludge bed design concept has been the most successful for up-scaling and implementation. The four top applications of high rate anaerobic reactor systems are for (Strydom and Britz, 1997):

- breweries and beverage industry ,
- distilleries and fermentation industry,
- food industry and
- pulp and paper.

Together, these industrial sectors account for 87% of the applications. However, the applications of the technology are rapidly expanding, including treatment of chemical and petrochemical industry effluents, textile industry wastewater, landfill lactates as well as applications directed at conversions in the sulphur cycle and removal of metals.

Furthermore, the UASB concept is also suitable for treatment of domestic wastewater in warm climates (RAP Bulletin, 1995).

### 2.2.3 Performance

One of the main benefits of the UASB concept is that it selects micro-organisms in the sludge with the best settling properties. In fact, the primary function is to wash out poorly settling organic matter and to retain the granule precursors in the reactor, enabling them to grow into full size granules. A prerequisite for the pelletization of sludge is therefore the maintenance of maximal bacterial growth (Hulshoff Poll et al., 1982). Favourable environmental conditions are necessary for anaerobic digestion. Factors like temperature, pH, VFA concentration, alkalinity, grease fibre and toxic substances all play a role in digester efficiency. Most digesters operate in the temperature range of 20 – 40 degrees Celsius (Mesophilic) (Britz et al., 1999).

The average full-scale design loading of the UASB of 682 full-scale plants surveyed was 10 kg COD/m<sup>3</sup>.day, while average full-scale design loading of the EGSB (slightly modified UASB) of 198 full-scale plants surveyed was 20 kg COD/m<sup>3</sup>.day COD removal efficiencies depend largely on wastewater type. However, the removal efficiency (with respect to the biodegradable COD) is generally in excess of 85 or even 90%. Peak loadings of up to 40 kg/m<sup>3</sup>/day can be obtained under optimum conditions (Britz et al., 1999). Table 2.2 compares the COD removal rate of earlier digestion processes to that of the current UASB and EGSB technologies.

**Table 2.2: COD Removal Rates of Some Anaerobic Digestion Processes**

Reactor Type	COD Removal Rate [kg/Vr.d]
Anaerobic Pond	1.8 - 2.1
Digester	5
Contact Process	5-7
UASB	10-18
EGSB	20-40



Table 2.2 clearly shows that the spontaneous immobilization of anaerobic sludge (UASB and EGSB) has a dramatic effect on the COD removal rate per cubic metre of reactor volume ( $V_r$ ). Currently, this is one of the primary motivators for the shift towards granular sludge bed technologies in anaerobic digestion processes and applications.

### **2.2.4 Shortcomings**

One major drawback of the UASB reactor is its extremely long start-up period. The unit generally requires between 2 and 8 months (start-ups of as long as 12 months has been documented) to develop granular anaerobic sludge, if the unit is initially seeded with non-granular anaerobic sludge (Liu et al., 2003). This restricts the application in areas where granules from operating UASB's are not readily available, since the operating efficiency and performance of these systems are mainly dictated by the extent of granulation that has occurred inside the reactor. The full potential of the UASB system cannot be exploited until granule formation are better defined and optimised (Britz and Van Schalkwyk, 2002).

Other lesser factors, such as hydraulic short-circuiting of the flow pattern in the sludge bed, hampers the reactor performance significantly by creating areas without movement known as dead zones. The dead zone fraction increases with a decrease in operating temperature (Singh and Viraraghavan, 2002). Variation of the sludge concentration along the reactor height depends on the gas production rate, load per unit area, type of COD, operating temperature, up-flow velocity and the settling characteristics of the sludge. At a lower pH level, COD removal decreases dramatically, to an average COD removal rate of 66.1%. A pH of less than 5.5, it was also found that any further lowering of the pH would lead to complete system failure. This is another one of the UASB's major shortcomings, since neutralization costs have an influence on the economic aspects of the system (W Trnovec and Britz., 1997).

## **2.3 Granule Composition**

A formal definition of UASB granules will now be given, followed by a discussion of the various organic and inorganic species that occurs in side the sludge.



### **2.3.1 Definition of UASB Granules**

UASB bioreactor operation is dependant on the spontaneous formation of granular anaerobic sludge with high settling velocities and high methanogenic activity (Britz et al., 1999), as was discussed in Section 2.2.1. The definition of a sludge granule is a symbiotic community of anaerobic micro-organisms which forms during wastewater treatment in an environment with a constant up-flow hydraulic regime. None of the individual species in the granular ecosystem are capable of degrading complex organic wastes individually (Lui et al., 2003). Granules can therefore be described as a spherical bio-film consisting of a densely packed symbiotic microbial consortium, living in absence of any support matrix.

Due to the absence of a support matrix, the flow conditions create a selective environment in which only those micro-organisms, capable of attaching to each other will survive and proliferate. Eventually these microbial aggregates shape into compact bio-films without any support matrix referred to as "granules". As a result of their large particle size (generally ranging from 0.5 to 2 mm in diameter), the granules resist wash-out from the reactor. The resistance to washout is further promoted by good settling velocities, permitting high hydraulic loads. Compact bio-films (or granules) allow for high concentrations of active micro-organisms and thus high organic space loadings in UASB reactors. A single gram of granular sludge organic matter (dry weight) can catalyse the conversion of 0.5 to 1 gram of COD per day to methane, carbon dioxide and biomass. Or in other words this means granular sludge can process its own body weight of wastewater substrate on a daily basis (Guiot and Gorur, 1986).

A well-adapted granulated anaerobic sludge meets the following requirements (Hulshoff Poll et al., 1982):

- Volatile Fatty Acids (VFA's) are completely broken down,
- the specific gravity of the sludge is high,
- the settling properties of the sludge are good (>0.5 m/s).

### **2.3.2 Inorganic Species**

Of all the inorganic species occurring in granules, calcium and phosphates were found to be the most prominent (Britz et al., 1999). Calcium-bound phosphorus was also

present more prominently in the core than in the exterior of the granule. The interior core portion contained abundant crystalline precipitates of calcium carbonate. Other minerals such as Mg, Fe, S, Al, Si, K, Na and Cu were also present, but exhibited no prominent pattern. Furthermore, the core portion of the granules also had a much higher ash content than the exterior layer, indicating that most of the inorganic compounds precipitated in the core of the granules. This phenomenon may be attributed to an increase in granule depth that lead to a higher pH level, thus aiding in the precipitation process inside the granule (see Figure 2.4). Table 2.3 shows the mineral content of UASB granules, ash content of the core, exterior and the entire granules are 94.5%, 26.4% and 40,3% (w/w) respectively (Uemura and Harada, 1994).

**Table 2.3: Mineral compositions of UASB granules (Uemura and Hadara, 1994)**

Component	Composition (g minerals/ 100 g ash)		
	Core	Exterior layer	Entire granule
<b>Ca</b>	36	30	35
<b>P</b>	2.3	3.8	3.5
<b>Ca-P</b>	1.9	2.3	2.3
<b>S</b>	0.33	2.3	1.4
<b>Fe</b>	0.26	0.34	0.27

Phosphorous deficiency reduces the UASB efficiency by 50%. This reduction can be revised by phosphate dosage. Overdosage of phosphate, which in practice is related to high effluent phosphate concentrations, was found to be economically and environmentally unviable. An empirical inorganic formula for the population make-up in anaerobic sludge was found to be  $C_5H_7O_2P_{0.06}$  (Alphenaar et al., 1993).

### 2.3.3 Organic Species (Extracellular Polymers)

Even though there are countless organic compounds present in the anaerobic microbial environment this section will primarily focus on extracellular polymers (ECP). These are by far the most important and abundant species. Under the correct environmental conditions, some of the microbial species in anaerobic sludge excrete these high molecular weight polymers ( $M_r > 10\ 000$ ). Substrate and pH play the most prominent part in ECP production, but the amount of ECP secreted also depends on the

composition of the wastewater. An increase in the C: P ratio normally leads to an increase in ECP formation.

The main components of ECP are proteins and carbohydrates. The former includes asparagines, glutamine and aniline, the latter include mannose and ramosse. Other compounds, like deoxyribonucleic acid (DNA), ribonucleic acid (RNA) and lipopolysaccarides, are present in lesser concentrations. As was the case with anaerobic granules, calcium and phosphates forms the largest fraction of the inorganic elements found in ECP. Calcium is ascribed to be important in the linking of the polymers. The optimal pH-level for ECP production was found to be close to 6 and phosphates were identified as a production enhancer. The main ECP producers have found to be Acidogenic bacteria. ECP production started after 20 – 40 hours and reached a stationary phase after approximately 100 hours (Britz et al., 1999).

## **2.4 Granule Structure and Population**

Anaerobic granules have been defined and their organic and inorganic compositions have been discussed, the next step will be to discuss their macro- and microscopic characteristics. The digestion process in (and around) granules will also be reviewed.

### **2.4.1 Macroscopic Granule Structure**

If the macroscopic characteristics of anaerobic sludge granules are studied, the structure generally shows a sponge like outer 0.1 mm, while the inner core exhibiting a black colour that contains abundant crystalline precipitates (Uemura and Harada 1995). The pinpoint size fraction (<0.5 mm) represented 80% of the total granule population, and the larger size granules represented approximately 20% per 10 ml granular sludge sample respectively (Britz and Van Schalkwyk, 2002).

Figure 2.3 shows anaerobic sludge granules from a UASB reactor treating wastewater from a recycle paper mill. The red arrows point to gas vents in the granules; this is where biogas is released. Anaerobic sludge granules are dense pellets with either a brown or black exterior that range in sizes from 0.25 to 5 mm in diameter.

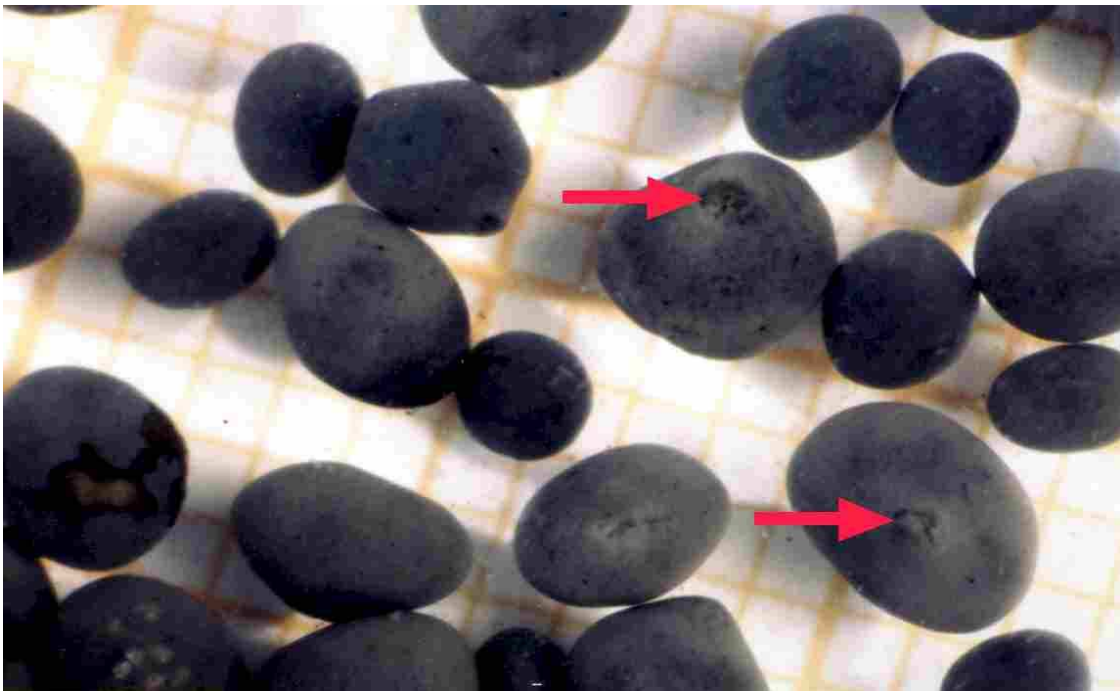


**Figure 2.3: Anaerobic Sludge Granules**

The size distribution in UASB reactors appears to be the result of the growth process from small particles to larger ones. Microbial growth is responsible for the layered structure in granules (see Section 2.4.2, Figure 2.4). Reactor turbulence does not cause granule breakage, nor does abrasion due to microbial activity result in significant reduction in granule size. Biomass washout is mainly from un-granulated sludge (Pereboom, 1994).

#### **2.4.2 Microscopic Granule Structure**

A granule's bacterial profile is heavily dependant on the substrate concentration, mass transfer and concentration of metabolites within the granules. Acidogenic species appears to be most prominent in the outer layer where the simple sugars are degraded. The volatile fatty acids (VFA's) produced as waste by these bacterial species diffuse inward due to concentration gradients, then becoming the primary food source for the syntrophic acetogens which populate the middle layer of the granule. In turn, the VFA's are broken down by the acetogenic species to form the key substrate used by the methanogenic bacteria in the granule core (see Figure 2.4). The surface of the granule consists mainly of gram negative bacteria in a matrix of gram positive microbes. The core, far more homogeneous, and consists mainly of gram negative microbes of the Methanothrix family (Britz et al., 1999).

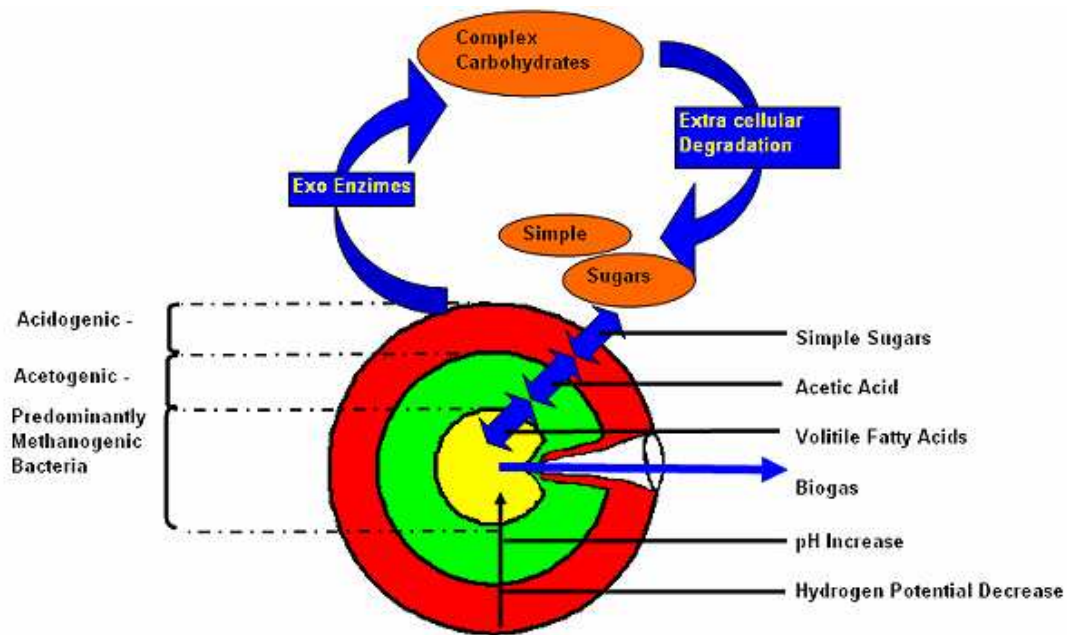


**Figure 2.4: Microbial layout and digestion process inside a UASB granule**

Figure 2.4 gives a visual summary of the staged digestion process in granulated anaerobic sludge. This process can be broken down into the following steps:

- Exo-enzymes are secreted by the outer layer micro-organisms,
- these enzymes degrade complex carbohydrates into simple sugars,
- which is absorbed and digested by the outer layer organisms,
- digestion products from these species diffuses deeper into the granules (due to a diffusion gradient induced by the digestion processes deeper in the granule),
- where it is consumed by the acidogenic species,
- the digestion products of these species then forms the primary food source of the microbes populating the core of the granule (Methanogens),
- the digestion products produced by these species (biogas) exits the granule via the biogas vent(s).

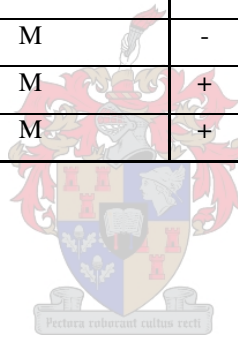
The microbial makeup of UASB granules is very complex. It varies with time, pH and other factors such as dilution rate and variations in feed rate and composition inside the anaerobic digester. Some sources claim that there might be more than 11000 species present (Lettinga et al., 1980). Although a great deal of research is still needed in this field, Table 2.4 gives a list of the more common species found in anaerobic sludge.

**Table 2.4: Some of the more common species found in granulated anaerobic sludge**

Organism	Type [Methanogen/Acidogen]	Gram stain	Temperature range °C	Motile / No motile	
Acetomicrobium flavidum	A	-	35-65	Motile	*
Acetomicrobium faecalis	A	-	55-74	Motile	*
Acetothermus paucivorans	A	-	50-60	Motile	*
Clostridium thermocellum	A	-	60-64	Motile	*
M. thermoautotrophicum	M	-	65-70	Motile	*
M. wolfei	M	-	55-65	Motile	*
M. thermoformicum	M	-	55-65	Motile	*
M.spec. Stamm	M	-	35-70	Motile	*
M. thermophila	M	-	50	Non-motile	*
M.spec. TAM	M	-	60	Non-motile	*
M.spec. CALS-1	M	-	60	Non-motile	*
M. thermoflexum sp. Nov.	M	+	60	Non-motile	
M.defluvii sp. Nov.	M	+	55	Non-motile	

**M. – Methanobacterium**

\* - (Winter and Zellner, 1990)



## **2.5 Granule Formation**

A four step model for the granulation process as suggested by literature will now be presented along with a discussion on known granulation enhances and inhibitors. The reason for this is to gain further insight into the granulation process and also to identify additives that might aid in the granulation process.

### **2.5.1 Anaerobic Bio-granulation**

Under normal culture conditions, it is believed that microbial cells would prefer a dispersed rather than aggregated state. Microbial granulation might be the result of cell response to a stressful environment that leads to the change in surface characteristics of bacteria. Cell surface hydrophobicity may mediate attachment by facilitating and maintaining specific receptor-ligand interactions, which leads to nucleus formation and



eventually granules. High hydrophobicity of micro-organisms is usually associated with the presence of fibrillar structure on the cell-surface and specific cell-wall proteins. Culture conditions such as starvation, substrate change, pH and temperature may also influence hydrophobic properties of the cell surface and granule formation (Liu et al., 2003).

For granulation to occur spontaneously in an anaerobic culture, a number of conditions have to be fulfilled. Based on the existing mechanisms a four step model can be derived (Liu et al., 2003).

1) Physical movement to initiate a bacterium-bacterium and/or bacterium-nuclei contact. Forces involved in this step are as follows:

- hydrodynamic force,
- diffusion force,
- gravity force (Hulshoff Pol et al., 1988),
- thermodynamic force (Thaveesri et al., 1995),
- cell mobility (Van Oudenaaden et al., 2003).

2) Initial active forces to stabilise multi-cellular contacts:

- van der Waals forces,
- opposite charge attraction,
- thermodynamic forces (Thaveesri and Daffonico, 1995),
- hydrophobicity (Van Loodsrecht et al., 1987),
- filamentous microbes can serve as a link to individual cells,
- hydrogen liaison (Teo et al., 2000),
- formation of ionic pairs/triplets (Mahoney et al., 1987),
- interparticulate bridging,
- cellular surface dehydration (Liu et al., 2003),
- cellular membrane diffusion,
- signalling and collective action in bacterial community (Oudenaaden et al., 2003).

3) Microbial forces needed to mature the initial nucleus to a granule:

- ECP production (Schmidt and Ahring, 1994),
- microbial growth inside cellular cluster,

- metabolic and genetic change induced by environment.
- 4) The steady-state, three-dimensional structure of the microbial aggregate shaped by the shear forces in its environment. The outer shape, the size of the granules are a function of the interaction between the granule and the hydrodynamic shear forces and substrate type and loading rate in its environment (Hulshoff Pol et al., 1983).

## 2.5.2 Granulations Accelerators and Inhibitors

The following constituents were identified from literature as either granulation enhancers or inhibitors:

- The presence of high energy sugars was the foremost factor influencing the growth of granular sludge in batch cultures. A COD:N:P ratio of 300:5:1 was recommended (Britz and Van Schalkwyk, 2002). One of the main granulation enhancing carbon sources was found to be peach cannery effluent. The typical make-up of PCE can be seen in Table 2.5, the significance of this will be discussed in Chapter 3.
- Hydrogen concentration and pH has proven to be the primary limiting factors in the anaerobic digestion and granulation process. High hydrogen concentrations inhibit acetogenic ethanol conversion and in the case of pH, methanogenesis is inhibited. It was also found that ethanol, butyrate and propionate slightly inhibit the methanogenic step. (Kalyuzhnyi, 1996). Hydrogen concentration and pH are therefore inhibitors to the granulation process.
- Both  $\text{Ca}^{++}$  and  $\text{Mg}^{++}$  aid the granulation process either by neutralising the negative charges on cell surfaces or as a result of “Van der Waals” attractive forces, or to function as cationic bridges between bacteria (Hulshoff Pol et al., 1988; Guiot and Gorur, 1988; Tay et al., 2002). Calcium and magnesium consequently aid granule formation.
- The addition of cationic polymer “AA 184 H” (produced by Ondeo Nalco Pacific Pte. Ltd.) during seeding could significantly accelerate the start-up of the UASB reactor. It was found that a maximum acceleration of 52% is achieved at a dosage of 80 mg/litre polymer (Show et al., 2004).
- Heavy metals tend to inhibit the granulation process, inhibition was found to decrease in the following order: Ni>Cu>Cd>Cr>Pb. Factors like high ammonia



concentration, dispersed solids, organic solvents, pesticides and long chain VFA's also tend to have a inhibitory effect on the granulation rate (Britz et al., 1999). Hence, foreign substances and heavy metals also have a tendency to inhibit granulation.

**Table 2.5: Average composition of PCE (Trnovec and Britz , 1997)**

<b>Average composition of fruit canning effluent (PCE) used as substrate [mg/l]</b>		
<b>Parameter</b>	<b>Average</b>	<b>Standard Deviation</b>
<b>pH</b>	5.54	1.4
<b>COD</b>	4432	297
<b>TS</b>	2114	625
<b>PO<sub>4</sub></b>	5.32	3.9
<b>Alkalinity</b>	25	6.5
<b>Glucose</b>	161.6	25.3
<b>Fructose</b>	389.7	34.6
<b>Sorbitol</b>	88.8	9.7
<b>Ca<sup>2+</sup></b>	21	Not Determined (nd)
<b>Co<sup>2+</sup></b>	<0.06	nd
<b>Fe</b>	7.9	nd
<b>K</b>	84	nd
<b>Mg</b>	15	nd
<b>Na</b>	65	nd
<b>Ni<sup>2+</sup></b>	<0.3	nd
<b>SO<sub>4</sub><sup>2+</sup></b>	12.8	nd
<b>S<sup>2-</sup></b>	0.03	nd

## **2.6 Bioreactors and Scale-up**

The primary goal of this research project is to gather enough data on the topic to allow for a conservative as possible scale-up to a granule producing reactor of economically viable size (see Chapter 1). This subsection is devoted to bioreactor scale-up considerations obtained from literature that is regarded as important to this specific case.

### **2.7.1 General Scale-up Considerations**

Geometric scale-up seems to be a logical requirement for successful bioreactor scale-up, yet in the majority of cases it does not give a suitable relationship between the most important mixing parameters. Two other types of process similarities can also be used for scale-up, namely kinematic and dynamic similarity. The former requires that all the velocities in the various parts of the bioreactor be similar. This can only be obtained through procedures like computational fluid dynamics an entire field of research on its own and will thus not be applicable at this stage. Dynamic similarity on the other hand requires that the ratio of all the forces be similar between the different scales.

In the case of dynamic scale-up the speed of the mixer is related to the average impeller (or baffle) macro-zone shear and typically decreases in scale-up. The average shear rate of the reactor is typically a factor of 10 times lower than the average impeller zone shear rate. It may take a minimum amount of shear stress to create a certain particle size, but the ultimate distribution of particle sizes usually relate to the length of time that a particle is exposed to that shear rate.

If one looks at solid liquid mass transfer, it is important to remember that going from off-bottom motion to complete uniformity requires much less mixing power than going from an on-bottom motion to an off-bottom suspension. Thus a much higher mass transfer rate is obtained at lower shear if going from an off-bottom suspension to a completely mixed situation (Oldshue, 1998).

During scale-up the following should always be taken into consideration (Oldshue, 1998):

- Pilot tanks are blending rich and full-scale tanks are blending poor. Therefore it is advisable to use relatively inefficient blending impellers on the pilot plant.

- One way of making the pilot tank more similar to the full scale tank is to make use of impellers with a relatively narrow blade width, to lower the amount of mixing in the pilot plant.
- It should also be beard in mind that the viscosity of the full-scale unit will appear much lower than the pilot plant, in the order of 10 to 50 times lower.
- Guard against compensating effects on the pilot plant that will give the impression that some parameter does not have an effect on the scale-up. For example: if the circulation times become longer, the shear rates become higher therefore, resulting in a compensating effect that will make the process output satisfactory.

### 2.7.2 General Design Parameters

The following parameters should be considered during the scale-up of anaerobic systems (Metcalf and Eddy, 2003):

- 1 One of the parameters of main importance in the scale-up of bioreactors is the tipspeed of the mixing device. Normally a tipspeed of between 2 and 5 m/s is sufficient for adequate mixing, but still low enough to avoid cell breakage and consequently, a lowering in product yield.
- 1 As stated earlier, the observed viscosity in smaller volumes is much higher than in larger volumes. Local shear forces around the impellor would thus be higher for the same amount of mixing.
- 1 Due to the fact that no oxygen is needed in anaerobic systems, the agitation of cultures need not be as vigorous as with aerobic systems.
- 1 Agitation should still be of large enough magnitude for liquid-solid (or feedstock to microbe) mass transfer to occur at a sufficient rate.

## 2.8 Matlab® Image Processing

Chapter 1 gives a short discussion of the main problems with regards to the methods of analysis used to determine the granule growth in Phase 1 and 2 of the study. In an attempt to overcome these problems, an image processor will be developed and tested in stage 2 of Phase 3 (Figure 1.2). A detail discussion of the shortcomings of the growth quantification methods used in Phase 1 and 2 (and various other methods) will be given in Chapter 5, where it is attempted to develop an alternative to currently used methods. This section highlights details from the literature that will be used to implement a digital

image processing programme for the quantification of growth of bio-granules during an incubation period.

The Image Processing toolbox is a collection of functions that is effectively an extension of the Matlab ® numeric computing environment. The toolbox supports a wide range of image processing operations, including:

- special image transformations,
- morphological operations,
- linear filtering,
- image analysis and enhancing,
- deblurring as well as,
- region of interest operations

Many of the toolbox functions are M-files, which is a series of statements that implement specialised algorithms for image processing. The capabilities of the image processing toolbox can also be extended by writing more M-files, and it can be used in combination with other toolboxes. The *Matlab® Image Processing Users Guide* can be obtained from [www.Mathworks.com](http://www.Mathworks.com).

In Chapter 5 this toolbox, along with basic Matlab ® will be used as a basis for the initial study and evaluation of a better method of growth quantification in granulated anaerobic sludge. This method will be an image processing computer programme that quantifies growth by comparing the amount of granules on digital images.

## **2.9 Summary**

Compared to other treatment methods, anaerobic digestion is an inexpensive means to remove the bulk of organic and nitrate loads in a wastewater stream. In their most basic forms, these units can be used as 'roughers' (anaerobic ponds and digesters) to remove the bulk of the COD load. A single high rate unit (like the UASB and EGSB) can remove up to 90% of the COD in less than 10 hours (Kato et al., 1994). Compared to its closest rival treatment method, anaerobic digestion produces on average 40% less sludge than aerobic digestion. Consequently, far less sludge has to be removed and treated and/or land filled. Aerobic digestion also needs aeration, which results in a much higher energy

consumption and operating cost. Because of this, the demand for- and applicability of anaerobic digestion to treat various types of effluents is growing daily.

Unlike most anaerobic processes where large footprint, effluent pre-treatment and low COD removal rates hampers the applicability of the system, the Up-flow Anaerobic Sludge Blanket Reactor (UASB) provides a state-of-the-art solution to effluent treatment. The UASB reactor is a fluidised bed reactor, therefore a relatively simple design. Influent is distributed into the granulated sludge bed at appropriately spaced inlets. The influent passes upwards through the anaerobic sludge where the micro-organisms in the granules come into contact with substrates. The “solid state catalyst” is composed of micro-organisms that naturally form granules (pellets) of 0.5 to 2 mm diameter. These granules have a high sedimentation velocity and thus resist wash-out from the system even at high hydraulic loads.

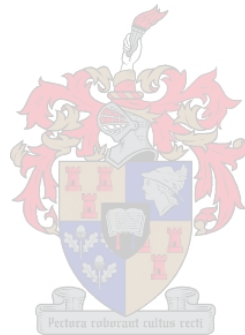
One major drawback of the UASB reactor is its extremely long start-up period. The unit generally requires between 2 and 8 months to develop granular anaerobic sludge, if initially seeded with normal anaerobic digester sludge. This restricts the application in areas where granules from operating UASB's are not readily available, since the operating efficiency and performance of these systems are mainly dictated by the quality of the granulated anaerobic sludge used. The full potential of the UASB system cannot be exploited until granule formation are better defined and optimised.

UASB bioreactor start-up (and operation) is heavily dependant on the spontaneous formation of granular anaerobic sludge with high settling velocities and high methanogenic activity. Granules can be described as spherical bio-film consisting of a densely packed symbiotic microbial consortium, living in a symbiotic environment in absence of any support matrix. Therefore, if this granulation process can be aided by any means, it would aid immensely in the applicability of arguably the most cost-effective means of removing organic waste from effluent streams namely high rate anaerobic digestion (or the UASB/EGSB systems to be more exact).

As in most biological systems, the inorganic species nitrogen, phosphates and calcium (except for carbon, oxygen and hydrogen) play an important role in granule growth. Phosphate, calcium and simple sugars are also vital for the granulation process to occur, as they are used in ECP production and the initial cell attachment process (nucleus

formation). ECP is long-chain C-H bonds which are secreted by some of the microbial species in order to protect them from their adverse environmental conditions.

As stated in Chapter 1, the aim of this research is to identify and quantify the key parameters that influence the granulation rate inside the reactors, as well as those factors/elements that have an effect on the scale-up process. Two types of process similarities can also be used for scale-up namely, kinematic and dynamic similarity. In the case of the latter, the speed of the mixer is related to the average impeller (or baffle) macro zone shear and typically decreases during scale-up. Kinematic similarity requires that all the velocities in the various parts of the bioreactor be similar. This can only be obtained through procedures like computational fluid dynamics, an entire field of research on its own and thus be applicable at this stage. Dynamic similarity on the other hand requires that the ratio of all the forces be similar between the different scales. Dynamic sale-up will form the basis of all the reactor designs done in this research project.



# *3. Initial Research and Bench-Scale Commissioning*

---

## **3.1 Introduction**

Chapter 3 is in actual fact an extension of the literature survey done in Chapter 2. The reason for devoting an entire chapter to the following work is because this research project is the Phase 3 (see Figure 1.2) of the larger WRC project and is heavily based on:

- 1) Research done at the Department of Food Science at the University of Stellenbosch on the artificial cultivation of UASB granules in lab scale reactors with 400 ml vessel volumes, or Phase 1 of the WRC project (Britz et al., 1999; Britz and Van Schalkwyk 2002),
- 2) And secondly, on the initial study done on the scale-up of the abovementioned reactors to bench-scale reactor volumes especially designed to give insight into parameters that might influence scale-up to even larger or more effective granule producing reactor systems, or Phase 2 of the WRC project (Els and Van Zyl, 2002).

The materials, design of experiments and findings that were used in Phase 1 and 2 form the basis of this research project. Therefore a detailed discussion of the first two phases of this project is given. The feed preparation, reactor loading and operating procedures can be seen in Section A1 of the Appendix.

In the original research (Phase 1), granular biomass was cultured in a linear shake bath at 35 °C and 150 rpm (Britz et al., 1999; Britz and Van Schalkwyk, 2002). The vessels had a volume of 450 ml and contained a sludge to feed ratio of 1: 3,5. Lactate, glucose,

sucrose and peach cannery effluent (Table 2.5) were used as feed, while  $\text{KH}_2\text{PO}_4$  served as a buffer component to avoid acidification. The sludge used in this study did contain small granules at the start of the experiment. – making this a study in granule enhancement- and not so much an actual granulation study. Since PCE will be used as COD source for the bench-scale reactors, this discussion will mainly focus on the results and conclusions drawn from vessels inoculated with this medium. The amount of granules was determined by physically counting the granules formed over a specific period of time by using a round glass container with a graded grid underneath.

With the abovementioned method, the accurate counting of granules was a near impossibility; the formed nuclei (miniature granules) were less than 0.5 mm in size and the sludge solution was a very cloudy and viscous. Another point worth mentioning is the difference in settling properties. If a sample is stirred in the usual fashion, most of the large granules will immediately move outward and then, the moment pouring starts and stirring stops, the granulated fraction of the reactor volume rapidly drop to the bottom of the sampling container. This phenomenon results in very large errors each time the sample is diluted or divided. Nonetheless an increase in ( $[\text{Number of Granules After}] * 100 / [\text{Number of Granules Before}]$ ) of between 46% and 600% (for PCE) was observed over the 14 to 20 day incubation period, depending on the batch of anaerobic sludge used. It was proven, even at this early stage of the project that the type of sludge used plays a vital role in the granulation process.

The pH profiles were measured to indicate metabolic activity of the acidogenic species, since the metabolic products produced by these species are volatile fatty acids, hence a drop in pH will occur as these products accumulate. The dispersed sludge samples showed a drop in pH to 6 within the first 3 days, with a slight climb over the next following days and then remained stable for the rest of the 20 day incubation period. The vessel inoculated with PCE and anaerobic sludge showed a volatile fatty acid (VFA) profile as displayed in Figure 3.1. A major peak in the in the propionic acid production occurred on day 4, with a steady decrease in propionic acid until the formation started to stabilise. The highest concentration of acetic acid was found on day 10 with a far less dramatic decrease than propionic acid to the stabilisation phase occurring in the last 4 days of the incubation period.



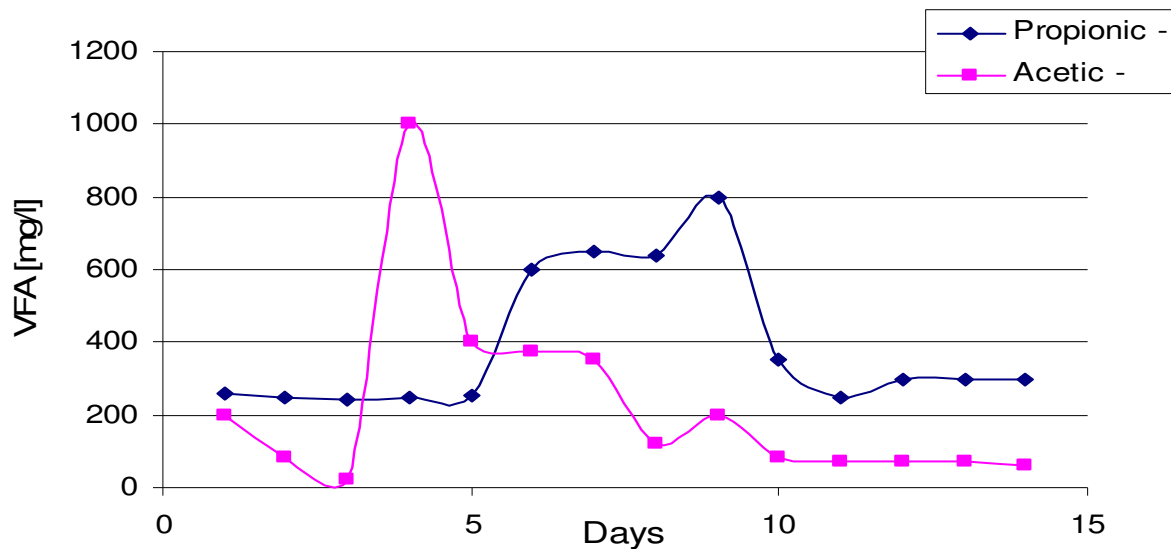


**Figure 3.1: VFA profiles of the major acidic metabolic products of sludge digesting PCE**

The conclusions were the following (Britz et al., 1999; Britz and Van Schalkwyk, 2002):

- Glucose, sucrose, lactate and PCE have proven to be granulation enhances.
- Bigger granules were found at the end than at the beginning of the experiment
- Shear forces applied to the biomass appeared to enhance granulation.
- The study proved that granulation can be enhanced using batch units inoculated with raw anaerobic sludge.
- A drop in pH over the first few days, followed by a gradual recovery to a neutral pH also seemed to aid in the granulation process.
- The type, age and concentration of the sludge used in the experiment, were also found to be of paramount importance to granule formation.

However, the methods used in the early studies done by the Department of Food Sciences at the University of Stellenbosch (400 ml Schott bottles on roller/shaker tables), did not facilitate scale-up to a reactor system capable of mass culturing anaerobic sludge to be sold commercially as inoculum for UASB reactors (Els and Van Zyl, 2003).

Chapter 3 proceeds with a detailed discussion of the Phase 2 bench-scale reactors, followed by a discussion of the biogas measuring units. The sludge-, feed preparation

and reactor operation can be seen in Section A1 of the Appendix. The rest of the chapter focuses is on the results and conclusions drawn from these initial stages of the WRC project. Based on these results and conclusions, the chapter will be ended off with a summary.

### 3.2 Reactor Design

To study the artificial granulation of anaerobic sludge in Phase 2 (see Figure 1.2), two bench scale reactors were designed to simulate the motion that was induced by the shaker tables on the 450 ml vessels in Phase 1. Both reactors were designed b Dr E.R. Els of the department of process engineering at the University of Stellenbosch. The following two subsections give a detailed discussion on the reactors.

#### 3.2.1 The 4.15 Litre Unit (R<sub>4.15</sub>)

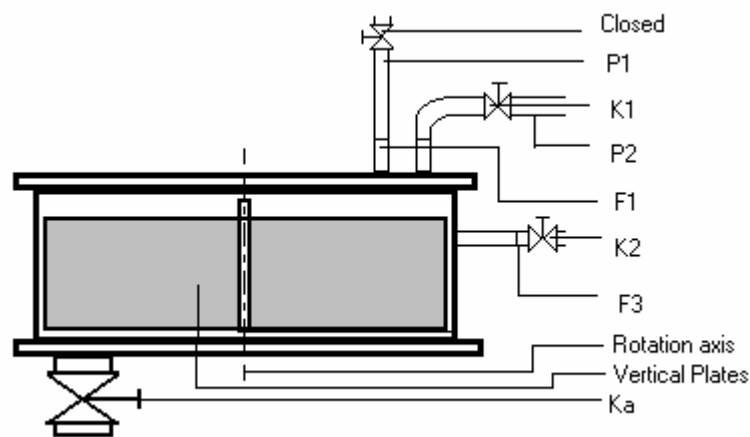


**Figure 3.2a: R<sub>4.15</sub>, Agitator Included**

The total operating volume of the first reactor is 4.145 litres. This reactor has, functioning as a stirring mechanism, two stainless steel plates (coloured grey on Figure 3.2a) mounted 180° on a vertical axis. The two plates oscillate through approximately 90° to induce a radial flow pattern inside the reactor. R<sub>4.15</sub> has a horizontal radius of about 15 cm, with a height of 12 cm. The mixer plates are 8 cm high and have a clearance of 0.8 cm from the side of the reactor. The reactor has a gas volume of 2 litres above the operational volume, and the main outlet valve is situated on the bottom of the unit. The materials of construction of the reactors are stainless steel. It has one

primary outlet valve ID 2.5 cm, and in the case of R<sub>4.15</sub>, three secondary in-/outlets, ID 1.25 cm (F1, 2, 3 on Figure 3.2a), for feeding and biogas disposal.



**Figure 3.2b: R<sub>4.15</sub>, Outside View**

Figure 3.2b gives an outside view of the reactor discussed above.

### 3.2.2 The 7.2 Litre Unit (R<sub>7.2</sub>)

The flow pattern induced by the mixer plate in R<sub>7.2</sub> (Figure 3.2a and b) is completely different from that of R<sub>4.15</sub>. R<sub>7.2</sub> has a single mixer plate mounted on a horizontal axis, which oscillates like a pendulum (if seen from the side) back and forth through 90°. In this case the reactor is a horizontal cylinder with a radius of 10 cm and a width of 40 cm.

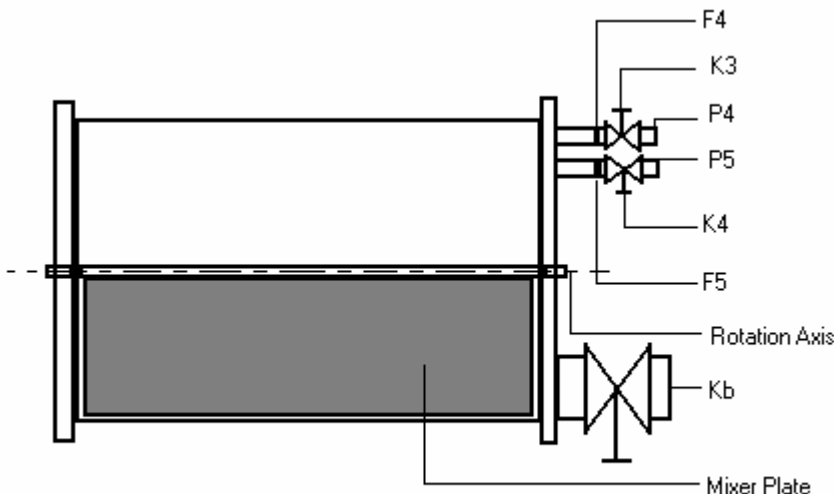


**Figure 3.3a: R<sub>7.2</sub>, Agitator Included**

The reactor has a total operational volume of 7.2 litres with a gas clearance (above the liquid) of 0.5 litres. R<sub>7.2</sub> has one primary outlet valve (Kb on Figure 3.3a) and only two secondary in/outlets (p4 and p5). In both R<sub>4.15</sub> and R<sub>7.2</sub>, the angle of the mixing plates can be adjusted if necessary. Both reactors have heating jackets, which can be used to

control the temperature inside with hot water. In the current situation, this is unnecessary, the room's temperature is kept constant at 35 °C.



**Figure 3.3b: R<sub>7.2</sub>, Outside View**

Figure 3.3b gives an outside view of the above mentioned reactor.

### **3.2.3 Gas Measuring Unit**

During the digestion process that occurs inside the reactor in the incubation period, biogas is formed, the biogas outlet is connected to a biogas measuring unit (Figure 3.4) to give insight on the amount of biogas produced and also the percentage of methane (via a Gas Chromatograph) in the produced gas. The gas from the reactor enters the 3-way valve at inlet B. The valve has two settings: B to A or A to C. The gas flows through B to A and into the glass container. Pressure builds up inside the unit and the water level is forced down, resulting in a rise in the water-level in the glass tube. As the water level in the tube rises, the buoy also rises, and moves past the top diode system. The light beam is broken, and a signal goes to the circuitry, which in turn sends a signal to the 3-way valve. The valve now switches to A to C.

The pressurised gas inside the glass container can now escape to the atmosphere. This causes the water-level in the glass container to rise, while simultaneously lowering the water level in the glass tube. The buoy moves downward, pass onto the lower set of diodes, again sending a signal to the circuitry and to the valve. The valve switches from B to A and this process is repeated. A counter is connected to the system and counts the amount of repetitions the unit makes. One can thus calculate the amount of gas produced. This system was also designed by Dr E R Els. The percentage methane in the biogas was measured in the exact same manner as used in phase 1 of the research (Britz and Van Schalkwyk, 2002).

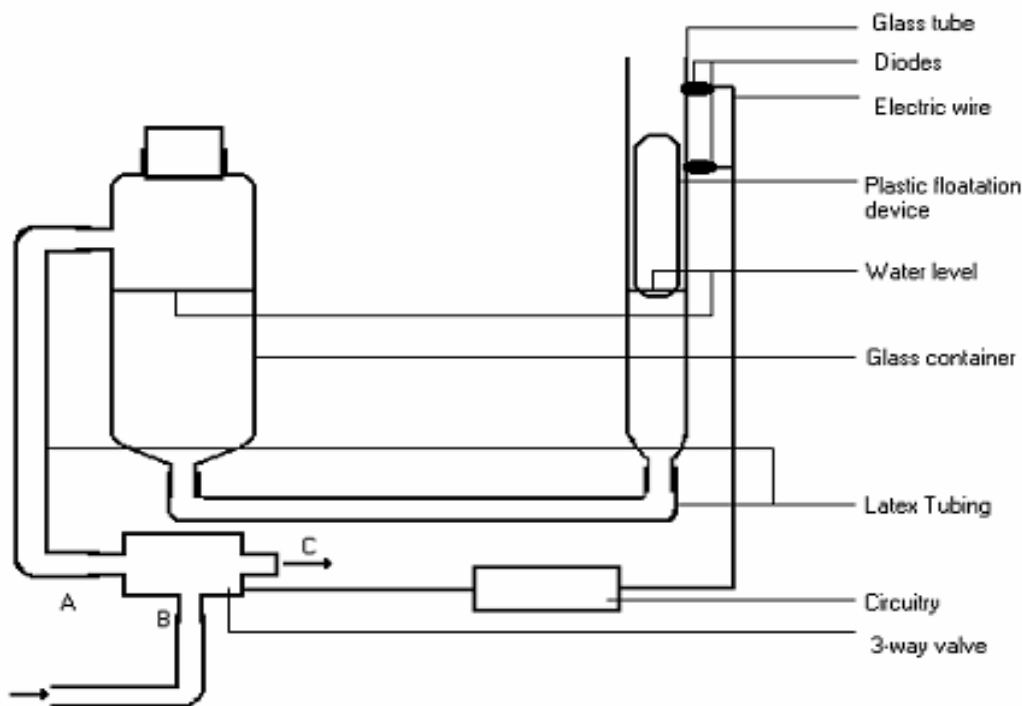
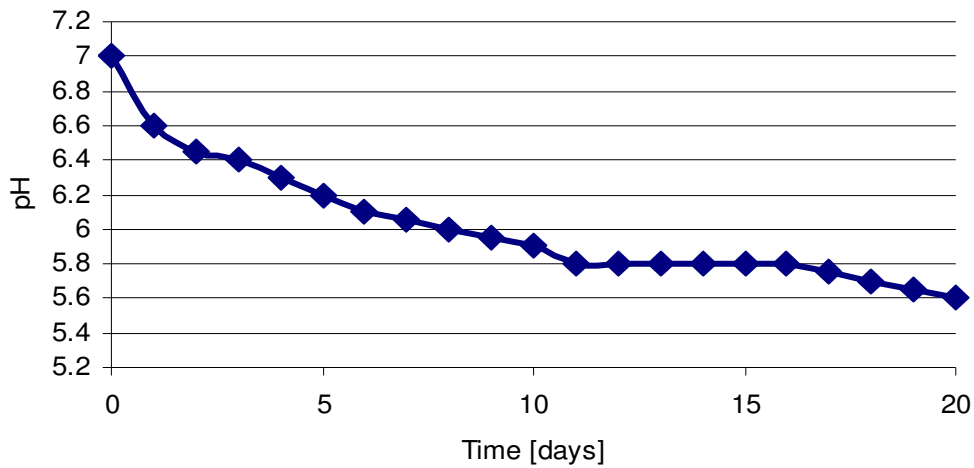


Figure 3.4: The Gas Measuring Unit

### 3.3 pH-Manipulation



If the reactors were fill and draw systems which were fed daily with a carbon feedstock of pH of 7 at a COD level of 2000 mg/l, for the 20 day incubation period, the pH vs. time distribution will be approximately that shown in Figure 3.5. Regrettably, this distribution is far from that needed for optimum granule formation. A pH of lower than 6.5 leads to a decrease in the overall methanogenic activity (Britz et al., 1999). At pH levels lower than 6, the methanogenic species go into hibernation and become completely dormant. Since these organisms are essential for granule formation, a stable pH above 6.5 must be maintained after the first four days of the 20 day incubation period. However, the activity of the acidogenic species needs to be high for ECP production to occur; hence a pH of less than 6.5 is also needed at some stage of the incubation period, albeit for the first 40 hours (see Section 2.3.3). A means had to be found to manipulate the pH in such a way as to optimise the environment of the bacteria to enable them to form granules.



**Figure 3.5: The Actual pH vs. Time Distribution**

Earlier studies on this topic have come to the conclusion that a pH distribution like that on Figure 3.6 is an optimum for granulation. Also, calcium promotes granulation (see Section 2.5.2). Therefore, to achieve the sort of distribution as seen on Figure 3.6, the buffer substance like  $\text{CaCO}_3$  and  $\text{KHCO}_3$  were added to increase the alkalinity with good results (Britz and Van Schalkwyk, 2002).

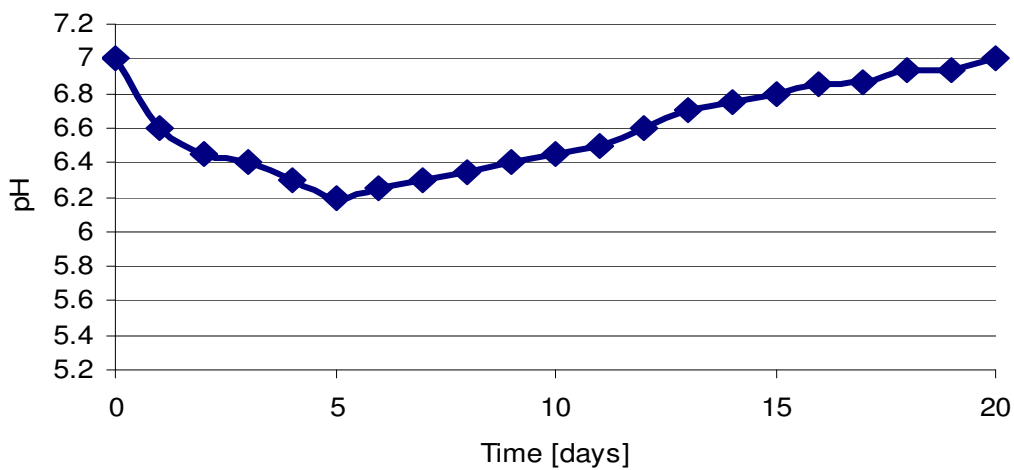


**Figure 3.6: Desired pH vs. Time Distribution**

From fairly early on in Phase 2, the alkalinity and pH problems proved to be far more of an issue than was the case in small vessel volumes used in Phase 1. Various additives and concentrations were experimented with (under advice from Prof TJ Britz at the Department of Food Science) as will be seen in the following section.

### 3.4 Results and Discussion

In this section, a discussion on the results obtained in Phase 2 of in this project will be given.

#### 3.4.1 Experimental Run 1

The aim of this experiment was to familiarise the operator with the reactor system, as well as with the nature of the biological system inside the reactors. The incubation time was set to 14 days. The results obtained are displayed in Figures 3.7 and 8.

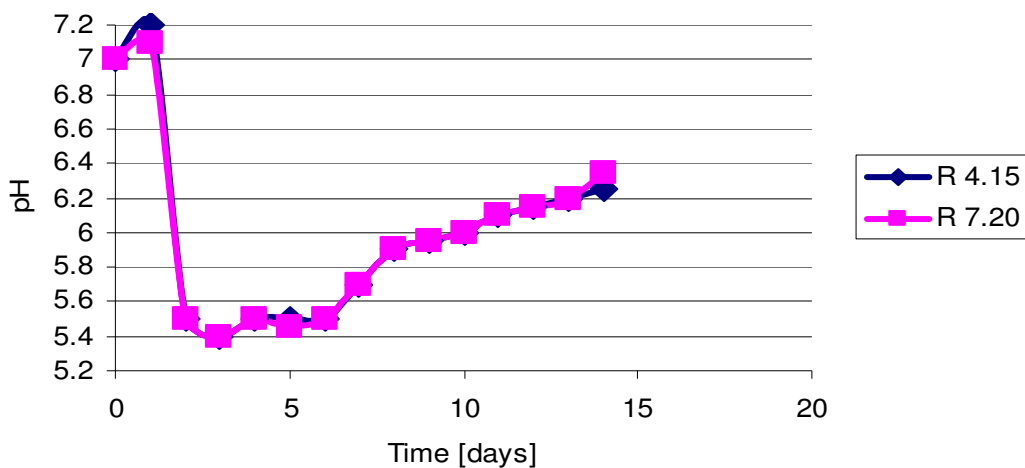


Figure 3.7: Experiment 1, pH vs. Time

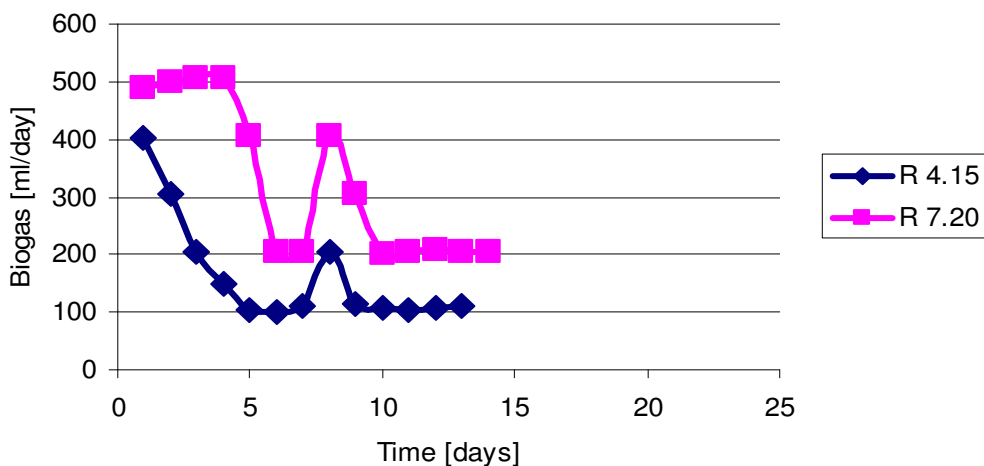


Figure 3.8: Experiment 1, Gas Production vs. Time

Experiment 1 demonstrated that  $\text{CaCO}_3$  at a concentration of 100 mg/litre in the feed does not provide adequate buffer capacity to the system. Furthermore, gas production decreased and methanogenic hibernation occurred at a pH lower than 6. It is of primary

importance that the feed medium is kept at 5°C even if sterilised (autoclaved: 5 minutes at 125 degrees Celsius). This is done to avoid deviations in gas production due to fermentation. As can be seen from the peak in Figure 3.8 on day 8, the operator ensured that this never happened again. It was established that, to avoid sludge being drained with used feed every day, the reactors must be shut down 20 minutes before opening the valves. This time allows the sludge to settle at the bottom of the reactors and the feed to clarify.

### 3.4.2 Experimental Run 2

The main aim of this experiment was to establish if the pH manipulation could be preformed more effectively. From hereon forward an incubation period of 20 days will be used.

It was evident that an additional 400 mg CaCO<sub>3</sub> added to the reactor volumes as deemed necessary (usually every two days for the 20 day incubation period) would not poison the system, as was the impression obtained from the literature (Mahoney et al., 1987). On the contrary, to UASB operation (300 mg/l proved poisonous, Mahoney et al., 1987) it was found that the additional 400 mg provided better buffer action in the system and no inhibition occurred. Literature also showed that Ca<sup>2+</sup> ions seem to enhance granule formation and growth (Mahoney et al., 1987). Therefore, a double benefit arises from using CaCO<sub>3</sub> as buffer. An increase in the percentage of methane in the biogas, indicating a rise in the methanogenic activity, confirmed this conclusion (see Figure 3.11).

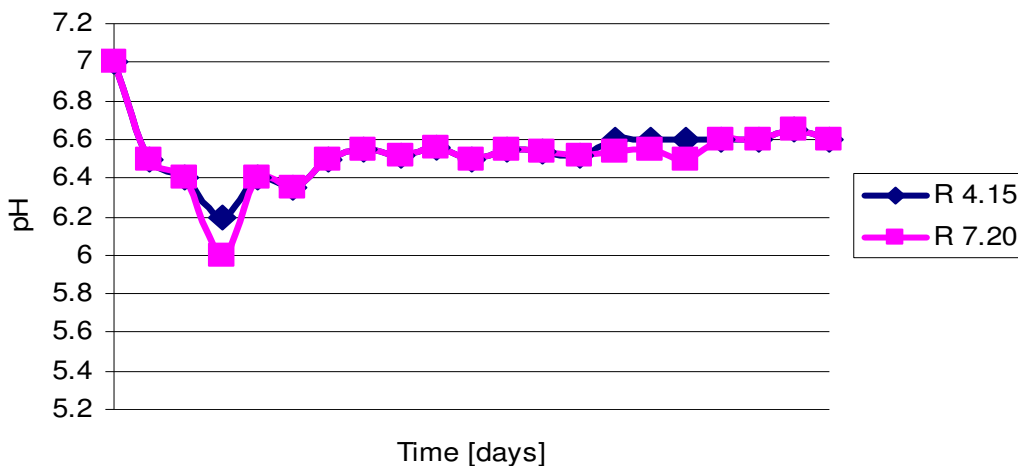
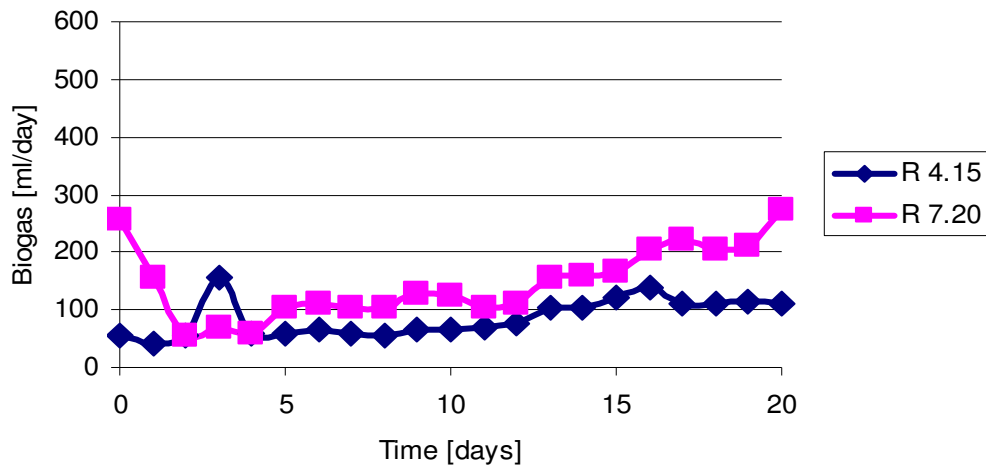
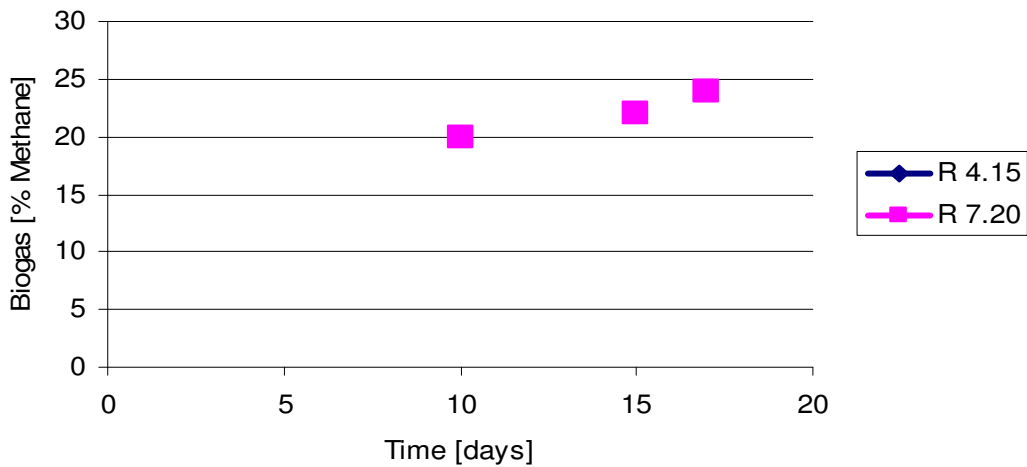


Figure 3.9: Experiment 2, pH vs. Time





**Figure 3.10: Experiment 2, Gas Production vs. Time**



**Figure 3.11: Experiment 2, % Methane in Biogas vs. Time**

It was established that the pH can be manipulated to the desired extent with the addition of  $\text{CaCO}_3$ , directly to the reactor volumes and it was decided that, after the initial pH drop, the pH must be kept above 6.5 at all times for optimum methanogenic activity and enhanced granulation (Britz et al., 1999). Hence the alkalinity, and so the buffering capacity of the system should be upped after the first 48 hours to ensure a adequate production of ECP, but also to avoid any further inhibition of the methanogenic species that is needed for granulation.

### 3.4.3 Experimental Run 3

The main aim of this experiment was to see if the pH could be kept above 6.5 after the initial decrease of the first few days. The second aim was to compare the granule growth inside the reactor with the growth of in earlier experimental runs.

R<sub>4.15</sub> had to be shut down on day 14 due to leaky seals at the base of the reactor. Figure 3.14 shows a steady increase in the percentage methane in the biogas, this implies that, with the increase in pH (and alkalinity) of the system, these organisms rapidly become more active.

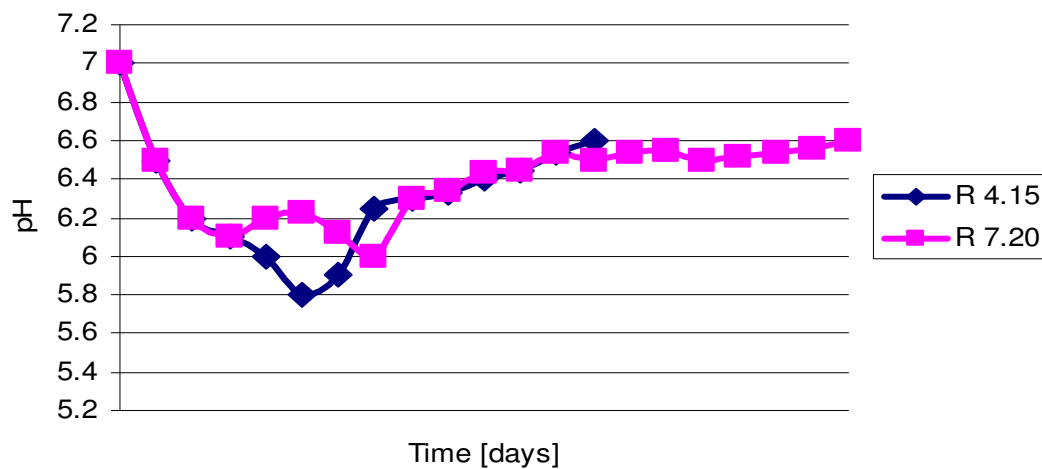


Figure 3.12: Experiment 3, pH vs. Time

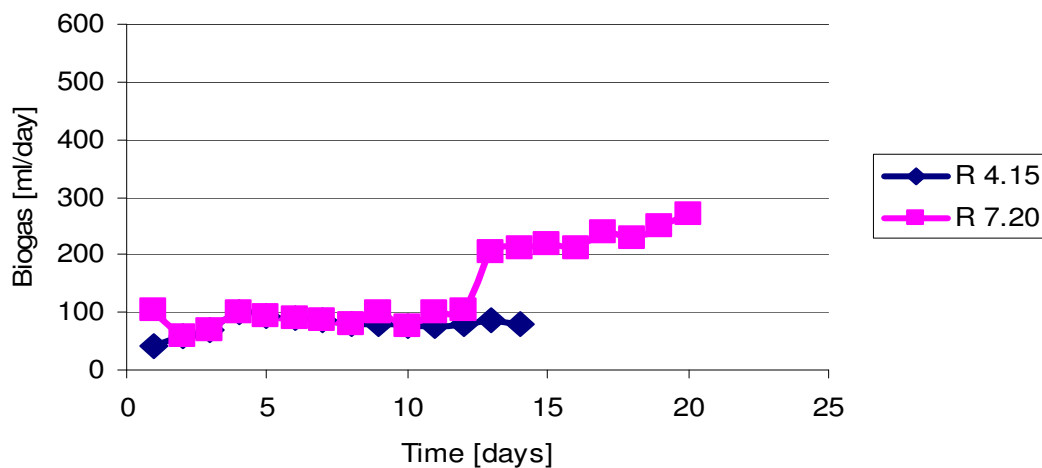
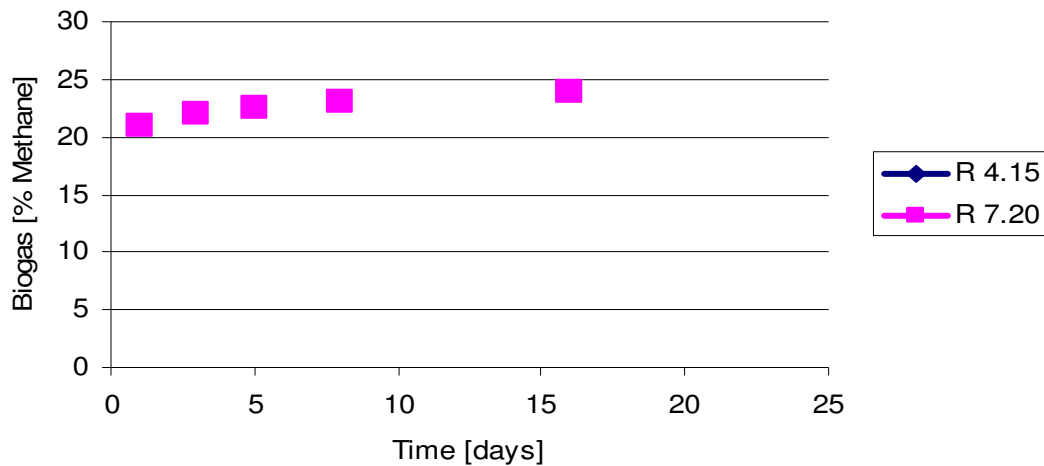


Figure 3.13: Experiment 3, Gas Production vs. Time



**Figure 3.14: Experiment 3, % Methane in Biogas vs. Time**

It was decided to increase the  $\text{CaCO}_3$  addition (as was needed) from 400 mg/l to 500mg/l in the next experiment. The reactors were both dismantled after this run and taken to the workshop to get the seals replaced.

#### 3.4.4 Experimental Run 4

For the fourth run, better quality sludge was obtained from the Athlone Sewerage Works. The reason for this is that the sludge used up to this point in time (Paarl Sewerage Works) did not give the desired results. Granule counts were only done visually at this stage and no significant amount of granulation occurred up to this point.

Figure 3.15 showed that 500 mg/litre of  $\text{CaCO}_3$  (added every two days for the 20 day incubation period) combined with the Athlone sludge resulted in a far smoother (or more damped) pH curve. The microbial activity (gas production) in experiment 4 was also far higher than in earlier experiments. The reason for this can be twofold: it can be due to the relatively high pH and alkalinity of the system and secondly the fact that the activity of the Athlone sludge was higher than its predecessor.

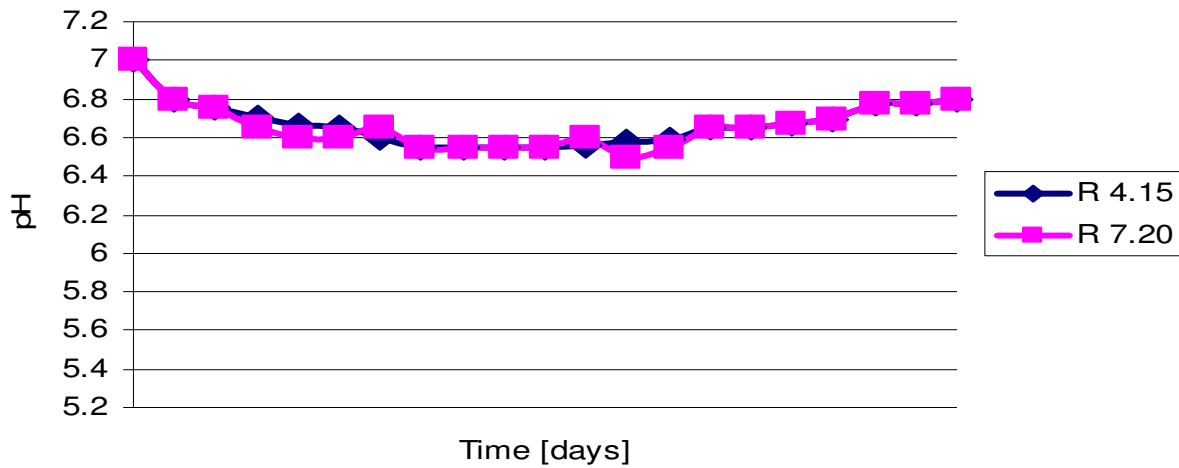


**Figure 3.15: Experiment 4, pH vs. Time**

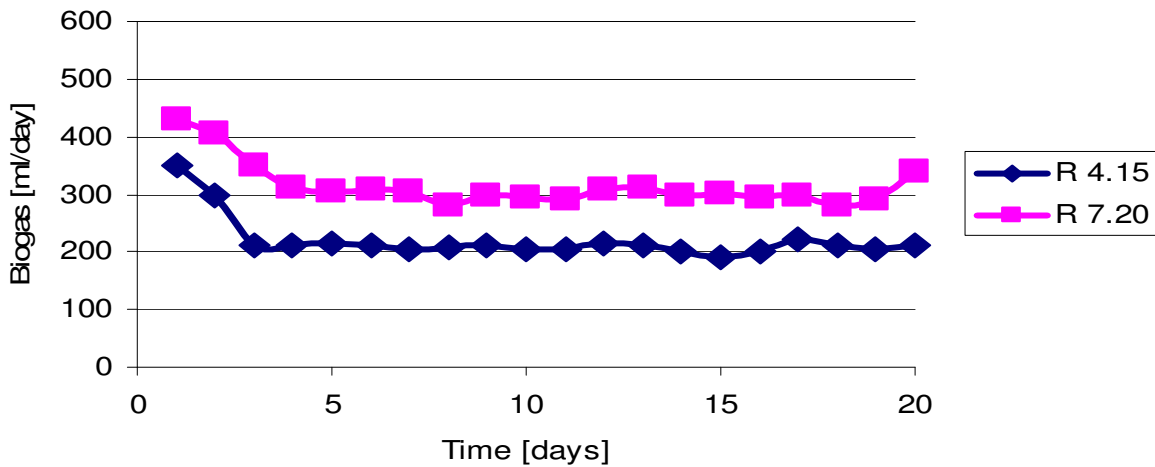


**Figure 3.16: Experiment 4, Gas Production vs. Time**

The method of granule growth comparison that was used was the sieve array and TSS method described in Laguna et al., 1999. A graphical presentation of this procedure is given in the Appendix Section A2. As can be seen from the quantitative growth comparison of the yields obtained from R<sub>4.15</sub> and R<sub>7.2</sub> (in this experimental run), Athlone sludge is a good medium for reactor inoculation (Figures 3.17).

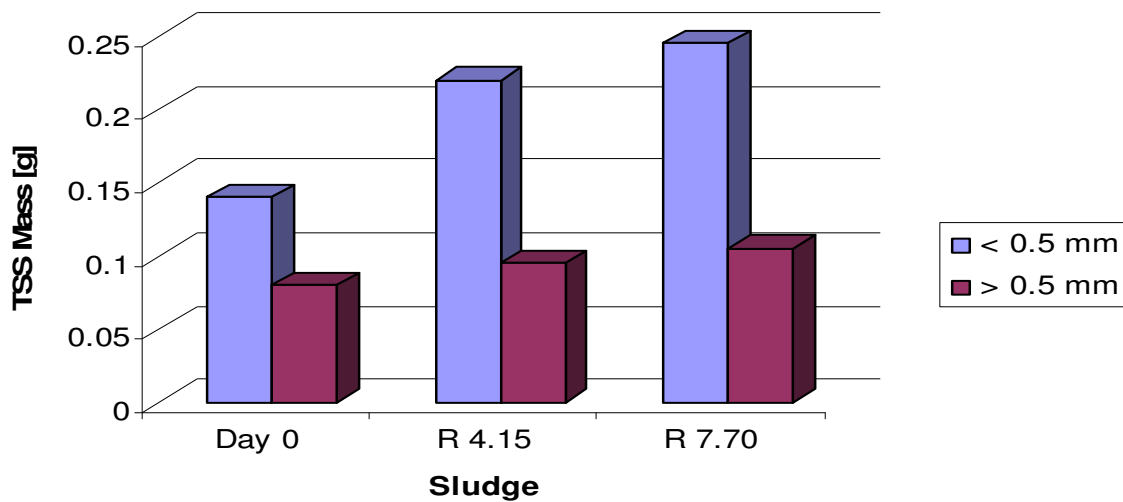


**Figure 3.17: Experiment 4, TSS Yield per Mass fraction**

As can be seen from Figure 3.17, there was a definite growth of granular biomass in sizes larger than 0.5- and smaller than 0.5 mm, if the Day 20 yields of both reactors are compared to the size distribution of the Day 0 inoculation sludge. Growth is especially evident in the sizes smaller than 0.5 mm, indicating a growth from small – to larger granules (as expected).

When calculating the total mass by adding the mass in each size range for the Day 0 (Day 0 on Figure 3.17), R<sub>4.15</sub> and R<sub>7.2</sub> sludge, it is clear that growth occurred in the Total Suspended Solids (TSS) in the reactors. The above-mentioned experiment was duplicated to ensure the results were accurate. Representative samples that were taken from the reactors are assumed to be a proper representation of the species in the sludge and that the results are indeed accurate.

Even though the initial drop in pH (to induce ECP production) was not as prominent as in earlier experiments. This run was by far superior to previous runs done on the two reactors in Phase 2. For R<sub>7.2</sub> the TSS was calculated at 0.08 grams per 50 ml sample of the reactor volume. This in turn can be converted to 2.02 kg of granules larger than 0.5mm produced per m<sup>3</sup> reactor volume per 20 days (MUG). These results verified the discussions on the type of sludge used and the fact that calcium promotes granulation (Britz and Van Schalkwyk, 2002; Mahoney et al., 1987). However, it is also in direct conflict with the hypothesis that calcium above a certain level starts to inhibit the

granulation process due to an increase in density of calcium saturated granules (Mahoney et al., 1987).

### **3.5 Summary**

The aim of the Phase 1 research was to see if UASB granules could be cultivated in an artificial environment. From this part of the project it was found that, with a certain number of parameters set in place (like feed composition, pH distribution, hydrodynamic force and temperature), growth does occur during the 20-day incubation period, albeit in 450 ml vessel volumes. However, even though economic potential of this project was identified at an early stage, the Phase 1 research (of the larger WRC project) did not facilitate scale-up or the study thereof. Because of this, two bench-scale bioreactors (with volumes in the order of 10 times larger) that would simulate the motion, were induced by the shaker tables on the 450 ml vessels.

So the second phase of the artificial cultivation of granulated anaerobic sludge was initiated. The aim of Phase 2 was two fold:

- To see if the artificial cultivation of anaerobic sludge granules can be achieved in volumes one order of magnitude larger than previous,
- To orientate the researcher in the workings of the reactor, anaerobic digestion – and the granulation process of anaerobic sludge, since he had no prior knowledge of either of these.

As stated above, the aim of Phase 2 was to determine whether or not the reactors can be optimised in such a way that an increase in granules in the anaerobic sludge can occur over 20 days. As can be seen from Figure 3.17, a definite increase in mass occurred in the sludge, along with definite increase in usable granule mass (explanation for the mass of usable granules can be obtained in Section A2 of the Appendix). It can then be concluded that anaerobic bio-granulation can be enhanced in larger artificial environments (Els and Van Zyl, 2002).

The pH-level plays a vital role in the process. At a pH lower than 6.5 a decrease in activity starts to occur in the methanogenic species and this is unacceptable, since these are some of the primary species needed for granulation to occur (see Table 2.2).

A definite decrease in gas production and consequently sludge activity also occurs at this pH level. It can be concluded that after the initial decrease (that initiates the granulation process by aid of ECP production); the pH should be increased to above 6.5 as quickly as possible without harming the system. This should be done between day 2 and day 4.

$\text{CaCO}_3$  plays a very important role in the stabilisation of the pH and the increase in alkalinity in the reactors. Initially 100 mg/l feed was added, but it was found later that an additional 500 mg per reactor is far more sufficient. Not only does the  $\text{CO}_3^{2-}$  work as an excellent buffer, but the  $\text{Ca}^{2+}$  also enhances flocculation, which at later stages leads to granulation in the sludge.

It can also be noted from Figure 3.15 that from day 14 onwards in Experiment 4, the sludge started to stabilise its own pH. In the beginning of the incubation period, the acidogenic bacterial are far more prominent than the methanogenic species. Reasons for this include an abundance of growth medium and a much faster doubling time than their methane producing counterparts. However, as the amount of by products (mostly VFA's) produced by these species increase, so does the inhibitory effect of the VFA's increase. Furthermore, even though VFA's are the primary food source for the methanogenic species, the resultant pH with an increase in concentration of VFA's therefore also inhibits the methanogenic step.

The answer lies in the addition of alkalinity or buffering capacity in the form of bicarbonates (in the form of  $\text{CaCO}_3$ ) to the reactor volume. This allows VFA formation to increase without having as large an effect on pH as would be the case without the buffering. The elevated pH levels allows for the methanogenic conversion of VFA's to biogas and thus resulting in a far higher methanogenic activity, which in turn aids in the granulation process and breaks down the VFA's. The resultant effect of the VFA removal is that the pH of the reactor volume increases. When the  $\text{CaCO}_3$  was at 100 mg/l, self-stabilisation did not occur (see Figure 3.5). Furthermore, results also show that calcium promotes granulation. The explanation given in the literature is that the divalent  $\text{Ca}^{2+}$  ion also enhances the formation of extra-cellular polymers (ECP), which in turn acts as a hydrogen sink that stabilises the pH. ECP is also needed for granulation (see Section 2.3.3). It is clear that the addition of  $\text{CaCO}_3$  in sufficient amounts has quite a few advantages and that this buffer is the best for use on this system.

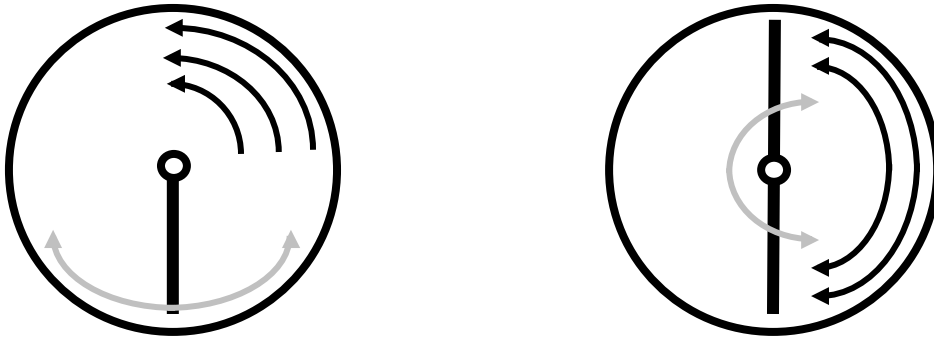
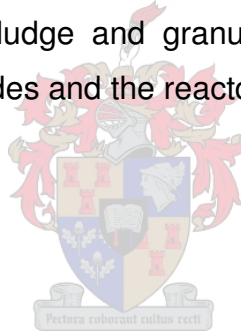


**Figure 3.18: Flow patterns in  $R_{7.2}$     Figure 3.19: Flow patterns in  $R_{4.15}$**

*(The grey arrows show the impellor movement)*

The concept used in the design of  $R_{7.2}$  proved to be better than the one used for  $R_{4.15}$  as can be gathered from the  $\text{CH}_4$  production and the amount of granulation that occurred in all experimental runs (Figure 3.17). This is possibly due to the fact that the agitator in  $R_{7.2}$  only goes to the middle of the reactor volume (see Figures 3.18 and 3.19), allowing liquid to easily escape over the top of the axis. This results in a lower maximum impellor shear than in  $R_{4.15}$ , where the sludge and granules are forced through the 5 mm openings between the impellor blades and the reactor shell.





# 4. Phase 3, Reactor Optimisation

---

## 4.1 Phase 3 Problem Statement

The final goal of the WRC project was to produce large quantities of anaerobic sludge granules in a short period of time (in the order of 500 kg in 20 days). These granules will then be used for the seeding of UASB reactors. This will shorten the start-up periods of this low maintenance, high throughput water treatment units - from approximately 300 days to less than 30 days.

Phase 1 of the larger WRC project proved that UASB granule growth can be enhanced artificially if a certain set of environmental conditions are met. These conditions included a pH between 6.5 and 7, simple sugars in the feed medium and a source of nitrogen and phosphate. The temperature was also kept at 35 °C for the entire 14 to 20 day incubation period. However, from an engineering point of view, this microbiological study contained some dire shortcomings. These included:

- the lack of a means to measure the biogas production and thus, the activity of the sludge,
- the means used to determine the granule growth (visual counting) was subjected to human error and was qualitative rather than quantitative in design and,
- the 450 ml reactor vessels on the shaker/roller tables did not facilitate scale-up or the study thereof.

As discussed in Chapter 3, Phase 2 was a study on the commissioning and initial performance of bench-scale bioreactors with volume one order of magnitude larger than the 450 ml vessel volumes used in Phase 1. From the results obtained from the four experimental runs done it was found that:

- not only could granulation be enhanced, but granules could be cultivated from dispersed anaerobic sludge,
- $\text{CaCO}_3$  ups the alkalinity of the system resulting in a higher methanogenic activity, more effective breakdown of VFA's produced by the acidogenic species and a larger granule yield in the end,
- however, at this point it was believed that a too high concentration of calcium would inhibit the granulation process (Mahoney et al., 1987), so it was only added when needed,
- a more accurate means of granule growth analysis was incorporated, but still had inadequacies (very time consuming and destructive),
- the sludge used as source of inoculum has a large effect on the final yield of the process,
- even though it was proven that granulation could be enhanced, it was clear that further process optimisation would be necessary (Els and Van Zyl, 2002).

Phase 3, the research represented in this thesis, can be defined as a bench-scale information gathering and optimisation study on the artificial cultivation of granulated anaerobic sludge over a 20 day incubation period. Parameters to be optimised include the following:

- sludge used as inoculum source,
- feed medium make-up,
- reactor configuration,
- reactor mixing speed,
- and internal surface area (ISA) variation.

Furthermore, Phase 3 will also be an attempt to bridge the gap between the microbiological study done in Phase 1 and a bioreactor design project, to ensure a conservative as possible scale-up to a pilot-scale granule producing reactor (Phase 4). Apart from the optimisation, the information gathering will also include the evaluation of methods used to quantify granule growth and a study on the actual and predicted absorption and production of granulation rate limiting parameters in the system, these include:

- COD,
- phosphates,
- nitrogen,

- calcium,
- TSS,
- carbon dioxide and
- methane.

The incubation period, temperature, sludge to feed ratio, and reactor operation (discussed in Section A1 in the Appendix) that was used in the early phases was replicated in Phase 4 in an attempt to make the results of the 3 phases as compatible as possible.

## 4.2 Background

From the results and conclusions reached in Chapter 3, it was decided to introduce a third test reactor into the project (see Figures 4.1 and 4.2). It was decided that this reactor should simulate the rolling motion that was found in the 500 ml Schott bottles on the roller tables. Since these conditions produced the highest yield of granules and the shape of the yielded granules were nearly spherical.

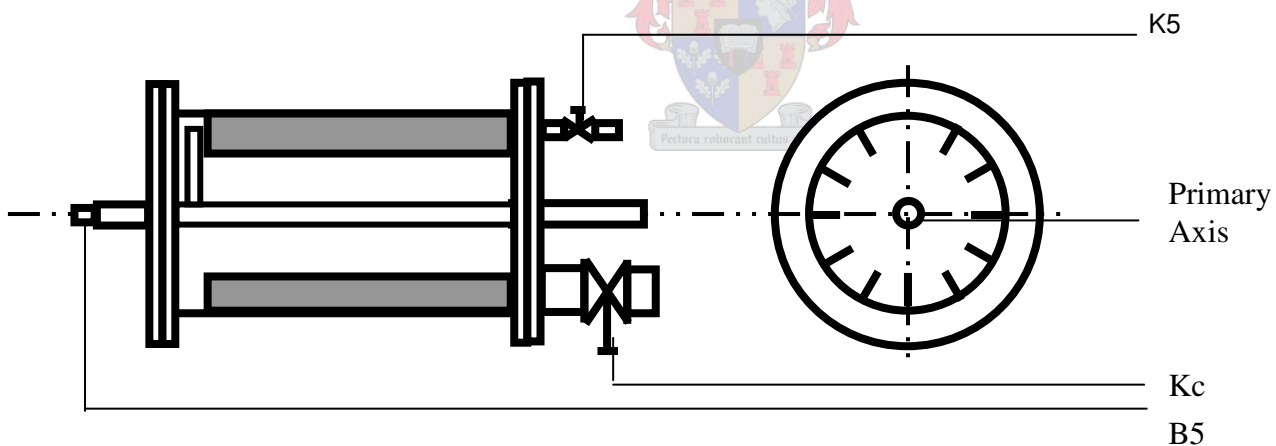


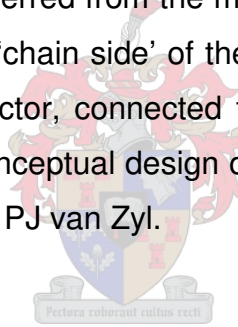
**Figure 4.1: R<sub>5.5</sub>, Baffles Included**

The flow pattern induced by the rolling motion in R<sub>5.5</sub> is completely different from that of R<sub>4.15</sub> and R<sub>7.2</sub>. R<sub>5.5</sub> has twelve baffles mounted on the inside shell of the reactor. The whole unit rotates around the horizontal axis, inducing a ball-mill-like rolling motion. This reactor is a horizontal cylinder with a radius of 8 cm and a width of 27 cm. It has a total operational volume of 5.5 litres with an air clearance above the liquid of 0.3 litres. R<sub>5.5</sub> has one primary outlet valve (Kc) and only one secondary in/outlet (K5). There is no heating jacket present here in R<sub>5.5</sub>, and the biogas exits via the biogas vent. This vent is situated at the back of the reactor.



**Figure 4.2: Outside view of the third reactor (R<sub>5.5</sub>)**

Figure 4.2 gives an outside view of the 5.5 litre unit. As can be seen this reactor is powered by an electrical motor with a variable speed converter to change the speed of rotation as desired. Power is transferred from the motor to the reactor via a drive chain. Valve Kc can be observed on the 'chain side' of the reactor and the biogas vent, to be seen on the other side of the reactor, connected to a biogas measuring unit as was discussed in Section 3.2.3. The conceptual design of this reactor was a combined effort of Dr E R Els, Prof L Lorenzen and PJ van Zyl.



### ***4.3 Identification of Sludge Prone to Granulation.***

The choice of the source of inoculum for the bioreactor to be seeded with is of utmost importance (Britz et al., 1999; Britz and Van Schalkwyk 2002; Els and Van Zyl 2002). The design may be 100% optimised with perfect flow patterns and a highly optimised synthetic food source, but without the proper sludge to seed the reactor with, no granulation will occur. In the following section, some of the criteria for sludge prone to effective granulation will be presented.

Digester sludge from three different wastewater treatment plants in the Cape Town and Boland area were chosen for the sludge screening process. Sludge A was the standard sludge used in the Department of Food Sciences. This sludge was prone to granulation, but still inadequate in terms of yields aimed to be achieved for this project. Sludge B, on the other hand a 'near legendary' inoculum to work with. The best results obtained up to

date by Department of Food Sciences were with this type of sludge. However, the anaerobic digesters of this specific plant was also 'near legendary' for their operational problems. The third sludge, Sludge C, has proven in the initial studies to be a sludge with very poor granulation properties.

The aim of these screening tests was to identify the sludge types that was, in granulation terms, somewhere in the range of a poor performer, an average sludge and a sludge with good granulation properties. The latter will be used for the duration of this study as the standard inoculum for bioreactor seeding.

### 4.3.1 Settability

The settlability test was done with the '1-liter cylinder method' as was discussed in Section A1.3 in the Appendix. The following results were obtained:

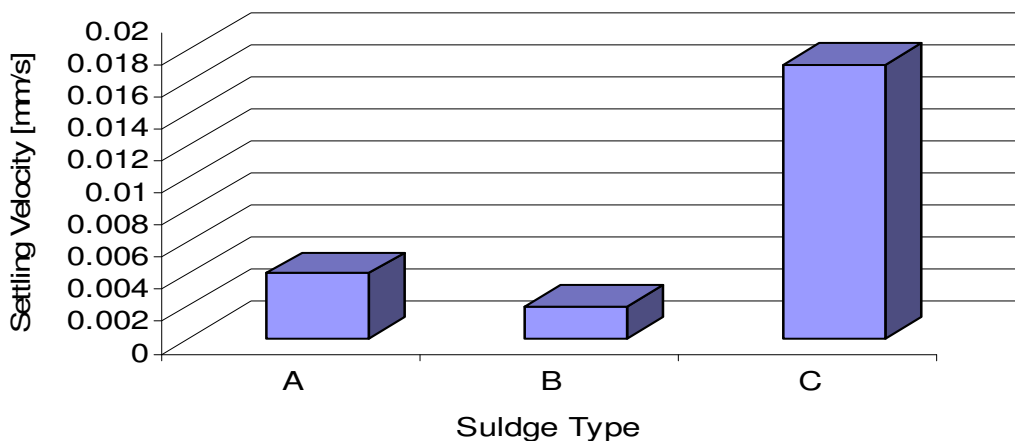


**Figure 4.3: Settling Velocities of Raw Sludge**

As can be seen in Figure 4.3, Sludge C had by far the shortest settling time, with sludge A more than 60% slower and sludge B nearly 90% slower. A possible reason for the good settlability of Sludge C is the fact that this sludge had a comparatively low viscosity, whereas A and B was thicker and visquous by nature. Even though literature states that good settling is a desired attribute for the anaerobic sludge granulation process, the exact opposite seemed to be true for the raw sludge obtained form the sewerage waterworks (Metcalf and Eddy, 2003). This observation is confirmed by the fact that dispersed microbes with a high activity usually have poor settling properties

due to gas formation. Therefore, Sludge B has in fact the most favourable settling properties due to its high gas production rate and resultant 'buoyancy' of microbes, which translates directly to a high microbial activity in the sludge.

### 4.3.2 pH

The pH screening test is divided into two categories: the pH history of the different digesters and secondly, the measured pH of the sludge after a period of separation from the digester (stored at 5 °C). This data was obtained from the operators working on the digesters at the various waterworks.

The comment on A was that the digesters had been stable for quite a while and a period of approximately three months were given. The digesters, from which sludge B was drawn, were started up approximately a month before the sample was taken. The operators commented that the unit was quite stable for the entire time after start-up. In the case of anaerobic digester shut down, the feed to the reactor is stopped. Theoretically no genetic drift will occur, since the micro-organisms will automatically go into a hibernation induced by a starved state. Sludge C was not stable at all. According to the operators at this plant, pH fluctuations occurred nearly weekly. This is damaging to the overall population make-up of the anaerobic sludge and will result in too a high concentration of acidogenic species and a lower than desired level of methanogens (the main precursors for granulation). The second test was to observe the stability of the pH of the sludge after it has been separated from the digester for a period of time. The results obtained from this test, after the three sludges were stored in separate 20-liter containers for 10 days, can be seen in Figure 4.4.

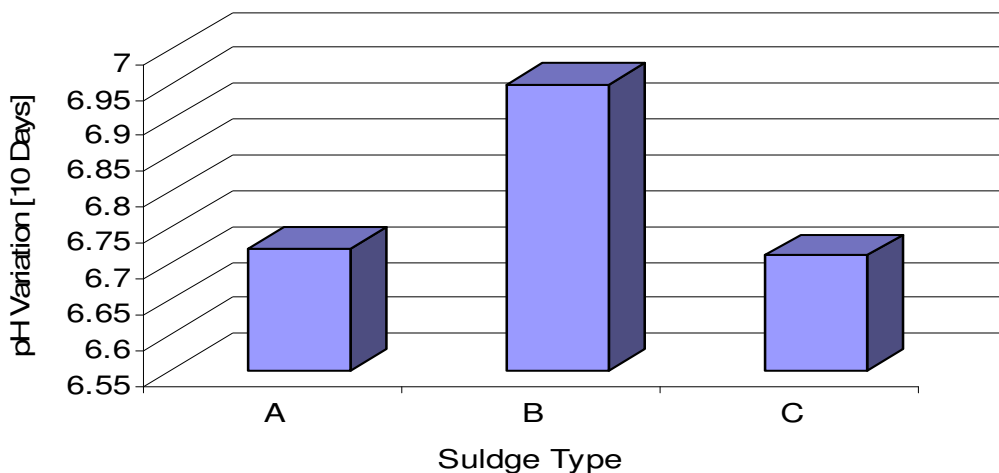
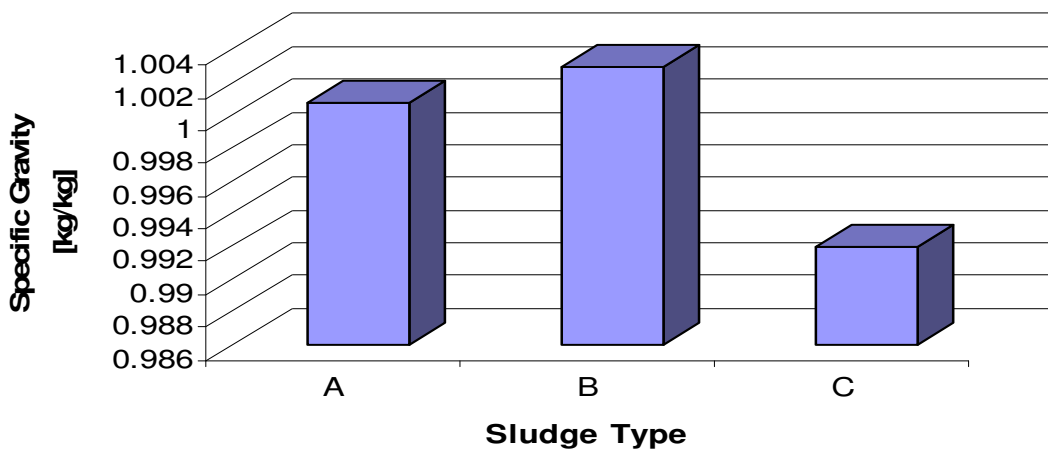


Figure 4.4: pH's of Raw Anaerobic Sludge

Figure 4.4 also shows a pH of 6.99 for Sludge B after 10 days of separation, Sludge A being the closest rival with a pH of 6.72. All three sludges were at a pH of 7.00 on the first day of the test. This test examined how stable the sludge actually is or rather how much buffering capacity (alkalinity) the system raw sludge possesses. The more stable the sludge, the smaller the decrease, due to the complete breakdown of VFA's by the methanogenic bacteria. Sludge B proved to be the most stable by far.

### 4.3.3 Specific Gravities

The specific gravities of the three sludges were compared in order to determine their solids (microbial) concentration. This is a very important parameter; as for a sludge with all the favourable requirements in place, the higher the ratio of bio-mass to water, the higher the yield of granules obtained will eventually.



**Figure 4.5: Specific Gravities of Raw Sludge**

Figure 4.5 show that Sludge B again gave the best results, with Sludge A in second place. However, the extremely low specific gravity of the third sludge definitely shows to some undesired properties.

### 4.3.4 Granule Size Distribution

This test is based on one of the main assumptions for this study; if granulation has already occurred to some extent in the digester, the necessary microbial precursors will be in place to allow for further granulation. To expand, one can say that the more continuous in terms of size distribution range the sludge is the more prone to



granulation the sludge will be. Based on the above, a sieve tray analysis (Laguna et al., 1999) was done for the three sludge types (Appendix: Section A2).

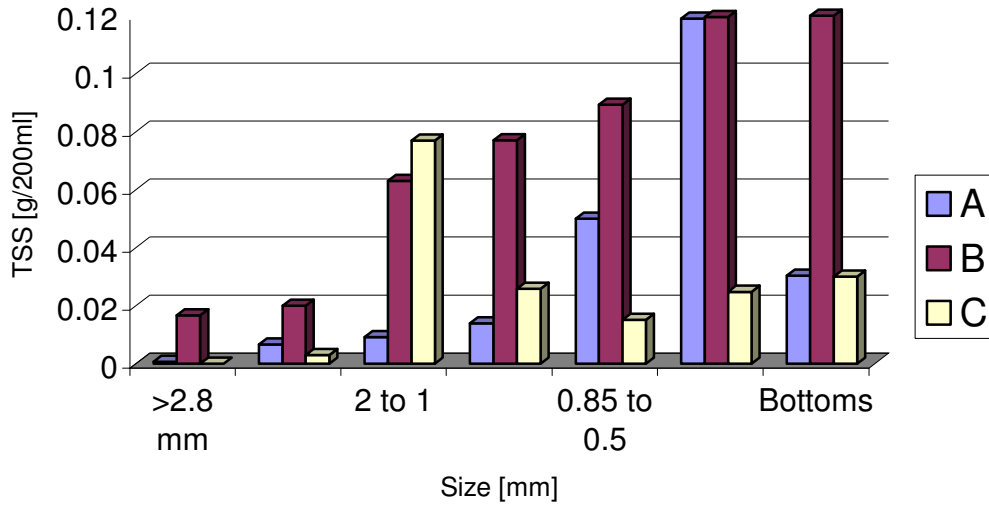


**Figure 4.6: Granule Size Distribution of Raw Anaerobic Sludge**

Sludge B has by far the most continuous granule size range distribution, with a gradual drop in mass over each segment of the size range (see Figure 4.6). This shows that even though there are mature granules in the sludge, new granules are still formed on a regular basis. All the necessary precursors are therefore assumed to be in place in this specific sludge.

### 4.3.5 Summarized results

Table 4.1 shows that there are some good properties in all three sludge types. Nevertheless, Sludge B has by far the most desired qualities. Based on the test results, type B will be used as a standard for the rest of the research done in this thesis.

**Table 4.1: Summarised Results of the Sludge Screening Tests**

Sludge	Log term pH stability	10 Day pH drop	Settlability [mm/s]	Specific Gravities	Granule size distribution
A	3 months	0.15	0.005	1.002	Discont.
B	3 weeks	0.01	0.001	1.004	Cont.
C	2 days	0.25	0.019	0.994	Discont.

Sludge B has approximately the same viscosity as tomato sauce (in the order of 1 Pa.s) with a pitch-black colour (see Figure 4.7, 'disperse') and a definite methanic odour indicating a high methanogenic activity. The sharp volatile fatty acid scent, which usually points to a high acidogenic activity, was completely absent. As can be noted from the above, it also has a density higher than that of water.



Figure 4.7: Raw Anaerobic Digester Sludge

#### 4.4 Reactor Feed Optimisation

Due to the fact that a single experimental run (and thus one data point) on the bioreactors takes 20 days, the effects of all the additives used in the process could not be studied by conventional means in the Phase 3 bench-scale bioreactors. To study these effects in detail, many data points are needed and if the 3 bench scale units were used, an extended period of time and considerable amount of resources would be required to perform this study. If the feedstock optimisation were ignored, a major shortcoming would occur in the study, since a limiting reactant might easily have been overlooked. Comprehensiveness was thus the key motivator for the feed medium optimisation study.

The aim of this study was threefold; to find optimum concentrations for additives that were known to aid in the granulation process, to search for and test of few additives that might aid in the granulation process; and thirdly, to identify the main limiting reactants (apart from pH and COD) in the feedstock. The feed optimisation study was done on

shaker tables (Britz et al., 1999). This technique was chosen because many tests can be done in parallel - shortening the time period dramatically. Due to the small reactor volumes, the amount of feedstock consumed could be kept to a minimum.

Three experimental runs were conducted with fifteen 250 ml Schott bottles used per run, yielding 45 data points in 60 days. Only nine data points could have been obtained with the three test reactors in this time period. The procedure can be summarised as using a basic feed medium (Appendix, Section A1), yielding an increase of 500% ( $TSS_{\text{before}}/TSS_{\text{after}}$ ) in granular biomass of diameter larger than 0.5 mm after 20 days on the shaker tables. This was used as the base case. For these tests, the concentration of one additive at a time was increased in regular intervals and the percentage increase in TSS carefully noted.

#### 4.4.1 Base Case and Growth Curve

A steady increase in granulated biomass occurred between day 8 and day 17. The last three days showed a rapid increase in granular biomass yielding a final increase of 500% ( $TSS_{\text{before}}/TSS_{\text{after}}$ ) over the 20 day incubation period (see Figure 4.8).

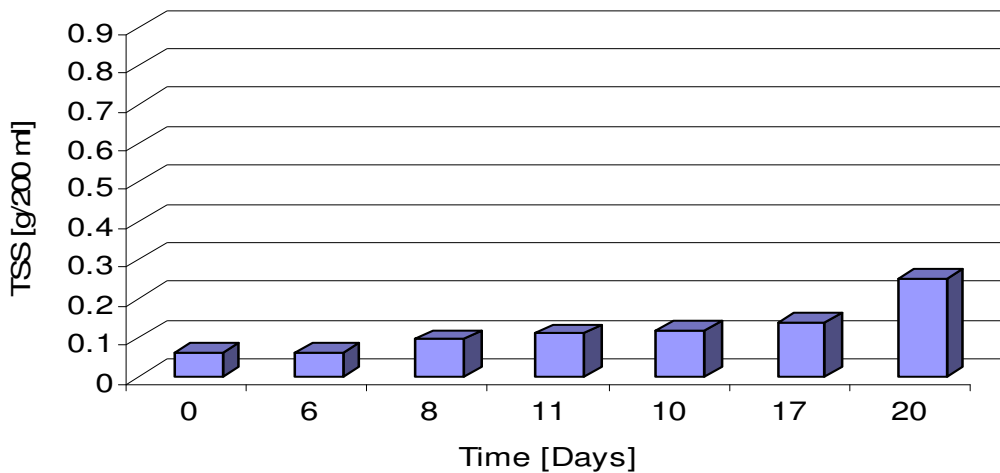


**Figure 4.8: Granule Growth over 20 Days**

#### 4.4.2 Variation of the CaCO<sub>3</sub> Concentration

The variation of CaCO<sub>3</sub> shows a gradual TSS yield increase from concentration of 200 mg/l, with a peak in the yield at the 400 mg/l region. This peak was followed by a gradual decrease in the 600 to 1100 mg/l region (see Figure 4.9).

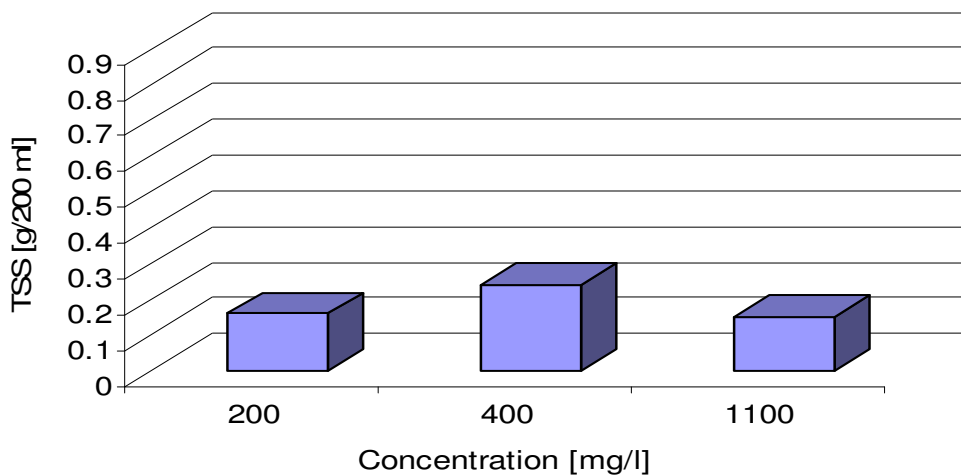


**Figure 4.9: Variation in CaCO<sub>3</sub> Concentration**

This increase can be attributed to the fact that CaCO<sub>3</sub> aids in the granulation process up to a certain point; beyond this concentration calcium becomes gradually inhibitory to microbial growth. At high calcium concentrations, the amount of calcium absorbed by the granules rises to such a level that the granule density increases excessively. This compact structure inside the granules inhibits the mass transfer of metabolites and waste inside the granules to such an extent that overall granule growth is inhibited (see Section 2.5.2).

#### 4.4.2 Feed Processing Through Filtration and Sterilisation

Filtering and autoclaving the feed do not increase the biomass yield enough to justify the time and effort spent on it (see Figure 4.10). The autoclaving process is extremely costly in a high throughput situation, rendering the scale-up economically less viable.

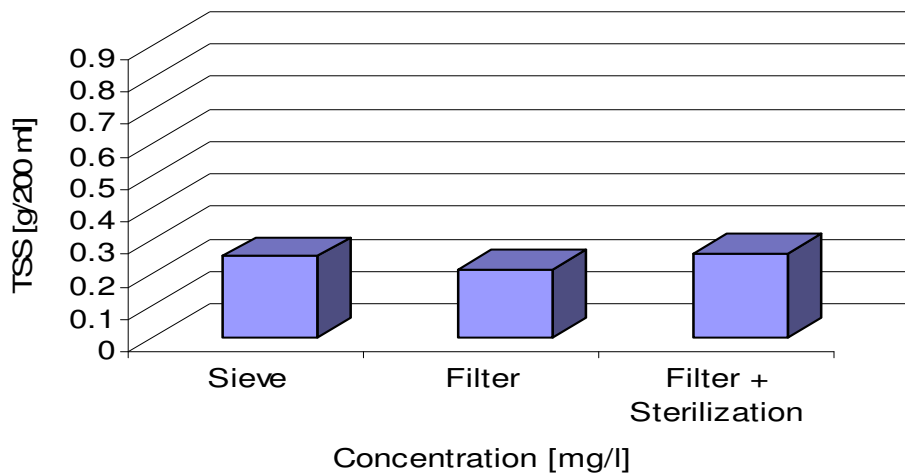


**Figure 4.10: Feed Variation**

#### 4.4.4 Variation of the $\text{KH}_2\text{PO}_4$ Concentration

Compared to the TSS yield of 500% for the basic feed medium (at 200 mg/l), phosphates are one of the key growth rate limiting reactants of this system, yielding a nearly 1800% increase in granular biomass in the 800 mg/l region (see Figure 4.11).

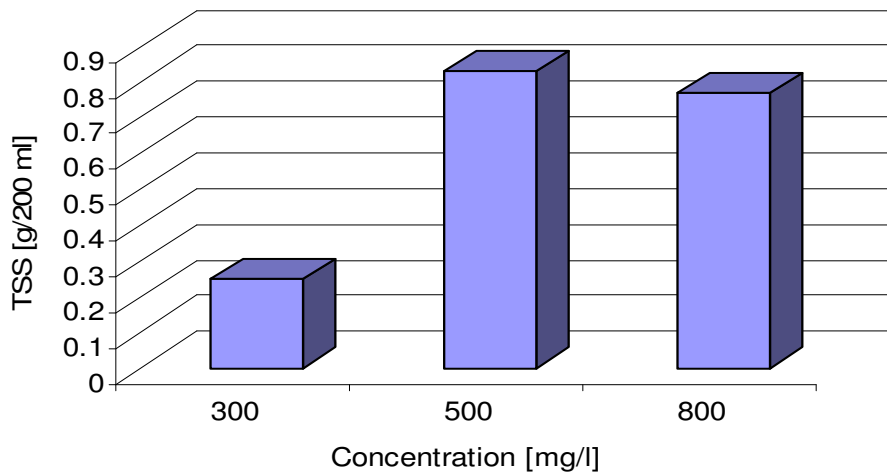


**Figure 4.11:  $\text{KH}_2\text{PO}_4$  Variation**

Phosphates have a positive effect on the hydrophobicity of cell walls and thus aid in the granulation process via local surface dehydration (Van Loosdrecht et al., 1987). The findings displayed in Figure 4.11 supports this theory. Phosphates also aid in the production of ECP, this will be discussed in greater detail in Chapter 7.

#### 4.4.5 pH Manipulation via $\text{Ca}(\text{OH})_2$

In this test, NaOH was replaced with  $\text{Ca}(\text{OH})_2$  as main pH manipulator additive in the feed. An increase of approximately 0.5 g/200 ml (TSS) was observed with  $\text{Ca}(\text{OH})_2$ , compared to only 0.24 g/200 ml (TSS) with NaOH (Figure 4.12). These results agree with the theory that monovalent anions (especially sodium and potassium) have a negative effect on granulation and should be avoided as far as possible in additives to feedstock's (Britz et al., 1999) and that calcium aids in the granulation process (Mahoney et al., 1987). The tests were done in triplicate to ensure accuracy.

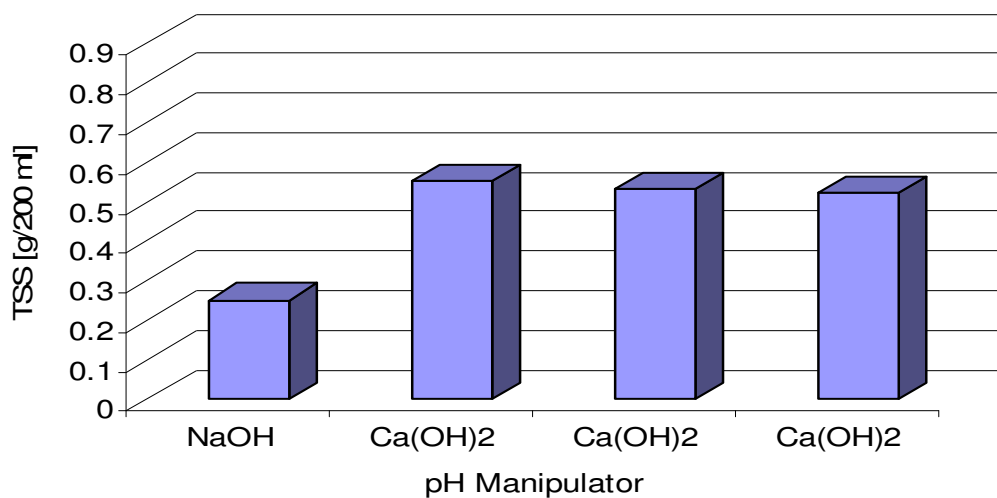
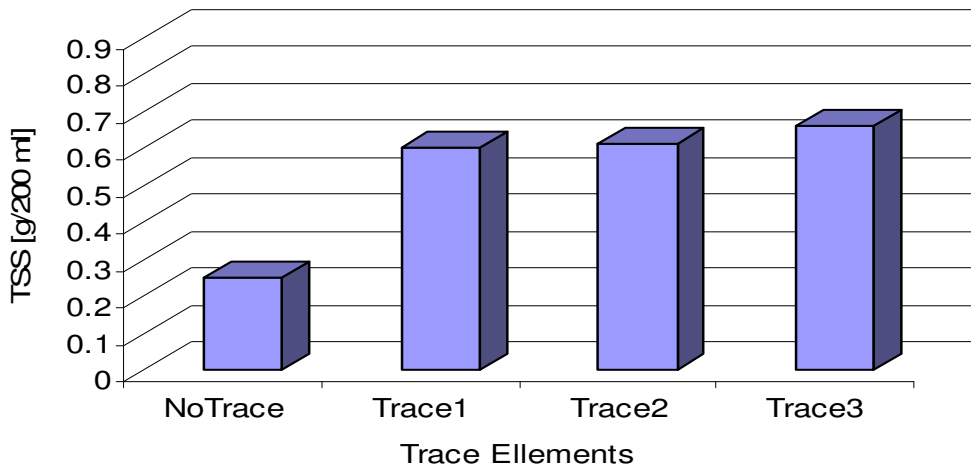


Figure 4.12: Feed pH Manipulation with  $\text{Ca}(\text{OH})_2$

#### 4.4.6 Trace Elements

Trace elements are defined as vitamins and minerals essential for microbial growth (Nel and Britz, 1985). 10 ml/litre was added to the feed to test whether these elements aid the granulation process. This led to an average increase of 0.58 gTSS/200 ml, 0.36 g better than without trace elements. Therefore, it can be concluded that trace elements definitely aid in the granulation process. Figure 4.13 reflects this conclusion. The trace element test was done in triplicate to ensure accuracy.



**Figure 4.13, Trace Elements**

#### 4.4.7 COD Variation

The Chemical Oxygen Demand (COD) of the feed were varied to study the effect of a higher COD on the occurred growth over the 20 day period. Figure 4.14 shows that a COD of up to 3000 mg/l yields satisfactory results. Further increase in the COD level of the feed resulted in a dramatic decrease in the yield of granular mass less than 0.5 mm (MUG) in diameter.

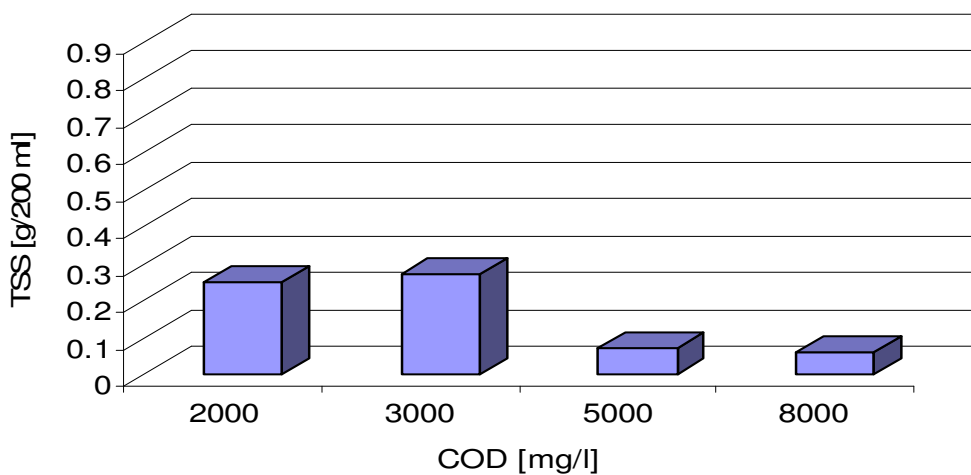


**Figure 4.14 COD Variation in Feed**

## ***4.5 Bioreactor Optimisation with Regards to Mixing Speed***

This section revolves around finding the mixing speed of the impellor (in the case of R<sub>4.15</sub> and R<sub>7.2</sub>), or the rotation speed (R<sub>5.5</sub>) at which the highest yield of usable granules are obtained. Another main objective will be to see which of the three reactor configurations gives the highest yield of usable granules, rather granular anaerobic colonies with a sieve diameter of larger than 0.5 mm (MUG). Results obtained by using the optimised feed will only be incorporated later in this chapter, since the feed optimisation and mixing speed optimisation were done in parallel. In other words, the optimum mixing speed will first be determined with the normal medium, in the following experimental run, done at the same mixing speed, the optimised medium will be incorporated (C and D on Figure 1.2). Due to resource and time considerations, only the best of the three reactors will then be optimised to produce the optimised process output (E on Figure 1.2).

Experimental procedures such as the loading, tapping and feeding of the reactors can be obtained from Section A1 of the appendix. The data analysis techniques used on the inoculum can be obtained from Section A1.2 of the Appendix. During the 20-day inoculation period, a number of different parameters are measured. These will include the biogas production volume, the methane concentration of the biogas, the amount of COD consumed on a daily basis and the amount of additives needed to buffer the system and maintain a relatively stable pH inside the reactors. At this point KHCO<sub>3</sub> was used to increase the alkalinity of the system. The reason for using this additive is that literature stated that too much calcium will inhibit the granulation process (Mahoney et al., 1987). However, it was found, in the feed optimisation study, that CaCO<sub>3</sub> provides sufficient buffering capacity at 400 mg/litre, but these results will only be incorporated in the next section.

### **4.5.1 Experimental Runs 1 to 5**

Runs 1 to 5 was done only on R<sub>4.15</sub> and R<sub>7.2</sub> of which the last three were discussed in detail in Chapter 3 (or Phase 2 of the WRC project). On the fifth run in Phase 2 large errors occurred in the final yields of both reactors probably caused by leaks that occurred on the worn out seals. The first five runs can mostly be considered commissioning and orientation runs done to become acquainted with the dynamics of a



biological system. This study proved above all that anaerobic bio-granulation can be enhanced in an artificial environment such as a bioreactor. The results also pointed to the fact that the mixing patterns induced by the two reactors were less than optimal, hence the irregular shape of the granules.

#### 4.5.2 Experimental Run 6

Run 6 was the first run during which reactor R<sub>5.5</sub> was commissioned. In Phase 2, pH manipulation was far more difficult an obstacle than anticipated. This was due to low alkalinity in the system, but was successfully counteracted by the addition of KHCO<sub>3</sub> to the basic feed medium. The mixing speed of the units was set to 2 revolutions per minute and the run was started. From the beginning R<sub>4.15</sub> proved to be a problematic reactor configuration: the many moving parts and the fact that sand entered the lower bearing and grinding of the seals, resulted in leaks.

R<sub>7.2</sub> proved to be the most temperamental as far as pH is concerned. This unit needed more additives per unit volume of feed medium than the other two reactors. In the case of R<sub>5.5</sub>, very little sludge was lost when the used feed was drawn off each day, and the measured activity, at the same mixing speed and feed composition, was higher than in the other two units. The relevancy of this will be proven later.

**Table 4.2: Experiment 6 Results**

AVG	R6R <sub>4.15</sub>	R6R <sub>5.5</sub>	R6R <sub>7.2</sub>	
pH	6.7	6.7	6.00	
CaCO <sub>3</sub>	381	381	381	mg/d
KHCO <sub>3</sub>	43	43	53	mg/d
CH <sub>4</sub>	28	36	30	dm <sup>3</sup> /d.Vr
COD	344	354	348	mg/d.Vr
MUG	3.34	4.3	3.74	Kg/Vr

Table 4.2 presents the average values of the pH, concentration of the additives added, the amount of methane produced and the COD consumed per day for the entire run. The average amount of CaCO<sub>3</sub> and KHCO<sub>3</sub> fed per litre of feed per day was exactly the same for the three units and the phosphate and urea content were also kept constant at 200 mg/l. From these results the pH problems in R<sub>7.2</sub> is clear. As is the case with the higher activity per unit reactor volume per day [cm<sup>3</sup>/(d.Vr)] in R<sub>5.5</sub> (with the Vr term from

hereon forward defined as 1 m<sup>3</sup> reactor volume). The amount of COD consumed by R<sub>5.5</sub> was also higher than in the other two units. R<sub>5.5</sub> proved superior by yielding a 650 % increase in granular mass over the 20-day period, exceeding the other units by 150 %.

### 4.5.3 Experimental Run 7

This run was commenced at 0.0275 m/s tipspeed (10 rpm). It was noted that a high concentration of sodium in the feed medium added to neutralise the acidic peach cannery effluent, has the tendency to de-flocculate the sludge in the early stages of the experiment. This lead to more sludge to be lost to feed extraction. No major leakages or problems occurred during this run.

**Table 4.3: Experiment 7 Results**

AVG	R7R <sub>4.5</sub>	R7R <sub>7.1</sub>	R7R <sub>5.5</sub>	
pH	6.5	6.5	6.6	
CaCO <sub>3</sub>	381	381	381	mg/d
KHCO <sub>3</sub>	57	57	57	mg/d
CH <sub>4</sub>	16	19	49	dm <sup>3</sup> /d.Vr
COD	233	292	221	mg/d.Vr
MUG	0.844	2.4	1.711	kg/Vr

After calculating the average values the methanogenic activity in R<sub>5.5</sub> was far higher than in the other two reactor configurations (Table4.3). Even though R<sub>7.2</sub> consumed more COD per unit reactor volume per day [mg/d.Vr], the unit still has a lower methanogenic activity than R<sub>5.5</sub>. In conjunction with the low pH it might (at this stage) be said that the environmental conditions inside this reactor are more suitable for the acidogenic micro-organisms, which cannot enhance bio-granulation on their own. A strong odour of volatile fatty acids from this reactor supports this theory.

After the experimental run was completed and the reactors washed, a 1.5 cm thick bio-film layer at the liquid level in R<sub>4.15</sub> was noted. This bio-film also occurred in R<sub>7.2</sub>, but was completely absent in R<sub>5.5</sub>. A possible reason for this is that R<sub>5.5</sub> is the only reactor where there is never a permanent water-air-reactor-shell interface, since the unit rotates around its own axis.

### 4.5.1 Experimental Run 8

The mixing speed of this experiment was set at 0.0825 (30 rpm). From the beginning, this experiment was plagued with problems. During the first few days, R<sub>4.15</sub> was shut down due to excessive leakages and sent in for repairs. pH manipulation was a severe problem and up to three times the normal amount of additives was added with little or no effect. On Day 10 a leak was spotted on R<sub>5.5</sub>. The unit was shut down and sent for repairs. The only reactor that survived the high mixing speeds was R<sub>7.2</sub>.

**Table 4.4: Experiment 8 Results**

AVG	R8R <sub>5.5</sub>	R8R <sub>7.2</sub>	
pH		6.39	
CaCO <sub>3</sub>	457	457	mg/d
KHCO <sub>3</sub>	119	119	mg/d
CH <sub>4</sub>		11	dm <sup>3</sup> /d
COD	424	424	mg/d
MUG		0.659	kg/Vr

Compared to Experiment 7, the KHCO<sub>3</sub> consumption was 300 % higher. Still it yielded a lower average pH and activity than in the previous experiments (Table 4.4). The yield of MUG dramatically decreased in comparison to previous (slower) experiments, and so did the activity of the methanogenic species. The COD consumption stayed high, though. The odour of volatile fatty acids was also very prominent in the used feed throughout the run. This indicates that the activity of the acidogenic species was excessive. After the completion of this run was finished, R<sub>7.2</sub> was also sent in for maintenance.

### 4.5.1 Experimental Run 9

Originally, Experiment 9 was to be done at 0.165 m/s tipspeed (60 rpm). Due to the 30 rpm run yielding such poor results, not to mention leakage problems experienced, it was decided to rather set the mixing speed of the run at 0.01375 m/s tipspeed (5 rpm). Previous results indicated that the optimum might lie in regions smaller than 10 rpm and no significant leakage problems occurred during this run.

The settling velocities of the reactor volumes were also measured at regular intervals. However, these have shown to have a negative effect on the overall activity of the methanogens, via the introduction of above normal levels of oxygen due to the nature of the settling tests (Section A1.3 of the Appendix). Settling tests on the reactor volumes were done in this run in an attempt to observe changes in settling velocity with regards to time.

**Table 4.5: Experiment 9 Results**

<b>AVG</b>	<b>R9R<sub>4.15</sub></b>	<b>R9R<sub>5.5</sub></b>	<b>R9R<sub>7.2</sub></b>	
<b>pH</b>	6.49	6.38	6.39	
<b>CaCO<sub>3</sub></b>	457	457	457	<b>mg/d</b>
<b>KHCO<sub>3</sub></b>	119	119	119	<b>mg/d</b>
<b>CH<sub>4</sub></b>	15	15	19	<b>dm<sup>3</sup>/d.Vr</b>
<b>COD</b>	339	392	440	<b>mg/d.Vr</b>
<b>MUG</b>	0.467	1.654	0.753	<b>Kg/Vr</b>

As can be seen in Table 4.5, the activities of this experiment do not co-ordinate with previous results. Here R<sub>7.2</sub> showed the best results with an activity of 19.28 cm<sup>3</sup> methane per day per unit reactor volume. If one interpolates between 0.0275m/s and 0.0055 m/s tipspeed, an activity of approximately 40 cm<sup>3</sup>/d.Vr can be expected. The only explanation for the low activity is possibly the introduction of oxygen via the settling tests done in this run. Some serious problems occurred in R<sub>4.15</sub> during this run, as can be seen from the MUG results. This means that destruction, rather than growth of granules occurred. The results from R<sub>7.2</sub> and R<sub>5.5</sub> were also far lower than expected.

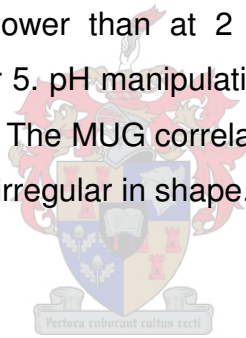
### 4.3.1 Experimental Run 10

Studying the results obtained from Experiments 6, 7 and 9, the mixing speed of the reactors were decreased even more, reaching a level of 0.00275 m/s (1 rpm).

**Table 4.6: Experiment 10 Results**

AVG	R10R <sub>5.5</sub>	
pH	6.65	
CaCO <sub>3</sub>	371	mg/d
KHCO <sub>3</sub>	86	mg/d
CH <sub>4</sub>	23	dm <sup>3</sup> /d.Vr
COD	272	mg/d.Vr
MUG	3.99	kg/Vr

As can be noted from Table 4.6, the activity (CH<sub>4</sub> produced) of the reactor was higher than at 5 rpm (Table 4.5), but lower than at 2 rpm (Table 4.2). Less COD was consumed than in either of run 2 or 5. pH manipulation was done with far less additives than in the higher agitation regime. The MUG correlates well with that obtained from run 6 (2 rpm), but granules were more irregular in shape.



## 4.6 Graphical comparison of results obtained

### 4.5.1 Mixing speed vs. Increase in Granular Mass

The increase in granular mass (MUG) was calculated for runs 6 to 10 (Appendix: Section A2.5). Figure 4.15a and b (focusing on the 0 to 0.03 m/s tipspeed range) represents these results for the 3 individual test reactors in graphical form.

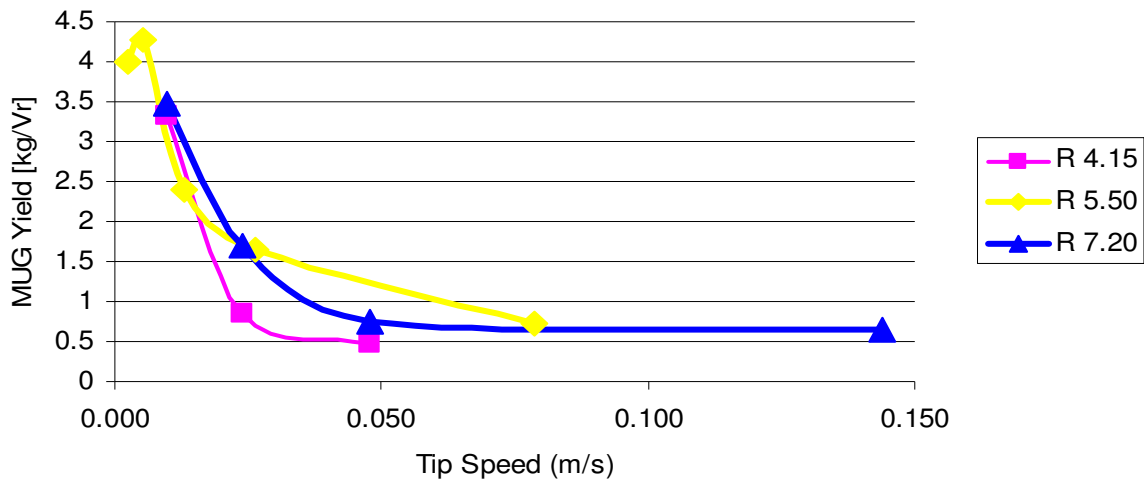


**Figure 4.15a: Yield (MUG) vs. Impellor Tipspeed**

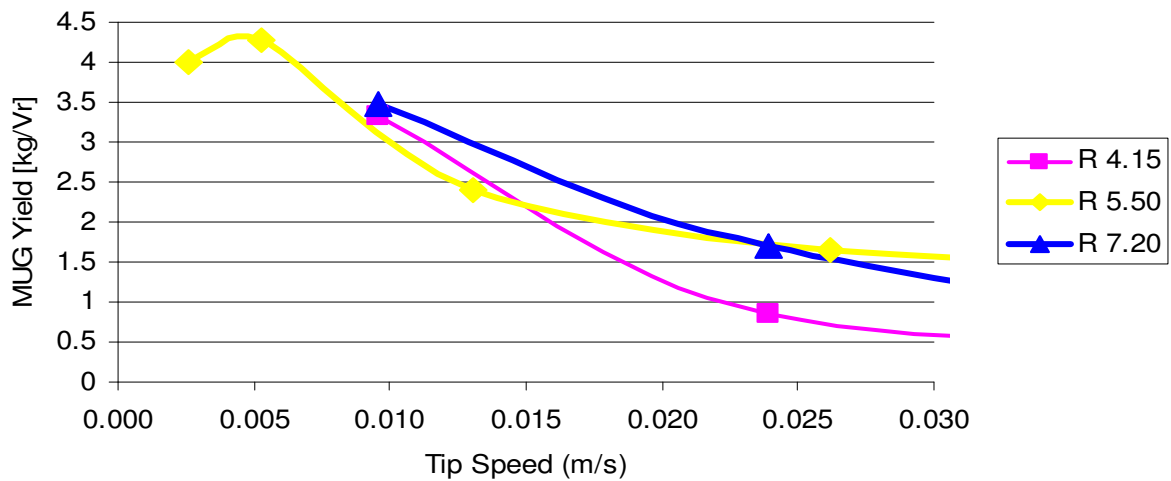


**Figure 4.15b: Yield (MUG) vs. Impellor Tipspeed**

As can be gathered from the graphs in Figure 4.15a and b, the yield of usable granules decreased dramatically in the region  $0.0055 \text{ m/s} < \text{tipspeed} < 0.05 \text{ m/s}$  for all three of the reactors. At high mixing speeds, nearly no enhancement of granulation occurred. Also from this it can be seen that  $R_{5.5}$  is by far the best reactor configuration. It showed on average a 25% larger increase in granular mass than its closest rival  $R_{7.2}$ , and  $R_{4.15}$ , the latter surely the worst granulation enhancement design. The shape and density of the granules produced by reactor  $R_{7.2}$  and reactor  $R_{4.15}$  are of a far lower quality than that produced by reactor  $R_{5.5}$ .

Originally it seemed that an inflection point occurred in the  $0.013 \text{ m/s}$  range for all three of the reactors. It was therefore decided to repeat this experiment, and the inflection point in the yield did not occur again. This might be attributed to the oxygen inhibition of

the methanogenic species, resulting in a lower than expected yield. This was caused by settling tests that were done on the reactor volumes in this experiment. If it is assumed that granules are 85% water, the best yield obtained was 4.3 kg usable granules per m<sup>3</sup> reactor volume per 20 days at a baffle speed of 0.0055 m/s with R<sub>5.5</sub>. From the abovementioned figures it can be seen that no data exists for the 4.15- and 7.2 liter reactors at the 0.00275 m/s tipspeed, the reason for this is that these low speeds are not attainable with this two units due to design constraints.

#### 4.5.2 Mixing Speed vs. Methane Produced

The amount of methane produced gives a good indication of the activity of the methanogenic species in the inoculums. This is important because filamentous methanogens are one of the main precursors for anaerobic granulation. In other words: if the methane production is low, no granulation will occur as the environmental conditions inside the reactor will be undesirable.

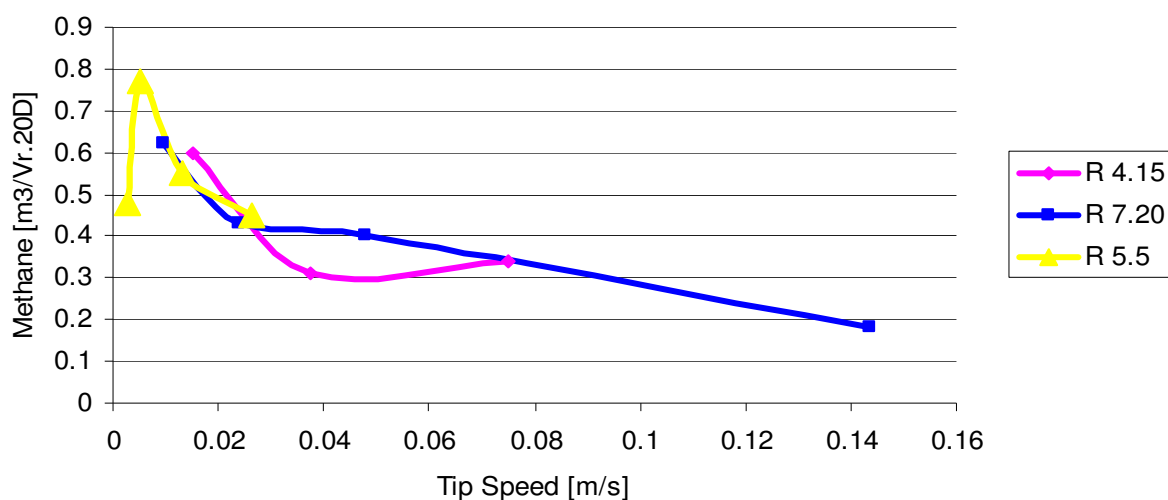


**Figure 4.16: Methane Produced vs. Mixing Speed**

It can be noted (Figure 4.16) that the largest amount of activity occurred in the 0.0055 m/s < tipspeed < 0.05 m/s range, with a gradual drop towards the higher agitation velocities. The inflection in the 0.01375 m/s range is also present, again hinting towards the unexpected drop in activity experienced in this experimental run. R<sub>5.5</sub> showed the highest average activity thus far.

### 4.5.3 Mineral Consumption vs. Mixing speed

pH manipulation is aided by  $\text{CO}_3^{2-}$  and NaOH.  $\text{CO}_3^{2-}$  is introduced in two forms. Firstly, in the form of  $\text{CaCO}_3$  to add calcium to the mineral pool and secondly, in the form of  $\text{KHCO}_3$  to up the alkalinity of the medium. At this stage it was still believed that levels in the order of 300 mg/litre  $\text{CaCO}_3$  will poison the granulation process (Mahoney et al., 1987), it was only proven from results obtained in the feed optimisation section that this is not the case. NaOH is only used in small quantities to do minor adjustments to the pH, since it has been proven that  $\text{Na}^+$  is slightly inhibitory to the granulation process (Britz and Van Schalkwyk, 2002).

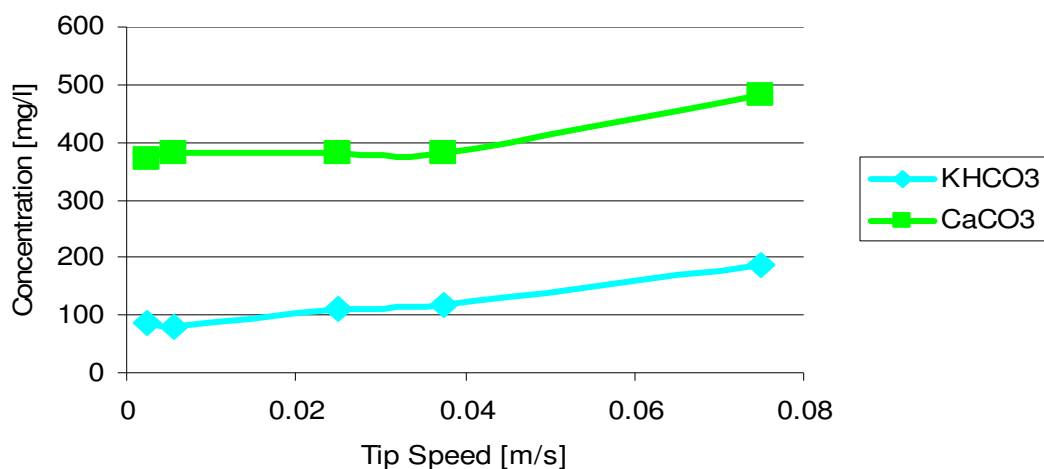


**Figure 4.17:  $\text{KHCO}_3$  and  $\text{CaCO}_3$  Consumed to Maintain pH vs. Mixing Speed**

Figure 4.17 evidently shows that, in order to maintain a relatively stable pH, the amount of  $\text{KHCO}_3$  (and resultant alkalinity) needed increased substantially. At a tipspeed of 0.075 m/s, an extra 100 mg/litre of  $\text{KHCO}_3$  was added. The same tendency occurs in the consumption of  $\text{CaCO}_3$ . In the lower mixing speeds the amount needed is approximately stable, but at higher mixing speeds, a dramatic increase can be noted. If Figure 3.16 and 3.17 is compared, a possible explanation for the larger amount of additives needed to maintain pH can be the build-up of organic acids in this system. This is supported by the fact that the overall COD consumption and thus the overall activity, increased at the higher mixing speeds (to be discussed in Section 4.5.5). However, the specific methanogenic activity dropped dramatically, resulting in a low conversion rate of organic acids.



### 4.5.5 COD Consumed vs. Mixing Speed

The amount of COD consumed gives an indication of the overall activity of the microbial community. That is to say the combined activity of the acetogenic-, acidogenic- and methanogenic subgroups, and a high activity of the latter two groups does not aid in the granulation process. This implies that when the amount of COD consumed is high and the amount of methane produced in the biogas is low, the environment inside the reactor is unsuitable for methanogenic anaerobes and therefore, not optimised for granulation. Figure 4.18 displays the COD consumption vs. mixing speed for the reactors.

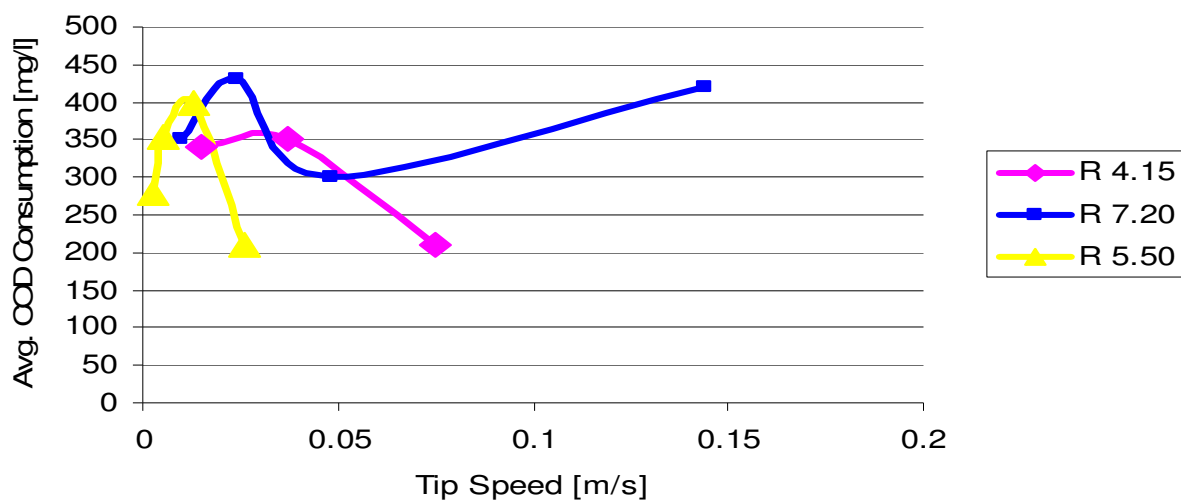


Figure 4.18: COD Consumption vs. Mixing Speed

R<sub>7.2</sub> consumed on average the most COD per day, but methanogenic activity in this unit is far lower than in R<sub>5.5</sub>. R<sub>4.15</sub> yielded the smallest consumption of COD, but also the lowest average activity and increase in biomass.

## 4.7 Optimised Process Output

This section combines the research in sections 4.5 and 4.6. Optimised feed was used in the reactor that showed overall the best results (R<sub>5.5</sub>), at a mixing speed that yielded the best results. The aim of this section of study is thus to produce the highest possible MUG yield per unit reactor volume.

### 4.7.1 Experimental Run 11

Based on the results taken from section 4.4, the feed composition was changed in the following way:

COD	2000 mg/l	
CaCO <sub>3</sub>	500 mg/l	
Urea	200 mg/l	
KH <sub>2</sub> PO <sub>4</sub>	800 mg/l	(originally 200 mg/l)
Trace Elements	10 ml/l	(originally none)
Ca(OH) <sub>2</sub>	Used for pH	(originally NaOH)
Adjustments in medium		

KHCO<sub>3</sub> was completely abandoned due to the superior results obtained with CaCO<sub>3</sub>.

The optimised feed was now inoculated, along with the correct amount of sludge into the 5.5 litre reactor (R<sub>5.5</sub>) and incubated for 20 days at 2 rpm (or 0.0055 m/s tipspeed).

These were the results:

**Table 4.7: Experiment 11 Results**

AVG	R11R <sub>5.5</sub>	
pH	6.6	
CaCO <sub>3</sub>	500	mg/d
KH <sub>2</sub> PO <sub>4</sub>	800	mg/d
CH <sub>4</sub>	25	dm <sup>3</sup> /d
COD	900	mg/d
MUG	14.3	Kg/Vr



#### 4.7.2 Experimental Run 12

This run was basically a confirmation test, to check the results obtained from Experiment 11. The following results were obtained:

**Table 4.8: Experiment 12 Results**

AVG	R12R <sub>5.5</sub>	
pH	6.6	
CaCO <sub>3</sub>	500	mg/d
KH <sub>2</sub> PO <sub>4</sub>	800	mg/d
CH <sub>4</sub>	43	cm <sup>3</sup> /d
COD	930	mg/d
MUG	15.2	kg/Vr

As can be seen from the results in Table 4.8, an even higher yield occurred.

## 4.8 Summary

Figure 4.20 contains the timeline of the project, as well as an account of how the yield increased over time.

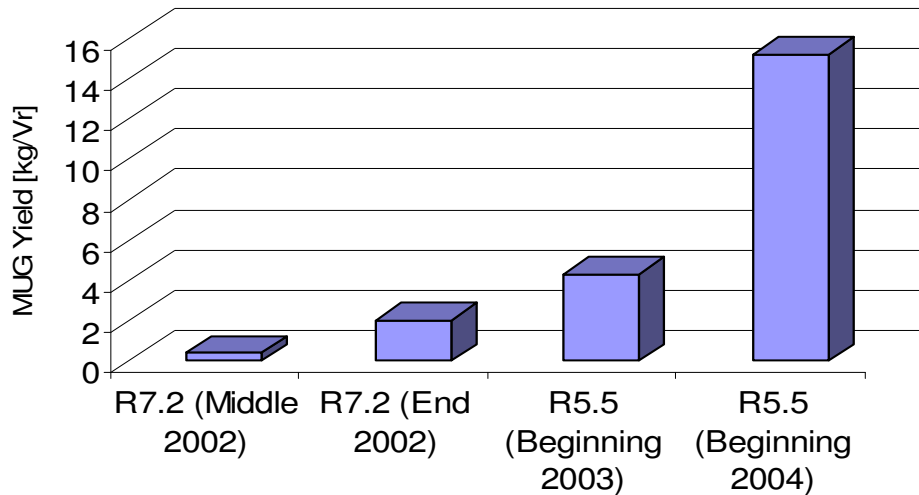


**Figure 4.19: MUG Timeline**

An increase in yield occurred over the reactor optimisation period. At the beginning of the optimisation study, yields estimated at 0.5 kg MUG were common. As the process and designs were optimised, this yield was upped to 2.02 kg MUG towards the end of 2002. In the beginning of 2003, the 5.5 litre reactor was introduced and a 100% increase (4.4 kg MUG) was experienced with the new reactor configuration. After the optimum mixing speed was obtained and the feed optimisation section of the study were completed this yield was increased substantially to 15.2 kg MUG. Therefore it can be concluded that the optimisation part of the study is considered successful.

Figure 4.15 contains what is probably the most important result. Clearly, R<sub>5.5</sub> is by far the best reactor configuration. It showed on average a 25% higher increase in granular biomass than the other two reactors, as well as a yield of 15.2 kg granules larger than 0.5 mm in diameter per cubic meter of reactor volume for 20 days (MUG).

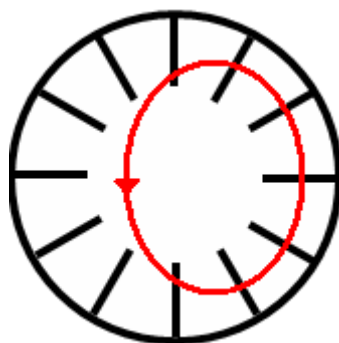


**Figure 4.20: Flow Patterns in R<sub>5.5</sub> (Red shows the sludge movement)**

This higher yield can possibly be attributed to the difference in mixing patterns that is induced by R<sub>5.5</sub>. Figure 4.20 shows the rotational movement induced on the reactor volume by the rotating shell and baffles. If this is compared to the configurations of R<sub>7.2</sub> and R<sub>4.15</sub> (Figures 3.18 and 3.19) it is clear that the motion induced on the sludge is far more uniform. Furthermore, the 5.5 litre unit induces a rolling effect, yielding more roundly shaped granules resulting in higher stability and a higher settling velocity.

From the optimisation of the feed medium used to enhance the spontaneous bio-granulation of anaerobic sludge, the following additive concentrations yielded the highest growth over the 20 day period\*\*:

COD	2000 mg/l
CaCO <sub>3</sub>	400 mg/l
Urea	200 mg/l
KH <sub>2</sub> PO <sub>4</sub>	800 mg/l
Trace Elements	10 ml/l
Ca(OH) <sub>2</sub>	Used for pH adjustments in medium

KHCO<sub>3</sub> was completely abandoned when it was proven that CaCO<sub>3</sub> provided adequate buffering capacity to the system and calcium did not inhibit the yield, at 400 mg/litre. A further reason for abandoning KHCO<sub>3</sub> that it was proven that monovalent anions like potassium have an inhibiting effect on granulation, this correlates well with findings from literature (Britz et al., 1999). To update, reactions and interactions between the various additives, once inside the medium, have not been studied. Slight changes to the optimised feed might therefore still occur in future.

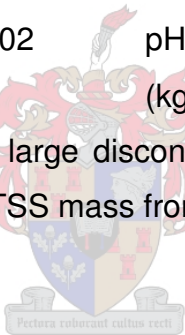
\*\* Compare to the Basic Feed Medium Composition in Section A1.2 of the Appendix

From Figure 4.16 it can be concluded that the highest methanogenic activity (a function of the amount of methane produced per time unit) occurred in the 1 to 5 rpm range. This supports the notion that methanogenic species aid in the granulation process (Metcalf and Eddy, 2003). It is also the mixing range in which the largest MUG yields were obtained.

A drastic increase in the consumption of additives (to maintain pH) occurs as the mixing velocity of the reactors increases. Not only will the granule yield drop dramatically above 0.1 mm/s, but it will be more expensive to operate in this range.

From the results obtained with the sludge used as inoculum in the tests, it is evident that this sludge (Sludge B) is prone to agglomeration and granulation. Here is some screening criteria to which a virgin anaerobic sludge should concur to:

Settlability:	<0.004	mm/s
$\Delta$ pH over 10 days:	<0.02	pH-units
Specific Gravity:	>1	(kg/kg)
Granule Size Distribution:	No large discontinuities, with a continuous decrease in TSS mass from 0 to 2mm.	



# 5. Growth Analysis

## Revision

---

### 5.1 Introduction

As stated in various articles, there is a dire need for a quantitative method to classify the anaerobic bio-granule growth (Britz et al., 1999, and Britz and Van Schalkwyk 2002, Els and Van Zyl, 2002). The methods currently used (visual counting and MUG) are not only operator dependant, but can lead to large errors, and/or can be very time consuming and cumbersome to perform.

Visual counting was the original method the Department of Food Sciences Phase 1 (Figure 1.2; Appendix: Section A8). With this method, a sample of granulated anaerobic sludge is diluted with water and the granules are physically counted. Even though the size range of the granules were from 'pinprick size' to nearly 2 mm in diameter, no distinction was made between the different sizes of these granules.

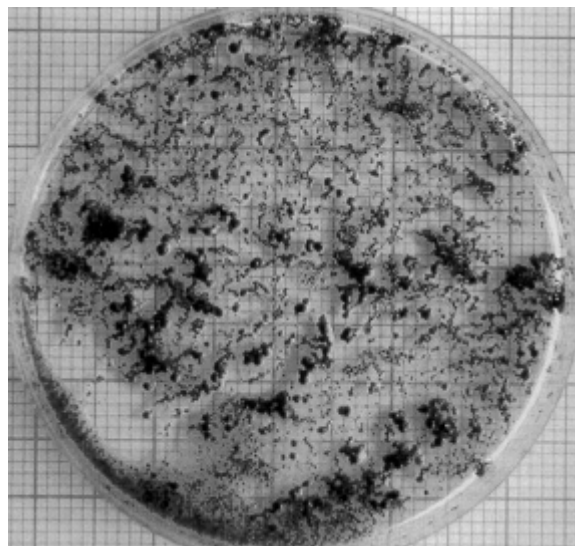


**Figure 5.1, Granulated Anaerobic Sludge (Britz and Van Schalkwyk, 2002)**

Figure 5.1 depicts a typical image of granulated and dispersed anaerobic sludge, it is nearly impossible to visually count the amount of 'granules' present, especially if one tries to count from 'pinprick' size.

In Phase 2, a more quantitative method of growth analysis was incorporated based on a discussion given in Laguna et al., 1999; a discussion of the 'MUG' method can be seen in Section A2 of the Appendix. However, the sieve-tray-TSS method is far from without problems. The main problem is that this is a destructive method due to the drying and long period of time the anaerobic micro-organisms are exposed to oxygen. To obtain accurate results, a sample of 200 ml must be drawn from the reactor volume. If this is done at Days 5, 10, 15 and 20, it has a dramatic impact on the overall growth in the reactor. This leads to a classic case of Heisenberg's uncertainty principle: "By observing, we disturb to such an extent that the observations that are made are not entirely accurate" (Powers, 1993).

Other problems include the time and resources needed to obtain the TSS masses. For example, if a sludge sample is divided into 3 size ranges, the TSS mass needs to be obtained for each size to produce accurate results. If this is then done for up to 6 (see Chapter 7) bioreactors at a time, 54 samples are generated every 5 days. If an average time to process 9 samples is taken at 4 hours, this procedure indeed proves to be very labour and time intensive. Laguna also discussed some of the other methods used to determine UASB granule growth in his 1999 article; Table 5.1 gives a summary of the advantages and disadvantages of these methods of analysis:

**Table 5.1: Currently Used Methods of Analysis for Determining Granule Growth (\*)**

<b>Method</b>	<b>Advantages</b>	<b>Disadvantages</b>
<b>Microscope Sizing (Visual Counting)</b>	Simple, Readily Available Apparatus (Microscope), Non-time-consuming, Non-destructive	Subjected to Human Error, Reproducibility Problems, Do Not Distinguish Between Different Sizes, Only Gives Granule Count
<b>Settling Velocities</b>	Simple, Readily Available Apparatus, Non-time-consuming, Non-destructive	Messy, Assumes Stoke's Law Apply, Introduces O <sub>2</sub> which Poisons Microbes, Only Gives Average Granule Size, Not the Number of Granules
<b>MUG</b>	Gives Histogram of Mass of Granules Per Size Range, Accurate	Destructive, Very Time Consuming, Do Not Give Granule Counts
<b>Image Analysis</b>	Non-time-consuming Once Implemented, Very Accurate Results, Gives Granule Count and Histogram of Sizes, Non-destructive	Expensive (approximately 10 000 \$US), Tedious Implementation and Calibration.
<b>Laser Analysis</b>	Non-time-consuming Once Implemented, Very Accurate Results, Gives Granule Count and Histogram of Sizes, Non-destructive	Expensive (approximately 60 000 \$US), Tedious Implementation and Calibration.

\* (Laguna et al., 1999)

Taking into account the above, a different method of analysis needs to be incorporated into this study. This method should abide to the following criteria:

- The tests should be non-destructive, meaning that after the analysis, it should be possible to return the sample to the bioreactor. This will avoid disturbances to the reactor volume that might affect the granule growth which, in turn, could lead to error propagation in the long run.
- These tests should be quantitative and not qualitative in nature, preventing possible human error that could have been experienced in the first method.
- It should be versatile and not only applicable to this study, as a substantial amount of work still needs to be done on this topic. It is thus advised that one standard method be used in future.
- The method should give the following information about the sample: the amount of granules, the size distribution of the granule population, the average granule diameter as well as the size of the largest granule. These properties form the basis of future studies.
- Finally, this method should not be time and resource consuming, due to the large amount of samples that needs to be processed. As was the case with both of the previously used methods.



An image analysis system or Digital Image Processor (DIP) was chosen, as this method is quick and easy to use once implemented. Due to financial constraints and the specific criteria desired for this project, it was decided to write a DIP in Matlab®, rather than purchasing an 'off the shelf' system. This chapter will entail a brief discussion on the programming and implementation procedure of the DIP, followed by the results and discussion section which will include a comparative study on the results obtained.

## ***5.2 Programming and Implementation***

The image processor is a computer programme written in Matlab® to run on a Windows® platform PC. The Matlab® code of the computer programme can be found in Section A5 of the Appendix. For the programme to work properly, it must first be calibrated.

Firstly, the calibration sheet needs to be photographed. This sheet is basically any sheet with dark circular shapes of known size. The closer these shapes are to the size of actual granules, the more accurate the calibration will be. Now, the digital camera is set up, details can be seen in Figure 5.2 (Section 5.3).

The image processor starts by giving the operator three choices. The first will be to calibrate the programme, the second to give known and already used calibration parameters and the third option is that of using the DIP to process digital images of granulated sludge.

If the first option is chosen, the operator will be asked to provide the directory path of the calibration image. Once the directory path is known, the next option is to automatically calibrate the pixel to millimetre conversion factor. The operator will be asked what the average diameter of the particles on the calibration page is. The calibration page is any sheet with a white back ground with dark curricular dots on of which the size is known (Section A1, in the Appendix).

After the auto-calibration, a black and white image is displayed on the on the screen, along with the grey threshold value (CLevel). This is the cut-off value for the black and white conversion, any other colours on the image lighter than this threshold value, will be displayed as white on the black and white image. Any colours darker than this value

will be displayed as black. This threshold value is the most important parameter for identifying granules, since it separates the darker granules from the lighter background. Next the operator must give the minimum cut-off size in millimetre. This will allow the DIP to ignore all the objects smaller than this given size. Two images will be displayed on the screen, the original and the processed image, with objects identified as granules showing as white dots on a black background. Particles smaller than the cut-off size does not feature on this image. If the operator is satisfied with the calibration, the image processor can be operated. If not, the calibration procedure can be repeated. A visual representation of the calibration can be seen in Section A1 of the Appendix.

After calibration, the DIP is ready to be used. The operator will at this stage be asked to give the directory path of the image that needs to be processed. The DIP will then yield the following; the total amount of objects identified as granules, the diameter of the largest object identified as a granule, as well as average diameter of all the identified granules. The original image will again be displayed, along with the black and white converted image and histogram of the granule size distribution of all the objects. A visual representation of the programme operation can be seen in Section 10.3.4 in the Appendix.



## **5.3 Materials and Methods**

### **5.3.1 Sampling Procedure**

Initially the reactor volume is mixed thoroughly to ensure the mix of granules, feed and sludge inside the reactors are as close to homogenous as possible. A 1 litre sample is taken from the reactor volume. This sample is again homogenised via light stirring and a 200 ml subsample is taken from the 1 litre volume. The rest of the large sample is re-inoculated into the reactor.

The sub sample is then passed through a 0.5x0.5 mm sieve and the tailings are returned to the reactor for further incubation. The granules left on top of the sieve is rinsed with water, removed from the sieve and then transferred to a Petri dish. This sample is further prepared by removing of all the particles that can visually be identified as not being granules. The test sample is now placed underneath the digital camera as

depicted in Figure 5.2. The final step before taking the picture is to ensure that there is enough space between the granules in the sample; this can be done by aid of a syringe needle. The reason for doing this is the image processor cannot distinguish between 2 small granules lying close to each other and 1 large granule; often leading to variations in the calculated MUG. A block flow diagram of this standard sampling procedure can be seen in Section A2 in the Appendix.

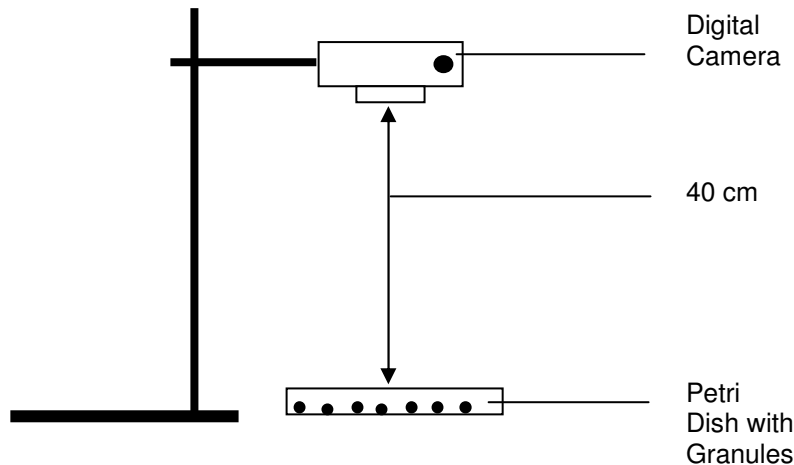


**Figure 5.2, Standard camera set-up for the DIP programme**

### 5.3.2 Calculations

Once the Total Suspended Solids (TSS) value for 200 ml sample is obtained (as discussed in Section A2 of the Appendix), the method described later in Section A2 can be used to obtain the Mass of Usable Granules (MUG). MUG is the total mass of granules with a diameter larger than 0.5 mm per cubic meter of reactor volume.

The MUG predicted by the DIP model (DIPMUG) is calculated by photographing the sample of granules larger than 0.5 mm, after which the image is processed by the DIP programme. The output of the programme then yields the following:

- 1 average particle diameter (AVG),
- 1 the number of particles in the sample (Nu) and
- 1 the largest particle diameter.

To obtain the mass of an average granule, the average particle diameter is multiplied by a constant:

$$\text{Mass of single particle} = \text{AVG} \cdot K \quad [6] \quad [5.1]$$

Now the total mass is estimated by multiplying the mass of a single particle with the amount of particles in the sample:

$$\text{DIPMUG} = K \cdot \text{AVG} \cdot N_u \quad [5.2]$$

The next step is to find a value for K as to minimise the sum of the squared error ( $SS_{\text{reg}}$ ) between the MUG and DIPMUG values for each sample in a given dataset (with n being the amount of samples in the dataset and i being the  $i^{\text{th}}$  sample in the given set):

$$SS_{\text{reg}} = \sum_{i=1}^n (\text{MUG}_i - \text{DIPMUG}_i)^2 \quad [5.3]$$

Once the optimised K value is known the model fit can be evaluated:

$$SS_{\text{total}} = \sum_{i=1}^n (\text{MUG}_i^2 - (1/n) \cdot (\sum_{i=1}^n \text{MUG}_i)^2) \quad [5.4]$$

Finally, to obtain the coefficient of determination ( $R^2$ ) the relative sizes of the variability explained by regression ( $SS_{\text{reg}}$ ) and the total measure of the adequacy of the model ( $SS_{\text{total}}$ ) is used:

$$R^2 = SS_{\text{reg}} / SS_{\text{total}} \quad [5.5]$$

[6] Even though the granules are of spherical geometry and the mass should be a function of  $\text{AVG}^3$ , it was found that the best fit of the model was obtained if AVG to the power 1 was used.

## 5.4 Results and Discussion

In this section, equations 5.1 to 5.5 will be used to compare the results of the normal MUG method to the results obtained for the same test samples using the DIP prediction (DIPMUG). These results will then firstly be evaluated statistically and then visually in the form of graphs, to see if the DIP can be used alongside the MUG calculations, or even replace it. The actual and predicted MUG results for all 3 test samples can be seen in Section A5 of the Appendix.

#### **5.4.1 Test Sample, Set 1 (200 ml)**

In MUG calculations, a 200 ml sample is drawn, passed through a 0.5x0.5 mm sieve and the TSS value (Appendix: Section A2) of the granules that did not pass through the sieve is obtained. As a first attempt, the entire granule sample in 1 Petri dish was photographed before sending the sample to the oven. The method discussed in section 5.3.2 was used to implement the DIP programme.

The initial images showed large variations in the calculated residuals where the MUG and DIPMUG is compared. A  $R^2$  value of 0.76 was obtained for the dataset, meaning that for 76% of the model predictions will be accurate. This value is a relatively good fit, but there is always a strive to higher accuracy.

#### **5.4.2 Test Sample, Set 2 (2x100 ml)**

Due to the large errors obtained in the first section (see Figures 5.3 to 5.6), for the second test set, the 200 ml samples were split and each half photographed separately. The total amount of granules for 2 images will then be compared to the 200 ml MUG of the same sample. This was done in attempt to deliver pictures with more space between granules, since this factor hampers the efficiency of the DIP programme. It is evident that the DIP preformed far better for the second dataset and yielded a classification rate of 93%. Thus, the technique of splitting the samples into 100 ml sub samples is definitely an improvement.

#### **5.4.3 Test Sample, Set 3 (4x50 ml)**

In the third test set, the sample was quartered. Yielding four, 50 ml sub-samples per (single) 200 ml sample. The reason was to study the performance of the DIP programme at an even lower dilution. The DIP prediction showed some large deviations in this section. A  $R^2 = 0.41$  was obtained, translating into an accurate prediction of only 41% of the data. One possible reason for this might be the small data set that was used, the

#### 5.4.4 Visual representation of DIPMUG vs. the actual MUG

Figure 5.3 represents the growth curve obtained from the 1 litre reactor for sample 3, showing the MUG and DIPMUG curves. The DIP predicted the day 5, 10 and 20 values to within < 20 % error range. The poor prediction of the day 15 values shows upon a possible error in the experimental procedure used on this sample.

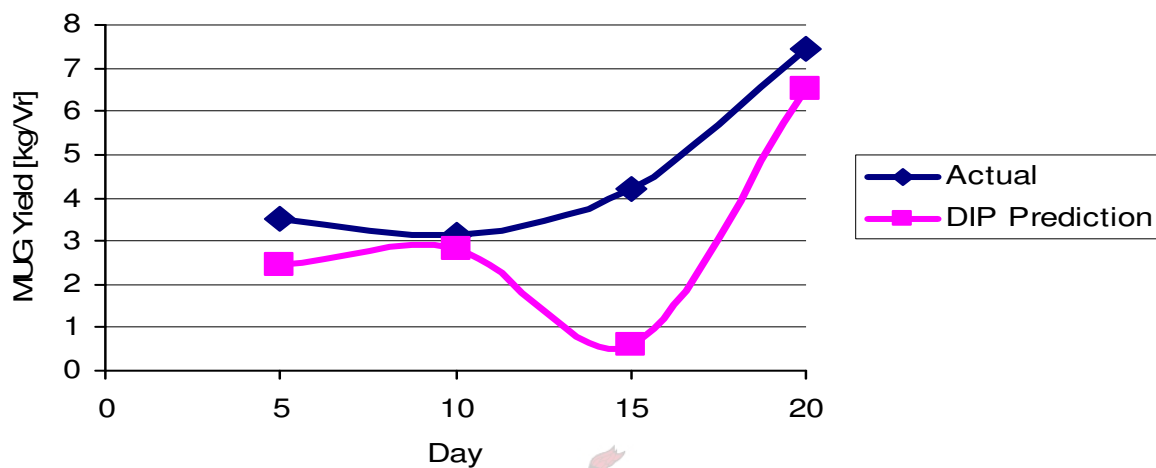


Figure 5.3: Actual MUG vs. DIP MUG for Run 3, 1 litre growth Curve (200 ml)

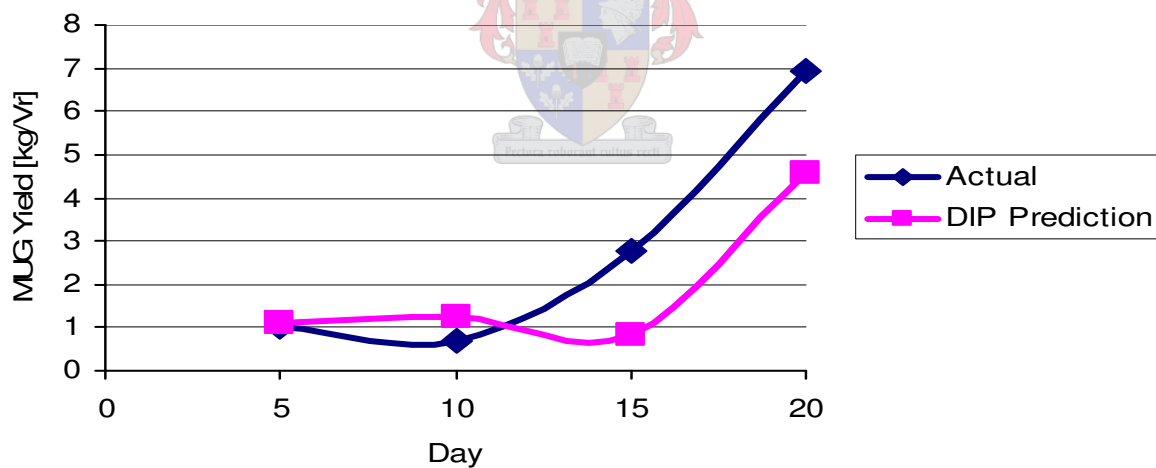
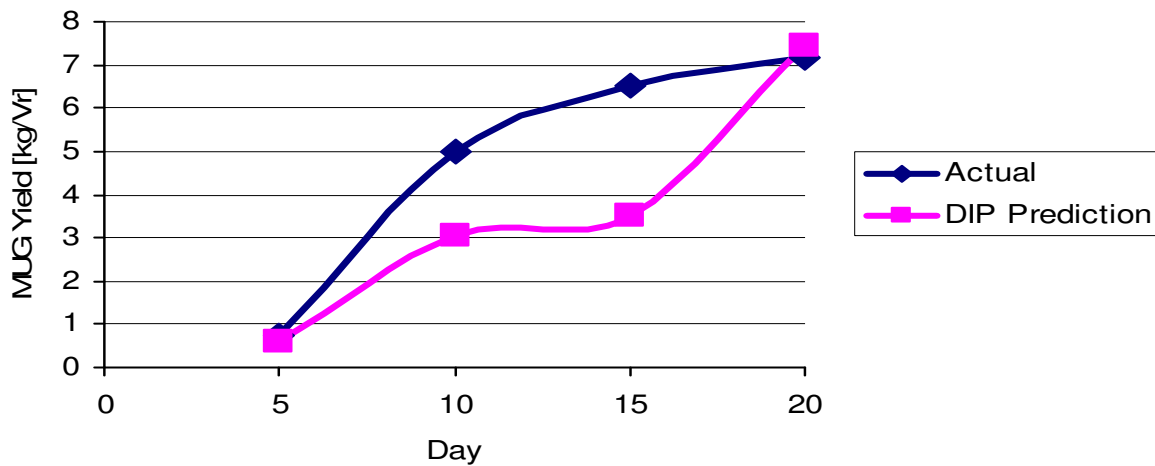


Figure 5.4: Actual MUG vs. DIP MUG for Run 3, 2 litre growth Curve (200 ml)

For the 2 litre reactor in run 3, a  $R^2 = 0.614$  was obtained. This indicates that the fit could be better, but 61% of the time the model will be accurate (Figure 5.4). One usually strives for higher  $R^2$  values.



**Figure 5.5: Actual MUG vs. DIP MUG for Run 3, 4 litre growth Curve (200 ml)**

For the 4 litre reactor a  $R^2 = 0.61$  was again measured (see Figure 5.5). The sampling of granulated anaerobic sludge can be very problematic, mostly due to the high settling rate of the sludge (up to 60 m/h). If a 1 litre sample is mixed, by the time the 200 ml sub sample is drawn, most of the large granules have again settled at the bottom of the container. Thus, only fines end up in the 200 ml sample to be tested. This leads to lower than actual MUG values from the test samples.

To study this phenomenon, the entire volume of the 1 litre reactor (Run 2) was split into 200 ml samples. This gave in 5 samples of 200 ml each. This 200 ml sub-samples were halved again leaving 100 ml samples for the DIP. In other words there were two images for every 200ml sample drawn. The amount and average size were added to calculate the total amount and average for the 200 ml sample. Due to time constraints, 200 ml samples were taken from the 2 and 4 litre reactors using the conventional method. Afterwards the rest of the reactor volumes were also passed through the 0.5x0.5 mm sieve and thoroughly washed with water. Therefore, the actual MUG for all three reactors could now be determined and compared to the 200 ml test samples that were first drawn from the reactors.

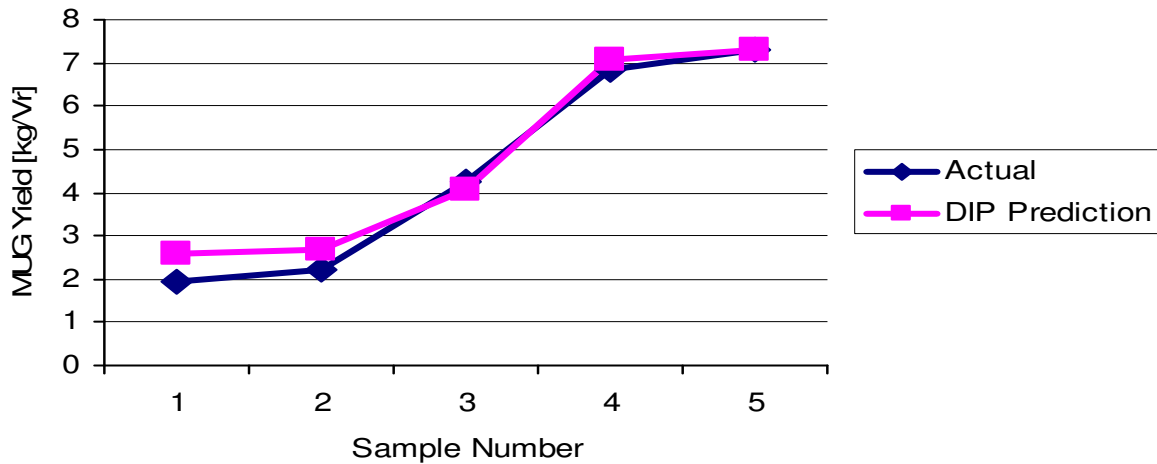


**Figure 5.6: Actual MUG vs. DIP MUG for Run 3, 1 litre test samples (2x100 ml)**

As can be seen in Figure 5.6, there is a close correlation between the DIP model and the actual data. Regression yielded a  $R^2 = 0.994$ , which is considered acceptable. The sample MUG increased drastically as the reactor volume decreased. A variation of more than  $5 \text{ kg/m}^3$  occurred between the first and last sample with an average of  $4.15 \text{ kg/m}^3$  for the test of 5 samples. This is twice higher than the value of the first 200 ml sample.

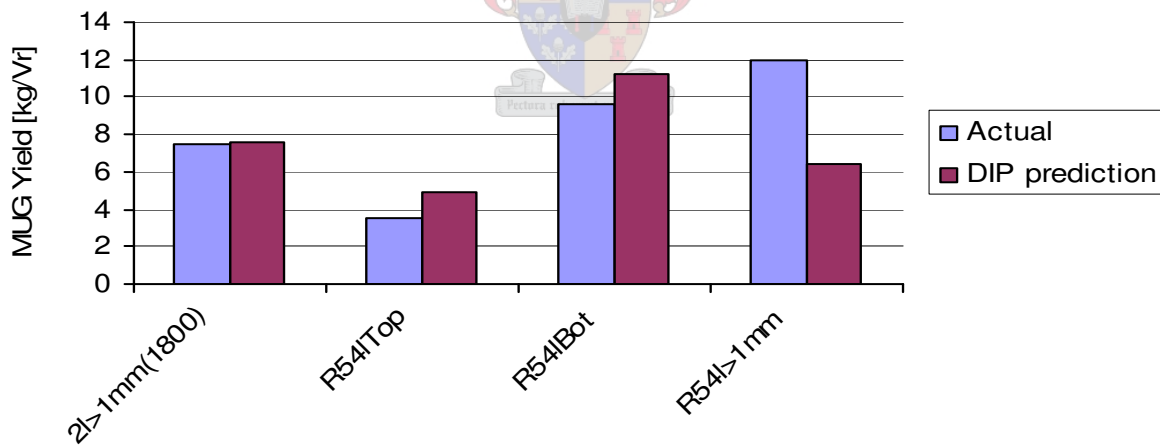


**Figure 5.7: Actual MUG vs. DIP MUG for Run 3, Diverse Test Samples (2x100ml)**

A few random samples were also processed to test the robustness of the DIP programme, Figure 5.7 clearly shows that a relatively good fit ( $R^2 = 0.71$ ) was obtained for all of the 2x100 ml random samples.



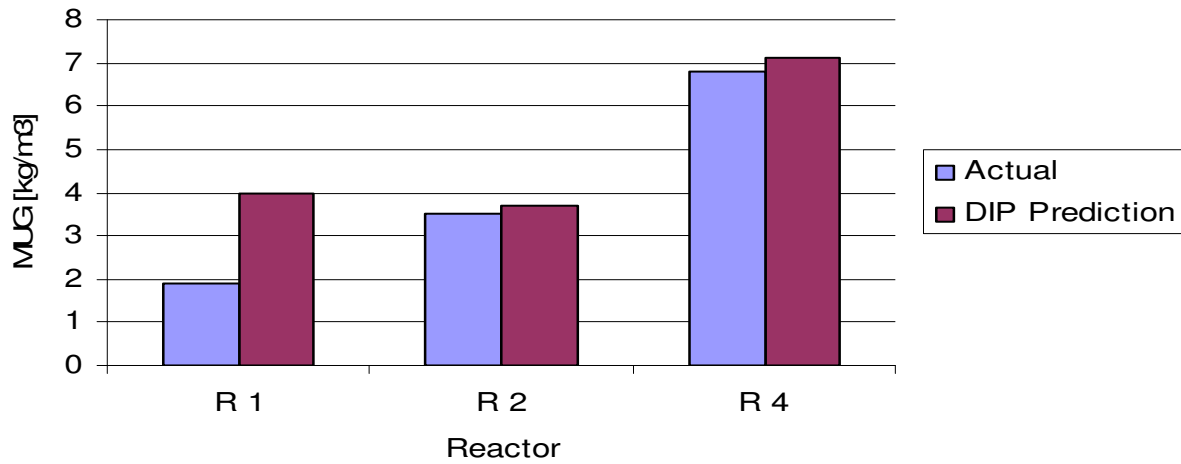


**Figure 5.8: Actual MUG vs. DIP MUG for 1, 2 and 4 Litre Reactors.**

Figure 5.8 displays a comparison of the MUG values generated by the standard method of sampling (200 ml) versus the MUG values obtained by actually passing the entire reactor volume through the TSS-MUG procedure. As can be seen from the figure, the 200 ml sample result was always less than the actual MUG and in the case of the 1 litre reactor, a 200% lower value occurred.

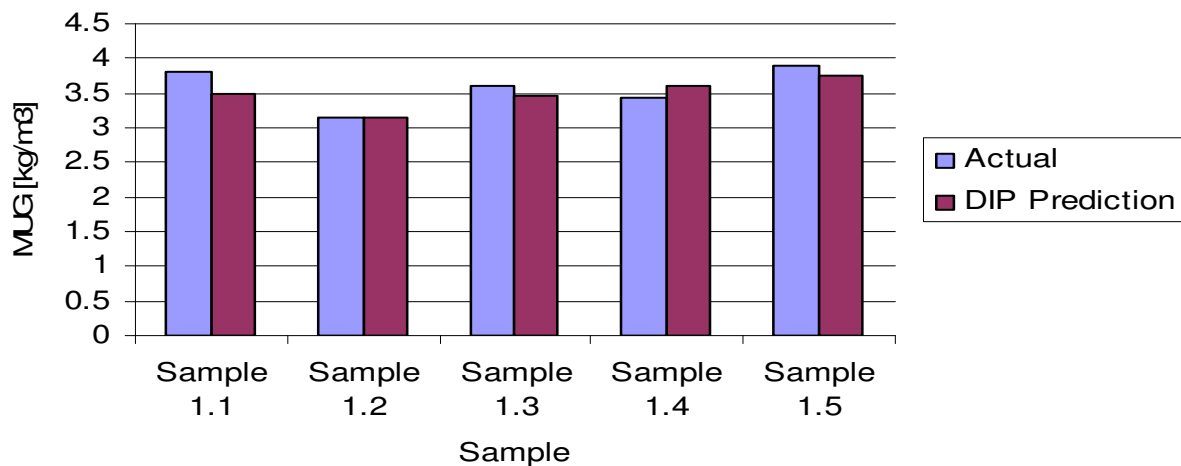


**Figure 5.9: 4 x 50 ml Actual MUG vs. DIPMUG**

## 5.5 Summary

The DIP model yielded satisfactory results for approximately 93% of the 2x100 ml sample sets and 71% of the 200 ml sample set batch. The worst results were obtained with the 4 x 50 ml samples: a  $R^2$  value of only 41%. Therefore, it can be concluded that it is far better to split the 200 ml to be used for TSS and MUG calculations into two 100ml samples before photographing them.

Even though the DIP is at this stage not 100% accurate, this programme delivers more detailed information on a sample than the conventional MUG tests. From the latter, only the dry mass can be retrieved, whereas the former provides the average particle size, amount of particles, biggest particle and also a size distribution of particles. Thus, even though the original MUG tests are still necessary to act as a benchmark for the DIP, incorporating the DIP model can lead to far more information than the conventional MUG tests. As stated earlier this 'new' information on average particle diameter and size distribution will form the basis of future studies.

From the studied test samples, it is evident that at some points large variations between the actual MUG and the DIPMUG values did occur. Various parameters like clusters of granules, a poor choice of greyscale and glare on the water in the test sample, to name a few, can have a negative effect on the DIP performance and should be prevented.

Figure 5.6 showed very interesting results in the study of how settling of large granules can affect the MUG obtained from the standard method of sampling used throughout this thesis. As the total volume (of the 1 litre reactor volume) is reduced, a far higher MUG yield is obtained for each 200 ml sub-sample drawn. Of the 5 sub-samples drawn from the 1 litre reactor sample, sample 1 will have a lower MUG than sample 2 and sample 2 lower than sample 3 and so forth. An average MUG for the reactor of  $6.3 \text{ kg/m}^3$  was found to be approximately 3 times higher than that of the first 200 ml sample drawn. Therefore it can be concluded that settling in samples drawn from any reactor has a negative effect on the MUG calculations - the calculated MUG will always be lower than the actual mass of granules inside the reactor. Nevertheless the obtained MUG results are still compatible, since the sampling techniques followed for all the reactors are standard. These results were also verified for the 2 litre and 4 litre reactors as can be seen from Figure 5.8.

One of the main limiting factors on the DIP is the digital camera resolution. In this study, a 1.3 mega-pixel camera was used. Even though the camera could be used with some success, the resolution was actually too low. Therefore, a digital camera with higher resolution is recommended to be used in the future. This will aid granule identification immensely, and the cut-off size could also be lowered, shedding even more light on the granule size distribution of the sample.

The results of the second test showed a dramatic increase in the percentage of correct classification. Consequently, two 100 ml sub-samples are recommended. This moves the DIP to achieve optimal results.

Further more the dip should be used in conjunction with MUG calculations. Since combination of the techniques sheds far more light on the sample characteristics than either does individually.

A light source that illuminates the sample from the bottom will induce a sharpened contrast between the granules and the background. This will also standardise the procedure even more, since natural light fluctuations will be eliminated.

Future growth prediction models should also attempt to predict the growth in each of the size ranges over the incubation period. The DIP yields a histogram of the size distribution of the granulated sample studied. If samples are drawn on Day 0, 5, 10, 15 and 20 of the incubation period is processed; a histogram of each sample will be obtained. The growth in each size range can thus be quantified. If one takes a typical particle breakage model used in mineral processing like for example the 'King' model (Hayes 1993) it can be inverted, to represent particle 'growth' rather than particle breakage. In other words, the same fundamental principles used to describe how ore breaks from one large rock to many smaller particles, can be inverted and used to describe how granules grow from dispersed sludge to mature granules. A growth function from fines to large particles, rather than the usual breakage from large particles to smaller will be obtained and with this, possibly the first function describing the granule growth that occurs in anaerobic sludge. By lengthening the growth rate parameters a function describing the growth in an actual UASB might also be possible. It is strongly recommended that a study and evaluation of such a model be incorporated into the later phases of the larger WRC project, since it would give a large amount of insight into the growth process.

# 6. ISA Variation

---

## 6.1 Introduction

The conservative scale-up of bioreactors is a very complex task, even if only one microbial species is present - let alone more than 11 000 species as is the case in anaerobic sludge. The conventional way of achieving this is to create a working lab-scale unit, optimise and enlarge the volume usually in the order of 2 to 5 fold, optimise again and repeat this procedure until the unit is of adequate volume. The classic scale-up procedure followed in reactor design is depicted in Figure 6.1. In the case of bioreactor design, far more process steps are needed to produce a conservative scale-up (Fogler, 1999; Letting et al., 1980; Metcalf and Eddy, 2003; Oldshue, 1998;).

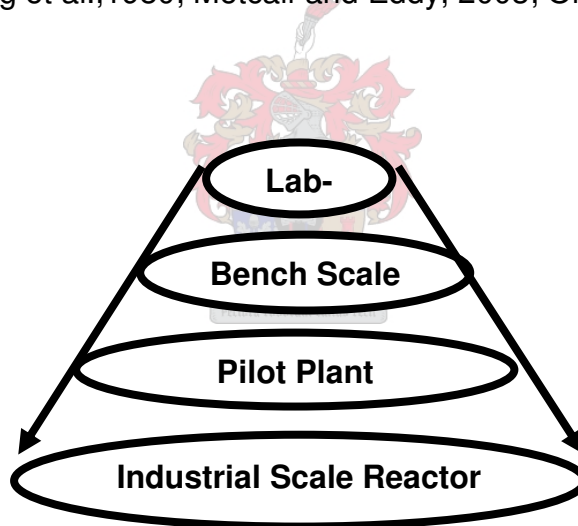


**Figure 6.1: Classic Scale-up Procedure followed in Reactor Design**

One key to a conservative scale-up is to have the speed at the tip of the impellor equal the velocity in both the laboratory- and the full-scale reactor (Metcalf & Eddy, 2003). If the impellor speed is too fast, it can destroy the bacteria; and if the tipspeed is too slow, the contents will not be well mixed and inadequate growth will occur due to local starvation in the dead zones and due to insufficient mass transfer. Typical speeds are in the range 5 to 7 m/s (Metcalf and Eddy, 2003). Speeds in the order of  $10^{-3}$  times less is needed for granulation to take place, as was proven in Chapter 4.

It seemed that internal surface area (ISA) has a large effect on the granulation rate inside the reactor: the larger the internal surface area is, the more shell-to-organism contact will occur inside the reactor. The more physical interaction occurring between the micro-organisms and a surface the more adverse the conditions for microbial life becomes. This leads to more ECP secreted by the ECP producing species in the community, in an attempt to protect themselves from their environment. The secreted ECP forms a protective layer between the micro-organisms and the surface and the higher the rate of ECP production, the higher the microbial growth and granulation inside the reactor.

To test this hypothesis it was decided to design 3 more reactors geometrically similar to the 5.5 litre reactor that will induce flow patterns as close as possible to that produced by  $R_{5.5}$ . The baffles were sized in such a manner as to be in the same tipspeed regime as was experienced with the 5.5 litre unit. The only variable that was varied on the reactors was the internal surface area. Due to financial and resource constraints it was decided to scaledown rather than to scale up. Another reason for this scale-down was that the units could be rotated on readily available roller tables of adequate speed, making the scale-down financially even more lucrative. Consequently, units with a volume of 1, 2 and 4 litres respectively were designed and constructed.

Section 6.2 contains the materials and methods used, along with a detailed discussion on the design of the 3 smaller units. The following presents the results that were obtained on the 3 smaller units as well as a discussion thereof. This is followed by a summary of the internal surface area variation section of this research.

## ***6.2 Materials and Methods***

To summarise, the requirements that the scale-down reactors should meet the following:

- the units should be smaller than 5.5 litre,
- the reactors should be as close as possible to the geometrical design of  $R_{5.5}$ ,
- they should vary in internal surface area, and
- they should have equal tipspeeds at every roller table speed setting.

The fourth requirement proved to be the most problematic in the scale-down, as the units are cylindrical and vary in diameter and in volume. Because of this, the units differ in rotation speeds at any given roller table setting, in turn resulting in a variation in tipspeeds inside the reactors.

### 6.2.1 Baffle Tipspeeds

The above mentioned problem was overcome by the following method:

The ratio of rotation for any two circular objects with no slip is given by:

$$\theta_{\text{Roller}} \cdot \pi \cdot D_{\text{roller}} = \theta_{\text{F}} \cdot \pi \cdot D_{\text{F}} \quad [6.1]$$

or

$$\theta_{\text{F}} = (D_{\text{roller}} / D_{\text{F}}) \cdot \theta_{\text{Roller}} \quad [6.2]$$

Since the reactor shell is welded to the flange, the rotational speed flange ( $\theta_{\text{F}}$ ) will be equal to the rotational speed of the shell ( $\theta_{\text{D}}$ ) and also to the rotational speed of the baffles ( $\theta_{\text{b}}$ ). To calculate the tipspeeds of the mixers, the following equation is used (Hibbeler et.al.,1997):

$$V_{\text{Tip}} = 2 \cdot \pi \cdot r \cdot \theta \quad [6.3]$$

Therefore, the tipspeeds of the baffles can be obtained in the following way:

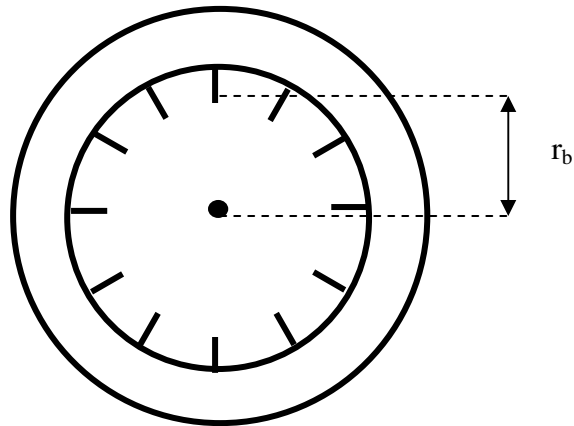


**Figure 6.2: Visual representation of the  $r_b$  value**

The clearance from the centre of the reactor to the tip of the baffle is described as the baffle clearance radius ( $r_b$ ). This value is needed to calculate the baffle tipspeeds from equation 6.3.

Thus: 
$$V_{\text{Tip}} = 2 \cdot \pi \cdot r_b \cdot (D_{\text{Roller}}/D_F) \cdot \theta_{\text{Roller}} \quad [6.4]$$

The rotational speed in rad/s of the rollers of the roller table can be obtained by counting the amount of revolutions that the rollers make per minute (**RPM**). This value can be converted to radians per second (rad/s) by the following.

$$\theta = 2 \cdot \pi \cdot \text{RPM}/60 \quad [6.5]$$

Now if Equation 6.5 is combined with 6.4, the following equation is obtained:

$$V_{\text{Tip}} = (4 \cdot \pi^2/60) \cdot (D_{\text{roller}}/D_F) \cdot \text{RPM}_{\text{Roller}} \cdot r_b \quad [6.6]$$

### 6.2.2 Reactor Design

If one looks closely to Equation 6.6 the following can be concluded:

$$V_{\text{Tip}} = K \cdot \text{RPM}_{\text{Roller}} \cdot r_b/D_F, \quad [6.7]$$

with K being a constant. In other words, for any given roller speed:

$$V_{\text{Tip}} \propto r_b \quad [6.8]$$

and

$$V_{\text{Tip}} \propto 1/D_F \quad [6.9]$$

However, the flanges come in pre-manufactured sizes, so the only variable that can be changed to manipulate the baffle tipspeed inside the reactors, is  $r_b$ . This was done and the following designs were obtained.

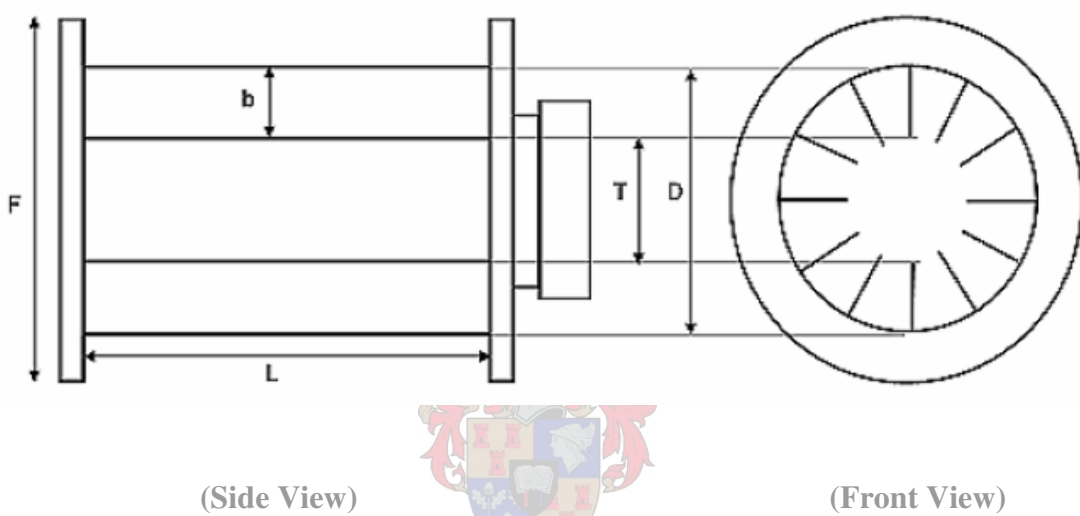


Figure 6.3, Front and Side View of Reactors

Table 6.1: Calculated Reactor Dimensions, for a 1, 2 and 4 litre scale-down of R<sub>5.5</sub>

Reactor	Volume	F	L	D	b	2*r <sub>b</sub>
Dimensions	[m <sup>3</sup> ]	[m]	[m]	[m]	[m]	[m]
R 1	1	0.14	0.164	0.1	0.018	0.064
R 2	2	0.16	0.213	0.12	0.023	0.074
R 4	3	0.2	0.268	0.16	0.033	0.094
R 5.5	5.5		0.275	0.16	0.03	0.1

Table 6.2: Comparison of Tipspeeds at a Given Roller Speed

Reactor	RPM F	RPM r <sub>b</sub>	rad/s r <sub>b</sub>	V(T) [m/s]
R 1	3.00	3.00	0.157075	0.0050
R 2	2.63	2.63	0.137441	0.0051
R 4	2.10	2.10	0.109953	0.0052
R 5.5		2	0.104717	0.0052



As can be seen from Table 6.2, the manipulation of  $r_b$  produced scaled down versions of  $R_{5.5}$  with nearly exactly the same tipspeeds in the same range that was experienced with the 5.5 litre unit. Therefore, since the 3 reactors are geometrically similar to  $R_{5.5}$  and they operate in the same baffle tipspeed range, the scale-down is considered successful.

### **6.2.3 Operating Procedure**

The operating procedure were exactly as was discussed in the previous sections. On Day 0 of the 20 day incubation period, the reactors were loaded with a ratio of 2 parts sludge to 7 parts feed. The sludge was filtered through a 1 mm sieve (to be consistent with previous runs) and to ensure that no granules that grew prior to the inoculation can affect the final results and the optimised feed was used.

Every day of the 20 day experimental run, used feed was drawn off, new feed was introduced (2/9 of the reactor volume) and the pH of the reactor volume was measured. On Days 0, 5, 10 and 20 samples were drawn from the reactor volume and filtered through a 0.5 mm sieve.

The 'filtrate' was re-inoculated into the reactor and the granules left on top of the sieve were photographed (of DIP) whereafter the TSS was obtained in order to calculate the MUG (see Section A2 in the Appendix). The pH was again manipulated to obtain the desired pH curve. In the case of the 3 scale-down reactors, the amount of biogas was not measured daily, due to the fact that these units rotated on a roller table.

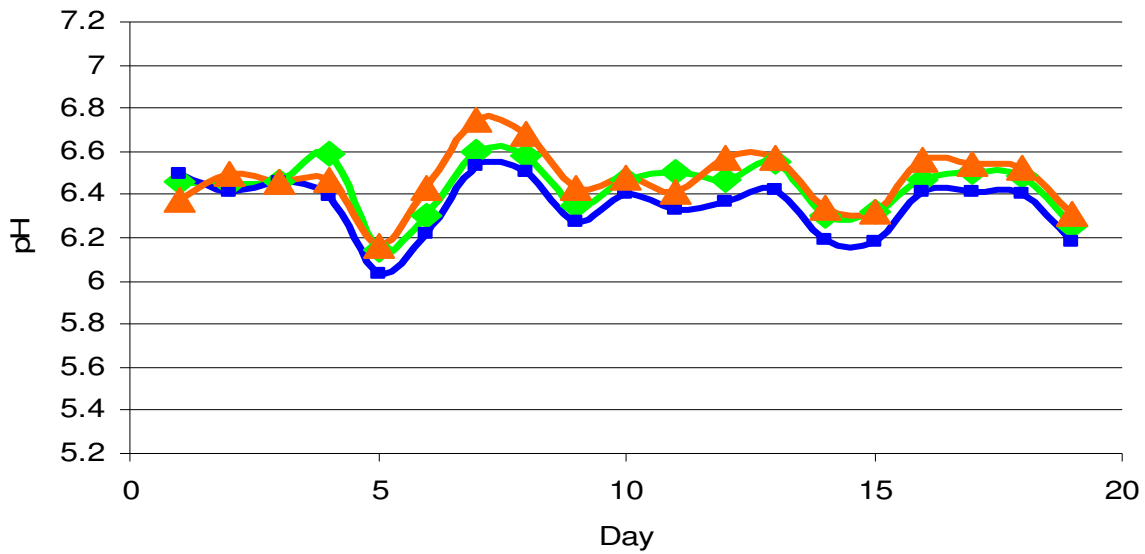
## **6.3 Results and Discussion**

Four experimental runs were performed on the 3 test units, the first of which was basically a commissioning run to become accustomed to the system and fix leaks. In the second run the baffle tipspeed was set to the equivalent of 1 RPM on the 5.5 litre unit (0.00275 m/s tipspeed). In the following experiment the speed were set to the equivalent of 2 RPM (0.055m/s tipspeed) and in the fourth experiment the tipspeed was set to 0.01375 m/s tipspeed. Results and measured values are represented in table form in Section A6 of the Appendix. From here on forth, orange will represent the 1 litre

unit, blue the 2 litre unit and green the 4 litre reactor. The following results were obtained:

### 6.3.1 Daily pH Log

The average pH of run 2 (0.0055 m/s tipspeed) was the closest to the classic pH curve, the latter proven to produce the best granulation yield. It is also clear from the Figure 6.4 to 6.6 that the 4 litre unit yielded the most stable pH for every run, followed by the 2 - and 1 litre reactors respectively.



*Pectera robustant cultus recti*  
**Figure 6.4: Run 2 pH vs. Time 0.00275 m/s.**

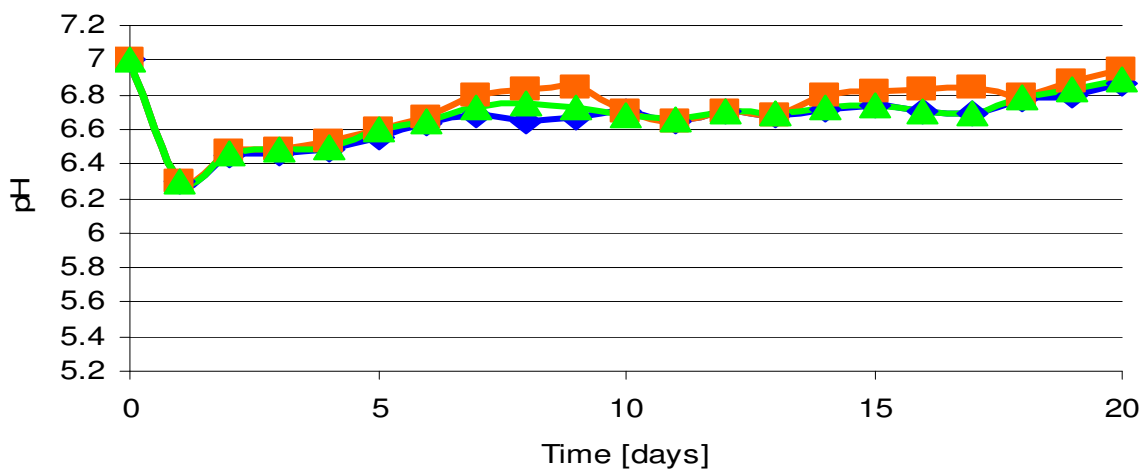


**Figure 6.5: Run 3 pH vs. Time 0.0055 m/s.**

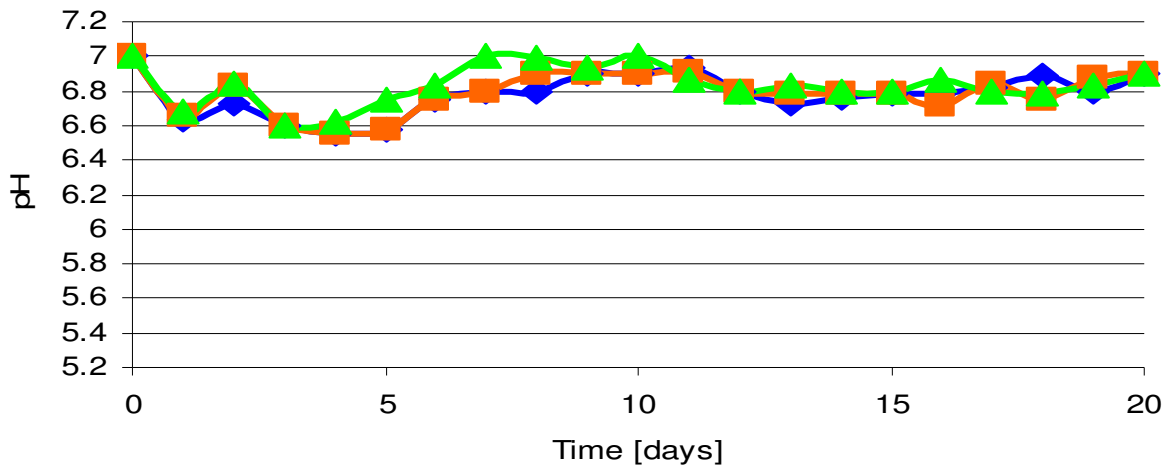


**Figure 6.6: Run 4 pH vs. Time 0.01375 m/s.**

### 6.3.2 Growth Curves

The same phenomenon that occurred in the pH measurements seemed to manifest itself in the MUG versus time plots (Figure 6.7 to 6.9). The 0.0055 m/s tipspeed yielded the best growth curves while the 4 litre unit yielded the best results at all the mixing speeds with the 1 litre unit yielding the poorest results. The growth curves obtained for the 4 litre unit also proved to be the closest to the ‘classic’ growth curves obtained in the earlier studies as discussed in Chapter 4.

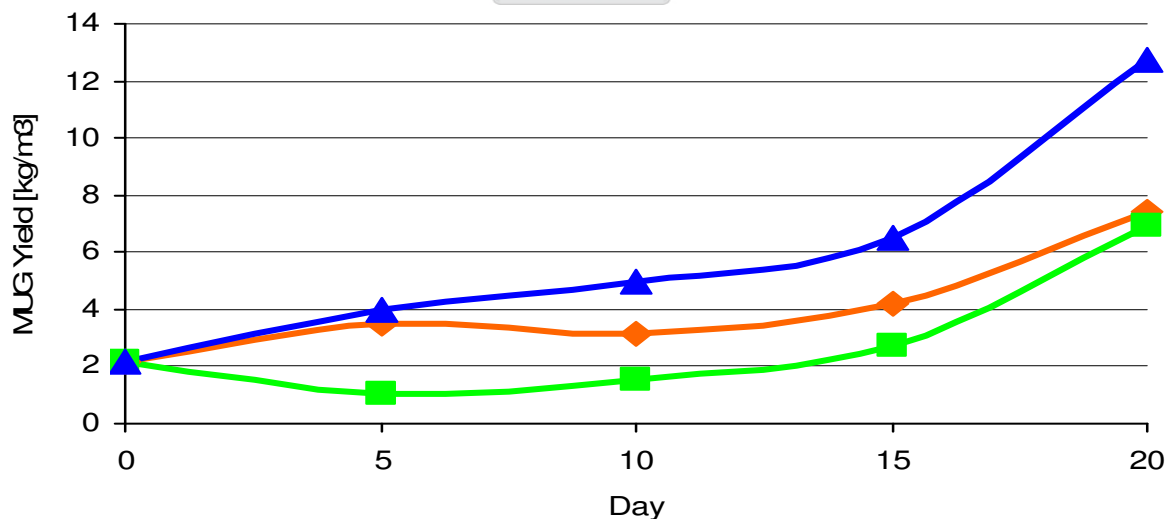


**Figure 6.7: Run 2 MUG vs. Time at 0.00275 m/s**

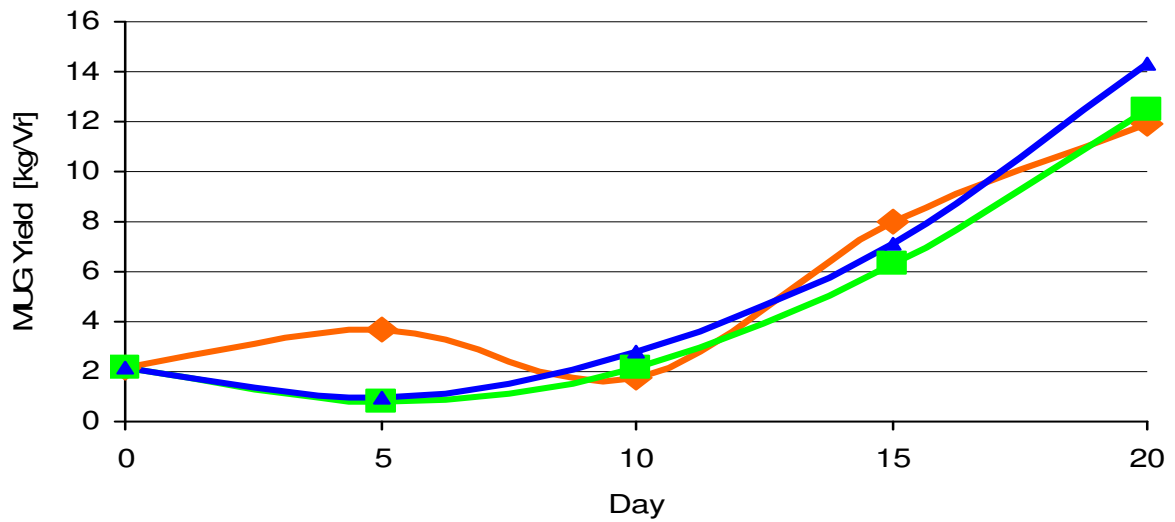


Figure 6.8: Run 3 MUG vs. Time at 0.0055 m/s

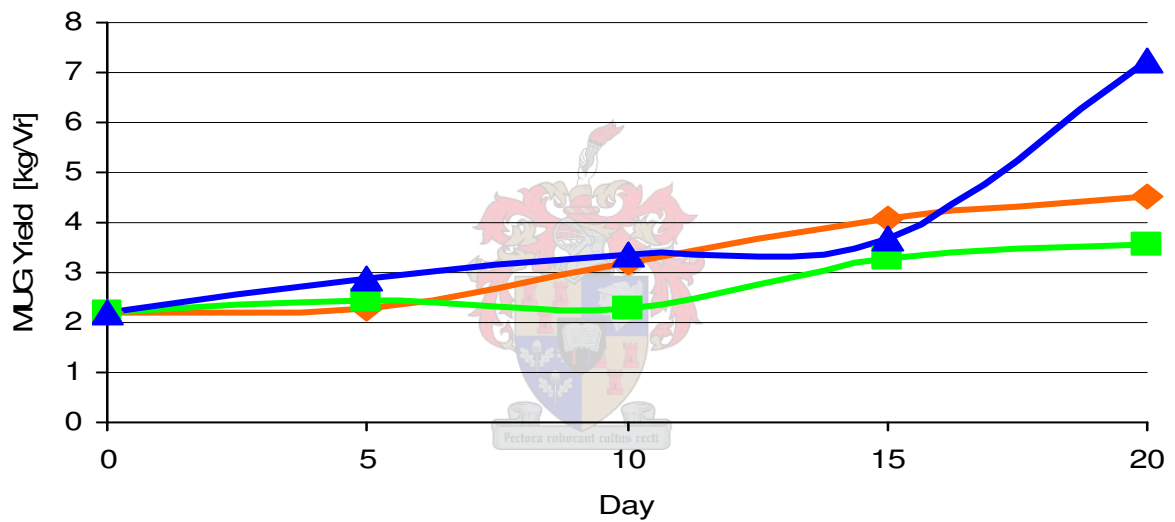
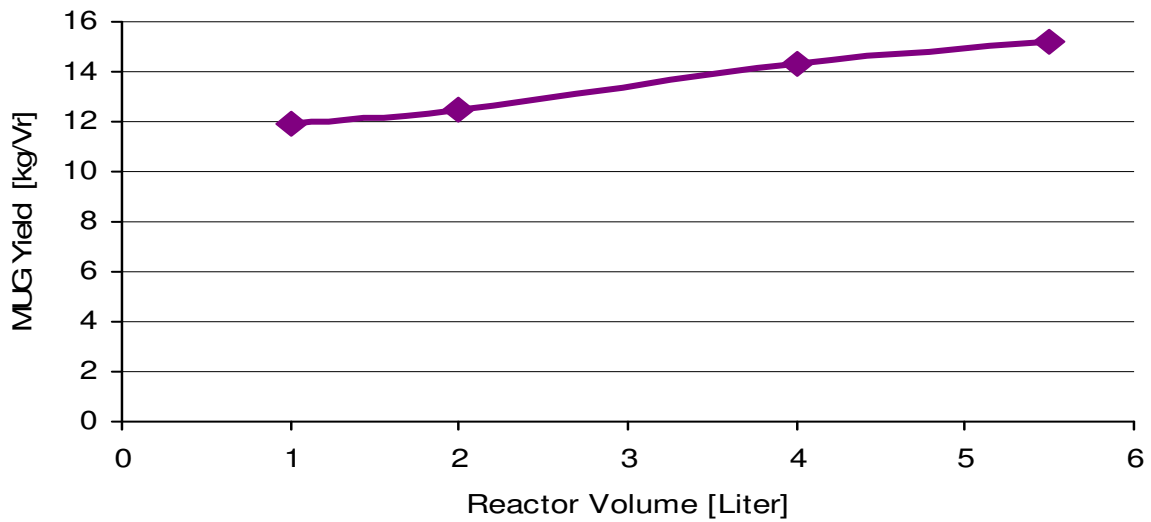


Figure 6.9: Run 4 MUG vs. Time at 0.01375 m/s

### 6.3.3 MUG vs. Tip speed

In this section the MUG versus tip speed yields of the 3 scale-down reactors is compared to each other, as well as to the yields obtained earlier at the same tip speeds with the 5.5 litre unit.



**Figure 6.10: MUG<sub>D20</sub> vs. Tipspeed for 1, 3, 4 and 5.5 litre units.**

Figure 6.7 confirms that, for any given tipspeed, an increase in volume of the reactor leads to an increase in the MUG yield.

### 6.3.4 MUG vs. Internal Surface Area (ISA)

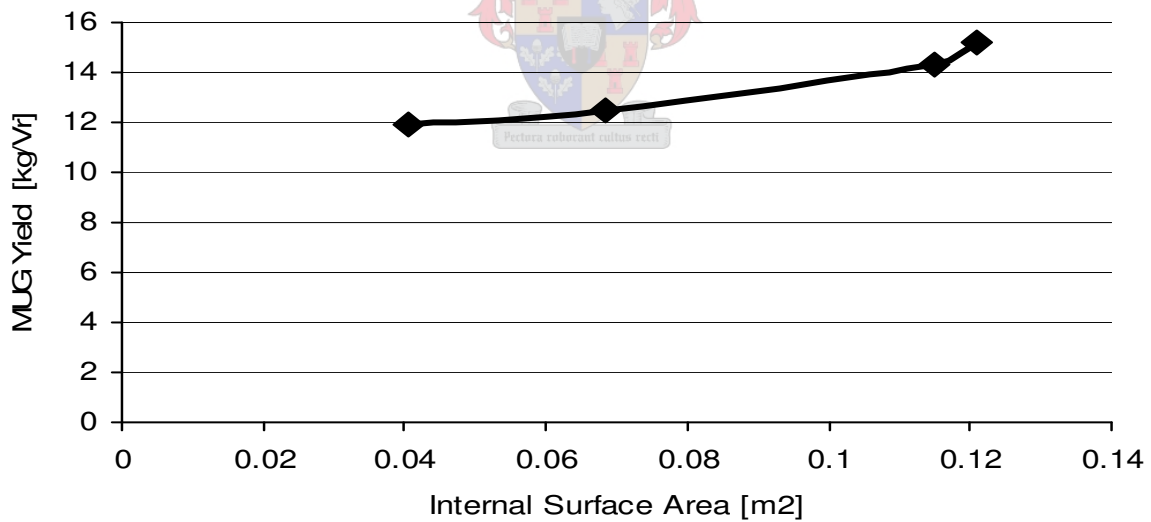


**Figure 6.11: MUG<sub>D20</sub> vs. Tipspeed for 1, 3, 4 and 5.5 litre units.**

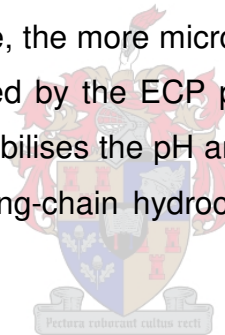
Figure 6.11 indicates quite a dramatic increase in the MUG yield per increase in the ISA. An increase of more than 3 kg/m<sup>3</sup> reactor volume occurred with an increase in ISA of only 0.06 m<sup>2</sup>. On the other hand, as the volume of the reactor increased so, did the ISA. But in Phase 1 of the WRC project, 5 litre Schott bottles with no baffles were used. It was found that the yield was inversely proportional to the volume of the Schott bottle

that was used on the roller tables. Therefore Figure 6.10 in Section 6.3.3 might be a bit misleading, as it may seem that it is the increase in volume that has an effect on the yield when it is in fact the internal surface area.

## **6.4 Summary**

If the calculations done in section 6.2.1 and 6.2.2 are considered, the only parameter that varied on the 3 scale-down units was the internal surface area (ISA). The tipspeed, feed and operating procedures were kept relatively constant to that in the optimisation of the 5.5 litre unit. The scaled-down unit design is therefore considered relatively conservative.

As discussed in section 6.3.1, the pH curves for the 4 litre reactor was the most stable and followed the 'classic' pH curve for optimal granulation. This might be attributed to the fact that the more ISA available, the more micro-organism-shell contact there will be, and the more ECP will be excreted by the ECP producers to protect them from their harsh environment. This in turn stabilises the pH and enhances growth, since ECP acts as a hydrogen sink due to the long-chain hydrocarbon nature of the secreted extra-cellular polymers.



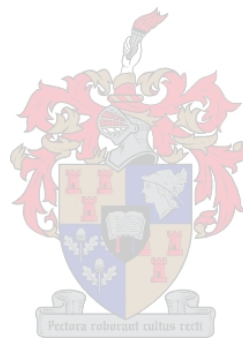
At a tipspeed of 0.0055 m/s (equivalent to 2 RPM in the large reactor), the highest yields of usable granules were obtained. The reasons for this might be that at lower rotation speeds, the mass transfer between the micro-organisms and the environment seems to deteriorate resulting in a slower growth and therefore a lower MUG yield. At tipspeeds of higher than 0.0055m/s on the other hand a dramatic decrease in MUG yield is again experienced. This might be because granule breakage starts to occur (possibly due to grinding) if the baffle or impellor speeds become higher than 0.0055m/s (See Chapter 4).

The 4 litre reactor exceeded its competitors performance in every run, giving the highest MUG yields for all the studied mixing speeds. The reason for this can be linked to the explanation given in the second paragraph of this summary. As was discussed earlier, ECP is a well known core component of anaerobic granules and are also required for the granulation process to initiate. Thus, the larger the ISA the higher the MUG yield will be.

Figure 6.11 in section 6.3.4 it can clearly shows that there is a dramatic increase of MUG yield with an increase in ISA of the test reactors. This occurrence can be linked to discussions given in paragraph 2 and 4 in this section. In the range studied, a  $40 \text{ kg/m}^3$  ISA occurred, - a very high value. Thus, the ISA of the bioreactor is one of the prime MUG Yield influencing parameters identified thus far.

Due to the time constraints only 3 mixing speeds could be studied (approximately 70 days). In future, a wider range of mixing speeds is recommended – this will show the effects of the ISA variation over a wider range.

The 3 test units can also be used for further optimisation of feed, since the base yields were laid down in this chapter. The units are ideal for this kind of research since they are small, does not require much resources and are scale models of the  $R_{5.5}$ .



# 7. *Mass Balance and Modelling*

---

## **7.1 Introduction**

Chapter 7 aims to perform the most extensive possible mass balance on the reactor, identified as the most successful from Chapters 3 and 4. In this way any interrelationships between the growth rate limiting parameters become apparent. Furthermore, a mass balance will provide information as to the composition of the anaerobic granules produced in the bioreactor.

Section A2 of the Appendix gives a brief discussion on the methods of analysis used to obtain the concentrations and masses of the various organic and inorganic species that plays a noteworthy role in the granulation reaction inside the reactor. Section 7.2 will be a theoretical overview the derivation of the mass balance. Section 7.3 contains the results and discussion of the consumption and production of the various species while section 7.4 gives the overall mass balance using the results from 7.3. This model equation (Equation 7.14 section 7.2) is then used to predict the yield after which the results are compared to the actual yields obtained for the TSS analysis. Section 7.4 also includes a discussion on the interrelationships between various granulation rate limiting parameters. The chapter ends off with a summary.

## **7.2 Theoretical Discussion**

All the parameters identified as playing even a limited role in the granulation process, can be measured or analysed (Section A2 Appendix). For this specific run, all input and output values are known. From basic reactor design theory it shows that for any system the following mass balance holds (Fogler, 1999):



$$\text{Accumulation} = \text{Generation} - \text{Destruction} + \text{Inflow} - \text{Outflow} \quad [7.1]$$

If it is assumed that no nuclear reactions occur within the reactor volume (which is hopefully the case) the generation and destruction terms can be considered legible. Therefore, for this specific case:

$$\text{Accumulation} = \text{Inflow} - \text{Outflow} \quad [7.2]$$

The inflow will be the fresh feed introduced; the outflow will be the used feed drawn off every day. The accumulation within the system will be the amount of increase in mass that occurs in the anaerobic sludge during the incubation period. Due to the thorough mixing in the reactor and the lack of precipitates identified in the sample analysis, the only precipitation of inorganics are assumed to occur will be inside the sludge granules.

Equation 7.2 can thus be modified to:

$$MI = [\text{Mass In}] - [\text{Mass Out}] \quad [7.3]$$

with MI being the overall increase in mass of the sludge (organic or inorganic) inside the reactor due to microbial growth, granulation and/or inorganic precipitation in the granules.

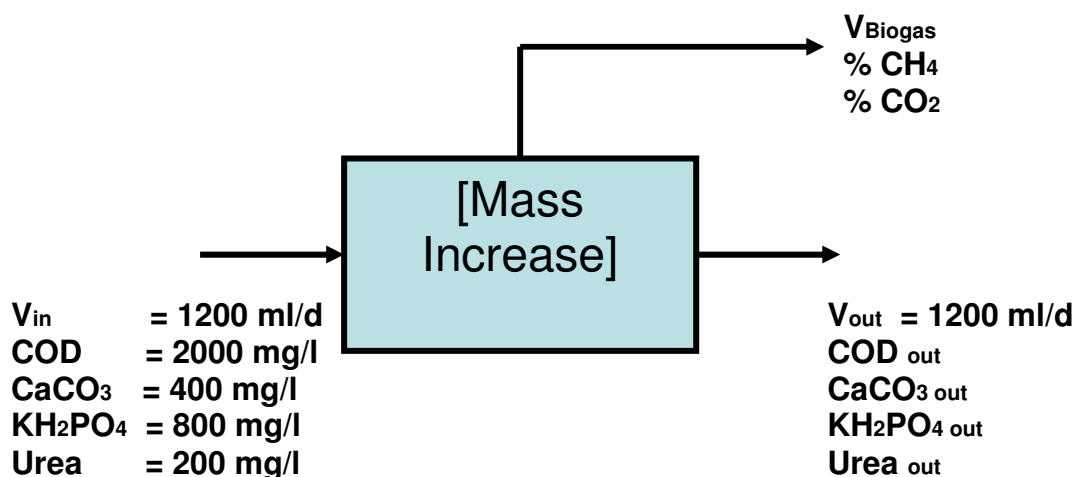


Figure 7.1: Mass Balance over 5.5 litre reactor

Figure 7.1 gives a visual summary of all the analysed parameters for this reactor feeding and tapping procedure. The increase in inorganic precipitates within the sludge granules can be written as:

$$MI_{Ca} = In_{Ca} - Out_{Ca} \quad [7.4]$$

$$MI_{PO4} = In_{PO4} - Out_{PO4} \quad [7.5]$$

$$MI_N = In_N - Out_N \quad [7.6]$$

or

$$MI_{inorganic} = MI_{Ca} + MI_{PO4} + MI_N \quad [7.7]$$

The organic mass balance is slightly more complicated, as the Chemical Oxygen Demand (COD) is only a measure of the amount of oxygen needed to completely break down all of the organics in the sample. Another problem is the fact that only a fraction of the actual COD is biodegradable. According to literature though (Metcalf and Eddy, 2003), this fraction remains relatively constant for any given type of effluent (like PCE used in the feed). Therefore, it is assumed that:

$$\text{Mass of Biodegradable Organics (MBO)} = \Psi * COD, \quad [7.8]$$

with  $\Psi$  being a constant obtained through experimental analysis. Therefore:

$$MI_{organic} = MBO_{in} - MBO_{out} - M_{CO2} - M_{CH4} \quad [7.9]$$

or

$$MI_{organic} = \Psi COD_{in} - \Psi COD_{out} - M_{Biogas} \quad [7.10]$$

or

$$MI_{organic} = \Psi COD_{consumed} - M_{Biogas} \quad [7.11]$$

Due to the nature of the TSS tests, the  $MI_{organic}$  and  $MI_{inorganic}$  cannot be separated. Only the total increase in dry mass ( $MI_{total}$ ) can be obtained.

$$MI_{total} = MI_{organic} + MI_{inorganic} \quad [7.12]$$

By incorporating equations 7.7 and 7.11 into equation 7.12, the following is true:

$$\begin{aligned} \mathbf{MI_{total}} = & (\mathbf{In_{Ca}} - \mathbf{Out_{Ca}}) + (\mathbf{In_{PO4}} - \mathbf{Out_{PO4}}) \\ & + (\mathbf{In_N} - \mathbf{Out_N}) + \mathbf{\Psi COD_{consumed}} - \mathbf{M_{Biogas}} \end{aligned} \quad \mathbf{[7.13]}$$

But  $MI_{total}$  is nothing more than the dry mass of the entire size distribution of the reactor volume:

$$\mathbf{MI_{total}} = \mathbf{TSS_{>1mm}} + \mathbf{TSS_{>1-0.5mm}} + \mathbf{TSS_{>0.5-0.25mm}} + \mathbf{TSS_{bottoms}} \quad \mathbf{[7.14]}$$

In the next section, equation 7.13 will be used to predict the  $MI_{total}$ . This will be compared to the experimental  $MI_{total}$  values obtained from equation 7.14 and TSS analysis of the reactor volume.

### ***7.3 Results and Discussion***

The mixing speed of  $R_{5.5}$  was set to 2 rpm or 0.0055 m/s (tipspeed) and inoculated in the usual manner with a 1:3.5 sludge to feed ratio. The feed had optimised quantities of inorganic additives. Since the maximum yield at 0.0055 m/s has been verified, again a single parameter was again altered in this experimental run. The altered parameter in this case was the size of the seeding sludge. Instead of using the normal 1 mm sieve to screen the sludge, a 0.5x0.5 mm screen (to study the effects this will have on the overall MUG yield of the reactor) was used. Graphical representations of the results of the analysis of the in- and output data will be given in this section (Represented in table form in Section A7 of the Appendix). Except for Figures 7.2, 3 and 7.7 and 8, graphical results will be displayed in the following way:

- 1 input variables will be displayed in blue;
- 1 output data will be displayed as pink dots on the days when the samples were taken;
- 1 a green curve through the output values shows, through interpolation, the daily values of the output variables; and
- 1 to obtain the daily amount consumed (yellow line) of the specific species, the interpolated output will be subtracted from the input value.

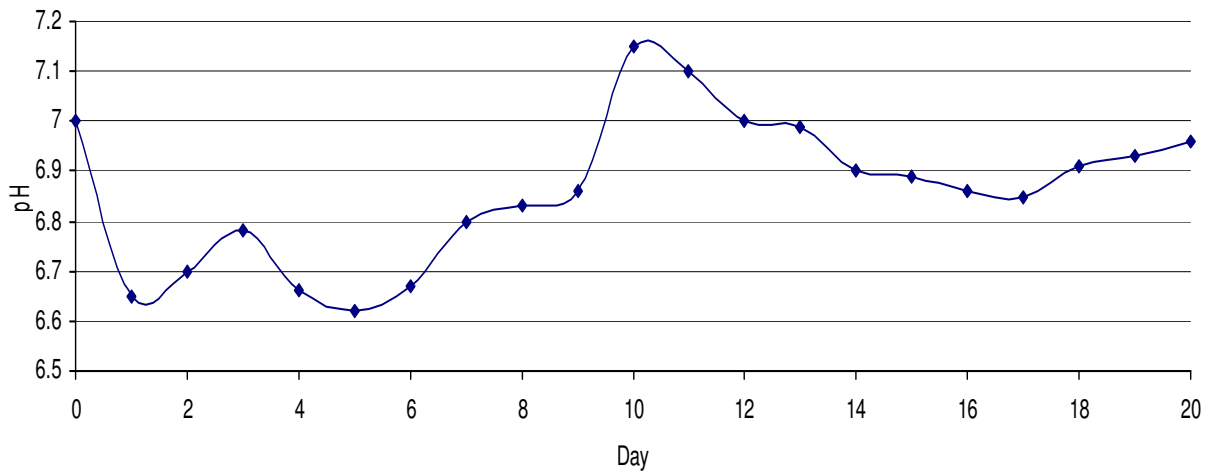


**Figure 7.2: pH vs. time for Mass Balance on R<sub>5.5</sub>**

The average pH was higher for this experiment than for the previous, possibly due to the finer nature of the sludge. The acidification phase lasted for 5 days after which the stabilisation phase started, peaking at Day 10, followed by a far more stable pH phase (the granule growth phase) occurring with a pH variation of less than 0.2 pH units occurring for the last 8 days of the run.

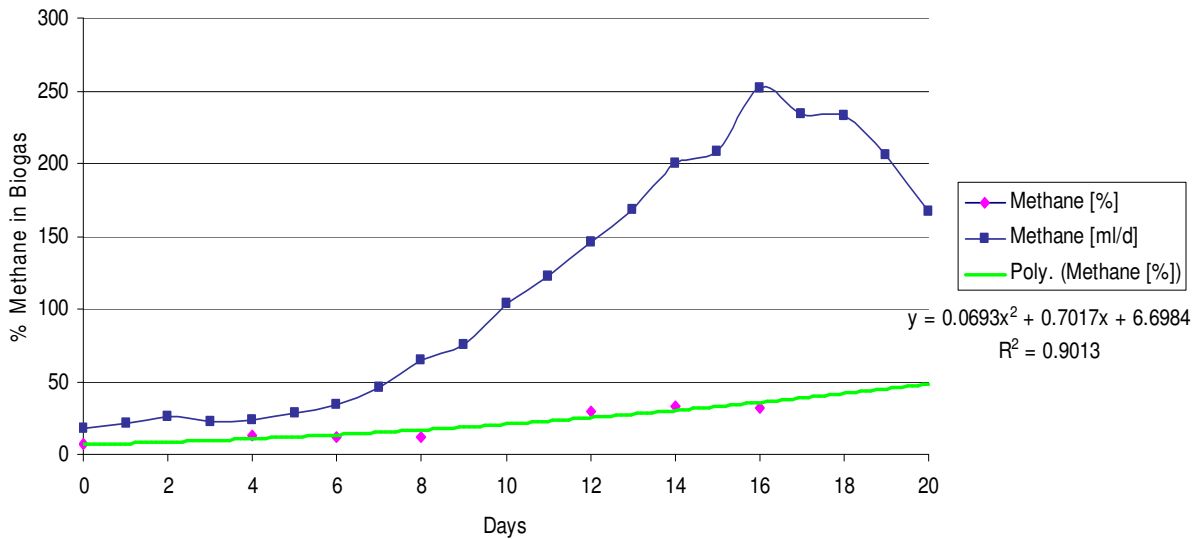


**Figure 7.3: Methane in Biogas Production vs. Time**

Figure 7.3 shows that the total methane (Methane [ml/d]) production increased dramatically after the acidification stage. It can also be noted that the methanogenic activity (Methane [%]) in the beginning of the run was very low. A possible reason for this might be the fact that the sludge was stored at 5°C for nearly 18 months as the

same sludge was used throughout this study. A peak occurred at Day 17, after which the total biogas production started to decrease.

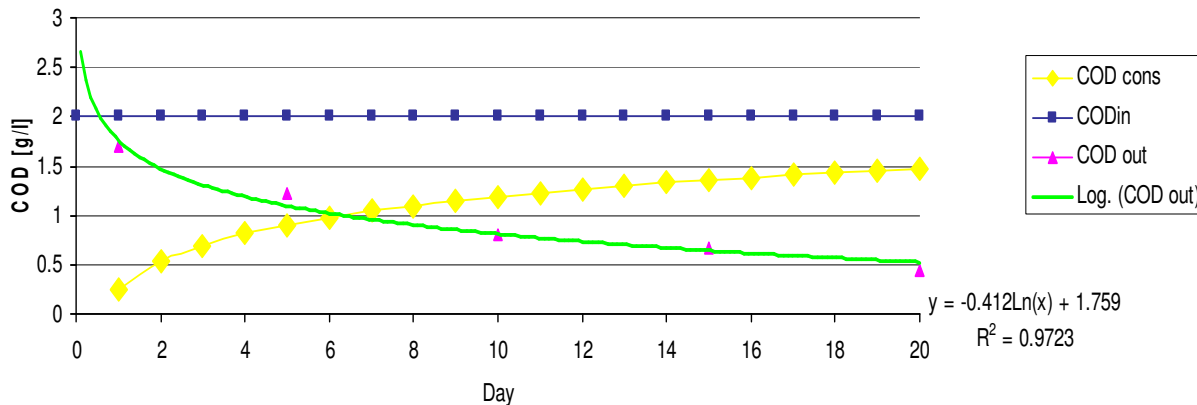


**Figure 7.4: COD Consumed vs. Time**

The influent (feed) COD was set to 2000 mg/l and the effluent (used feed) COD measured at regular intervals. From this data (Figure 7.4) it is evident that COD consumption was very low in the acidification stage. This can probably be attributed to the low activity of the sludge in the first 5 days. The COD removal rate reached approximately 80 % at the end of the 20 day incubation period.

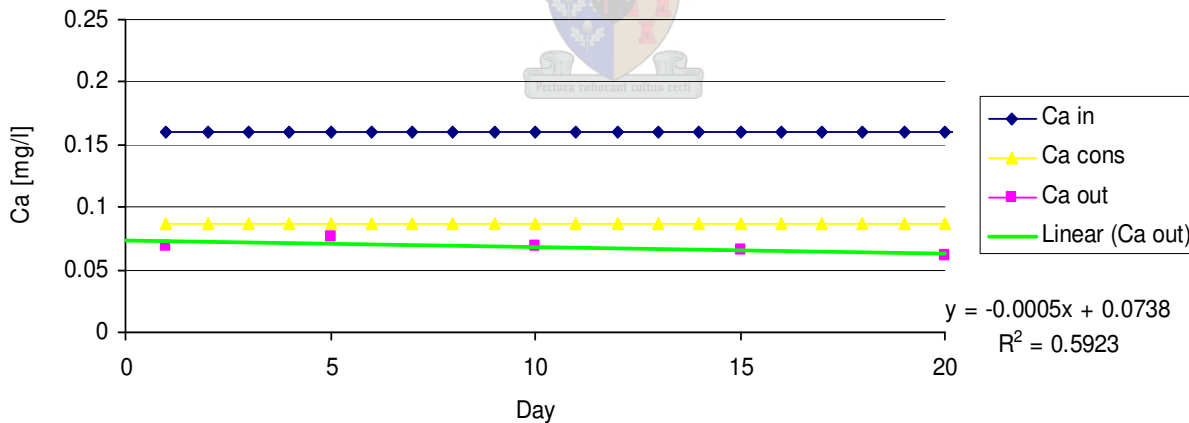


**Figure 7.5: Calcium consumption vs. time**

As shown in Figure 7.5, the calcium consumed (Ca cons) each day increased very slowly from the beginning to the end of the run. No dramatic in- or decreases in the consumption rate were observed.

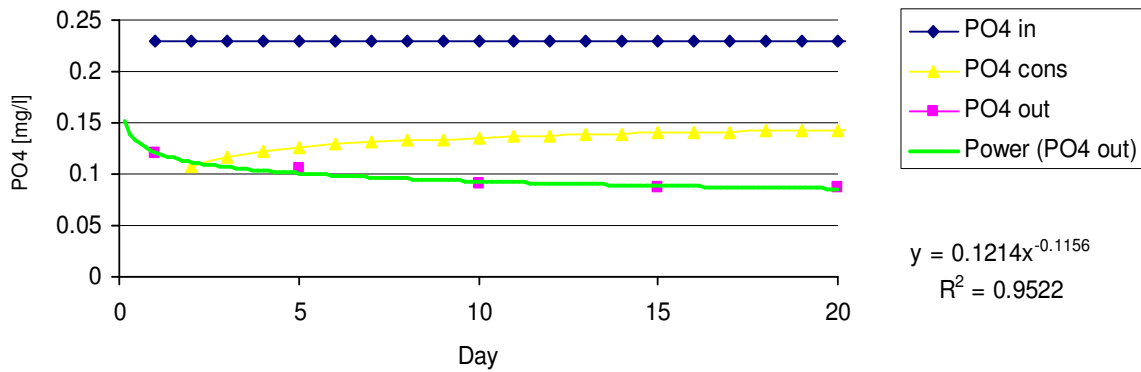


**Figure 7.6: Phosphate Consumption vs. Time**

The phosphate consumption occurred directly proportional to the COD. Even though a low consumption rate was observed in the beginning of the run became a gradual increase, it slowed down in the stabilisation phase (Figure 7.5 and 7.6).

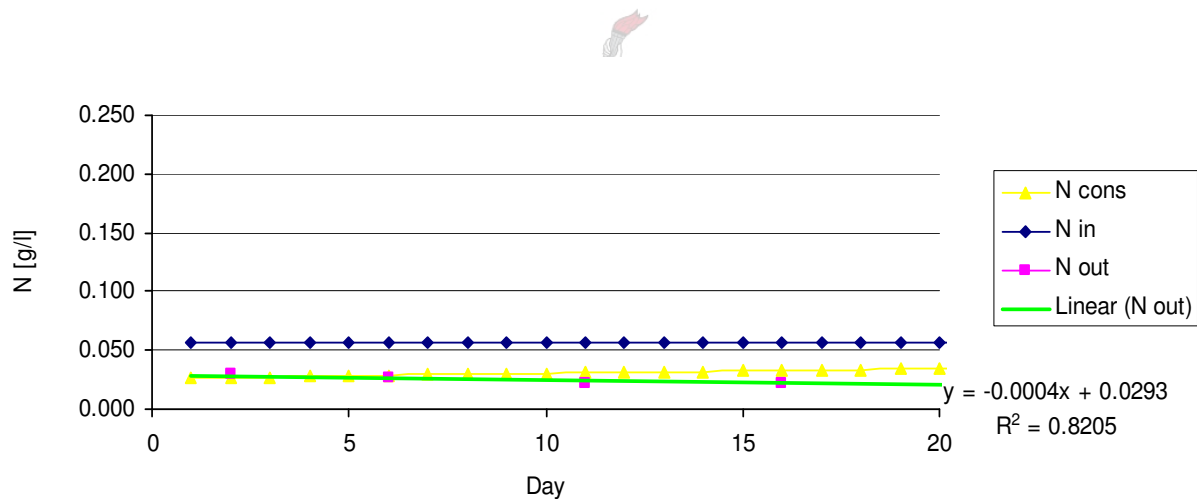


**Figure 7.7: Nitrogen Consumption vs. Time**

Nitrogen was absorbed by the biomass (N cons) in much the same manner as calcium.

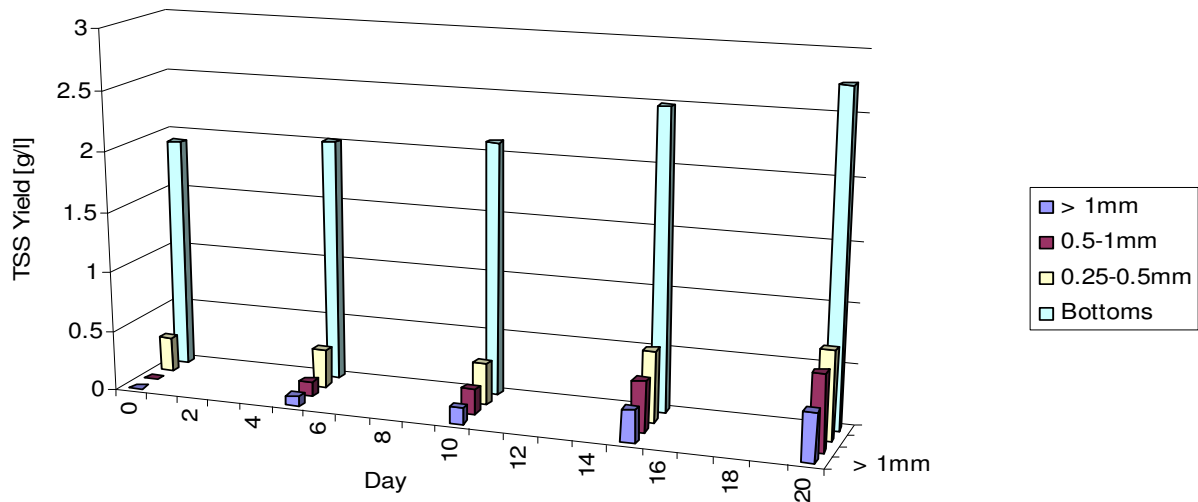


**Figure 7.8: Mass Increase in Each Size Range vs. Time (i)**

Figure 7.8 displays the growth that occurred during the 20 day incubation period: a definite increase in mass occurred in every size range, with the highest amount of growth occurring in the smaller size ranges.

## 7.4 Mass Balance and Modelling

As was discussed in section 7.2, a mass balance was done to predict the yield that will be obtained from the bioreactor after 20 days.

### 7.4.1 Mass Balance Predictions Compared to TSS values

Figure 7.9 shows the TSS values obtained for each size range over the 20 days. It can be noted that the growth curve followed near exactly the same shape for all the size ranges.

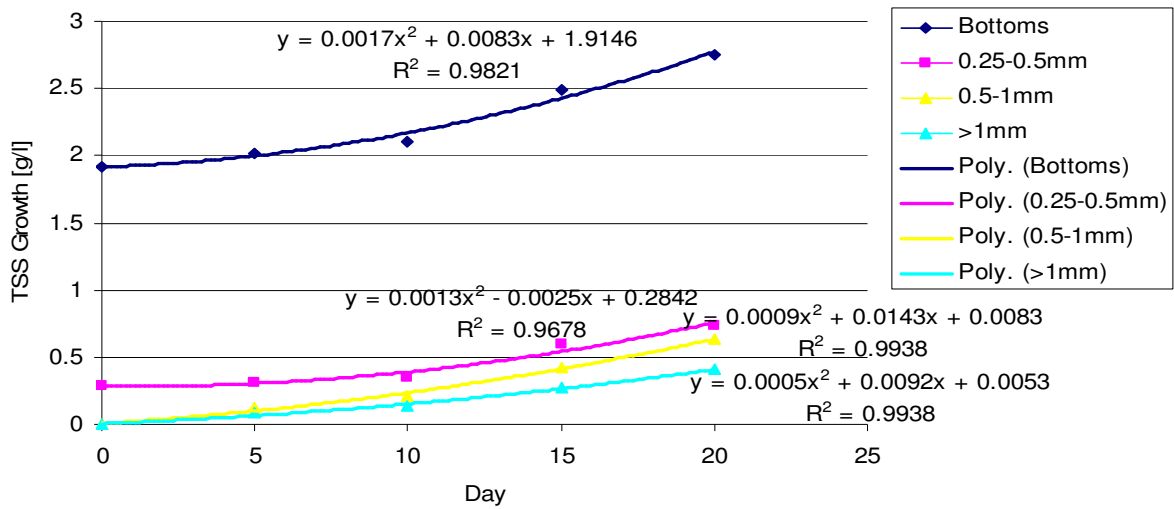


**Figure 7.9: Mass Increase in Each Size Range vs. Time (ii)**

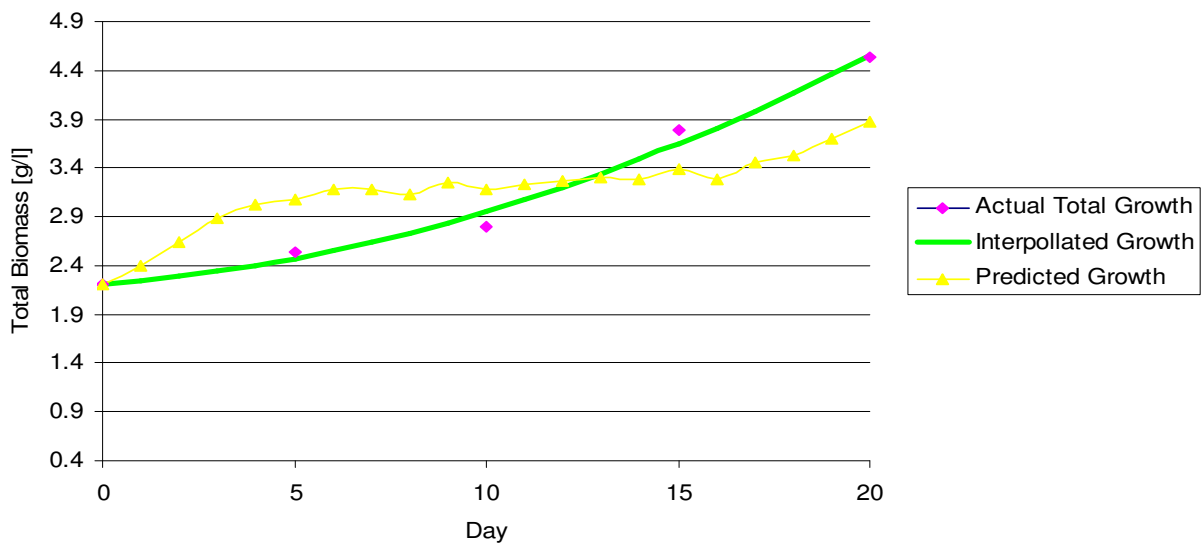


**Figure 7.10: Total Biomass Increase vs. Time**

Figure 7.10 represents the total growth (pink dots), interpolation curve of the total growth (green line) as well as the model prediction of the growth (yellow). As can be seen, the model overestimated the growth for the first 11 days, crosses the actual growth curve at day 13, until eventually underestimating the actual growth that occurred.



## 7.4.2 Summary of the Final Experimental Run

Table 7.1 summarises the results obtained from experimental run 13. The details on the mass balance and measured values can be seen in the appendix.

**Table 7.1: Results Run 13**

AVG	RunR <sub>5.5</sub>	
pH	6.8	
CaCO <sub>3</sub>	500	mg/d
KH <sub>2</sub> PO <sub>4</sub>	800	mg/d
CH <sub>4</sub>	19.6	cm <sup>3</sup> /d
COD	886	mg/d
MUG	3.6	kg/Vr

## 7.5 Summary

Figure 7.3 and 7.4 shows that the amount of COD consumed increases with the amount of biogas produced for the largest part of the run. The deviation towards the end of the run did not occur in previous runs and can probably be attributed to a leak in the biogas pipe or something similar that led to a lowering in the amount of biogas measured each day. Nevertheless, it can be concluded from these and previous runs that the amount of COD consumed is nearly directly proportional to the amount of biogas produced for any given period. This correlates well with statements made by Metcalf and Eddy, 2003.

The figures mentioned above also indicated that the methanogenic activity increased as the incubation time increased, which in turn led to an increase in the COD consumed. Therefore, the higher the methanogenic activity (or rather, the more active the methanogenic bacteria gets) the higher the consumption of COD will be (Els and Van Zyl, 2002).

When Figures 7.4, 7.5 and 7.9 are compared, one notice that in all the size ranges, growth is relatively slow in the first 15 days of the incubation period, with approximately 60 % of the total increase in biomass occurring in the final 3 days of the incubation. Yet, if one looks at COD consumption, the exact opposite is true; 60% of the total increase in COD consumption occurred within the first 10 days. This phenomenon clearly shows that COD must be converted to something other than biomass or biogas in the first 10

days of the run (Figure 7.3). The only other conversion that can take place is COD to extra cellular polymers (ECP). This conclusion compares well to statements made in literature (Britz et. al., 1999). It means that before the stabilisation phase, the microbes (acidogens) convert most of the COD to ECP in attempt to buffer the pH of their environment. After the pH has stabilised, COD is used for growth, and since the concentration of ECP is high in the last section of the run, the granulation rate also increases dramatically in the last few days (Figures 7.8 and 7.9).

If one compares Figures 7.5, 7.6 and 7.7 to Figure 7.4, it becomes clear that the consumption of inorganic species increases with the length of incubation period. The same can be said for if the COD consumption and growth is compared (Figure 7.8). Nitrogen and calcium increased linearly with time, but the amount of phosphates consumed showed a direct proportionality to COD consumption. Thus, the phosphates seem to be used for exactly the same operations as COD. In other words in the acidification stage phosphates are used for the production of ECP and at later stages used for metabolic activity and growth. Therefore, phosphates have proven to be by far the most prominent inorganic species in ECP. This correlates well with findings from literature (see Section 2.3.3).

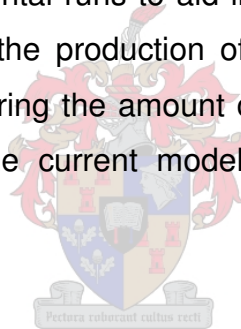
In previous runs, a 1 x 1 mm sieve was used to filter the sludge and a MUG of approximately 15 kg/Vr (Vr being one cubic meter of reactor volume) was produced. In this run the sieve diameter was halved (0.5 x 0.5 mm) and the MUG obtained after 20 days under exactly the same conditions (0.0055 m/s tipspeed in the 5.5 litre reactor) decreased by more than 70 % to only 3.6 kg/Vr. Therefore, particle size of the inoculation sludge is concluded to have a dramatic effect on the final yield. Based on these results it might be added that granules tend to grow much faster from smaller 'crushed' (by the sieve) granules than from dispersed sludge. The finer the sludge the slower the formation of granules will be, since the nuclei which are the precursors to granules, are smaller.

Figure 7.10 displays the actual measured values of growth over the 20 day incubation period compared to the predictions of the mass balance. The mass balance predictions are a bit optimistic in the acidification stage of the run. Possibly due to the fact that most of the nutrients used in this stage are used for ECP production, not growth (Britz et al., 1999). Since the model (at this point in time) does not account for ECP, the growth predictions will be high. In the stabilisation phase, the mass balance crosses the actual

values - yielding a lower than actual growth prediction in the end. Yet the day 20 prediction was still within 0.5 grams of the Day 20 TSS value.

If the results obtained from this operational run (Table 7.1) is compared to the results of experimental runs 11 and 12 (Tables 4.7 and 4.8, chapter 4), the average pH is about 0.2 pH units higher than the previous runs at the same tipspeeds (0.0055 m/s). Yet the amount of methane produced and the MUG obtained after 20 days were far lower than before. It can therefore be concluded that in a fine inoculation sludge, the overall methanogenic activity is significantly lower. This is probably due to the fact that the methanogens are 'protected' and aided by the acetogenic and acidogenic species inside the granules, enabling them to have a much higher activity (see Figure 2.4). The MUG of was also far less as was discussed earlier in this section.

The main recommendation of chapter 7 is probably the fact that the mass balance should be done on more experimental runs to aid in the accuracy to better the current model. In future mass balances, the production of extra-cellular polymers should be accounted for. A means of measuring the amount of ECP should be established. This can then be incorporated into the current model to hopefully produce even more accurate results.



# 8. *Final Conclusions and Recommendations*

---

---

Studies done earlier (Britz et al., 1999, Britz and Van Schalkwyk, 2002) showed that granulation can be artificially enhanced on lab-scale (450 ml reactor volume). The reactors used did not facilitate scale-up or the study thereof. The 2 larger reactors (specifically designed for the study of scale-up parameters) proved not only to enhance granulation, but also allowed granule formation to occur (to some extent) from dispersed sludge in the inoculum (see 3.17 Section 3.4.4). This is one of the most fundamental discoveries of the entire study; namely that the cultivation and enhancement of anaerobic bio-granules can be achieved artificially. However, the irregularly shaped granules formed, indicated that the flow patterns inside these reactors were less than optimal (Els and Van Zyl, 2002). Consequently, a third lab scale reactor was incorporated into the study, with flow patterns completely different those which occurred in the 4.15 and 7.2 litre units.

The research done in Chapter 3 confirmed a drop of approximately 2 pH units (7 to nearly 5) occurs naturally within the first 4 days of operation. This can probably be attributed to the fact that the doubling times of the organic acid producing bacteria (acidogens) have a far shorter doubling time than the methanogenic species, hence the drop in pH. At a pH lower than 6, the methanogenic species become dormant and death starts to occur. These methane producing species form the initial granule nuclei as well as the core of mature granules - thus vital for granulation to occur (Britz and Van Schalkwyk, 2002). External intervention is therefore needed to maintain a pH above 6 in the reactor volume. On the other hand, the ECP producers that also play a key role in the granulation process only become active at a pH lower than 6.5. Extra-cellular polymers (ECP) are vital for the formation of embryonic granules (also known as nuclei) in the first few days of operation (Britz et al., 1999). To accommodate all of these factors, the pH should be allowed to drop below 6.3 (acidification phase), but then intervention

should start immediately. This can be done by increasing the feed pH to 7.5, which will allow stabilisation of the reactor pH over the next few days (stabilisation phase), resulting in a near neutral pH at the end of the incubation period (growth phase).

From day 14 onwards in Experiment 4, the sludge started to stabilise its own pH (Figure 3.15). In the beginning of the incubation period, the acidogenic bacteria are far more prominent than the methanogenic species. Reasons for this include an abundance of growth medium and a much faster doubling time than their methane producing counterparts. However, as the amount of by products (mostly VFAs) produced by these species increase, so does the inhibitory effect of the VFAs increase. Furthermore, even though VFAs are the primary food source for the methanogenic species, the resultant drop in pH with an increase in concentration of VFAs therefore also inhibits the methanogenic step. The answer lies in the addition of alkalinity or buffering capacity in the form of bicarbonates (in the form of  $\text{CaCO}_3$ ) to the reactor volume. This allows VFA formation to increase without having as large an effect on pH as would be the case without the buffering. The elevated pH levels allows for the methanogenic conversion of VFAs to biogas and thus resulting in a far higher methanogenic activity, which in turn aids in the granulation process and breaks down the VFAs. The resultant effect of the VFA removal is that the pH of the reactor volume increases. When the  $\text{CaCO}_3$  was at 100 mg/l, self-stabilisation did not occur (see Figure 3.5). Furthermore, results also show that calcium promotes granulation. The explanation given in the literature is that the divalent  $\text{Ca}^{2+}$  ion also enhances the formation of extra-cellular polymers (ECP), which in turn acts as a hydrogen sink that stabilises the pH. ECP is also needed for granulation (see Section 2.2.3). It is clear that the addition of  $\text{CaCO}_3$  in sufficient amounts has quite a few advantages and that this buffer is the best for use on this system.

The following proved to be essential characteristics for a sludge when used in a granulation study:

- 1 a pH variation of less than 0.1 pH units 10 days after being separated from the digester,
- 1 a specific gravity larger than 1, and
- 1 a continuous granule size distribution in the virgin sludge in the 0 to 2.5 mm range.

The last is probably the most important parameter, because even though there are mature granules in the sludge, new granules are still formed on a regular basis. Formation continues during the incubation process.

The feed optimisation proved that the suggested feedstock composition (COD:N:P = 300:5:1) was far from adequate for the reactor configurations used. The following feedstock configuration is recommended:

COD	2000	mg/l
CaCO <sub>3</sub>	400	mg/l
Urea	200	mg/l
KH <sub>2</sub> PO <sub>4</sub>	800	mg/l
Trace Elements	10	ml/l
Ca(OH) <sub>2</sub>	Used for pH adjustments in medium	

This configuration led to a more than 500% higher MUG yield than before. A COD:N:P ratio of 10:1:4 generates far better results. It was also proven that trace elements and the elimination of monovalent anions like Na<sup>+</sup> and K<sup>+</sup> result in higher yields, hence KHCO<sub>3</sub> was completely abandoned (Britz et al., 1999). The reason for this is that monovalent anions neutralise the resultant negative charge on the bacterial cell. Consequently the formation of ionic bonds with divalent anions (Ca<sup>2+</sup>) cannot occur (Mahoney et al., 1987). The high phosphate concentration aids the increase in cell hydrophobicity, and it has proven to be one of the primary building blocks of ECP (Van Loosdregt, 1887).

The results from the mixing speed optimisation section of the study (Chapter 4) indicated that the radial flow patterns induced by R<sub>5.5</sub> are superior to the other two configurations, with regards to granule production. The optimal baffle tipspeed of 0.0055 m/s was identified and it was proven that a tipspeed larger this leads to a dramatic lowering in the MUG in any configuration. One explanation for the performance of the 5.5 litre unit is the fact that low tipspeeds can be maintained, but mixing of the sludge and feedstock will still be high enough for sufficient mass transfer to occur. The rolling motion induced on the sludge by the rolling shell also aids the 'rounding' of the granules, improving settling properties.

In the field of microbial granulation, a dire need exists to classify granule growth. Current methods are not only operator dependant, but can lead to large errors and/or

destructive in nature (Laguna et al., 1999). Because of this, an initial study was performed in search of a growth determining procedure that would abide to the following criteria:

- a non-destructive nature;
- quantitative testability;
- provide information as to the size distribution and number of granules ; and
- be less time consuming than other methods.

The chosen method was a digital image processing model written and compiled in Matlab ®. For this method, the sample was sieved, diluted and then photographed with a digital camera. The image is fed to the image processor and the sample analysis is obtained. Various samples and dilution ratios were tested to obtain the predicted MUG (DIPMUG) This was then compared to the actual MUG results obtained by the conventional means (Appendix: Section A5). Results varied in accuracy, but in the end it was found that a 200 ml reactor volume sample split into 2 x 100 ml sub-samples yielded the best results with R<sup>2</sup> values ranging from 0.71 to 0.99. This and the fact that very small sample sets were used, emphasise the fact that this was only an initial study, setting the design criteria and initial model into place. Much more research still needs to be done on this topic.

In Chapter 7 it was proven that the amount of COD consumed increases with the amount of biogas produced for the largest fraction of the run. Thus, the amount of COD consumed is nearly directly proportional to the amount of biogas produced for any given period (Metcalf and Eddy, 2003). The methanogenic activity increased with an increase in the incubation time, which in turn led to an increase in the COD consumed. Thus it can be concluded that the higher the methanogenic activity (or rather, the more active the methanogenic bacteria gets), the higher the consumption of COD will be.

The study showed further that in all the size ranges, growth is relatively slow in the first 15 days of the incubation period, with approximately 60 % of the total increase in biomass occurring in the final 3 days of the incubation. Yet, if one looks at COD consumption, the exact opposite is true. 60% of the total increase in COD consumption occurs within the first 10 days. This phenomenon shows that COD must be converted to something other than biomass or biogas in the first 10 days of the run. The only other conversion that can take place is COD to ECP. Therefore, before the stabilisation phase,



the microbes (acidogens) convert most of the COD to ECP to buffer the pH and to protect them from their environment. After the pH has stabilised, COD is used for growth, and since the concentration of ECP is high in the last section of the run, the granulation rate also increases dramatically (growth phase) in the last few days.

The consumption of inorganic species increased with the length of incubation period, along with COD consumption and growth. Nitrogen and calcium increased marginally with time, but the amount of phosphates consumed showed a direct proportionality to COD consumption. Thus, it can be concluded that phosphates are used for exactly the same operations as COD. That is to say, during the acidification stage phosphates are used for the production of ECP and at later stages, it is used for metabolic activity and growth. Therefore, phosphates are by far the most prominent inorganic species in ECP. This finding correlates well with those in the literature (see Chapter 2).

In previous experimental runs, a 1 x 1 mm sieve was used to filter the sludge and a MUG of approximately 15 kg/Vr was obtained. In this run, the sieve diameter was halved (0.5 x 0.5 mm) and the MUG obtained after 20 days under exactly the same conditions ( 0.0055 m/s tipspeed in the 5.5 litre reactor) decreased by more than 70 % to only 3.6 kg/Vr. Particle size of the inoculation sludge therefore has a dramatic effect on the final yield. Based on these results it might be added that granules tend to grow much faster from smaller 'crushed' (by the sieve) granules than from fine sludge. And the finer the sludge, the slower the formation of granules will be, since the nuclei which are the precursors to granules are smaller.

The mass balance prediction was found to be a bit high in the acidification stage of the run. This could be attributed to the fact that most of the nutrients used in this stage go towards ECP production, not growth. Since the model (at this point in time) does not account for ECP, the growth predictions will be high. In the stabilisation phase, the mass balance crosses the actual values yielding a lower than actual prediction in the end. However, the Day 20 prediction was still within 0.5 grams of the day 20 TSS value.

The results from the internal surface area (ISA) variation section of the study showed a definite increase in the rate of granulation, with an increase in the ISA of the reactor at constant tipspeed. Therefore, the granulation process seems greatly aided by an increase in the microbe-to-surface contact time. The more shear or 'friction' the cells experience the more ECP will be produced, to protect them from their environment. As



was stated in Chapter 2, ECP is also one of the prime precursors for the granulation process. The higher the ECP production, the higher the rate of granulation will be. Anything that aids ECP production, no matter how cruel to the microbes, will thus also aid the granulation process. If the same line of reasoning is used, the long start-up period of the UASB can be accounted for in the following manner: due to the very low level of cell-to-surface contact inside the UASB, ECP production would not be as prominent, and therefore the overall ECP production- and granulation rate would be much lower.

Even though the DIP is at this stage not 100% accurate, this programme delivers more detailed information on a sample than the conventional MUG tests. From the latter, only the dry mass could be retrieved, whereas the DIP provides the average particle size, amount of particles, biggest particle and also a size distribution of particles. Thus, even though the original MUG tests are still necessary to act as a benchmark for the DIP, incorporating the DIP model can lead to far more information than the conventional MUG tests. As stated earlier this 'new' information on average particle diameter and size distribution will form the basis of future studies.

Future growth prediction models should also attempt to predict the growth in each of the size ranges over the incubation period. The DIP yields a histogram of the size distribution of the granulated sample studied. If samples are drawn on Day 0, 5, 10, 15 and 20 of the incubation period is processed; a histogram of each sample will be obtained. The growth in each size range can thus be quantified. If one takes a typical particle breakage model used in mineral processing like for example the 'King' model (Hayes 1993) it can be inverted, to represent particle 'growth' rather than particle breakage. In other words, the same fundamental principles used to describe how ore breaks from one large rock to many smaller particles, can be inverted and used to describe how granules grow from dispersed sludge to mature granules. A growth function from fines to large particles, rather than the usual breakage from large particles to smaller will be obtained and with this, possibly the first function describing the granule growth that occurs in anaerobic sludge. By lengthening the growth rate parameters a function describing the growth in an actual UASB might also be possible. It is highly recommended that a study and evaluation of such a model be incorporated into the later phases of the larger WRC project, since it would give a large amount of insight into the growth process.

One of the main problems was leakage at the rubber seals on the reactors. These seals were situated where a rotating axis passed through the stationary reactor shell (R<sub>4.15</sub> and R<sub>7.2</sub>) or vice versa (R<sub>5.5</sub>). Leakages caused by sand that entered the mechanical seal and then grinding away at the rubber until the watertight seal started to leak.

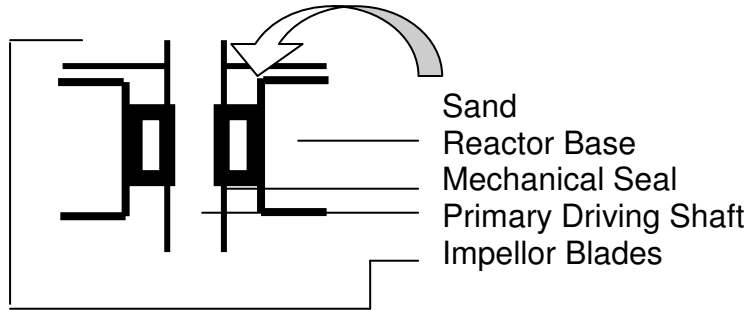


**Figure 8.1: Mechanical Seal at Reactor Base**

Sand is a quite a common occurrence in anaerobic sludge. In a high throughput situation, would be difficult to separate the sludge from the sand, due to the similar settling properties. Therefore, whatever reactor configuration is used, avoid using mechanical seals at the base of the reactor, as was the case with R<sub>4.15</sub>.

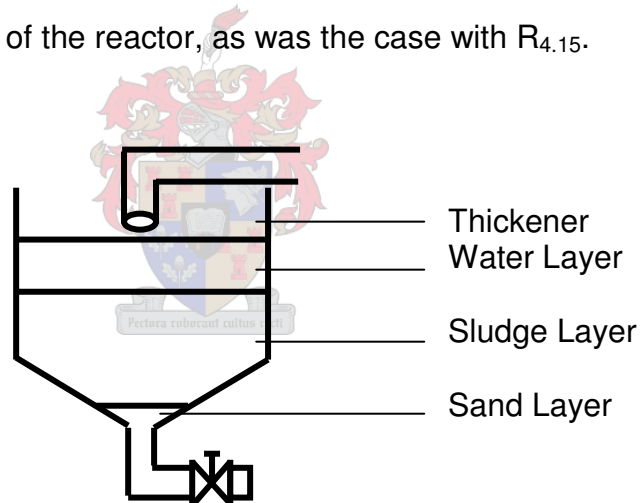


**Figure 8.3: Basic Thickener Design**

The compositions and consistency of anaerobic sludge are notorious for its major fluctuations from one batch to the following. Therefore, in a high throughput situation, a sludge pre-treatment unit should be incorporated into the design. A thickener will probably be the most economic pre reaction treatment system for this application. This unit will be able to separate the watery (undesirable) part of the sludge from the more visquous part. Another advantage is that the most of the sand that enters the system can be separated from the anaerobic sludge and this will in turn result in a longer lifespan of the pump and seals in the system.

As discussed earlier, one of the main criteria for separation of granulated anaerobic sludge from sand, plant and animal rests is the differences in settling velocity. It is therefore recommended that a fluidised bed be incorporated into the design to serve as a post-reaction treatment unit. The following discussion gives the basic advantages obtained by incorporating the fluidised bed design, as can be seen in Figure 8.4.

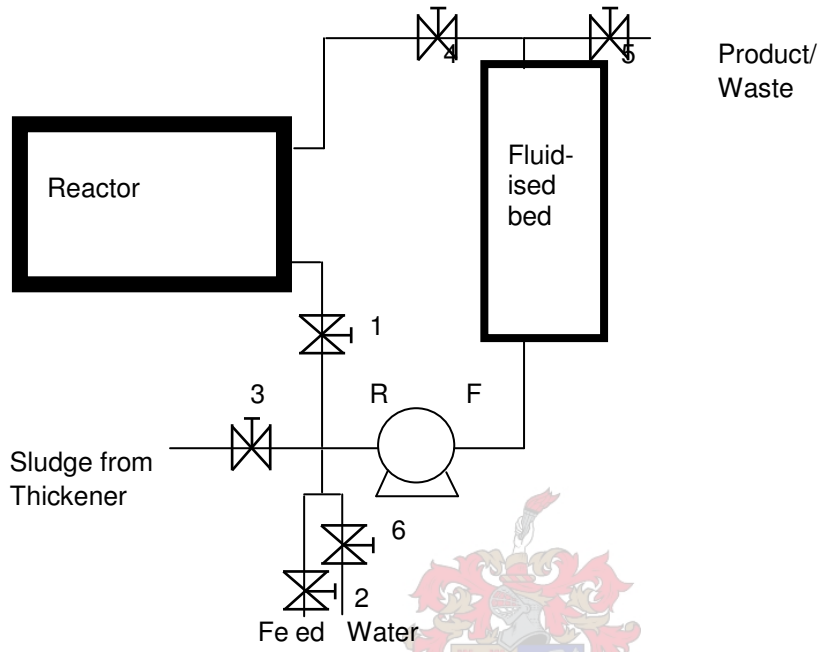


**Figure 8.4: PFD of Reactor and Fluidised Bed**

This system holds the following advantages:

- 1 ungranulated sludge can be returned to the reactor via the fluidised bed,
- 1 the average particle diameter of the product can be altered by manipulating the up-flow velocity through the fluidised bed,
- 1 the sludge can be washed before entering the reactor.

# 9. References

---

1. Agrawal LK, Hadada H, Okui H. (1997) *Treatment of dilute wastewater in a UASB reactor at a moderate temperature: Performance aspects*. *Jou. Ferm. Bio.* Vol. 83, No 2, pp. 179-184.
2. Alpenaar PA, Sleyster R, De Reuver P. (1993) *Phosphorus requirement in high-rate anaerobic waste water treatment*. *Water Research*, Vol. 27, No. 5, pp. 749-756.
3. Armante PM & Tong L. (2002) *Minimum agitation speed for off-bottom suspension of solids in agitated vessels provided with multiple flat-blade impellers*. *Proc.Mix.-Chem.and Biochem. App.* :Part ii.
4. Batstone DJ, Keller J, Blackall LL. (2004) *The influence of substrate kinetics on microbial community structure in granular anaerobic biomass*. *Water Research*, Vol. 38, pp. 1390 – 1404.
5. IEA BIOENERGY, (1996), *Biogas from Municipal Solid Waste, Overview of Systems and Markets for Anaerobic Digestion of MSW*, Danish Energy Agency, 11 Landemaerket, DK 1119, Copenhagen K, Denmark.
6. Britz TJ, Trnovec W, Van Schalkwyk C, Roos P, (1999) *Enhanced granulation in up-flow anaerobic sludge bed digesters (UASB) by process induction and microbial stimulation*. WRC Report. No 677/1/99,
7. Britz TJ & Van Scalkwyk C. (2002) *Development of a method to enhance granulation in a laboratory batch system*. *Water SA* Vol. 28 No 1.
8. Buswell, A.M. & W.D. Hatfield, (1936), *Anaerobic Fermentations*, State of Illinois Department of Registration and Education, Bulletin 32, Urbana, IL, USA.
9. De Zeew W. (1980) *Accumulation of digested sewerage sludge during start-up of an UASB*.

10. Els ER, Van Zyl PJ. (2002), *Optimisation of enhanced bio-granulation*. University of Stellenbosch, Undergraduate Thesis. 88 pages
  11. Els ER, Van Zyl PJ, Volkwyn A. (2003), *Bioreactor feed optimisation for enhanced bio-granulation*. University of Stellenbosch, Undergraduate Thesis. 70 pages.
  12. Fogler HS, (1999) *Elements of chemical reaction engineering*. 3<sup>rd</sup> Edition, Prentice Hall. 967 pages.
- Franklin RJ, (2001) *Full scale experience with anaerobic treatment of industrial wastewater*. Wat. Sci. Technol. 44(8) pp. 1-6.
13. Guiot, S.R. & Gorur, S.S., *Nutritional and environmental factors contributing to microbial aggregation during UBF start-up* Wat.Sci.Tech. Vol. 23. No.3, pp. 51-57
  14. Hayes, P., "*Process principles in Minerals & Materials Production*" (1993) 1<sup>st</sup> Edition, Hayes Publishing Co. 730 pages.
  15. RC Hibbler (1993) *Engineering mechanics DYNAMICS*. Prentice Hall International, 7<sup>th</sup> edition, 618 pages.
  16. Hulshoff Pol. L.W., de Zeew. W.J., and Lettinga G. (1982) *Cultivation of well-adapted palletized methanogenic sludge*. Bio.technol. Letters Vol.4 No.5, pp. 329-332.
  17. Hulshoff Pol. L.W., de Zeew. W.J., and Lettinga G. (1983) *Granulation in UASB reactor*. Water Sci. and Technol. 8/9, pp. 291-304.
  18. Hulshoff Pol LW, Heijnekamp K, Lettinga G. (1988) *The selection pressure as driving force behind the granulation in anaerobic sludge*. Granular anaerobic sludge: microbiology and technology, pp.153-61.
  19. Hulshoff Pol LW, De Castro Lopes SI, Lettinga G. (2003) *Anaerobic sludge granulation*. Water Research.



20. Koberle, Erwin, (1995), *Animal Manure Digestion Systems in Central Europe*, In: Proceedings of the Second Biomass Conference of the Americas, August 21-24, 1996, Portland, OR, National Renewable Energy Laboratory (NREL), 1617 Cole Blvd., Golden, CO, USA.
21. Laguna A, Quattara A, Gonzalez R O, Baron O, Fama G, El Mamounti R, Guiot S, Monroy O, Macarie H, (1999). *A simple and low cost technique for determining the granulometry of up-flow anaerobic sludge blanket reactor sludge*. Wat.Sci.Tech. Vol 40, pp 1 – 8.
22. Lettinga, G., A. F. M. van Velsen, S. W. Hobma, W. De Zeeuw, A. Klapwijk. (1980) *Use of up-flow sludge blanket reactor concept for biological wastewater treatment, especially for anaerobic treatment*. Biotechnol. Bioengineer. Vol 22, pp. 699-734.
23. Liu Y, Yang SF, Tay JH.( 2003) *Cell hydrophobicity is a triggering force of bio-granulation*. Enz. And Microb. Technol. Vol 37, pp. 76-78.
24. Liu Y, Xu HL, Yang SF. (2003) *Mechanisms and models for anaerobic granulation in up-flow anaerobic sludge blanket reactor*. Water Research, Vol 37, pp. 661 – 673.
25. Lusk, P., Wheeler, P. and Rivard, C., editors, (1996), *Deploying Anaerobic Digesters: Current Status and Future Possibilities*. NREL, 1617 Cole Blvd., Golden, CO, USA.
26. Mahoney EM, Varangu LK, Cairns WL. (1987) *The effect of calcium on microbial aggregation during UASB reactor start-up*. Water Sci. Technol. Vol 19, pp. 249-60.
27. Metcalf & Eddy. (2003) *Wastewater engineering treatment and reuse*. 4<sup>th</sup> Edition, McGraw Hill, 1249 pages.
28. Oldshue JY. (1995) *Geometric relationships for scale-up of diverse mixing processes*. Oldshue. Tech. Int.
29. Pereboom JHF. (1994) *Size distribution model for methanogenic granules from full scale UASB and IC reactors*. Wat.Sci.Tech. Vol. 30. No.12.
30. Powers T. (1993) *Heisenberg's War*. Da Capo Press, 1<sup>st</sup> edition

31. RAP Bulletin (1995), *Rural Energy, Medium and Large Scale Biogas Systems in the Asia-Pacific Region*, (1995), ISSN 1011-6443, Regional Office for Asia and the Pacific, Food and Agricultural Organization, Maliwan Mansion, 39 Phra Atit Road, Bangkok 10200, Thailand.
32. Schmidt JE, Ahring BK, (1994), *ECP in granular sludge from different UASB reactors*. Appl Microbiol Biotechnol. Vol 42, pp. 457-62.
33. Show K-Y, Wang Y, Foong S-F. (2004), *Accelerated start-up and enhanced granulation in up-flow anaerobic sludge blanket reactors*. Elsevier Ltd.
34. Singh KS & Viraraghavan T. (2002) *Modelling of sludge blanket height and flow patterns in UASB reactors treating municipal waste water*. Wastewater treatment
35. Smith, W.H. & Frank, J.R., (1998) *Methane from Biomass: A Systems Approach*, Elsevier Applied Science, London, United Kingdom, pp 500.
36. Standard Method – *Water Suspended Solids*, (1990), South African Buro of Standards. SABS Method 1049:1990.
37. Uremura S, Harada H. (1995) *Inorganic composition and microbial characteristics of methanogenic granular sludge grown in a thermophillic up-flow anaerobic sludge blanket reactor*. Appl. Microbiol. Biotechnol., Vol. 43, pp. 358 – 364.
38. Tattersson GB. (2002) *Scaling based upon similarity and scale matching concepts*. Proc.Mix.-Chem.and Biochem. App. Part ii.
39. Tay JH, Xu HL, Teo KC. (2000) *Molecular mechanism of granulation I: H<sup>+</sup> translocation-dehydration theory*. Journ. Environ. Eng.
40. Tay JH & Liu QS. (2001) *The effects of shear force on the formation, structure and metabolism of anaerobic granules*. App. Microbiol.Biotechnol Vol 57 pp. 227-233.
41. Teo KC, Xu HL, Tay JH. (2000) *Molecular mechanisms of granulation-II: proton translocating theory*. Environ. Eng. Vol 126, pp. 411-418.

42. Thaveesri J & Daffonchio D. (1995) *Granulation and sludge bed stability in UASB reactors in relation to surface thermodynamics*. Appl Environ Microbiol Vol 61, pp. 3681-3686.
43. Trnovec W & Britz TJ. (1998) *Influence of organic loading rate and hydraulic retention time on the efficiency of a UASB bioreactor treating canning factory effluent*. Water SA Vol. 24, No. 2.
44. Van Der Haegen B, Ysebaert E, Favere K, Van Wambeke M, (1992). *Acedogens in relation to in-reactor granule yield*. Wat.Sci.Tech. Vol 25, pp21 – 29.
45. Van Loosdregt MCM, Lyklema J, Norde W, Schraa G. (1987) *Electrophoretic mobility and hydrophobicity as a measure to predict the initial steps of bacterial adhesion*. Appl Environ Microbiol Biotechnol Vol 53, pp.1898-1901
46. Van Oudenaaren A, N Mittal, Budrene EO. (2003) *Motility of E-coli cells in clusters formed by chemotactic aggregation*. PNAS, Vol. 100, No 23, pp. 13259 – 13263.
47. Vining GG, (1998) *Statistical methods for engineers*. Brooks/Cole Publishing company.
48. Wilkie, A.C., Van Horn, H.H. Powers, W.J. and Riedesl, K.J. (1995), *Anaerobic Treatment Technology - An Integrated Approach to Controlling Manure Odors*. In: International Livestock Odor Conference Proceedings '95, New Knowledge in Livestock Odour,. Iowa State University College of Agriculture, Ames, IA, USA. pp. 223-277.
49. Winter J & Zellner G. (1990) *Thermophillic anaerobic degradation of carbohydrates – metabolic properties of micro-organisms from different phases*. FEMS Micro.Biol. Rev 75, pp. 139 – 154.
50. Yu HQ & Tay JH. (2001) *The roles of calcium in sludge granulation during UASB reactor start-up*. Water Research Vol. 35, No 4, pp. 1057 – 1060.



# Appendix

---

---

## A1. Operational Procedures

### A1.1 Reactor Operation

To obtain results that could be compared directly to that of experiments done on the shaker and roller tables, the exact same sludge to feed ratio's, feed composition, feeding and tapping methods and incubation periods (20 days) were used. The reactor operation can be summarized as follows:

- Day 0 – The units were loaded with a 2:7 ratio (by volume) of sludge to feed.
- Day 1 to 20 – The reactor was stopped once each day to allow the sludge to settle, 2/7 of the reactor volume of used feed is removed and replaced with an equal volume of fresh feed.
- Day 1 to 20 – The pH of the reactor volume was also measured on a daily basis measured and the necessary pH adjustments are made to the fresh feed before introducing it into the reactor.
- Day 1 to 20 – The amount of biogas produced and the fraction of methane was also measured to get an indication of the microbial (and methanogenic) activity during the incubation period.

### A1.2 Feed Composition and Sludge Preparation

Table A1 display the composition of this basic feed medium.

**Table A1: Composition of Basic Feed Medium**

Additive	Amount
PCE (COD)	2 000 mg/l
KH <sub>2</sub> PO <sub>4</sub>	200 mg/l
Urea	200 mg/l
CaCO <sub>3</sub>	100 mg/l
NaOH	pH Manipulator

The peach cannery effluent (PCE) was diluted to 2000 mg/l with distilled water. The reason for the low COD was found to be that the granulation rate increases if microbial growth occurs in a semi-starved state (see Section 2.5.1). Further additives include  $\text{KH}_2\text{PO}_4$  (source of phosphate), Urea (source of nitrogen) and  $\text{CaCO}_3$  (for alkalinity and calcium). These were added to the diluted PCE and the suspension was mixed until all the organics were dissolved. The pH was set to 7 with NaOH.

The raw anaerobic digester sludge was prepared by passing it through a 1 x 1 mm sieve to ensure that no granules larger than this were present at the beginning of the incubation period.

### **A1.3 Sludge Screening Tests**

In almost all earlier studies done on anaerobic sludge, one problem stands out; the lack of methods to quantify the sludge (Britz et al., 1999; Britz and Van Schalkwyk, 2002; Els and Van Zyl, 2002). That is to say, there is no way to answer the following question: is this a good sludge or not? A more accurate question would be: Which parameters should be measured and compared to be able to make a decision on using the sludge in a given system or not; and if a given sludge is used, what adjustments should be made to optimise the system for the sludge?

The following are some examples of parameters that should be measured and compared to make conclusions about how prone a sludge would be to granulation.

#### **A1.3.1 Density ( $\rho$ )**

The following procedure can be used to measure the density.

- Take a 1 dm<sup>3</sup>-measuring unit.
- Place unit on laboratory scale, zero the scale.
- Fill the unit with the sludge feed mix that is going to be fed to the reactor.
- Make sure that all the chemicals have been added beforehand.
- Place unit on zeroed scale and record the mass, and
- multiply the mass by 1000 to obtain the density in kg/m<sup>3</sup>.

### A1.3.2 Settling time ( $t_s$ )

The main reason why the settling time of the sludge is important is the belief that most of the better types of sludge have longer settling times. The following method is recommended for determining  $t_s$ :

- Make up 1 litre of sludge, feed and additives.
- Shake the sludge-feed mix thoroughly and allow to stand overnight at 5 degrees Celsius. This will inhibit sludge activity that might affect the settling time.
- Mark the level of the sludge layer ( $L_s$ ),
- Now shake the mix thoroughly once more and start timing the second the agitation has stopped.
- If the sludge reaches  $L_s$  again, the timer can be stopped, the reading on the timer can be recorded as  $t_s$ .

### A1.4 DIP Calibration

1. The first step in calibrating the DIP is to take a digital photograph of the calibration sheet with the set-up depicted in Figure 5.1. Like for example Figure A1.1, of which the average 'particle' diameter is known. The average particle diameter of this specific image is 2.475 mm.

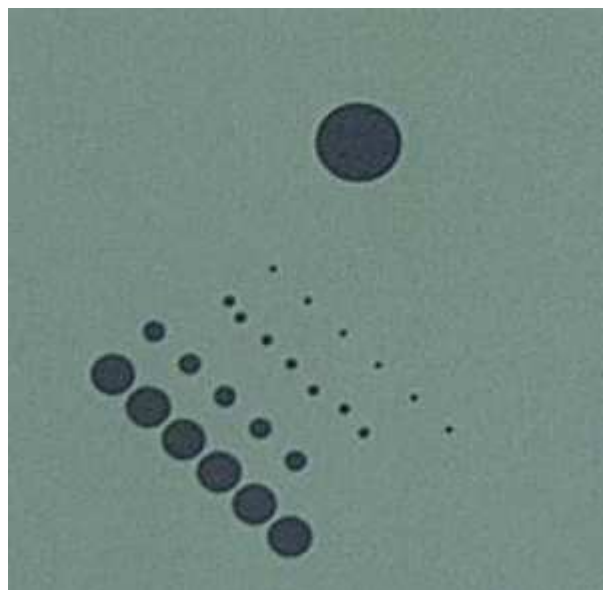


**Figure A1.1 Calibration image used for calibration of the DIP program (particles: 1x10mm; 6x5mm; 5x2mm; 7x1mm and 6x0.4mm)**

2. Now the operator is asked for the minimum cut-off size, and the average particle diameter. Normally the cut-off size is set to  $>0.5$  mm (or 0.4mm) and the average particle diameter can be calculated for the given calibration image.
3. The DIP program now automatically calculates the pixel to millimetre (ptmm) conversion.



**Figure A1.2: Calibration image used for calibration of the DIP program**

4. The next step is to obtain an adequate greyscale cut-off (CLevel) and minimum cut-off size (Cut) to ensure the circles are correctly identified and nothing else.



**Figure A1.3: DIP Calibrator Output (CLevel = 0.4, Cut = 0.2 mm)**



**Figure A1.4: DIP Calibrator Output (CLevel = 0.4, Cut = 0.5 mm)**

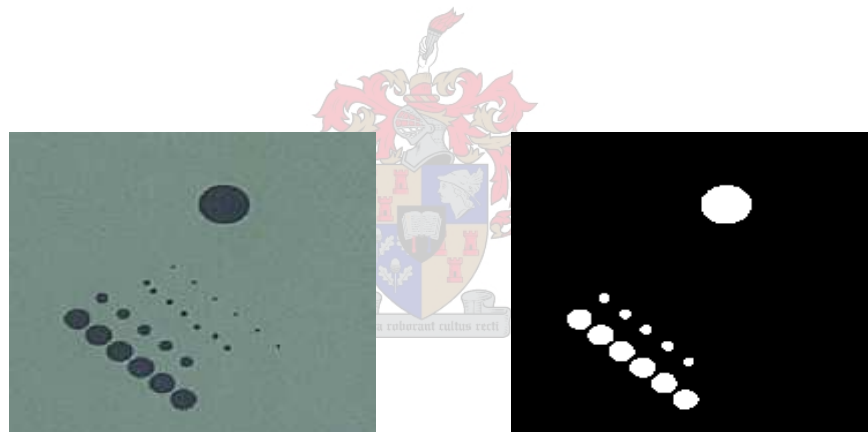


**Figure A1.5: DIP Calibrator Output (CLevel = 0.4, Cut = 1 mm)**

6. Figure A1.3 to A1,5 gives an example of how the minimum cut-off size is used. As can be seen from Figure 10.4, if a low cut-off value is chosen, all of the particles on the image are identified, since the smallest particles has a diameter of 0.4 mm. If the 'Cut' value is upped to 0.5 mm, the row of smallest particles is discarded and only particles bigger than this value is identified. In Figure A1.5, Cut is set to 1mm and only the >1mm particles are identified. The reason for using this is to make the DIP program more robust. And because particles

smaller than 0.5 mm are usually regarded as impurities and small flocks of dispersed sludge.

7. If the operator is visually satisfied with the pixel-to-millimetre conversion factor (ptmm), the greyscale cut-off level (CLevel) and the minimum cut-off size (cut), the DIP now displays these calculated values on the screen. These values can be saved and at later stages used as input for the DIP if calibration is not deemed necessary.

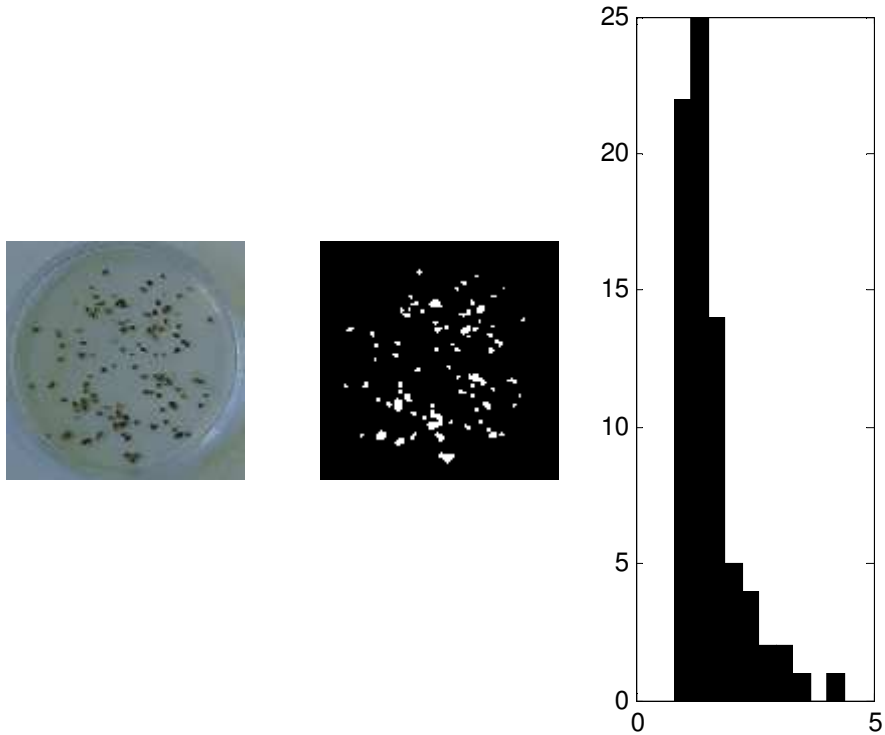
#### **A1.4 DIP Operation**

1. By aid of the digital camera set-up (Figure 5.1) photograph the sample. An image to the likes of Figure A1.6 will be obtained.



**Figure A1.6: Typical subsample image ready for DIP processing**

- This image is now transferred to the PC via data cable and stored in the appropriate directory.
- One the DIP is run it will ask for the name and directory path to the image.



CLevel : 0.3500  
 Total amount of recognised particles : 76  
 Avg particle diameter : 1.5498  
 Largest Particle : 4.3801  
 Standard Deviation : 0.65985

**Figure A1.7: Correct DIP program output**

- Problems might arise if the grey threshold (CLevel) is chosen poorly results like the following might be obtained.

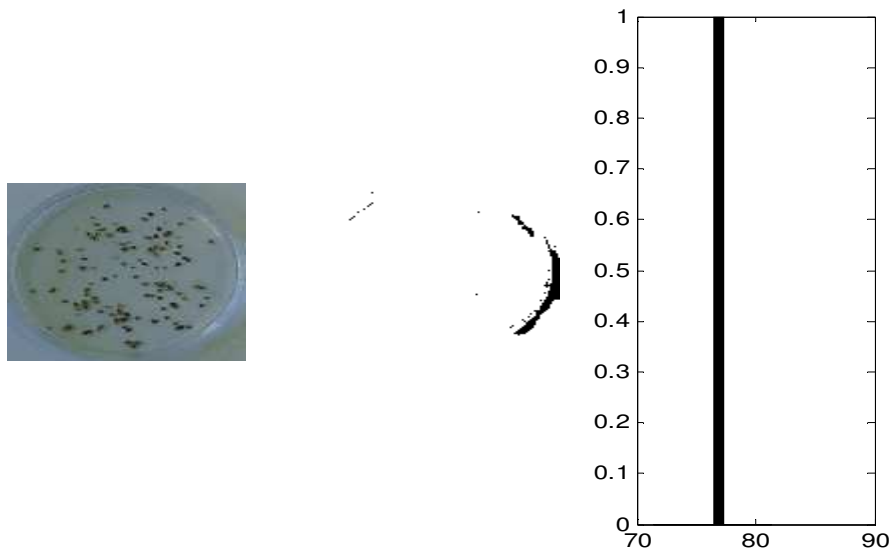


**Figure A1.8: Too high grey scale (CLevel = 0.55)**

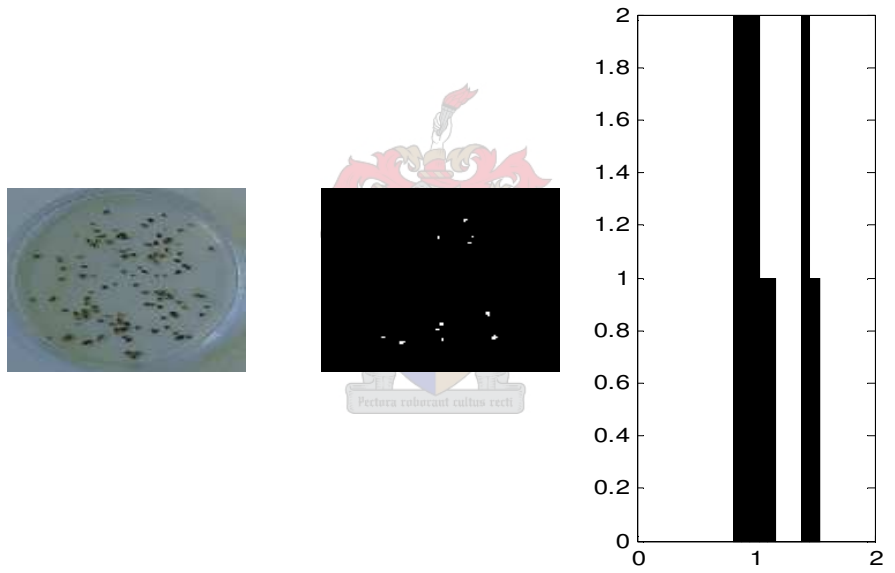


**Figure A1.9: Too low grey scale (CLevel = 0.2)**



## A2 Analytical Procedures

### A2.1 COD Analysis

First, 0.3 ml of COD Solution A and 2.3 ml of COD Solution B is added to a clean test tube. To dilute the sample, 2 ml of distilled water is added and the mixture is stirred vigorously. 1 ml of the test sample is added and the test tube is again stirred vigorously. The mixture is brought to a temperature of 150 °C for 120 minutes. The COD test tube is placed in a light spectrum analyser and the COD value of the sample is obtained. To acquire the actual COD value of the sample, the value needs to be multiplied by 3 in order to compensate for the dilution rate. A flow sheet of the COD sample analysis can be seen in Figure A2.1.

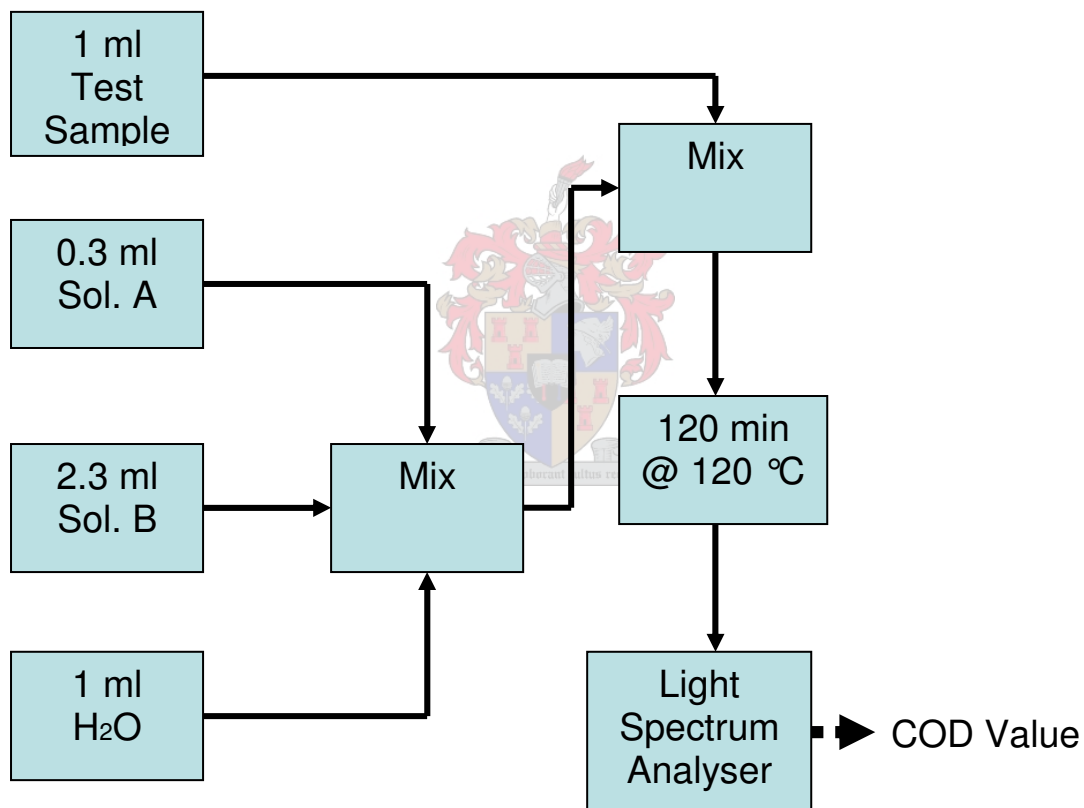


Figure A2.1: Chemical Oxygen Demand (COD) Analysis

## A2.2 Sample Preparation for TSS

The granulated anaerobic sludge sample that needs to be analysed is drawn from the desired reactor at first. The sample is thoroughly mixed and a 200 ml sub-sample is extracted. This smaller sample is then passed through a sieve array 1x1 mm, 0.5x0.5 mm, 0.25x0.25 mm in size, with a bottoms pan used to capture the un-granulated sludge. The granulated residue captured on each individual sieve is then passed through the TSS analysis (Section A2.3) to determine the granules size distribution. This can then in turn be used to calculate the total growth-, and growth that occurred in each size fraction during the incubation period.

## A2.3 Total Suspended Solids (TSS) [g/200ml]

Up to this point, the TSS analysis has been the cornerstone method for analysing the growth that occurred in the reactors. The crucible and filter is dried for 3 hours at 105 °C in a convection oven, to ensure that all the water vapour has been removed. The crucible and filter is then removed from the oven and placed in a water-free environment to cool down to room temperature after which they are weighed and the weight is logged as  $TSS_{c+f}$ . The dried filter is placed in a Buchner-type vacuum system and the sample is poured on top of the filter, the vacuum is initiated and the filter paper is sucked dry. The sample and filter is removed and placed in the crucible allowed to dry for another 3 hours at 105 °C. The sample is cooled down in the same way as before and weighed; the weight of the crucible-sample-filter system is logged as  $TSS_{c+f+s}$ . The total suspended solids of the sample can now be calculated as follows:

$$TSS_{\text{sample}} = TSS_{c+f+s} - TSS_{c+f} \quad [A.1]$$

Equation 7.1 proves that, if the dry mass of the crucible and filter is assumed to stay constant (a valid assumption since it was dried before and after sample filtration), the difference will yield the sample dry mass, or sample TSS. A flow sheet of the TSS procedure can be seen in Figure A2.2.

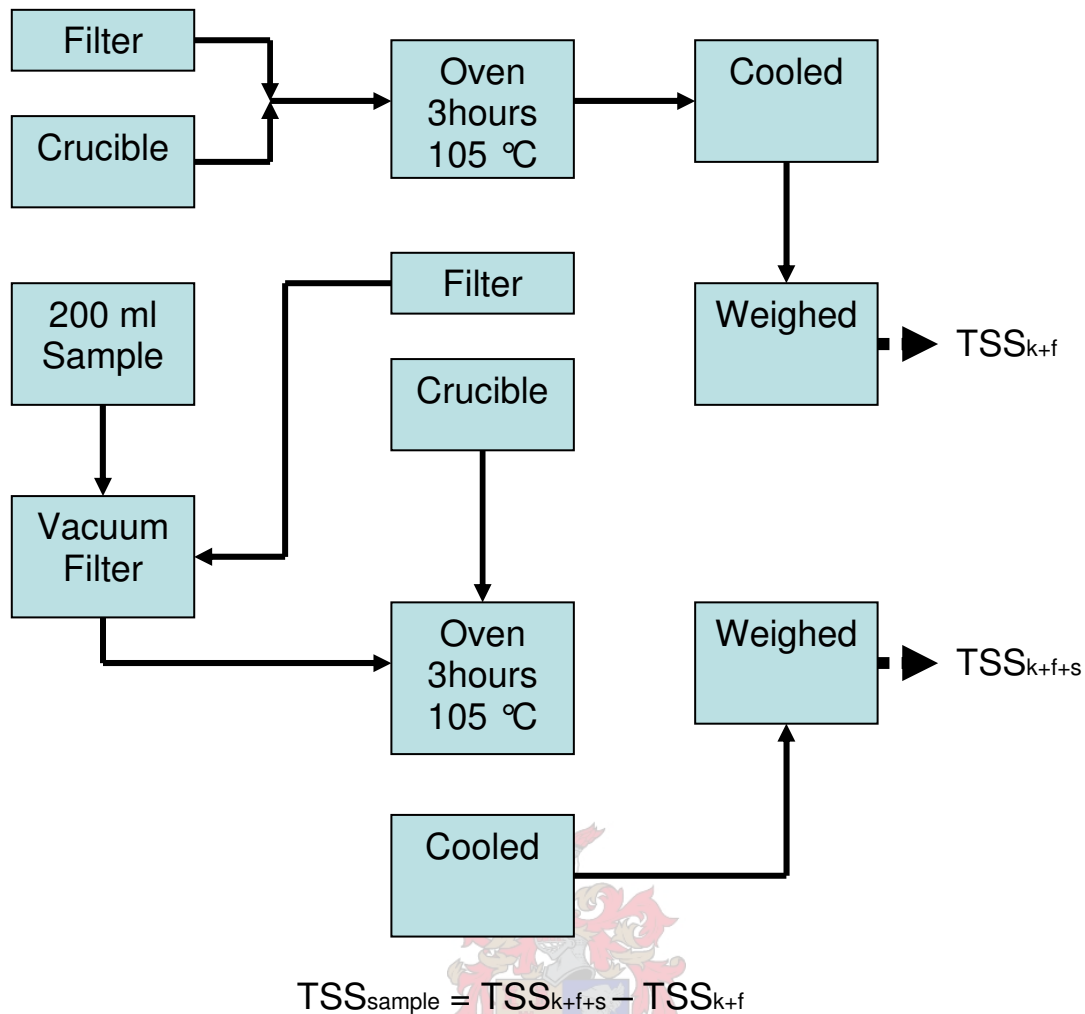


**Figure A2.2 : Total Suspended Solids (TSS) Procedure**

## A2.4 Biogas and Methane Production

As discussed in Chapter 3, the reactors were connected to biogas measuring units to measure the volume of gas produced per day. This was done with a biogas measuring unit that was connected to a gas counter. The gas samples were also analysed for the percentage methane and -carbon dioxide by aid of a gas chromatograph.

## A2.5 MUG and DIPMUG Analysis

Once the Total Suspended Solids (TSS) value for 200 ml sample is obtained, the following method can be used to obtain the Mass of Usable Granules (MUG) MUG is the total mass of granules with a diameter larger than 0.5 mm per cubic meter of reactor volume.

$$\text{MUG [kg/m}^3] = \alpha \cdot \text{TSS [g/200 ml sample]} \quad [\text{A.2}]$$

To calculate the value of  $\alpha$ , a dimensional analysis must firstly be performed to convert g/200ml to kg/m<sup>3</sup>:

**Table A2.1: Dimensional Analysis [g/200ml] to [kg/m<sup>3</sup>]**

<b>g</b>	<b>5 x 200 ml</b>	<b>1000 litre</b>	<b>1kg</b>
<b>200 ml</b>	<b>1 litre</b>	<b>1 m<sup>3</sup></b>	<b>1000 g</b>

Secondly, it is assumed that granules are 85% (weight) water. Therefore, the actual wet mass of granules will be:

$$\text{Actual Wet Mass} = [\text{Dry mass}] * [100/15] \quad [\text{A.3}]$$

If Table A2.1 and equation A.3 are combined, we find the following:

$$\begin{aligned} \alpha &= (5 * 1000 / 1000) * (100 / 15) \\ &= 33.33 \text{ [200ml/g]} * [\text{kg/m}^3 \text{ reactor volume}] \end{aligned} \quad [\text{A.4}]$$

Thus:

$$\text{MUG} = 33.3 * \text{TSS}_{\text{g/200ml}} \quad [\text{kg/m}^3 \text{ reactor volume}] \quad [\text{A.5}]$$

This method is more quantitative and accurate in nature, since the granulated sample is first passed through a sieve array. This array is normally a 1mm, 0.5 mm and a 0.25mm sieve trays stacked on top of each other with a bottoms pan to catch the un-granulated sludge (sizes smaller than 0.25 mm). Therefore, the sludge is separated into > 1mm granules, a 1 to 0.5 mm-, and 0.5 to 0.25 mm size range, leaving the un-granulated section of the sludge behind. While still on the sieve, the samples are thoroughly washed with water, to ensure that no ECP or dispersed sludge particles are trapped in the sample. Each size range is carefully removed from the sieve trays and the TSS mass of each individual size range is calculated (Std Methods et al., 1993). These dry mass values can now be compared to other samples analyzed in the same manner. For example, the sludge feed mix on Day 0 and Day 20 can be compared to calculate the growth in each size range or the total growth that occurred during the 20-day incubation

period. A flow sheet of this procedure can be seen in Figure A2.3. The main advantage is that unlike the previously discussed visual method, this method is quantitative and human error does not play as big a role as was the case in the first method. The DIPMUG method developed in Chapter 5 is also displayed in Figure A2.3.

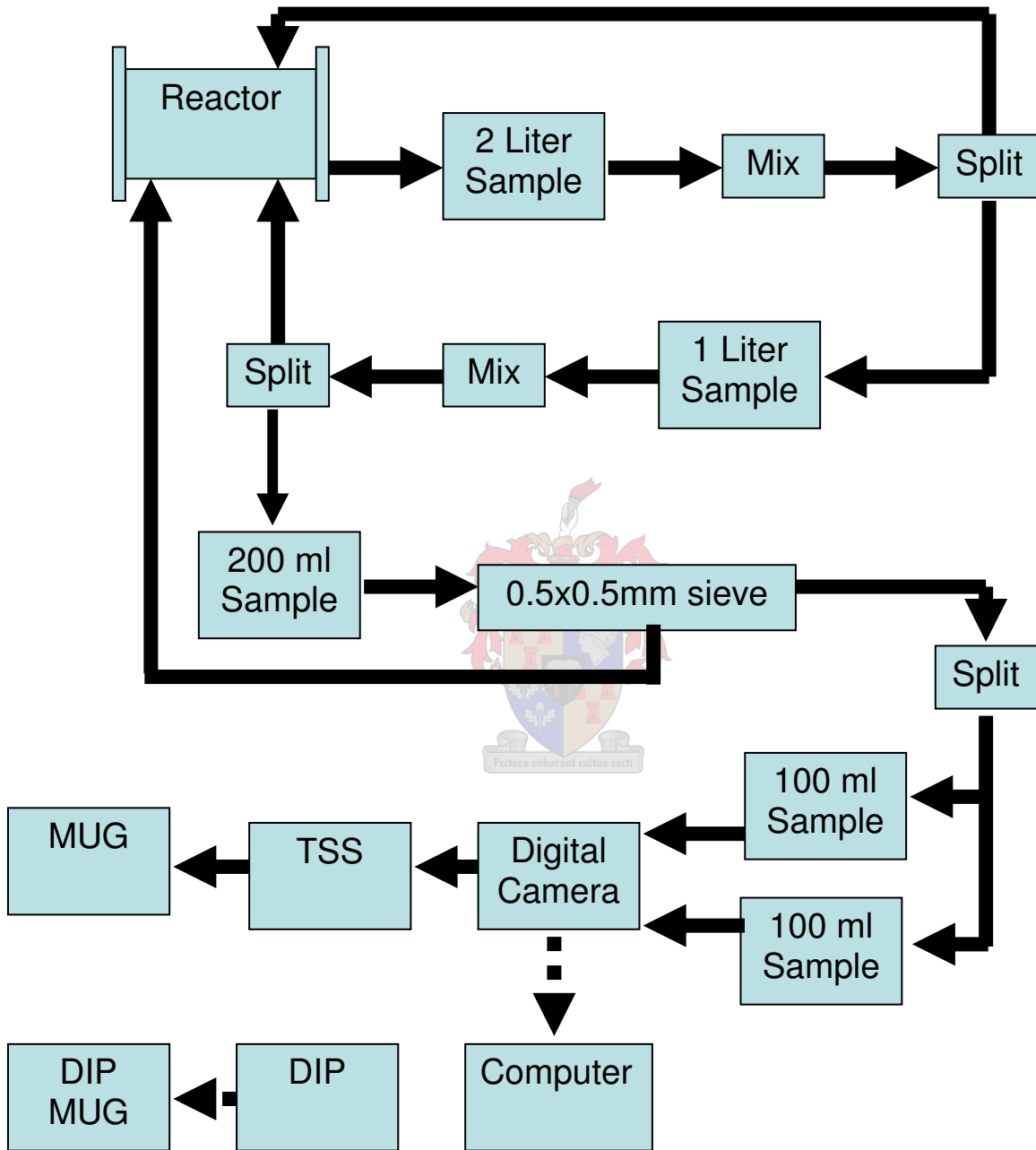


**Figure A2.3: Standard sampling method used for granulated sludge to obtain the MUG and DIPMUG values**

## A2.6 Inorganic Analysis

As stated earlier, various inorganic compounds were also added to the feed for pH stabilisation and growth enhancement. The values of these species were kept constant in the feed throughout the run at:

800	mg/l	$\text{KH}_2\text{PO}_4$
400	mg/l	$\text{CaCO}_3$
200	mg/l	Urea

The input concentrations were thus known. To obtain the concentrations of these species in the used feed (output concentration), the samples were analysed by the Department of Soil Science of the University of Stellenbosch.

## A3 Chapter 3, Experimental Results

**Table A3.1: Experimental Run 1, R<sub>4.15</sub>**

Day	pH	Biogas [ml]	% Methane
0	7	402	
1	7.2	305	
2	5.5	205	
3	5.4	150	
4	5.5	105	
5	5.5	102	
6	5.5	110	
7	5.7	205	
8	5.9	115	
9	5.9	106	
10	6.0	104	
11	6.1	106	
12	6.1	111	
13	6.2	100	
14	6.3		
15			
16			
17			
18			
19			
20			

**Table A3.2: Experimental Run 1, R<sub>7.2</sub>**

Day	pH	Biogas [ml]	% Methane
0	7.0	490	
1	7.1	500	
2	5.5	506	
3	5.4	505	
4	5.5	405	
5	5.4	205	
6	5.5	205	
7	5.7	405	
8	5.9	305	
9	5.9	202	
10	6.0	205	
11	6.1	208	
12	6.2	203	
13	6.2	205	
14	6.4		
15			
16			
17			
18			
19			
20			

**Table A3.3: Experimental Run 2, R<sub>4.15</sub>**

Day	pH	Biogas [ml]	% Methane
0	7.0	55	
1	6.5	40	
2	6.4	55	
3	6.2	155	
4	6.4	60	
5	6.4	60	
6	6.5	67	
7	6.6	60	
8	6.5	55	
9	6.6	67	
10	6.5	65	
11	6.6	70	
12	6.5	75	
13	6.5	105	
14	6.6	105	
15	6.6	120	
16	6.6	140	
17	6.6	110	
18	6.6	110	
19	6.7	115	
20	6.6	110	

**Table A3.4: Experimental Run 2, R<sub>7.2</sub>**

Day	pH	Biogas [ml]	% Methane
0	7.0	255	
1	6.5	155	
2	6.4	55	
3	6.0	70	
4	6.4	60	
5	6.4	105	
6	6.5	112	
7	6.6	105	
8	6.5	105	
9	6.6	129	
10	6.5	126	
11	6.6	104	
12	6.5	110	
13	6.5	155	
14	6.5	160	
15	6.6	165	
16	6.5	203	
17	6.6	223	
18	6.6	205	
19	6.7	211	
20	6.6	274	

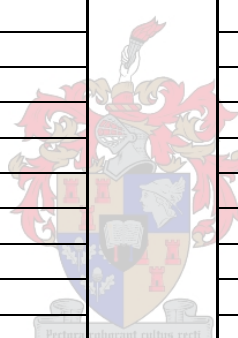


**Table A3.5: Experimental Run 3, R<sub>4.15</sub>**

Day	pH	Biogas [ml]	% Methane
0	7	40	
1	6.5	60	
2	6.2	70	
3	6.1	100	
4	6.0	95	
5	5.8	90	
6	5.9	87	
7	6.3	80	
8	6.3	79	
9	6.3	75	
10	6.4	78	
11	6.4	80	
12	6.5	85	
13	6.6	80	
14			
15			
16			
17			
18			
19			
20			

**Table A3.6: Experimental Run 3, R<sub>7.2</sub>**

Day	pH	Biogas [ml]	% Methane
0	7.0	105	
1	6.5	60	
2	6.2	70	
3	6.1	100	
4	6.2	95	
5	6.2	90	
6	6.1	87	
7	6.0	80	
8	6.3	100	
9	6.3	75	
10	6.4	100	
11	6.4	105	
12	6.5	205	
13	6.5	210	
14	6.5	220	
15	6.6	213	21
16	6.5	240	
17	6.5	230	22
18	6.5	250	
19	6.6	270	22.5
20	6.6		

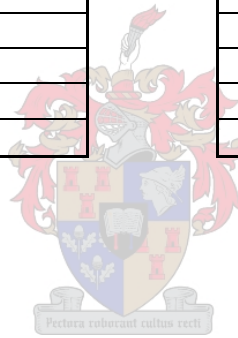


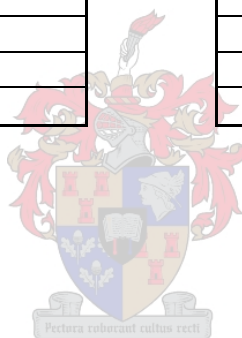


**Table A3.7: Experimental Run 4, R<sub>4.15</sub>**

Day	pH	Biogas [ml]	% Methane
0	7.0		
1	6.8	350	
2	6.8	300	
3	6.7	210	
4	6.7	212	
5	6.7	215	
6	6.6	210	
7	6.55	205	
8	6.55	208	
9	6.55	210	
10	6.55	205	
11	6.56	205	
12	6.58	215	
13	6.59	210	
14	6.65	200	
15	6.65	190	
16	6.67	200	
17	6.69	222	
18	6.77	210	
19	6.78	205	
20	6.8	210	

**Table A3.8: Experimental Run 4, R<sub>7.2</sub>**

Day	pH	Biogas [ml]	% Methane
0	7		
1	6.8	430	
2	6.75	405	
3	6.65	350	
4	6.6	312	
5	6.6	305	
6	6.65	310	
7	6.55	304	
8	6.55	280	
9	6.55	300	
10	6.55	295	
11	6.6	290	
12	6.5	310	
13	6.55	312	
14	6.65	300	
15	6.65	302	
16	6.67	295	
17	6.69	297	
18	6.77	280	
19	6.78	290	
20	6.8	340	



## A4. Chapter 4, Experimental Results

Table A4.1a : Experimental Run 6, R<sub>4.15</sub>

Measured Data								Fitted Curves	
Day	pH	CaCO <sub>3</sub>	KHCO <sub>3</sub> [mg/l]	COD <sub>in</sub> [mg]	COD <sub>out</sub> [mg/l]	Clicks	% CH <sub>4</sub>	COD curve [mg]	CH <sub>4</sub> curve
0	7	200		6440					
1	6.63	200		1840	1350	95		1299	11.14
2	6.2	400		1840		121		1177	11.71
3	6.42	400		1840		78		1062	12.29
4	6.55	400		1840		124		955	12.86
5	6.55	400		1840		203		856	13.43
6	6.56	400		1840	983.7	198	14	764	14.00
7	6.6	400		1840		209		679	14.57
8	6.6	400		1840		200		603	15.14
9	6.6	400		1840		183		534	15.71
10	6.6	400		1840		239		472	16.29
11	6.63	400		1840		222		418	16.86
12	6.66	400		1840	282.3	227		372	17.43
13	6.6	400		1840		259	18	333	18.00
14	6.69	400	250	1840		255		302	18.57
15	6.7	400	250	1840		260		279	19.14
16	6.77	400	100	1840		280		263	19.71
17	6.77	400	100	1840		275		255	20.28
18	6.91	400		1840		260		254	20.86
19	6.95	400	200	1840		280		261	21.43
20	6.98	400			330	288		276	22.00

139.97    8000    900

OneClick	3.3	cm <sup>3</sup> /click	
=			
Tap vol	920	cm <sup>3</sup>	88
Clearance	3578.23	cm <sup>3</sup>	
Press	101325	Pa [kg/mss]	
Temp	308	K	
R	8.314	[kPa.m <sup>3</sup> /kMol.K]	
CH <sub>4</sub>	16	g/mol	
COD in	2000	mg/l	
D0 Feed	3.22	l	

Table A4.1b : Experimental Run 6, R<sub>4.15</sub>

Calculated values					
COD consumed [mg]	Bio Gas produced [cm <sup>3</sup> ]	CH <sub>4</sub> produced [cm <sup>3</sup> /day]	Mol CH <sub>4</sub> produced per day	Mass CH <sub>4</sub> [g]	Day
					0
5141	313.5	34.9	0.0014	0.022	1
663	399.3	46.8	0.0019	0.030	2
778	257.4	31.6	0.0013	0.020	3
<b>885</b>	<b>409.2</b>	<b>52.6</b>	<b>0.0021</b>	<b>0.033</b>	4
984	669.9	90.0	0.0036	0.057	5
1076	653.4	91.5	0.0036	0.058	6
1161	689.7	100.5	0.0040	0.064	7
1237	660	99.9	0.0040	0.063	8
1306	603.9	94.9	0.0038	0.060	9
1368	788.7	128.4	0.0051	0.081	10
1422	732.6	123.5	0.0049	0.078	11
1468	749.1	130.6	0.0052	0.083	12
1507	854.7	153.8	0.0061	0.097	13
1538	841.5	156.3	0.0062	0.099	14
1561	858	164.2	0.0065	0.104	15
1577	924	182.2	0.0072	0.115	16
1585	907.5	184.1	0.0073	0.117	17
1586	858	178.9	0.0071	0.113	18
1579	924	198.0	0.0078	0.125	19
1564	950.4	209.1	0.0083	0.132	20
<b><u>29.99</u></b>	g	<b><u>2451.8</u></b>	<b><u>0.0970</u></b>	<b><u>1.552</u></b>	g
		<b><u>0.592</u></b>	[m <sup>3</sup> CH <sub>4</sub> /Vr.20Days]		

Table A4.2a : Experimental Run 7, R<sub>4.15</sub>

Measured Data								Fitted Curves	
Day	pH	CaCO <sub>3</sub> [mg/l]	KHCO <sub>3</sub> [mg/l]	COD <sub>in</sub> [mg]	COD <sub>out</sub> [mg/l]	Clicks	% CH <sub>4</sub>	COD curve [mg]	CH <sub>4</sub> curve
0	7	200		6440					
1	6.78	200		1840	961	95		1081	11.75
2	6.14	400	200	1840		211		1183	11.87
3	6.17	400	200	1840		78		1267	11.99
4	6.2	400		<u>1840</u>		<u>124</u>		1334	12.11
5	6.28	400		1840		206		1384	12.23
6	6.41	400	200	1840		198		1416	12.35
7	6.45	400	200	1840	1416	209		1431	12.46
8	6.46	400		1840		166		1428	12.58
9	6.46	400		1840		183	12.7	1407	12.70
10	6.46	400		1840		148		1369	12.82
11	6.48	400		1840		170		1314	12.94
12	6.51	400	200	1840		195		1241	13.05
13	6.51	400	200	1840		180		1150	13.17
14	6.31	400		1840		131		1042	13.29
15	6.46	400		1840		82		917	13.41
16	6.5	400		1840		179		774	13.53
17	6.8	400		1840		200		614	13.65
18	6.78	400		1840		185		436	13.76
19	6.9	400		1840		130		240	13.88
20	6.9	400			240	171	14	27	14.00

136.96      8000      1200

OneClick = 3.333 cm<sup>3</sup>/click  
 Tap vol 920 cm<sup>3</sup>  
 Press 101325 Pa [kg/mss]  
 Temp 308 K  
 R 8.314 [kPa.m<sup>3</sup>/kMol.K]  
 CH<sub>4</sub> 16 g/mol  
 COD in 2000 mg/l  
 D0 Feed 3.22 l

Table A4.2b : Experimental Run 7, R<sub>4.15</sub>

Calculated values					
COD consumed [mg]	Bio Gas produced [cm <sup>3</sup> ]	CH <sub>4</sub> produced [cm <sup>3</sup> /day]	Mol CH <sub>4</sub> produced per day	Mass CH <sub>4</sub> [g]	Day
					0
5359	316.635	37.2	0.0015	0.024	1
657	703.263	83.5	0.0033	0.053	2
573	259.974	31.2	0.0012	0.020	3
<b>506</b>	<b>413.292</b>	<b>50.0</b>	<b>0.0020</b>	<b>0.032</b>	4
456	686.598	84.0	0.0033	0.053	5
424	659.934	81.5	0.0032	0.052	6
409	696.597	86.8	0.0034	0.055	7
412	553.278	69.6	0.0028	0.044	8
433	609.939	77.5	0.0031	0.049	9
471	493.284	63.2	0.0025	0.040	10
526	566.61	73.3	0.0029	0.046	11
599	649.935	84.8	0.0034	0.054	12
690	599.94	79.0	0.0031	0.050	13
798	436.623	58.0	0.0023	0.037	14
923	273.306	36.6	0.0015	0.023	15
1066	596.607	80.7	0.0032	0.051	16
1226	666.6	91.0	0.0036	0.058	17
1404	616.605	84.9	0.0034	0.054	18
1600	433.29	60.1	0.0024	0.038	19
1813	569.943	79.8	0.0032	0.051	20
<b>20.35</b>	g	<b>1392.8</b>	<b>0.0551</b>	<b>0.882</b>	g
		<b>0.336</b>	<b>[m<sup>3</sup> CH<sub>4</sub>/Vr.20Days]</b>		

Table A4.3a : Experimental Run 9, R<sub>4.15</sub>

Measured Data								Fitted Curves	
Day	pH	CaCO <sub>3</sub> [mg/l]	KHCO <sub>3</sub> [mg/l]	COD <sub>in</sub> [mg]	COD <sub>out</sub> [mg/l]	Clicks	% CH <sub>4</sub>	COD curve [mg]	CH <sub>4</sub> curve
0	7	200		6440					
1	6.15	200		1840	810	99		826	19.40
2	6.23	200	200	1840		30	19	836	19.47
3	5.86	500	400	1840		97		840	19.53
4	6.6	500		<b>1840</b>		<b>60</b>		838	19.60
5	6.15	500	200	1840		57	20	831	19.66
6	6.2	500	200	1840		80		818	19.73
7	6.27	500		1840		99		799	19.79
8	6.36	500		1840		82	22	775	19.86
9	6.39	500		1840	775	94	19	745	19.92
10	6.34	500		1840		115		709	19.99
11	6.5	500		1840		33		668	20.05
12	6.56	500		1840		112		620	20.12
13	6.66	500		1840		102		567	20.18
14	6.68	500	500	1840		127	20	509	20.25
15	6.72	500	500	1840		110		445	20.31
16	6.7	500		1840		59	16.1	374	20.38
17	6.72	500		1840		121		299	20.44
18	6.66	500	500	1840		189	24	217	20.51
19	6.69	500		1840		135		130	20.57
20	6.8	500			130	179		37	20.64

136.24    9600    2500



OneClick  
 = 3.333 cm<sup>3</sup>/click  
 Tap vol 920 cm<sup>3</sup>  
 Press 101325 Pa [kg/mss]  
 Temp 308 K  
 R 8.314 [kPa.m<sup>3</sup>/kMol.K]  
 CH<sub>4</sub> 16 g/mol  
 COD in 2000 mg/l  
 D0 Feed 3.22 l

Table A4.3b : Experimental Run 9, R<sub>4.15</sub>

Calculated values					
COD consumed [mg]	Bio Gas produced [cm <sup>3</sup> ]	CH <sub>4</sub> produced [cm <sup>3</sup> /day]	Mol CH <sub>4</sub> produced per day	Mass CH <sub>4</sub> [g]	Day
					0
5614	329.967	64.0	0.0025	0.041	1
1004	99.99	19.5	0.0008	0.012	2
1000	323.301	63.2	0.0025	0.040	3
<b>1002</b>	<b>199.98</b>	<b>39.2</b>	<b>0.0016</b>	<b>0.025</b>	4
1009	189.981	37.4	0.0015	0.024	5
1022	266.64	52.6	0.0021	0.033	6
1041	329.967	65.3	0.0026	0.041	7
1065	273.306	54.3	0.0021	0.034	8
1095	313.302	62.4	0.0025	0.040	9
1131	383.295	76.6	0.0030	0.049	10
1172	109.989	22.1	0.0009	0.014	11
1220	373.296	75.1	0.0030	0.048	12
1273	339.966	68.6	0.0027	0.043	13
1331	423.291	85.7	0.0034	0.054	14
1395	366.63	74.5	0.0029	0.047	15
1466	196.647	40.1	0.0016	0.025	16
1541	403.293	82.4	0.0033	0.052	17
1623	629.937	129.2	0.0051	0.082	18
1710	449.955	92.6	0.0037	0.059	19
1803	596.607	123.1	0.0049	0.078	20
<b><u>29.52</u></b>	g	<b><u>1327.7</u></b>	<b><u>0.0525</u></b>	<b><u>0.841</u></b>	g
		<b><u>0.321</u></b>	[m <sup>3</sup> CH <sub>4</sub> /Vr.20Days]		

Table A4.4a : Experimental Run 6, R<sub>7.2</sub>

Measured Data								Fitted Curves	
Day	pH	CaCO <sub>3</sub> [mg/l]	KHCO <sub>3</sub> [mg/l]	COD <sub>in</sub> [mg]	COD <sub>out</sub> [mg/l]	Clicks	% CH <sub>4</sub>	COD curve [mg]	CH <sub>4</sub> curve
0	7	200		11000			16		17.62
1	6.38	200		3200	1350	79		2260	18.12
2	5.96	400		3200		231		2047	18.62
3	6.2	400		3200		113		1847	19.11
4	6.42	400		3200		180		1661	19.61
5	6.6	400		3200		266	21	1488	20.11
6	6.75	400		3200	983.7	334		1328	20.60
7	6.78	400		3200		360		1182	21.10
8	6.76	400		3200		395		1048	21.60
9	6.7	400		3200		232	24.4	928	22.10
10	6.7	400		3200		345		821	22.59
11	6.68	400		3200		377		727	23.09
12	6.56	400		3200	282.3	362		647	23.59
13	6.68	400		3200		358		580	24.08
14	6.68	400	250	3200		448		526	24.58
15	6.72	400	250	3200		477		485	25.08
16	6.77	400	100	3200		578	24	457	25.58
17	6.86	400	100	3200		330		443	26.07
18	6.88	400		3200		307		442	26.57
19	6.95	400	200	3200		445		454	27.07
20	6.98	400			330	412		479	27.56

126.08    7200    700

OneClick

= 2.857 cm<sup>3</sup>/click

Tap vol 1600 cm<sup>3</sup>

Press 101325 Pa [kg/mss]

Temp 308 K

R 8.314 [kPa.m<sup>3</sup>/kMol.K]

CH<sub>4</sub> 16 g/mol

COD in 2000 mg/l

D0 Feed 5.5 l



**Table A4.4b : Experimental Run 6, R<sub>7.2</sub>**

<b>Calculated values</b>					
<b>COD consumed [mg]</b>	<b>Bio Gas produced [cm<sup>3</sup>]</b>	<b>CH<sub>4</sub> produced [cm<sup>3</sup>/day]</b>	<b>Mol CH<sub>4</sub> produced per day</b>	<b>Mass CH<sub>4</sub> [g]</b>	<b>Day</b>
					0
8740	225.703	40.9	0.0016	0.026	1
1153	659.967	122.9	0.0049	0.078	2
1353	322.841	61.7	0.0024	0.039	3
<b>1539</b>	<b>514.26</b>	<b>100.8</b>	<b>0.0040</b>	<b>0.064</b>	4
1712	759.962	152.8	0.0060	0.097	5
1872	954.238	196.6	0.0078	0.124	6
2018	1028.52	217.0	0.0086	0.137	7
2152	1128.515	243.7	0.0096	0.154	8
2272	662.824	146.5	0.0058	0.093	9
2379	985.665	222.7	0.0088	0.141	10
2473	1077.089	248.7	0.0098	0.157	11
2553	1034.234	243.9	0.0097	0.154	12
2620	1022.806	246.3	0.0097	0.156	13
2674	1279.936	314.6	0.0124	0.199	14
2715	1362.789	341.8	0.0135	0.216	15
2743	1651.346	422.3	0.0167	0.267	16
2757	942.81	245.8	0.0097	0.156	17
2758	877.099	233.0	0.0092	0.148	18
2746	1271.365	344.1	0.0136	0.218	19
2721	1177.084	324.5	0.0128	0.205	20
<b>51.95</b>	g	<b>4470.8</b>	<b>0.1769</b>	<b>2.830</b>	g
		<b>0.630</b>	[m <sup>3</sup> CH <sub>4</sub> /Vr.20Days]		

Table A4.5a : Experimental Run 7, R<sub>7.2</sub>

Measured Data								Fitted Curves	
Day	pH	CaCO <sub>3</sub> [mg/l]	KHCO <sub>3</sub> [mg/l]	COD <sub>in</sub> [mg]	COD <sub>out</sub> [mg/l]	Clicks	% CH <sub>4</sub>	COD curve [mg]	CH <sub>4</sub> curve
0	7	200		11000					
1	6.81	200		3200	1243	49		1388	20.81
2	6.35	400	200	3200		36		1513	21.09
3	6.21	400	200	3200		48		1617	21.37
4	6.2	400		<b>3200</b>		<b>43</b>		1702	21.65
5	6.08	400		3200		50		1765	21.94
6	6.14	400		3200		70	24.6	1809	22.22
7	6.3	400		3200	1809	72		1832	22.50
8	6.3	400		3200		180		1835	22.78
9	6.32	400	200	3200		263		1818	23.06
10	6.35	400	200	3200		264	20	1780	23.34
11	6.4	400		3200		200		1722	23.62
12	6.52	400		3200		221		1644	23.90
13	6.52	400		3200		234		1546	24.18
14	6.42	400		3200		297		1427	24.46
15	6.52	400	200	3200		211		1288	24.74
16	6.49	400	200	3200		293		1128	25.02
17	6.55	400		3200		200		948	25.30
18	6.6	400		3200		260		748	25.59
19	6.7	400		3200		232		528	25.87
20	6.7	400			528	247	27.1	287	26.15

135.48      8000      1200

*Pectera robustant cultus recti*

OneClick = 3.333 cm<sup>3</sup>/click  
 Tap vol 1600 cm<sup>3</sup>  
 Press 101325 Pa [kg/mss]  
 Temp 308 K  
 R 8.314 [kPa.m<sup>3</sup>/kMol.K]  
 CH<sub>4</sub> 16 g/mol  
 COD in 2000 mg/l  
 D0 Feed 5.5 l

**Table A4.5b : Experimental Run 7, R<sub>7.2</sub>**

<b>Calculated values</b>					
<b>COD consumed [mg]</b>	<b>Bio Gas produced [cm<sup>3</sup>]</b>	<b>CH<sub>4</sub> produced [cm<sup>3</sup>/day]</b>	<b>Mol CH<sub>4</sub> produced per day</b>	<b>Mass CH<sub>4</sub> [g]</b>	<b>Day</b>
					0
9612	163.317	34.0	0.0013	0.022	1
1687	119.988	25.3	0.0010	0.016	2
1583	159.984	34.2	0.0014	0.022	3
<b>1498</b>	<b>143.319</b>	<b>31.0</b>	<b>0.0012</b>	<b>0.020</b>	4
1435	166.65	36.6	0.0014	0.023	5
1391	233.31	51.8	0.0021	0.033	6
1368	239.976	54.0	0.0021	0.034	7
1365	599.94	136.7	0.0054	0.087	8
1382	876.579	202.1	0.0080	0.128	9
1420	879.912	205.4	0.0081	0.130	10
1478	666.6	157.4	0.0062	0.100	11
1556	736.593	176.1	0.0070	0.111	12
1654	779.922	188.6	0.0075	0.119	13
1773	989.901	242.2	0.0096	0.153	14
1912	703.263	174.0	0.0069	0.110	15
2072	976.569	244.4	0.0097	0.155	16
2252	666.6	168.7	0.0067	0.107	17
2452	866.58	221.7	0.0088	0.140	18
2672	773.256	200.0	0.0079	0.127	19
2913	823.251	215.3	0.0085	0.136	20
<b>43.47</b>	g	<b>2799.3</b>	<b>0.1108</b>	<b>1.772</b>	g
		<b>0.394</b>	<b>[m<sup>3</sup> CH<sub>4</sub>/Vr.20Days]</b>		

Table A4.6a : Experimental Run 8, R<sub>7.2</sub>

Measured Data								Fitted Curves	
Day	pH	CaCO <sub>3</sub> [mg/l]	KHCO <sub>3</sub> [mg/l]	COD <sub>in</sub> [mg]	COD <sub>out</sub> [mg/l]	Clicks	% CH <sub>4</sub>	COD curve [mg]	CH <sub>4</sub> curve
0	7	200		11000					
1	6.79	200		3200	1600	110	9.29	1411	13.69
2	6.6	400		3200		41		1235	14.32
3	6.4	400		3200		59		1071	14.94
4	6.2	400		<b>3200</b>		<b>40</b>		918	15.57
5	6.15	400	200	3200		38	18	778	16.19
6	6.1	400	200	3200		50	20.1	651	16.82
7	6.22	400	400	3200		50		535	17.44
8	6.24	400	400	3200		55		431	18.07
9	6.2	400	400	3200		74		340	18.69
10	6.2	400	400	3200	340	87	20.57	261	19.32
11	6.22	400		3200		102		194	19.94
12	6.24	400	200	3200		149		139	20.57
13	6.22	400		3200		125		96	21.19
14	6.22	400	500	3200		125		66	21.82
15	6.12	400	500	3200		95		47	22.44
16	6.22	400	200	3200		109		41	23.06
17	6.3	400		3200		112		47	23.69
18	6.33	400	500	3200		130		65	24.31
19	6.35	400		3200		133	23	95	24.94
20	6.3	400			95	145		137	25.56

132.62    8000    3900

OneClick

= 3.333 cm<sup>3</sup>/click

Tap vol 1600 cm<sup>3</sup>

Press 101325 Pa [kg/mss]

Temp 308 K

R 8.314 [kPa.m<sup>3</sup>/kMol.K]

CH<sub>4</sub> 16 g/mol

COD in 2000 mg/l

D0 Feed 5.5 l

**Table A4.6b : Experimental Run 8, R<sub>7.2</sub>**

<b>Calculated values</b>					
<b>COD consumed [mg]</b>	<b>Bio Gas produced [cm<sup>3</sup>]</b>	<b>CH<sub>4</sub> produced [cm<sup>3</sup>/day]</b>	<b>Mol CH<sub>4</sub> produced per day</b>	<b>Mass CH<sub>4</sub> [g]</b>	<b>Day</b>
					0
9589	366.63	50.2	0.0020	0.032	1
1965	136.653	19.6	0.0008	0.012	2
2129	196.647	29.4	0.0012	0.019	3
<b>2282</b>	<b>133.32</b>	<b>20.8</b>	<b>0.0008</b>	<b>0.013</b>	4
2422	126.654	20.5	0.0008	0.013	5
2549	166.65	28.0	0.0011	0.018	6
2665	166.65	29.1	0.0012	0.018	7
2769	183.315	33.1	0.0013	0.021	8
2860	246.642	46.1	0.0018	0.029	9
2939	289.971	56.0	0.0022	0.035	10
3006	339.966	67.8	0.0027	0.043	11
3061	496.617	102.1	0.0040	0.065	12
3104	416.625	88.3	0.0035	0.056	13
3134	416.625	90.9	0.0036	0.058	14
3153	316.635	71.1	0.0028	0.045	15
3159	363.297	83.8	0.0033	0.053	16
3153	373.296	88.4	0.0035	0.056	17
3135	433.29	105.4	0.0042	0.067	18
3105	443.289	110.6	0.0044	0.070	19
3063	483.285	123.5	0.0049	0.078	20
<b>63.24</b>	g	<b>1264.6</b>	<b>0.0500</b>	<b>0.801</b>	g
		<b>0.178</b>	<b>[m<sup>3</sup> CH<sub>4</sub>/Vr.20Days]</b>		

Table A4.7a : Experimental Run 9, R<sub>7.2</sub>

Measured Data								Fitted Curves	
Day	pH	CaCO <sub>3</sub> [mg/l]	KHCO <sub>3</sub> [mg/l]	COD <sub>in</sub> [mg]	COD <sub>out</sub> [mg/l]	Clicks	% CH <sub>4</sub>	COD curve [mg]	CH <sub>4</sub> curve
0	7	200		11000					
1	6.79	200		3200	1600	110	9.29	1411	13.69
2	6.6	400		3200		41		1235	14.32
3	6.4	400		3200		59		1071	14.94
4	6.2	400		<b>3200</b>		<b>40</b>		918	15.57
5	6.15	400	200	3200		38	18	778	16.19
6	6.1	400	200	3200		50	20.1	651	16.82
7	6.22	400	400	3200		50		535	17.44
8	6.24	400	400	3200		55		431	18.07
9	6.2	400	400	3200		74		340	18.69
10	6.2	400	400	3200	340	87	20.57	261	19.32
11	6.22	400		3200		102		194	19.94
12	6.24	400	200	3200		149		139	20.57
13	6.22	400		3200		125		96	21.19
14	6.22	400	500	3200		125		66	21.82
15	6.12	400	500	3200		95		47	22.44
16	6.22	400	200	3200		109		41	23.06
17	6.3	400		3200		112		47	23.69
18	6.33	400	500	3200		130		65	24.31
19	6.35	400		3200		133	23	95	24.94
20	6.3	400			95	145		137	25.56

132.62      8000      3900

OneClick

= 3.333 cm<sup>3</sup>/click

Tap vol 1600 cm<sup>3</sup>

Press 101325 Pa [kg/mss]

Temp 308 K

R 8.314 [kPa.m<sup>3</sup>/kMol.K]

CH<sub>4</sub> 16 g/mol

COD in 2000 mg/l

D0 Feed 5.5 l

**Table A4.7b : Experimental Run 9, R<sub>7.2</sub>**

<b>Calculated values</b>					
<b>COD consumed [mg]</b>	<b>Bio Gas produced [cm<sup>3</sup>]</b>	<b>CH<sub>4</sub> produced [cm<sup>3</sup>/day]</b>	<b>Mol CH<sub>4</sub> produced per day</b>	<b>Mass CH<sub>4</sub> [g]</b>	<b>Day</b>
					0
9589	366.63	50.2	0.0020	0.032	1
1965	136.653	19.6	0.0008	0.012	2
2129	196.647	29.4	0.0012	0.019	3
<b>2282</b>	<b>133.32</b>	<b>20.8</b>	<b>0.0008</b>	<b>0.013</b>	4
2422	126.654	20.5	0.0008	0.013	5
2549	166.65	28.0	0.0011	0.018	6
2665	166.65	29.1	0.0012	0.018	7
2769	183.315	33.1	0.0013	0.021	8
2860	246.642	46.1	0.0018	0.029	9
2939	289.971	56.0	0.0022	0.035	10
3006	339.966	67.8	0.0027	0.043	11
3061	496.617	102.1	0.0040	0.065	12
3104	416.625	88.3	0.0035	0.056	13
3134	416.625	90.9	0.0036	0.058	14
3153	316.635	71.1	0.0028	0.045	15
3159	363.297	83.8	0.0033	0.053	16
3153	373.296	88.4	0.0035	0.056	17
3135	433.29	105.4	0.0042	0.067	18
3105	443.289	110.6	0.0044	0.070	19
3063	483.285	123.5	0.0049	0.078	20
<b>63.24</b>	g	<b>1264.6</b>	<b>0.0500</b>	<b>0.801</b>	g
		<b>0.178</b>	<b>[m<sup>3</sup> CH<sub>4</sub>/Vr.20Days]</b>		

**Table A4.8a : Experimental Run 6, R<sub>5.5</sub>**

Measured Data								Fitted Curves	
Day	pH	CaCO <sub>3</sub> [mg/l]	KHCO <sub>3</sub> [mg/l]	COD <sub>in</sub> [mg]	COD <sub>out</sub> [mg/l]	Clicks	% CH <sub>4</sub>	COD curve [mg]	CH <sub>4</sub> curve
0	7	200		8660			16		16.70
1	6.53	200		<b>2440</b>	<b>1350</b>	<b>105</b>		<b>1421</b>	<b>17.19</b>
2	5.95	400		2440		114		<b>1318</b>	17.69
3	6.1	400		2440		120		<b>1219</b>	18.18
4	6.2	400		<b>2440</b>		<b>100</b>		<b>1125</b>	<b>18.67</b>
5	6.64	400		2440		187	19	<b>1035</b>	19.16
6	6.64	400		2440	983.7	221		<b>951</b>	19.66
7	6.6	400		2440		360		<b>871</b>	20.15
8	6.75	400		2440		344		<b>795</b>	20.64
9	6.7	400		2440		151	21	<b>725</b>	21.13
10	6.72	400		2440		430		<b>659</b>	21.63
11	6.75	400		2440		327		<b>598</b>	22.12
12	6.6	400		2440	282.3	267		<b>541</b>	22.61
13	6.67	400		2440		290		<b>489</b>	23.10
14	6.7	400	250	2440		290		<b>442</b>	23.60
15	6.72	400	250	2440		364		<b>400</b>	24.09
16	6.75	400	100	2440		503	24	<b>362</b>	24.58
17	6.92	400	100	2440		280		<b>329</b>	25.07
18	6.91	400		2440		331		<b>300</b>	25.57
19	6.95	400	200	2440		416		<b>276</b>	26.06
20	6.98	400			330	400		<b>257</b>	26.55

139.78    8000    900

OneClick

=

3.3

cm<sup>3</sup>/click

Tap vol  
Clearance

1220

cm<sup>3</sup>

88

Press

101325

Pa [kg/mss]

Temp

308

K

R

8.314

[kPa.m<sup>3</sup>/kMol.K]

CH<sub>4</sub>

16

g/mol

COD in

2000

mg/l

D0 Feed

4.33

l



**Table A4.8b : Experimental Run 6, R<sub>5.5</sub>**

<b>Calculated values</b>					
<b>COD consumed [mg]</b>	<b>Bio Gas produced [cm<sup>3</sup>]</b>	<b>CH<sub>4</sub> produced [cm<sup>3</sup>/day]</b>	<b>Mol CH<sub>4</sub> produced per day</b>	<b>Mass CH<sub>4</sub> [g]</b>	<b>Day</b>
					0
<b>7239</b>	<b>346.5</b>	<b>59.6</b>	<b>0.0024</b>	<b>0.038</b>	1
1122	376.2	66.5	0.0026	0.042	2
1221	396	72.0	0.0028	0.046	3
<b>1315</b>	<b>330</b>	<b>61.6</b>	<b>0.0024</b>	<b>0.039</b>	4
1405	617.1	118.3	0.0047	0.075	5
1489	729.3	143.3	0.0057	0.091	6
1569	1188	239.4	0.0095	0.152	7
1645	1135.2	234.3	0.0093	0.148	8
1715	498.3	105.3	0.0042	0.067	9
1781	1419	306.9	0.0121	0.194	10
1842	1079.1	238.7	0.0094	0.151	11
1899	881.1	199.2	0.0079	0.126	12
1951	957	221.1	0.0087	0.140	13
1998	957	225.8	0.0089	0.143	14
2040	1201.2	289.3	0.0114	0.183	15
2078	1659.9	408.0	0.0161	0.258	16
2111	924	231.7	0.0092	0.147	17
2140	1092.3	279.2	0.0110	0.177	18
2164	1372.8	357.7	0.0142	0.226	19
2183	1320	350.5	0.0139	0.222	20
<b><u>40.91</u></b>	g	<b><u>4208.3</u></b>	<b><u>0.1665</u></b>	<b><u>2.664</u></b>	g
		<b><u>0.758</u></b>	<b><u>0.1665</u></b> [m <sup>3</sup> CH <sub>4</sub> /Vr.20Days]		

Table A4.9a : Experimental Run 7, R<sub>5.5</sub>

Measured Data								Fitted Curves	
Day	pH	CaCO <sub>3</sub> [mg/l]	KHCO <sub>3</sub> [mg/l]	COD <sub>in</sub> [mg]	COD <sub>out</sub> [mg/l]	Clicks	% CH <sub>4</sub>	COD curve [mg]	CH <sub>4</sub> curve
0	7	200		8600					
1	6.55	200		2400	1243	229		1408	12.03
2	6.4	400	200	2400		528		1550	12.98
3	6.56	400	200	2400		481		1669	13.93
4	6.6	400		<b>2400</b>		<b>388</b>		1765	14.88
5	6.58	400		2400		360		1837	15.84
6	6.5	400		2400		321	16.5	1886	16.79
7	6.75	400		2400	1886	352		1912	17.74
8	6.6	400		2400		333		1914	18.69
9	6.65	400	200	2400		308		1894	19.64
10	6.55	400	200	2400		432	21	1850	20.60
11	6.58	400		2400		360		1783	21.55
12	6.6	400		2400		300		1692	22.50
13	6.54	400		2400		432		1578	23.45
14	6.55	400		2400		500		1441	24.40
15	6.65	400	200	2400		359		1281	25.36
16	6.6	400	200	2400		523		1098	26.31
17	6.6	400		2400		400		891	27.26
18	6.55	400		2400		368		661	28.21
19	6.7	400		2400		421		408	29.16
20	6.81	400			408	495	30	132	30.12

138.92      8000      1200



OneClick  
 = 3.333 cm<sup>3</sup>/click  
 Tap vol 1200 cm<sup>3</sup>  
 Press 101325 Pa [kg/mss]  
 Temp 308 K  
 R 8.314 [kPa.m<sup>3</sup>/kMol.K]  
 CH<sub>4</sub> 16 g/mol  
 COD in 2000 mg/l  
 D0 Feed 4.3 l

**Table A4.9b : Experimental Run 7, R<sub>5.5</sub>**

<b>Calculated values</b>					
<b>COD consumed [mg]</b>	<b>Bio Gas produced [cm<sup>3</sup>]</b>	<b>CH<sub>4</sub> produced [cm<sup>3</sup>/day]</b>	<b>Mol CH<sub>4</sub> produced per day</b>	<b>Mass CH<sub>4</sub> [g]</b>	<b>Day</b>
					0
7192	763.257	91.8	0.0036	0.058	1
850	1759.824	228.4	0.0090	0.145	2
731	1603.173	223.4	0.0088	0.141	3
<b>635</b>	<b>1293.204</b>	<b>192.5</b>	<b>0.0076</b>	<b>0.122</b>	4
563	1199.88	190.0	0.0075	0.120	5
514	1069.893	179.6	0.0071	0.114	6
488	1173.216	208.1	0.0082	0.132	7
486	1109.889	207.5	0.0082	0.131	8
506	1026.564	201.7	0.0080	0.128	9
550	1439.856	296.6	0.0117	0.188	10
617	1199.88	258.5	0.0102	0.164	11
708	999.9	225.0	0.0089	0.142	12
822	1439.856	337.7	0.0134	0.214	13
959	1666.5	406.7	0.0161	0.257	14
1119	1196.547	303.4	0.0120	0.192	15
1302	1743.159	458.6	0.0181	0.290	16
1509	1333.2	363.4	0.0144	0.230	17
1739	1226.544	346.0	0.0137	0.219	18
1992	1403.193	409.2	0.0162	0.259	19
2268	1649.835	496.8	0.0197	0.315	20
<b>25.55</b>	g	<b>5624.9</b>	<b>0.2226</b>	<b>3.561</b>	g
		<b>1.023</b>	<b>[m<sup>3</sup> CH<sub>4</sub>/Vr.20Days]</b>		

Table A4.10a : Experimental Run 9, R<sub>5,5</sub>

Measured Data								Fitted Curves	
Day	pH	CaCO <sub>3</sub> [mg/l]	KHCO <sub>3</sub> [mg/l]	COD <sub>in</sub> [mg]	COD <sub>out</sub> [mg/l]	Clicks	% CH <sub>4</sub>	COD curve [mg]	CH <sub>4</sub> curve
0	7	200		8600					
1	5.86	200		2400	550	142		573	14.26
2	6.07	200	200	2400		35		592	14.66
3	5.76	500	400	2400		42	17	604	15.06
4	5.2	500		<b>2400</b>		<b>30</b>		612	15.46
5	5.31	500	200	2400		29	14	614	15.87
6	6.28	500	200	2400		45		612	16.27
7	6.32	500		2400		60		603	16.67
8	6.35	500		2400		105	18	590	17.08
9	6.35	500		2400	590	127	19	571	17.48
10	6.52	500		2400		212		547	17.88
11	6.55	500		2400		84		518	18.29
12	6.71	500		2400		99		484	18.69
13	6.7	500		2400		154	16	444	19.09
14	6.71	500	500	2400		181		399	19.50
15	6.65	500	500	2400		211	17	349	19.90
16	6.71	500		2400		143		293	20.30
17	6.66	500		2400		225		232	20.71
18	6.6	500	500	2400		304		166	21.11
19	6.8	500		2400		184	25	95	21.51
20	6.8	500			95	240		18	21.92

133.91    9600    2500



OneClick  
 = 3.333 cm<sup>3</sup>/click  
 Tap vol 1200 cm<sup>3</sup>  
 Press 101325 Pa [kg/mss]  
 Temp 308 K  
 R 8.314 [kPa.m<sup>3</sup>/kMol.K]  
 CH<sub>4</sub> 16 g/mol  
 COD in 2000 mg/l  
 D0 Feed 4.3 l

**Table A4.10b : Experimental Run 9, R<sub>5.5</sub>**

<b>Calculated values</b>					
<b>COD consumed [mg]</b>	<b>Bio Gas produced [cm<sup>3</sup>]</b>	<b>CH<sub>4</sub> produced [cm<sup>3</sup>/day]</b>	<b>Mol CH<sub>4</sub> produced per day</b>	<b>Mass CH<sub>4</sub> [g]</b>	<b>Day</b>
					0
8027	473.286	67.5	0.0027	0.043	1
1808	116.655	17.1	0.0007	0.011	2
1796	139.986	21.1	0.0008	0.013	3
<b>1788</b>	<b>99.99</b>	<b>15.5</b>	<b>0.0006</b>	<b>0.010</b>	4
1786	96.657	15.3	0.0006	0.010	5
1788	149.985	24.4	0.0010	0.015	6
1797	199.98	33.3	0.0013	0.021	7
1810	349.965	59.8	0.0024	0.038	8
1829	423.291	74.0	0.0029	0.047	9
1853	706.596	126.4	0.0050	0.080	10
1882	279.972	51.2	0.0020	0.032	11
1916	329.967	61.7	0.0024	0.039	12
1956	513.282	98.0	0.0039	0.062	13
2001	603.273	117.6	0.0047	0.074	14
2051	703.263	139.9	0.0055	0.089	15
2107	476.619	96.8	0.0038	0.061	16
2168	749.925	155.3	0.0061	0.098	17
2234	1013.232	213.9	0.0085	0.135	18
2305	613.272	131.9	0.0052	0.084	19
2382	799.92	175.3	0.0069	0.111	20
<b>45.28</b>	g	<b>1696.0</b>	<b>0.0671</b>	<b>1.074</b>	g
		<b>0.308</b>	<b>[m<sup>3</sup> CH<sub>4</sub>/Vr.20Days]</b>		

Table A4.11a : Experimental Run 10, R<sub>5.5</sub>

Measured Data								Fitted Curves	
Day	pH	CaCO <sub>3</sub> [mg/l]	KHCO <sub>3</sub> [mg/l]	COD <sub>in</sub> [mg]	COD <sub>out</sub> [mg/l]	Clicks	% CH <sub>4</sub>	COD curve [mg]	CH <sub>4</sub> curve
0	7	200		8600					
1	6.69	200		2400	1722.6	348	5.5	1605	10.84
2	6.39	200	400	2400		200		1526	11.80
3	6.14	400	400	2400		41		1451	12.76
4	6.36	600		<b>2400</b>		<b>124</b>		1382	13.73
5	6.4	600		2400		130		1318	14.69
6	6.5	400		2400	1266.3	120		1259	15.65
7	6.55	400		2400		135	22.6	1205	16.61
8	6.6	400		2400		270		1156	17.57
9	6.56	400		2400		116	22.5	1112	18.53
10	6.6	400	500	2400	1074.6	164		1073	19.50
11	6.65	200		2400		200		1040	20.46
12	6.7	200		2400		148		1011	21.42
13	6.75	400		2400		167	20.33	987	22.38
14	6.8	400		2400		162		969	23.34
15	6.8	400		2400		202	23	955	24.30
16	6.8	400		2400	1071.9	230		947	25.26
17	6.8	400		2400		230		943	26.23
18	6.78	400	500	2400		275		945	27.19
19	6.83	400		2400		277	29	952	28.15
20	6.88	400			891	300	27	964	29.11

139.58    7800    1800



= 3.333 cm<sup>3</sup>/click  
 Tap vol 1200 cm<sup>3</sup>  
 Press 101325 Pa [kg/mss]  
 Temp 308 K  
 R 8.314 [kPa.m<sup>3</sup>/kMol.K]  
 CH<sub>4</sub> 16 g/mol  
 COD in 2000 mg/l  
 D0 Feed 4.3 l

**Table A4.11b : Experimental Run 10, R<sub>5.5</sub>**

<b>Calculated values</b>					
<b>COD consumed [mg]</b>	<b>Bio Gas produced [cm<sup>3</sup>]</b>	<b>CH<sub>4</sub> produced [cm<sup>3</sup>/day]</b>	<b>Mol CH<sub>4</sub> produced per day</b>	<b>Mass CH<sub>4</sub> [g]</b>	<b>Day</b>
					0
6995	1159.884	125.7	0.0050	0.080	1
874	666.6	78.7	0.0031	0.050	2
949	136.653	17.4	0.0007	0.011	3
<b>1018</b>	<b>413.292</b>	<b>56.7</b>	<b>0.0022</b>	<b>0.036</b>	4
1082	433.29	63.6	0.0025	0.040	5
1141	399.96	62.6	0.0025	0.040	6
1195	449.955	74.7	0.0030	0.047	7
1244	899.91	158.1	0.0063	0.100	8
1288	386.628	71.7	0.0028	0.045	9
1327	546.612	106.6	0.0042	0.067	10
1360	666.6	136.4	0.0054	0.086	11
1389	493.284	105.7	0.0042	0.067	12
1413	556.611	124.6	0.0049	0.079	13
1431	539.946	126.0	0.0050	0.080	14
1445	673.266	163.6	0.0065	0.104	15
1453	766.59	193.7	0.0077	0.123	16
1457	766.59	201.0	0.0080	0.127	17
1455	916.575	249.2	0.0099	0.158	18
1448	923.241	259.9	0.0103	0.165	19
1436	999.9	291.1	0.0115	0.184	20
<b>31.40</b>	g	<b>2667.0</b>	<b>0.1055</b>	<b>1.689</b>	g
		<b>0.485</b>	<b>[m<sup>3</sup> CH<sub>4</sub>/Vr.20Days]</b>		

TableA4.12a : Experimental Run 11, R<sub>5.5</sub>

Measured Data								Fitted Curves	
Day	pH	CaCO <sub>3</sub> [mg/l]	KHCO <sub>3</sub> [mg/l]	COD <sub>in</sub> [mg]	COD <sub>out</sub> [mg/l]	Clicks	% CH <sub>4</sub>	COD curve [mg]	CH <sub>4</sub> curve
0	7	200		11000					
1	5.92	200		3200	370	117		386	23.08
2	5.99	200	200	3200		99	22	398	23.27
3	5.72	500	400	3200		76		406	23.47
4	5.96	500		<b>3200</b>		<b>76</b>		412	23.67
5	6.02	500	200	3200		73	25	414	23.87
6	6.13	500	200	3200		79		413	24.07
7	6.2	500		3200		173	26	408	24.27
8	6.37	500		3200		118	25	400	24.47
9	6.24	500		3200	400	219		389	24.67
10	6.35	500		3200		171		374	24.87
11	6.35	500		3200		125		356	25.06
12	6.57	500		3200		150		334	25.26
13	6.62	500		3200		168		310	25.46
14	6.61	500	500	3200		217	21	281	25.66
15	6.68	500	500	3200		219		250	25.86
16	6.72	500		3200		187		215	26.06
17	6.65	500		3200		252		177	26.26
18	6.6	500	500	3200		317	29	135	26.46
19	6.8	500		3200		260		90	26.66
20	6.75	500			90	300		42	26.86

134.25    9600    2500



OneClick  
 = 3.333 cm<sup>3</sup>/click  
 Tap vol 1600 cm<sup>3</sup>  
 Press 101325 Pa [kg/mss]  
 Temp 308 K  
 R 8.314 [kPa.m<sup>3</sup>/kMol.K]  
 CH<sub>4</sub> 16 g/mol  
 COD in 2000 mg/l  
 D0 Feed 5.5 l



Table A4.12b: Experimental Run 11, R<sub>5,5</sub>

Calculated values					
COD consumed [mg]	Bio Gas produced [cm <sup>3</sup> ]	CH <sub>4</sub> produced [cm <sup>3</sup> /day]	Mol CH <sub>4</sub> produced per day	Mass CH <sub>4</sub> [g]	Day
					0
10614	389.961	90.0	0.0036	0.057	1
2802	329.967	76.8	0.0030	0.049	2
2794	253.308	59.5	0.0024	0.038	3
<b>2788</b>	<b>253.308</b>	<b>60.0</b>	<b>0.0024</b>	<b>0.038</b>	4
2786	243.309	58.1	0.0023	0.037	5
2787	263.307	63.4	0.0025	0.040	6
2792	576.609	139.9	0.0055	0.089	7
2800	393.294	96.2	0.0038	0.061	8
2811	729.927	180.1	0.0071	0.114	9
2826	569.943	141.7	0.0056	0.090	10
2844	416.625	104.4	0.0041	0.066	11
2866	499.95	126.3	0.0050	0.080	12
2890	559.944	142.6	0.0056	0.090	13
2919	723.261	185.6	0.0073	0.118	14
2950	729.927	188.8	0.0075	0.120	15
2985	623.271	162.4	0.0064	0.103	16
3023	839.916	220.5	0.0087	0.140	17
3065	1056.561	279.5	0.0111	0.177	18
3110	866.58	231.0	0.0091	0.146	19
3158	999.9	268.5	0.0106	0.170	20
<b>65.61</b>	g	<b>2875.3</b>	<b>0.1138</b>	<b>1.820</b>	g
		<b>0.405</b>	<b>[m<sup>3</sup> CH<sub>4</sub>/Vr.20Days]</b>		

## A5. Chapter 5, Experimental Results

### A5.1 Matlab ® Programme Layout

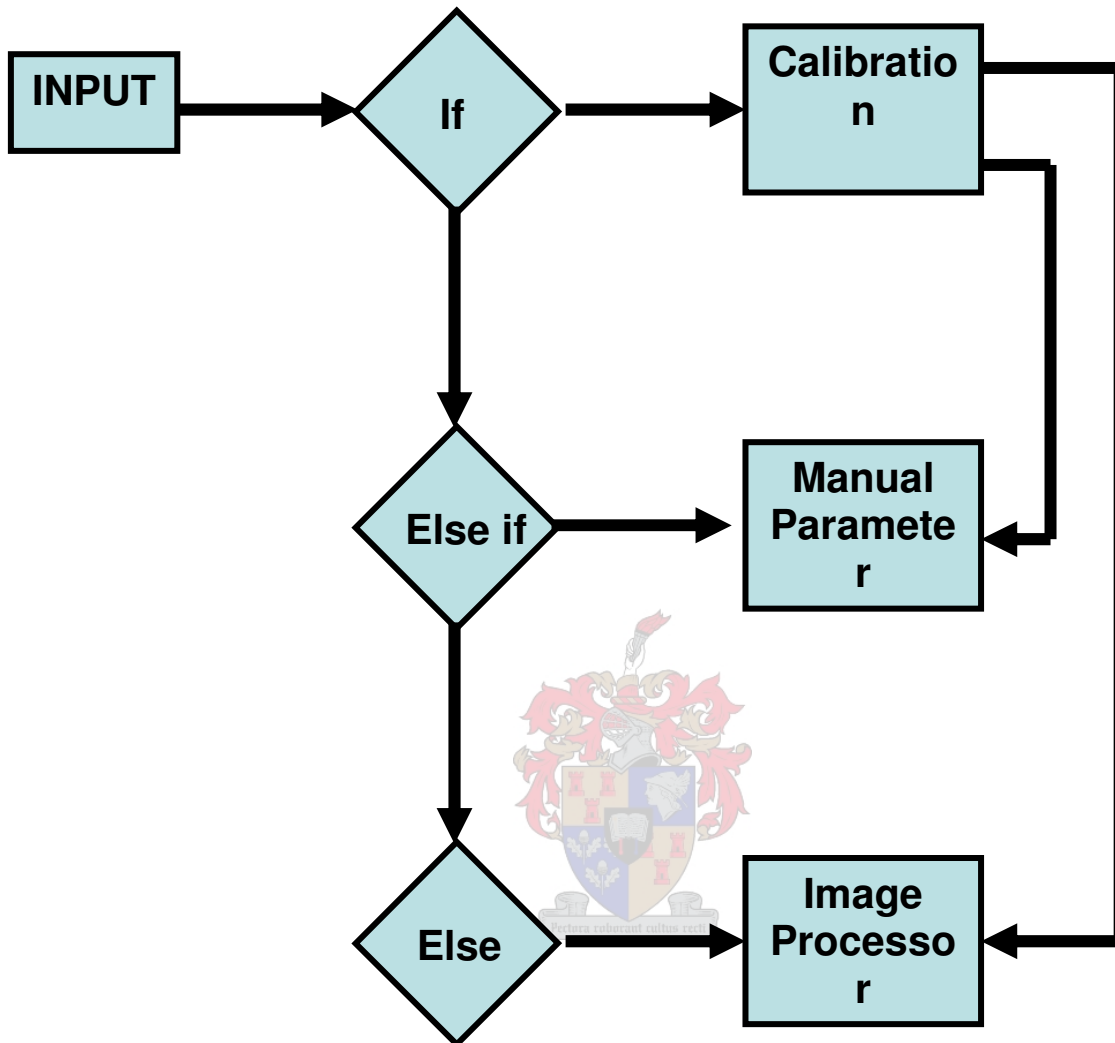
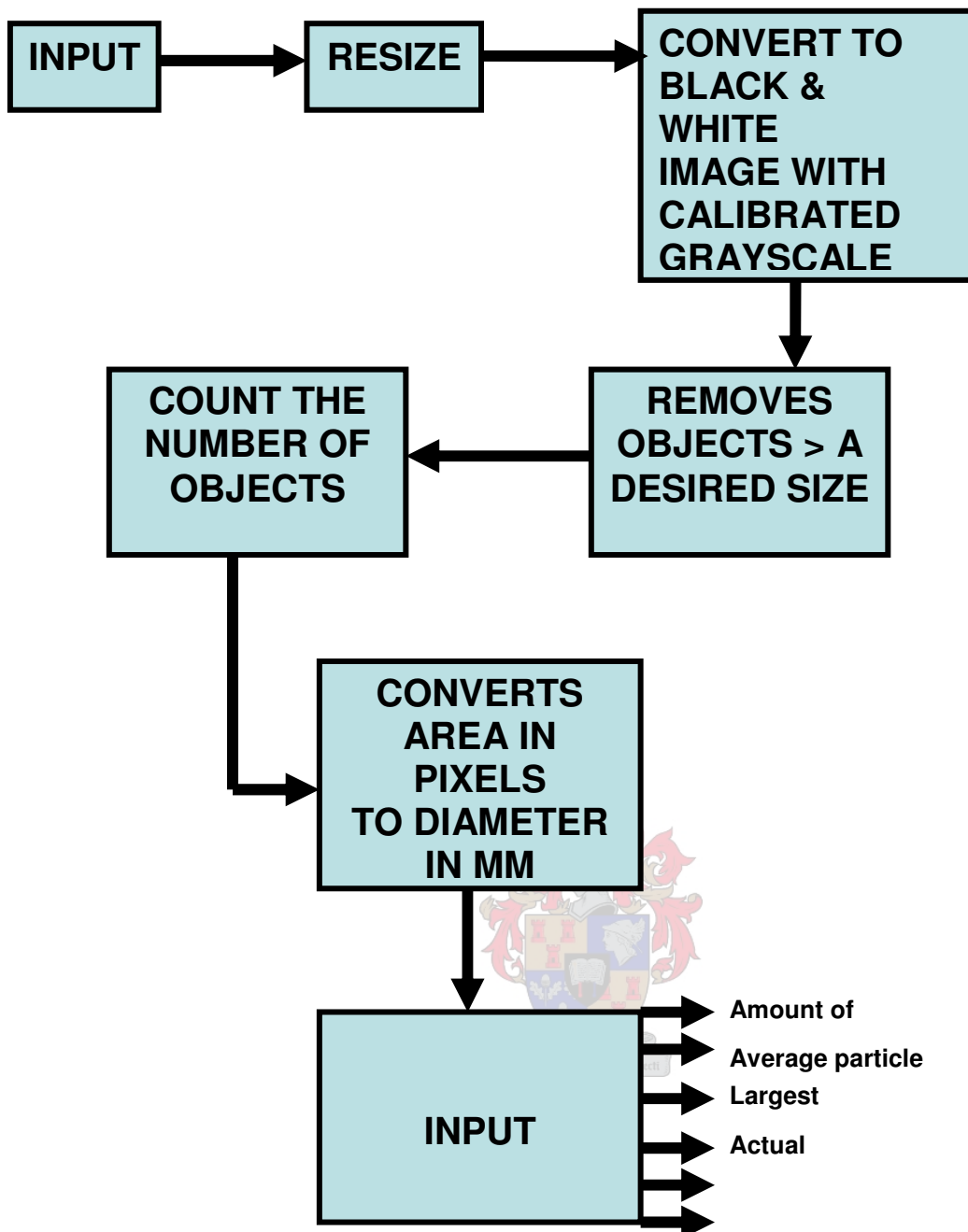


Figure A5.1 : Main Program Layout of the DIP Program



**Figure A5.2: Block Flow Diagram of Image Processing Section of the DIP Program**

### **A5.2 Matlab ® DIP Program Source Code**

```

disp('Please give the directory path of the desired image');
disp('If calibration is desired press 1');
V = input('Directory Path : ');
if V == 1
    S = input('Directory Path : ');
    CI = imread('C:\MATLAB6p5\work\Calibration.jpg'); %S
    CI2 = imresize(CI,[1000,1000]);
  
```

```

CLevel = graythresh(CI2);
Cbw = ~im2bw(CI2,CLevel);
Cchoice2=input('Press 1 to autocalibrate pixel to mm ratio');
if Cchoice2 == 1
    Cse = strel('disk',2);
    Cbw2 = imopen(Cbw,Cse);
    [Clabeled,numObjects] = bwlabel(Cbw2,4);
    CGraindata = regionprops(Clabeled,'basic');
    D=0;
    for f = 1:numObjects
        d(f)=(((CGraindata(f).Area)*4/pi)^0.5);
        D=D+d(f);
    end
    Davg = (D/numObjects);
    Inptmm = input('Wat is die gemiddelde partikkel grotte?');
    ptmm = Davg/Inptmm;
end
imshow(Cbw);
CLevel
CChoice = input('Happy ? with gray, 1 if not');
while CChoice == 1
    Clevel=input('New Greyscale');
    cut = input('Cutoff size? ');
    Cbw = ~im2bw(CI2,CLevel);
    d=round(cut*ptmm);
    Cse = strel('disk',d);
    Cbw2 = imopen(Cbw,Cse);
    subplot(1,2,1);imshow(CI2);
    subplot(1,2,2);imshow(Cbw2);
    CChoice = input('Happy ? ,1 if not');
end
disp('values: ');
ptmm
cut
CLevel
elseif V == 2

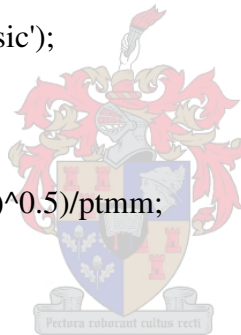
```



```

ptmm = input('Pixel to mm conversion factor : ');
cut = input(' Minimum cut-off size mm : ');
Clevel = input(' Graythreshold cut-off value : ');
else
    %In = input('C:\MATLAB6p5\work\Im1.bmp');
    I = imread('C:\MATLAB6p5\work\Calibration.jpg');
    I2 = imresize(I,[1000,1000]);
    CLevel = graythresh(I2);
    bw = ~im2bw(I2,CLevel);
    d=round(cut*ptmm);
    se = strel('disk',d);
    bw2 = imopen(bw,se);
    N=0;
    [labeled,numObjects]=bwlabel(bw2,4);
    N=numObjects;
    Graindata = regionprops(labeled,'basic');
    A=0;
    for K=1:N
        d(K)=(((Graindata(K).Area)*4/pi)^0.5)/ptmm;
        A=A+d(K);
    end;
    Maxg = (((max([Graindata.Area]))*4/pi)^0.5)/ptmm;
    Avg = (A/N);
    disp(['Total amount of recogized particles : ', num2str(N)]);
    disp(['Avg particle diameter   : ',num2str(Avg)]);
    disp(['Largest Particle : ',num2str(Maxg)]);
    subplot(1,3,1),imshow(I2);
    subplot(1,3,2),imshow(bw2);
    subplot(1,3,3),hist(d,10);
end

```



### A5.3 Experimental Results

Table A5.1a: 200 ml Sample MUG and DIPMUG

Sample	Number	Avg	Largest	Stddiv	Tot Number	Tot Avg
2l	11	1.28	1.88	0.34	11	1.28
4l	43	1.4	3.18	0.59	43	1.4
R3D51l	25	1.05	1.5	0.21	25	1.05
R3D101l	22	1.365	2.0982	0.4	22	1.365
R3D151l	6	1.0375	1.146	0.1	6	1.0375
R3D201l	60	1.15	1.83	0.364	60	1.15
R3D52l	12	1	1.58	0.25	12	1
R3D102l	12	1.088	2.25	0.4	12	1.088
R3D152l	7	1.29	2.36	0.588	7	1.29
R3D202l	31	1.08	1.8	0.27	45	1.08
R3D54l	5	1.243	1.9718	0.416	5	1.243
R3D104l	26	1.24	1.94	0.31	26	1.24
R3D154l	34	1.1	1.8	0.29	34	1.1
R3D204l	60	1.08	1.37	0.42	60	1.08
R4D201l	68	1.1769	2.738	0.455	68	1.1769
R4D202l	72	1.72	12.608	1.7188	72	1.72
R4D204l	117	1.5861	9.9821	1.204	117	1.5861

Table A5.1b: 200 ml Sample MUG and DIPMUG

Tot Vol	MUG	DIPMUG	(MUG - DIPMUG)^2	MUG^2
44.23232	1.3142	1.32697	0.000163063	1.727122
189.1183	6.22	5.673549	0.298608695	38.6884
82.46438	3.49545	2.473931	1.043500557	12.21817
94.33925	3.129	2.830177	0.089294976	9.790641
19.55584	4.22783	0.586675	13.25800882	17.87455
216.7635	7.4236	6.502905	0.847679283	55.10984
37.698	1.03199	1.13094	0.009791103	1.065003
41.01542	0.713	1.230463	0.267767667	0.508369
28.36775	2.763	0.851032	3.655620295	7.634169
152.6769	6.924	4.580307	5.492896878	47.94178
19.52442	0.723	0.585733	0.018842319	0.522729
101.282	4.99	3.038459	3.808513055	24.9001
117.4921	6.52484	3.524763	9.000462006	42.57354
203.5692	7.185	6.107076	1.16192015	51.62423
251.4117	11.91782	7.542352	19.14472062	142.0344
389.0434	12.517	11.6713	0.715207137	156.6753
582.9798	14.3147	17.48939	10.07867791	204.9106

**Total**                      94.10023                      68.89167454      815.799

**Ssreg**                                      68.89167  
**SStotal**                                      294.9253  
**Rsq**    0.76641

**Table A5.2a: 2 x 100 ml Sample MUG and DIPMUG**

Sample	Number	Avg	Largest	Stddiv	Tot Number	Tot Avg
R51I1.1	10	1.13	2.4	0.376		
R51I1.2	8	1.185	2.32	0.38	18	1.154444
R51I2.1	12	1.134	1.32	0.26		
R51I2.2	7	1.13	1.5	0.27	19	1.132526
R51I3.1	16	1.019	1.7	0.215		
R51I3.2	13	1.237	1.914	0.329	29	1.116724
R51.4.1	22	1.3	2.8	0.56		
R51I4.2	21	1.314	2.2	0.514	43	1.306837
R51I5.1	22	1.24	2.98	0.505		
R51I5.2	25	1.2373	2.9897	0.587	47	1.238564
R54Ibo1	18	1.179	1.795	0.3185		
R54Ibo2	14	1.266	2.057	0.3389	32	1.217063
R54IOrder1	26	1.424	2.89	0.573		
R54IOrder2	36	1.4415	4.08	0.714	62	1.434161
R54>1mm	60	1.758	4.7	0.8495	60	1.758
2l>1mm(1800)	48	1.255	2.518	0.391	48	1.255

**Table A5.2b: 2 x 100 ml Sample MUG and DIPMUG**

Sample	Tot Vol	MUG	DIPMUG	(MUG - DIPMUG)^2	MUG^2
R51I1.1					
R51I1.2	65.28037	1.96411	2.611215	0.418744622	3.857728
R51I2.1					
R51I2.2	67.5988	2.1974	2.703952	0.256594807	4.828567
R51I3.1					
R51I3.2	101.7375	4.2611	4.069499	0.036710905	18.15697
R51.4.1					
R51I4.2	176.5335	6.85577	7.061338	0.042258219	47.00158
R51I5.1					
R51I5.2	182.8746	7.291	7.314983	0.000575172	53.15868
R54Ibo1					
R54Ibo2	122.3489	3.518	4.893954	1.893250401	12.37632
R54IOrder1					
R54IOrder2	279.3359	9.58752	11.17344	2.515129178	91.92054
R54>1mm	331.3654	11.9844	13.25462	1.613450719	143.6258
2l>1mm(1800)	189.244	7.49	7.569758	0.006361402	56.1001

**Total**                      55.1493                      6.783075426    431.0263

**Ssreg**                                      6.783075  
**Sstot**                                      93.08797  
**RR**    0.927133

**Table A5.3a: 4 x 50 ml Sample MUG and DIPMUG**

Sample	Number	Avg	Largest	Stddiv	Tot Number	Tot Avg
1	25	0.9699	1.269	0.154		
2	27	0.986	2.128	0.28		
3	22	1.034	1.7	0.25		
4	26	1.041	1.6799	0.25	100	1.006835
5	23	1.056	1.6763	0.26		
6	19	1.0089	1.3366	0.176		
7	14	1.0831	1.5757	0.24		
8	29	1.0773	1.7436	0.28	85	1.057202
9	18	1.14	2.104	0.38		
10	8	1.244	1.83	0.4		
11	23	1.167	2.093	0.36		
12	21	0.962	1.27	0.3	70	1.107357
13	33	0.99	2.18	0.26		
14	0.25	1.0313	1.726	0.24		
15	25	1.0176	1.519	0.21		
16	31	1.144	2.071	0.28	89.25	1.051337
17	23	1.3	2.8	0.45		
18	25	1.1185	1.8563	0.29		
19	22	1.038	2.11	0.268		
20	26	1.1109	2.45	0.41	96	1.141478

**Table A5.3b: 4 x 50 ml Sample MUG and DIPMUG**

Sample	Tot Vol	MUG	DIPMUG	(MUG - DIPMUG)^2	MUG^2
1					
2					
3					
4	316.2972	3.820753	3.510899	0.096009582	14.59816
5					
6					
7					
8	282.3021	3.132585	3.133553	9.36923E-07	9.813091
9					
10					
11					
12	243.5134	3.666071	2.702998	0.927509452	13.44008
13					
14					
15					
16	294.7727	3.445082	3.271977	0.029965478	11.86859
17					
18					
19					
20	344.2515	3.943832	3.821192	0.01504061	15.55381

Total 18.00832 1.068526059 65.27373

Ssreg 1.068526  
Sstot 0.41378



## A7. Chapter 6, Experimental Results

Table A6.1: Chapter 6, Experimental Results

Sample	K+f	K+f+s	TSS	MUG
D0	157.8233	157.8893	0.066	2.19714
R3D51l	158.3732	158.4782	0.105	3.49545
R3D101l	172.53	172.624	0.094	3.12926
R3D151l	175.3712	175.4982	0.127	4.22783
R3D201l	187.4806	187.7036	0.223	7.42367
D0			0.066	2.19714
R3D52l	163.9461	163.9771	0.031	1.03199
R3D102l	167.9284	167.9744	0.046	1.53134
R3D152l	164.6344	164.7174	0.083	2.76307
R3D202l	157.3717	157.5797	0.208	6.92432
D0			0.066	2.19714
R3D54l	151.241	151.361	0.12	3.9948
R3D104l	157.2242	157.3742	0.15	4.9935
R3D154l	157.8233	158.0193	0.196	6.52484
R3D204l	159.2964	159.6794	0.383	12.75007
D0			0.066	2.19714
R4D51l	153.3321	153.4421	0.11	3.6619
R4D101l	152.1783	152.2323	0.054	1.79766
R4D151l	163.2951	163.5361	0.241	8.02289
R4D201l	160.6276	160.9856	0.358	11.91782
D0			0.066	2.19714
R4D52l	157.7336	157.7566	0.023	0.76567
R4D102l	187.3598	187.4238	0.064	2.13056
R4D152l	175.3172	175.5062	0.189	6.29181
R4D202l	156.8559	157.2319	0.376	12.51704
D0			0.066	2.19714
R4D54l	172.3947	172.4237	0.029	0.96541
R4D104l	153.2561	153.3391	0.083	2.76307
R4D154l	186.3467	186.5597	0.213	7.09077
R4D204l	154.7407	155.1707	0.43	14.3147
D0			0.066	2.19714
R5D51l	153.3321	153.4011	0.069	2.29701
R5D101l	152.1783	152.2743	0.096	3.19584
R5D151l	163.2951	163.4171	0.122	4.06138
R5D201l	160.6276	160.7632	0.1356	4.514124
D0			0.066	2.19714
R5D52l	157.7336	157.8066	0.073	2.43017
R5D102l	187.3598	187.4288	0.069	2.29701
R5D152l	175.3172	175.4152	0.098	3.26242
R5D202l	156.8559	156.963	0.107111	3.565729
D0			0.066	2.19714
R5D54l	172.3947	172.4807	0.086	2.86294
R5D104l	153.2561	153.3571	0.101	3.36229
R5D154l	186.3467	186.4567	0.11	3.6619
R5D204l	154.7407	154.9584	0.217694	7.247048

## A7 Chapter 7, Experimental Results

**Table A7.1a: Experimental Run 13 Results**

Day	pH	Clicks	Ca in	N in	PO4 in	Ca Measured	Ca out
0	7	58	0.16	0.056	0.2296		0.073
1	6.65	89	0.16	0.056	0.2296	0.06896	0.073
2	6.7	134	0.16	0.056	0.2296		0.073
3	6.78	137	0.16	0.056	0.2296		0.073
4	6.66	145	0.16	0.056	0.2296		0.073
5	6.62	167	0.16	0.056	0.2296	0.07616	0.073
6	6.67	171	0.16	0.056	0.2296		0.073
7	6.8	196	0.16	0.056	0.2296		0.073
8	6.83	230	0.16	0.056	0.2296		0.073
9	6.86	222	0.16	0.056	0.2296		0.073
10	7.15	260	0.16	0.056	0.2296	0.06896	0.073
11	7.1	267	0.16	0.056	0.2296		0.073
12	7	278	0.16	0.056	0.2296		0.073
13	6.99	288	0.16	0.056	0.2296		0.073
14	6.9	312	0.16	0.056	0.2296		0.073
15	6.89	301	0.16	0.056	0.2296	0.0656	0.073
16	6.86	344	0.16	0.056	0.2296		0.073
17	6.85	307	0.16	0.056	0.2296		0.073
18	6.91	300	0.16	0.056	0.2296		0.073
19	6.93	265	0.16	0.056	0.2296		0.073
20	6.96	220	0.16	0.056	0.2296	0.06176	0.073

**Table A7.1b: Experimental Run 13 Results**

N Mesured	N out	PO4 Measured	KH2PO4out	Biogas [ml]	%CH4 M	%CH4
	0.0293			135.14		13.07
0.0299915	0.0289	0.119966	0.12	207.37		10.09
	0.0285		0.11	312.22	7.12	8.13
	0.0281		0.11	319.21		7.09
	0.0277		0.10	337.85		6.87
0.026404	0.0273	0.105616	0.10	389.11		7.36
	0.0269		0.10	398.43	12.6	8.47
	0.0265		0.10	456.68		10.10
	0.0261		0.10	535.9	11.6	12.14
	0.0257		0.09	517.26		14.50
0.02245775	0.0253	0.089831	0.09	605.8	12	17.07
	0.0249		0.09	622.11		19.75
	0.0245		0.09	647.74		22.45
	0.0241		0.09	671.04		25.07
	0.0237		0.09	726.96	30	27.50
0.0219555	0.0233	0.087822	0.09	701.33		29.64
	0.0229		0.09	801.52	33	31.39
	0.0225		0.09	715.31		32.66
	0.0221		0.09	699	32	33.34
	0.0217		0.09	617.45		33.33

0.02174025	0.0213	0.086961	0.09	512.6	32.53
------------	--------	----------	------	-------	-------

**Table A7.1c: Experimental Run 13 Results**

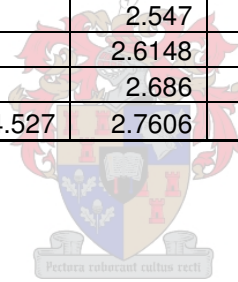
CODin	COD out Measured	COD out	Methane [ml]	Methane [g]	CO2 [ml]	CO2 [g]	CODconsumed
2.00			17.66	0.013	117.480	0.231	
2.00	1.70	1.759	20.93	0.015	186.444	0.366	0.24
2.00		1.473	25.39	0.018	286.828	0.563	0.53
2.00		1.306	22.64	0.016	296.572	0.583	0.69
2.00		1.188	23.20	0.017	314.646	0.618	0.81
2.00	1.22	1.096	28.64	0.020	360.467	0.708	0.90
2.00		1.021	33.75	0.024	364.679	0.716	0.98
2.00		0.957	46.11	0.033	410.570	0.806	1.04
2.00		0.902	65.05	0.046	470.851	0.925	1.10
2.00		0.854	74.98	0.054	442.282	0.869	1.15
2.00	0.80	0.810	103.39	0.074	502.408	0.987	1.19
2.00		0.771	122.89	0.088	499.222	0.981	1.23
2.00		0.735	145.44	0.104	502.295	0.987	1.26
2.00		0.702	168.22	0.120	502.819	0.988	1.30
2.00		0.672	199.89	0.143	527.070	1.035	1.33
2.00	0.67	0.643	207.86	0.148	493.472	0.969	1.36
2.00		0.617	251.61	0.180	549.911	1.080	1.38
2.00		0.592	233.60	0.167	481.707	0.946	1.41
2.00		0.568	233.02	0.166	465.984	0.915	1.43
2.00		0.546	205.77	0.147	411.683	0.809	1.45
2.00	0.44	0.525	166.73	0.119	345.872	0.679	1.48

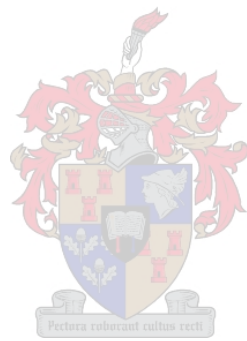
**Table A7.1d: Experimental Run 13 Results**

Ca cons	N cons	PO4 cons	MI inorganic	MI organic	MI cum	Day	Bottoms
0.087	0.027			2.204	2.204	0	1.91748
0.087	0.027	0.108	0.222	-0.020	2.406	1	
0.087	0.028	0.118	0.232	0.208	2.644	2	
0.087	0.028	0.123	0.237	0.442	2.883	3	
0.087	0.028	0.126	0.241	0.584	3.029	4	
0.087	0.029	0.129	0.244	0.628	3.076	5	2.013354
0.087	0.029	0.131	0.247	0.728	3.179	6	
0.087	0.030	0.133	0.249	0.725	3.177	7	
0.087	0.030	0.134	0.251	0.675	3.130	8	
0.087	0.030	0.135	0.252	0.797	3.253	9	
0.087	0.031	0.137	0.254	0.724	3.182	10	2.109228
0.087	0.031	0.138	0.255	0.775	3.234	11	
0.087	0.032	0.138	0.257	0.807	3.267	12	
0.087	0.032	0.139	0.258	0.839	3.301	13	
0.087	0.032	0.140	0.259	0.814	3.277	14	
0.087	0.033	0.141	0.260	0.917	3.381	15	2.492724
0.087	0.033	0.141	0.261	0.815	3.280	16	
0.087	0.034	0.142	0.262	0.999	3.466	17	
0.087	0.034	0.143	0.263	1.066	3.533	18	
0.087	0.034	0.143	0.264	1.226	3.694	19	
0.087	0.035	0.144	0.265	1.414	3.883	20	2.7465

**Table A7.1e: Experimental Run 13 Results**

<b>0.25-0.5</b>	<b>0.5-1</b>	<b>&gt;1</b>	<b>Total</b>	<b>Bottoms</b>	<b>0.25-0.5</b>	<b>0.5-1</b>	<b>&gt;1</b>	<b>Total</b>
0.28652	0	0	2.204	1.9146	0.2842	0.0083	0.0053	2.2124
				1.9246	0.283	0.0235	0.015	2.2461
				1.938	0.2844	0.0405	0.0257	2.2886
				1.9548	0.2884	0.0593	0.0374	2.3399
				1.975	0.295	0.0799	0.0501	2.4
0.315172	0.1266	0.0814	2.536526	1.9986	0.3042	0.1023	0.0638	2.4689
				2.0256	0.316	0.1265	0.0785	2.5466
				2.056	0.3304	0.1525	0.0942	2.6331
				2.0898	0.3474	0.1803	0.1109	2.7284
				2.127	0.367	0.2099	0.1286	2.8325
0.343824	0.20889	0.13431	2.796252	2.1676	0.3892	0.2413	0.1473	2.9454
				2.2116	0.414	0.2745	0.167	3.0671
				2.259	0.4414	0.3095	0.1877	3.1976
				2.3098	0.4714	0.3463	0.2094	3.3369
				2.364	0.504	0.3849	0.2321	3.485
0.5924	0.42411	0.27269	3.781924	2.4216	0.5392	0.4253	0.2558	3.6419
				2.4826	0.577	0.4675	0.2805	3.8076
				2.547	0.6174	0.5115	0.3062	3.9821
				2.6148	0.6604	0.5573	0.3329	4.1654
				2.686	0.706	0.6049	0.3606	4.3575
0.7405	0.633	0.407	4.527	2.7606	0.7542	0.6543	0.3893	4.5584





## **A8. WRC Project**

### **Phase 1 (Lab-Scale)**

- 1999 to 2002
- Conducted on shaker and roller tables in 450 ml vessel volumes
- Feed medium consisted of simple sugars and a COD:N:P:Ca ratio of 20:2:2:1 was used.
- Incubation periods of 20 days (@ 35 Degrees Celsius)
- 2/7 reactor volume fresh feed every day
- Large granules were found at the end of the incubation period than at the beginning
- Thus it was found that granulation can be enhanced in a artificial environment simulating the up-flow regime of a UASB system

### **Phase 2 (Bench-Scale Commissioning)**

- Mid to end 2002
- Conducted in reactors one order of magnitude larger than Phase 1 vessels
- All parameters were constant except for volume and agitation method (in order to facilitate scale-up and the study thereof)
- The findings from the experiments done showed that not only could granulation be enhanced, but granules could be grown from dispersed sludge.
- However, it was obvious from these experiments that the system is far from optimised. It was also found that the methods of analysis used in phase 1 was completely inadequate for the bench-scale and later phase 4 and 5 work.

### **Phase 3 (Bench-Scale Optimisation)**

- 2003 to 2004
- Another reactor was commissioned, simulating the movement of the phase 1 units on the roller tables, baffles were included.
- This study was firstly to optimise the system with regards to the sludge used, feed medium composition, reactor configuration and mixing speed.
- Secondly the research was preoccupied with obtaining as much as possible information that would aid in the scale-up to Phase 4. Thirdly, it was aimed to revise the methods of analysis that was used in phase 1.

### **Phase 4 (Pilot Plant)**

- 2005 onwards
- The aim of Phase 4 is to design, and optimise a reactor one order of magnitude larger than those used in phase 3.

### **Phase 5 (Industrial size bioreactor)**

- This unit should be of volume large enough to produce enough granules to seed a industrial size UASB